UNIVERSITÀ DEGLI STUDI DI PARMA

Dottorato di Ricerca in Scienze Chimiche

Ciclo XXIX (2014-2016)

Design and Synthesis of New Calix[6]arene-based Molecular Switches

Coordinatore:
Chiar.mo Prof. Roberto Cammi

Tutor:
Chiar.mo Prof. Arturo Arduini

Dottoranda: Valeria Zanichelli

2017

Abstract

This PhD thesis describes the design, the synthesis and the characterization of calix[6]arene-based molecular machine prototypes, and the study of their dynamic properties triggered by external stimulation. Initially, the ability of a calix[6]arene wheel to increase the rate of a nucleophilic substitution reaction on a complexed guest was demonstrated, and by virtue of these results a new supramolecularly assisted strategy for the synthesis of oriented rotaxanes was set up. Then, the properties of new hydroxy- and bis(*N*-phenylureido)-calix[6]arene derivatives were steered, and the effects of the structural modification of the different macrocycle's domains were evaluated. The ability of calix[6]arenes to form oriented complexes with dialkylviologen-based axles was then exploited for the synthesis of single and double station constitutionally isomeric rotaxanes, whose ability to behave as molecular level shuttles was proved. Moreover, the design, the synthesis and the characterization of an oriented calix[6]arene-based catenane, and the study of its electrochemical and dynamic properties were developed. As last part of this thesis, the study of possible synthetic pathways towards the synthesis of oriented calix[6]arene-based dimers and containers is reported.

Keywords: molecular machines, molecular shuttles, rotary motors, pseudorotaxanes, rotaxanes, catenanes, molecular flasks, calix[6]arenes, viologen salts, cyclic voltammetry, self-assembly, supramolecular chemistry.

CONTENTS:

PREFACE

GENERAL INTRODUCTION

General introduction

"Atoms are letters. Molecules are the words. Supramolecular entities are the sentences and chapters."

J. M. Lehn, 1987

Every chemical species can be considered as a specific entity endowed with an intrinsic and peculiar asset of structural information that delineates its physical properties and determines its reactivity. The exhaustive comprehension of these properties is of crucial importance for chemists, in order to exploit these characteristics for the development of modern nanotechnologies.

At the beginning of the last century, when J. D. van der Waals first devised the theoretical bases of non-covalent interactions,[1] it emerged the idea that these weak but highly specific intermolecular attractive forces could play a significant role in governing a variety of chemical processes. This promoted the rising of several modern concepts such as the definition of "receptor" formulated by P. Ehrlich,[2] the "lock-and-key" mechanism by E. Fisher[2,3] and the bases of coordination chemistry by A. Werner,[2,4] that dictated the beginning of modern chemistry. The re-elaboration of these conceptions, together with the progresses of synthetic chemistry, paved the way for the birth of Supramolecular Chemistry,[5] a highly interdisciplinary field defined as *the chemistry beyond the molecules*, that focuses on aggregates made up of a discrete number of assembled components, held together by non-covalent interactions. In the following decades, the pioneering work of D. J. Cram,[6] C. J. Pedersen[7] and J. M. Lehn[8] contributed to define the principles and methods of this new branch of chemistry, up to the extension of the concept of "machine" down to the molecular level, as initially envisaged by R. Feynman.[9] More recently, these ideas were finally applied in the design and synthesis of several systems able to perform programmed tasks upon

1 Margenau, H.; Kestner, N. R. *Theory of Intermolecular Forces*, Elsevier, 1969; Maitland, G. C.; Smith, E. B. *Chem. Soc. Rev.* **1973**, *2 (2)*, 181.

2 Lehn, J. M. *Perspectives in Coordination Chemistry*, VCH, Basel, 1992.

3 Fischer, E. *Ber. Dtsch. Chem. Ges.* **1894**, *27 (3)*, 2985-2993.

4 Constable, E. C.; Housecroft, C. E. *Chem. Soc. Rev.* **2013**, *42 (4)*, 1429-1439.

5 Lehn, J. M. *Supramolecular Chemistry*, VCH, Weinheim, 1995.

6 Cram, D. J. *Angew. Chemie Int. Ed.* **1988**, *27 (8)*, 1009-1020.

7 Pedersen, C. J. *Angew. Chemie Int. Ed.* **1988**, *27 (8)*, 1021-1027.

8 Lehn, J.-M. *Angew. Chemie Int. Ed.* **1988**, *27 (1)*, 89-112.

9 Feynman, R. *Eng. Sci.* **1960**, *23*, 22-36.

proper external stimulation, and the results achieved in this field by J.-P. Sauvage,[10] J. F. Stoddart[11] and B. L. Feringa[12] were awarded in 2016 with the Nobel Prize in Chemistry.[13]

This thesis deals with the design, the synthesis and the characterization of calix[6]arene-based molecular machine prototypes, that can exhibit a directional motion triggered by external stimulation. In particular, these studies have been focused on:

- *Chapter 1*: the state of the art of mechanically interlocked species as molecular level machines and their perspectives as working devices;

- *Chapter 2*: the ability of calix[6]arene derivatives to increase the rate of a nucleophilic substitution reaction on a complexed guest, and to supramolecularly assist the synthesis of oriented pseudorotaxanes and rotaxanes;

- *Chapter 3*: the steering of the properties of tris(*N*-phenylureido)calix[6]arene derivatives, through the structural modification of its different domains;

- *Chapter 4*: the synthesis, the characterization and the study of the dynamic properties of calix[6]arene-based single and double station rotaxanes, that can behave as molecular level shuttles;

- *Chapter 5*: the design, the synthesis and the characterization of two constitutionally isomeric calix[6]arene-based catenanes, through an intramolecular ring closing metathesis strategy, and the study of their electrochemical and dynamic properties;

- *Chapter 6*: the possible synthetic pathways towards the preparation of oriented calix[6]arene-based dimers.

[10] J. P. Sauvage *Acc. Chem. Res.* **1990**, *23 (10)*, 319-327; Sauvage, J. P. *Acc. Chem. Res.* **1998**, *31 (10)*, 611-619; Champin, B.; Mobian, P.; Sauvage, J. P. *Chem. Soc. Rev.* **2007**, *36 (2)*, 358-366.

[11] Balzani, V.; Gómez-López, M.; Stoddart, J. F. *Acc. Chem. Res.* **1998**, *31 (7)*, 405-414; Balzani, V.; Credi, A.; Raymo, F.; Stoddart, J. *Angew. Chem. Int. Ed* **2000**, *39 (19)*, 3348-3391; Gómez-López, M.; Preece, A. J.; Stoddart, J. F. *Nanotechnology* **1996**, *7*, 183-192.

[12] Browne, W: R.; Feringa, B. L. *Nat. Nanotechnol.* **2006**, *1 (1)*, 25-35; Feringa, B. L. *Acc. Chem. Res.* **2001**, *34 (6)*, 504-513; Feringa, B. L. *J. Org. Chem.* **2007**, *72* (*18)*, 6635-6652.

[13] Leigh, D. A. *Angew. Chem. Int. Ed.* **2016**, **55**, *14506-14508*.

CHAPTER 1

MECHANICALLY INTERLOCKED SPECIES AS MOLECULAR LEVEL MACHINES: STATE OF THE ART AND PERSPECTIVES AS WORKING DEVICES

1.1 General aspects of Supramolecular Chemistry

One of the ultimate goals for contemporary chemists is to control the assembly and the functions of artificial nano-sized structures with the highest possible degree of precision. The miniaturization of the components and the availability of responsive devices are in fact key issues for the development of modern nanotechnologies.

The most promising strategy for controlling the aggregation at the nanometer level is provided by the *bottom up* approach, which starts from nanoscale objects (namely atoms or molecules) to build up ordered nanostructures endowed with specific functions,[1] relying on the principles of *Supramolecular Chemistry.*[2] This branch of chemistry focuses on systems composed by a discrete number of spontaneously assembled subunits, that are held together through non-covalent interactions.

While traditional chemistry deals with covalent bonds, supramolecular chemistry takes advantage of weaker and reversible interactions between either charged or neutral chemical species, including hydrogen and halogen bonding, metal coordination, hydrophobic and van der Waals forces, as well as π-π, CH-π and Coulombic interactions. Although these forces are considerably weaker than covalent bonds, they can be exploited for the formation of highly stable supramolecular complexes when used in a co-operative manner. Moreover, the presence of reversible interactions allows the possibility to obtain stimuli-responsive assemblies, whose aggregation can be tuned through external inputs.

A peculiar class of supramolecular complexes that combines these interesting features is represented by Host-Guest adducts[3]. Usually, the term *host* is used to describe a large molecule or aggregate, such as a synthetic macrocycle, endowed with a central hole or cavity, that possesses convergent binding sites (Lewis basic donor atoms, hydrogen bonds donors, …). The *guest* could be an ion, a neutral species or a more complex molecule that exhibits divergent and complementary binding sites. When compared to their acyclic analogues, the complexes formed by macrocyclic hosts exhibit an increased stability by virtue of the *macrocyclic effect*[4]: this phenomenon relates not only to the chelation of the guest *via* multiple binding sites on the host, but also to the rigidity and the preorganization[5] of the receptor, that

[1] Yu, H. D.; Regulacio, M. D.; Ye, E.; Han, M. J. *Chem. Soc. Rev.* **2013**, *42*, 6006-6018.

[2] Steed, J. W.; Atwood, J. L. *Supramolecular Chemistry*, 2013; Lehn, J. M. *Angew. Chem. Int. Ed. Engl.* **1990**, *29 (11)*, 1304-1319 and **1988**, *27*, 89-112; Desiraju, G. R. *Curr. Sci.* **2005**, *88*, 374-380.

[3] Gale, P. A.; Steed, J. W. *Supramolecular Chemistry*, John Wiley & Sons, Ltd: Chichester, UK, 2012.

[4] Melson, G. A. *Coordination Chemistry of Macrocyclic Compounds*; Springer US: Boston, MA, 1979.

[5] Cram, D. J. *Angew. Chem. Int. Ed.* **1986**, 1039-1134; Fiedler, D.; Leung, D. H.; Bergman, R. G.; Raymond, K. N. *Acc. Chem. Res*. **2005**, *38*, 351-360; Sada, K.; Takeuchi, M.; Fujita, N.; Numata, M.; Shinkai, S.; *Chem. Soc. Rev.* **2007**, *36*, 415-435; e) Meyer, C. D. C.; Joiner, S.; Stoddart, J. F. *Chem. Soc. Rev*. **2007**, *36,* 1705-1723; Filby, M. H.; Steed, J. W. *Coord. Chem. Rev.* **2006**, *250,* 3200-3218; Antonisse, M. M. G.; Reinhoudt, D. N. *Chem. Commun*. **1998**, 443-448.

guarantee a higher overall free energy gain upon complexation of the guest. In addition to the host's preorganization, another crucial parameter in determining the affinity between an host and its guest is complementarity[5]: in order to provide an efficient complexation, the binding sites of the host must be suitably organized in space and simultaneously contact and attract the binding sites of the guest without generating internal strains or repulsions.

In the last decades, the properties of a wide range of natural and synthetic receptors have been studied, and countless examples of working devices and molecular machines prototypes whose behavior is governed by non-covalent interactions have been proposed. Indeed, supramolecular chemistry expanded into the fields of materials chemistry and nanoscience with many real and potential applications.

1.2 Mechanically interlocked molecules (MIMs)

In the simplest instance, a pseudorotaxane (see **Figure 1.1a**) is a supramolecular complex constituted by a molecular species having a linear symmetry that threads a macrocycle. Commonly, the term *wheel* refers to the cyclic component, while the term *axle* refers to the threaded linear molecule. The assembly is held together by non-covalent interactions, and the thermodynamic stability of the complex is determined by the nature and the extent of the intermolecular forces between the components.

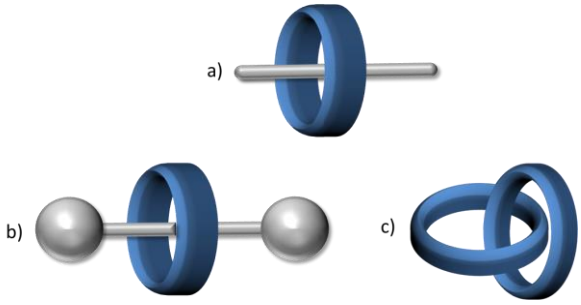

Figure 1.1 *Schematic representation of (a) a [2]pseudorotaxane, (b) a [2]rotaxane, and (c) a [2]catenane.*

The insertion, at the termini of the axle, of two bulky substituents (whose dimension is larger than the inner diameter of the macrocycle), gives rise to the formation of a new chemical compound defined as rotaxane (see **Figure 1.1b**). In this class of molecules, the axial component is mechanically confined within the macrocycle by the presence

of the *"stoppers"*. If the threaded dumbbell is constituted by a cyclized molecule, the originated interlocked molecule is defined as catenane (see **Figure 1.1c**). For [*n*]pseudorotaxanes, [*n*]rotaxanes and [*n*]catenanes, the number of components of the species is indicated between square-brackets before the name.

A plethora of different architectures based on these motifs composed by a variable number of elements connected to each other have been realized. The schematic representations of some interlocked structures, including polyrotaxanes, daisy-chain assemblies, dendritic and polymeric structures, such as polycatenanes and knots[6] are reported in **Figure 1.2**.

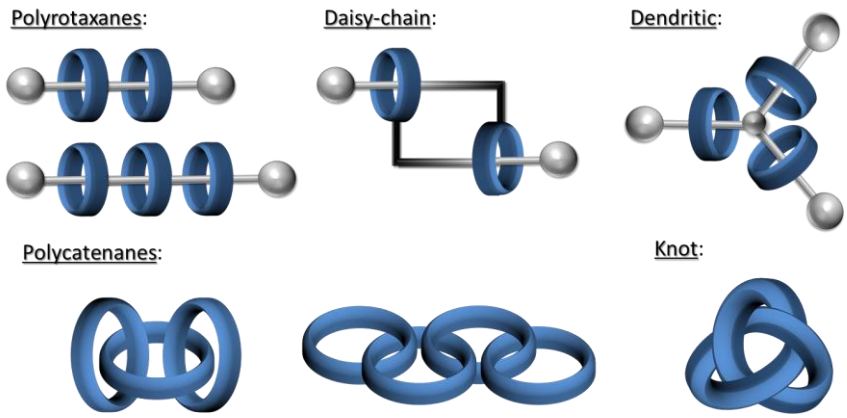

Figure 1.2 *Schematic representation of mechanically interlocked complex architectures.*

1.2.1 Synthetic approaches for the synthesis of MIMs

MIMs are synthetically challenging targets, mainly because of the inherent difficulty in arranging in space two or more independent molecules such that the desired mechanical bond can be formed in a predictable way. Methods for MIMs synthesis, in particular for catenanes and rotaxanes, have remarkably improved since the first reports of their synthesis in low yield relying on statistical attempts. The most effective synthetic strategies so far devised require the preventive formation of a [*n*]pseudorotaxane precursor, in which the axial component (eventually half-dumbbell-shaped) and the macrocycle are preventively organized in the correct mutual arrangement, by virtue of the intermolecular recognition between the components.[7]

[6] *Molecular Catenanes, Rotaxanes and Knot* (Eds.: J. P. Sauvage, C. O. Dietrich-Buchecker) Wiley-VCH, Weinheim, 1999.

[7] Philp, D.; Stoddart, J. F. *Synlett* **1991**, 445-458.

These methods, collectively referred to as *passive template* approaches, have been extended to a wide range of template motifs and increasingly complicated interlocked structures, often in excellent yields.[8]

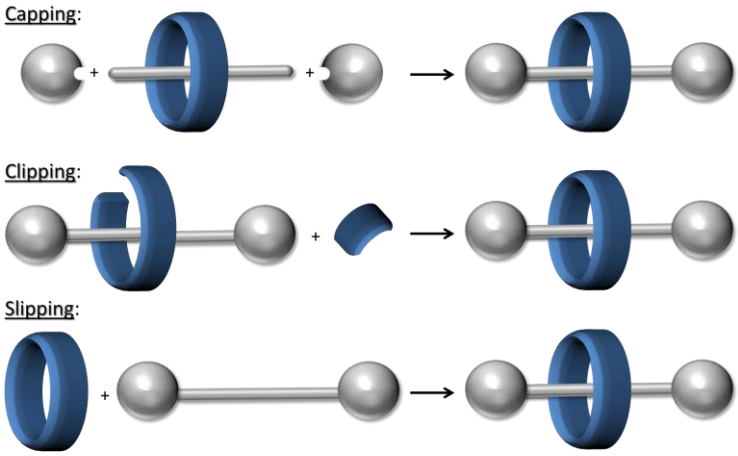

Figure 1.3 *Synthetic approaches for rotaxanes synthesis*

The *capping* strategy (**Figure 1.3** top) takes advantage of the presence of reactive moieties at the termini of the complexed axle, to which the bulky stoppers are covalently linked, in order to achieve the formation of the corresponding interlocked rotaxane.

In the *clipping* strategy (**Figure 1.3** middle), the only partially formed macrocycle is clipped around the pre-existing dumbbell of the rotaxane. Again, the placement and the initial folding of the ring around the axle are driven by supramolecular interactions.

Another strategy for the synthesis of rotaxanes is the *slippage*[9] (**Figure 1.3** bottom). This approach consists in the separate synthesis of the rotaxane components (i.e. the wheel and the fully stoppered axle), that are afterwards heated in solution so that the macrocycle can slip over the dumbbell's stoppers and form the thermodynamically favored interlocked product. The rate constants for these processes are highly affected by the size complementarity between macrocycles and stoppers.

[8] Hubin, T. J.; Busch, D. H.; *Coord. Chem. Rev.* **2000**, *200-202*, 5-52.

[9] Asakawa, M.; Ashton, P. R.; Ballardini, R.; Balzani, V.; Belohradsky, M.; Gandolfi, M. T.; Kocian, O.; Prodi, L.; Raymo, F. M.; Stoddart, J. F.; Venturi, M. *J. Am. Chem. Soc.* **1997**, *119*, 302-310; Raymo, F. M.; Houk, K. N.; Stoddart, J. F. *J. Am. Chem. Soc.* **1998**, *120 (36)*, 9318-9322.

As far as catenanes are concerned, one of the simplest approaches is to clip a second ring around an already complete macrocycle. This can be accomplished by the intramolecular reaction between the ends of a sufficiently long threaded axle, or by the intermolecular reaction of a preformed pseudorotaxane with an appropriate linker.

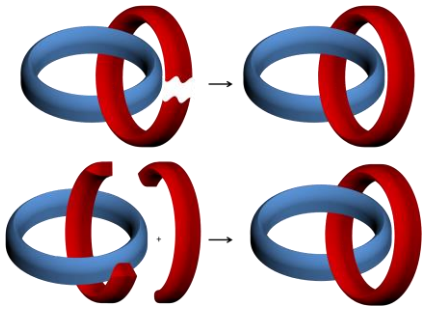

Figure 1.4 *Synthetic approaches for catenanes synthesis*

An elegant and complementary strategy for the synthesis of interlocked species is the *active template* method. Leigh and co-workers introduced this novel approach in which a reactive unit embedded in the macrocycle, typically a metal ion, both pivots the organization of the components and mediates the formation of the mechanical bond.[10] A growing number of different metal-catalyzed reactions have been exploited for the realization of rotaxanes and catenanes,[11] including the copper(I)-catalyzed terminal alkyne-azide cycloaddition[12] (the ''click'' reaction), palladium- and copper-catalyzed alkyne couplings[13] and oxidative Heck couplings.[14] An appealing characteristic of this approach is that the reactions that exclusively proceed through a threaded intermediate allow the formation of several otherwise inaccessible mechanically linked macromolecules. Moreover, these syntheses do not need permanent recognition elements between the components and, if the catalyst turns over, only a sub-stoichiometric amount of metal is required.

[10] Crowley, J. D.; Goldup, S. M.; Lee, A. L.; Leigh, D. A.; McBurney, R. T. *Chem. Soc. Rev.* **2009**, *38*, 1530-154.

[11] Goldup, S. M.; Leigh, D. A.; McGonigal, P. R.; Symes, M. D.; Long, T.; Wu, J. *J. Am. Chem. Soc.* **2009**, *131 (43)*, 15924-15929; Sato, Y.; Yamasaki, R.; Saito, S. *Angew. Chem. Int. Ed.* **2008**, *48*, 504-507.

[12] Aucagne, V.; Hänni, K. D.; Leigh, D. A.; Lusby, P. J.; Walker, D. B. *J. Am. Chem. Soc.* **2006**, *128*, 2186-2187.

[13] Saito, S.; Takahashi, E.; Nakazono, K. *Org. Lett.* **2006**, *8*, 5133-5136.

[14] Crowley, J. D.; Hänni, K. D.; Lee, A. L.; Leigh, D. A. *J. Am. Chem. Soc.* **2007**, *129*, 12092-12093.

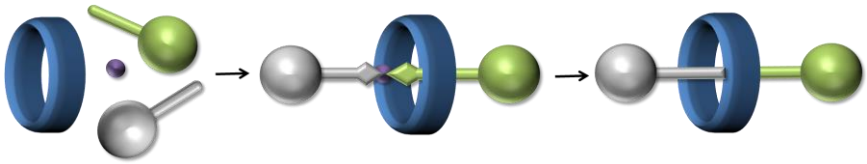

Figure 1.5 *Schematic illustration of active metal template synthesis: the formation of a covalent bond between the gray and green ''half-thread'' units to generate the rotaxane is promoted by a metal catalyst (violet), and takes place through the cavity of the macrocycle (blue).*

1.2.2 Synthesis of MIMs under kinetic and thermodynamic control

All the previously described strategies require a precise orientation of two or more molecules before performing the last step, in which the formation of covalent bonds permanently fixes the shape of the entwined final molecule. If these intermolecular stabilizing forces are retained in the transition state and irreversible stoppering reactions are employed, the interlocking process proceeds under kinetic control (see **Figure 1.6** left). However, this latter strategy may result in the irreversible formation of undesired byproducts, such as non-complexed dumbbells or non-catenated rings, that therefore lower the efficiency of the processes with loss of starting material.

Since the formed interlocked compounds are usually lower in free energy than their non-mechanically blocked counterparts, this suggests that their synthesis could also be efficiently performed under thermodynamic control.[15] This approach involves the use of reversible bonds to ultimately provide the most thermodynamically stable product (see **Figure 1.6** right):

[15] Dichtel, W. R.; Miljani, O. S.; Zhang, C. W.; Spruell, J. M.; Patel, K.; Aprahamian, I.; Heath, J. R.; Stoddart, J. F. *Acc. Chem. Res.* **2008**, *41 (12)*, 1750-1761.

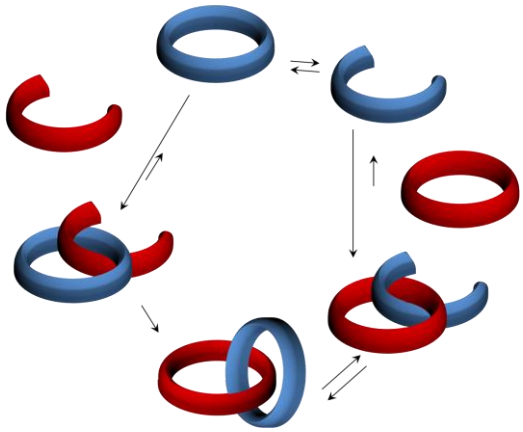

Figure 1.6 *Both kinetic and thermodynamic control have been exercised in the catenanes synthesis. Kinetically controlled reactions (left) proceed through a pseudorotaxane formation, followed by an irreversible ring closure, while thermodynamically controlled pathways (right) rely on reversible opening of one macrocycle, followed by the coordination to the second ring, and finally by the reversible closure.*

The appeal of this synthesis lies in the fact that dynamic mechanical bonds combine the robustness of covalent linking with the reversibility of non-covalent interactions: these features consent to operate in equilibrium conditions, and undesired kinetic side products can be recycled to maximize the formation of the most stable target compound.
This new method has already been put into practice to prepare several complex architectures[16] and novel materials[17].

1.3 Application of MIMs as molecular level machines

Among the characteristics of interlocked molecules, the possibility to trigger a controlled mechanical motion of one component relative to another through external energy inputs, that is to behave as *molecular level machines*, is a compelling property.

[16] Aricò, F.; Chang, T.; Cantrill, S. J.; Khan, S. I.; Stoddart, J.F. *Chem. Eur. J.* **2005**, *11*, 4655-4666.

[17] Steuerman, D. W.; Tseng, H. R.; Peters, A. J.; Flood, A. H.; Jeppesen, J. O.; Nielsen, K. A.; Stoddart, J. F.; Heath, J. R. *Angew. Chem. Int. Ed.* **2004**, *43*, 6486-6491.

When chemists and material scientists started developing the ability to orchestrate molecular movements in such multistate systems,[18] these became interesting building blocks of contemporary molecular nanotechnology.

The chemical information stored within the components of these devices strictly influences their working modes. For instance, if two or more binding sites are inserted in a rotaxane dumbbell, the macrocycle can interact alternatively with each of them, and the system can exist as two different co-conformations, whose population depends on their relative thermodynamic stability. In properly designed systems, the equilibrium between the species can be governed through an appropriate energy input (chemical, electrochemical or photochemical), since the external stimulus can tune the affinity of the wheel for the different stations present on the linear component. As a result, the macrocycle can translate back and forth along the threaded dumbbell to reach the most stable conformation: such structures represent the simplest models of a *molecular shuttle*.[19] As an arbitrary example, a molecular shuttle realized by Stoddart and coworkers is reported (see **Figure 1.7**).[20] The axial component of the assembly is decorated with two electron-rich sites, a 1,5-dioxynaphtalene (DNP) and a tetrathiafulvalene (TTF), and a cyclobis(paraquat-*p*-phenylene) is used as wheel.

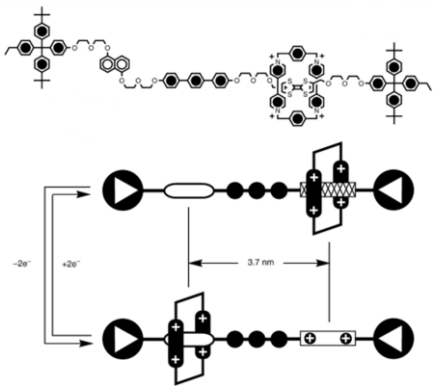

Figure 1.7 *Example of molecular shuttle (adapted from ref.20, copyright © 1999-2016 John Wiley & Sons.*

[18] Stoddart, J. F. *Angew. Chem. Int. Ed.* **2014**, *53*, 11102-11104; Pierro, T.; Gaeta, C.; Talotta, C.; Casapullo, A.; Neri, P. *Org.Lett.* **2011**, *13 (10)*, 2650-2653.

[19] Silvi, S.; Arduini, A.; Pochini, A.; Secchi, A.; Tomasulo, M.; Raymo, F. M.; Baroncini, M.; Credi, A. *J. Am. Chem. Soc.* **2007**, *129 (44)*, 13378-13379; Leigh, D. A.; Troisi, A.; Zerbetto, F. *Angew. Chem. Int. Ed. Engl.* **2000**, *39 (2)*, 350-353; Anelli, P. L.; Spencer, N.; Stoddart, J. F. *J. Am. Chem. Soc.* **1991**, *113 (13)*, 5131-5133.

[20] Tseng, H. R.; Vignon, S. A.; Stoddart, J. F. *Angew. Chem. Int. Ed. Engl.* **2003**, *42 (13)*, 1491-1495.

In the ground state, the macrocycle encircles the TTF station because of the strong charge transfer interaction between the positively charged host and the electron-rich guest. Exploiting the redox properties of the TTF moiety, the translation of the wheel towards the DNP station is induced by electrostatic repulsions that arise upon the oxidation of the TTF to TTF^{2+}. The subsequent reduction of TTF^{2+} to TTF restores the initial situation.

In the case of catenanes, the rings can rotate with respect to one another. When one ring is significantly larger than the other, the term *circumrotation* is often used to describe the translation of the smaller annulus around the larger one. This translational movement in a [2]catenane architecture was demonstrated by the same group exploiting an electrochemically triggered strategy very similar to the one employed in the case of rotaxanes. The catenane is constituted by a cyclobis(paraquat-*p*-phenylene) annulus ($CBPQT^{4+}$) entwined with a second ring that bears a 1,5-dioxynaphthalene (1/5DN) and a tetrathiafulvalene (TTF) recognition sites (see **Figure 1.8**). Since in solution the affinity of $CBPQT^{4+}$ for TTF is higher (K > 8000 M^{-1}) than the one for naphthalene derivatives, the wheel resides preferentially around the first station. Upon oxidation of the TTF, the wheel circumrotates along the crown ether until the 1/5DN unit occupies the cavity.

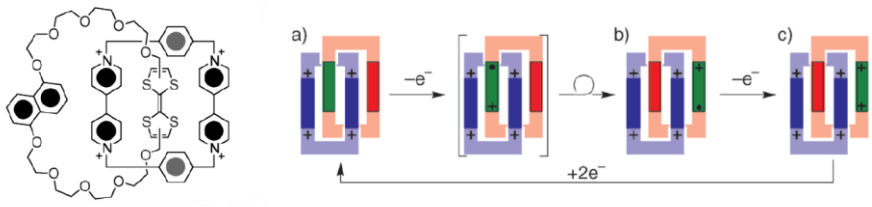

Figure 1.8 *Example of circumrotating [2]catenane Copyright © American Chemical Society.*

The main obstacle preventing the integration of these switching systems with current technologies is the gap between molecular and real-devices scale: in fact, the extension of the stimuli-induced motion to the macroscopic level generally requires organization, cooperation and coherence of many molecular-level units, and these goals are still challenging to reach.[21] For instance, mechanical switches embedded into polymeric matrices have been exploited to alter their optical properties. The rotaxanes and catenanes that rely on charge-transfer interactions between the components intrinsically involve changes in absorption, and therefore in color, as a consequence of

[21] Key, E. R.; Leigh, D. A.; Zerbetto, F.; *Angew. Chem. Int. Ed.* **2007**, *46*, 72-191; Van Dongen, S. F. M.; Cantekin, S.; Elemans, J. A. A. W.; Rowan, A. E.; Nolte, R. J. M. *Chem.Soc.Rev.* **2014**, *43*, 99-122.

shuttling. The incorporation of these systems into a solid or liquid-crystalline polymers gives rise to electrochromic devices, in which a macroscopic color change occurs on application of an external input.[22] Mechanical switches have also been utilized to affect the mechanical properties of materials. For instance, the incorporation of configurational switches, especially based on azobenzene moieties, allowed to reversibly control contraction–extension cycles through photoisomerization, and other physical properties such as viscosity and solubility could be similarly tuned.[23] Also, many solid-state molecular electronic devices based on electrochemically switchable supramolecular units have been reported.[24] Other interesting examples of application of molecular level machines are displayed in **Figure 1.9**.

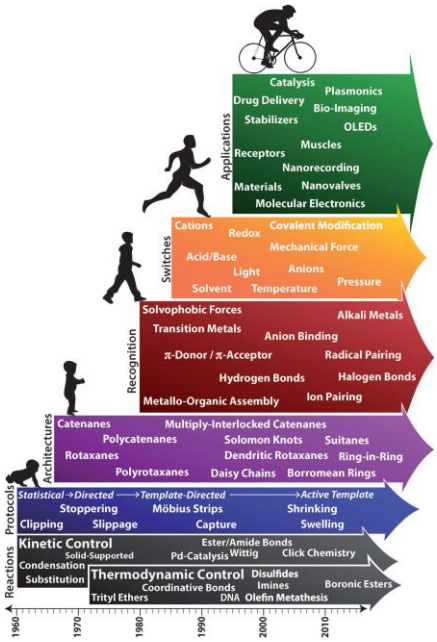

Figure 1.9 *Timeline for the growth of research on the mechanically-interlocked molecules and their applications proposed by Stoddart (reprinted from ref. 18, copyright © Wiley-VCH).*

22 Steuerman, D. W.; Tseng, H. R.; Peters, A. J.; Flood, A. H.; Jeppesen, J. O.; Nielsen, K. A.; Stoddart, J. F.; Heath, J. R. *Angew. Chem. Int. Ed.* **2004**, *43*, 6486-6491.

23 Natansohn, A.; Rochon, P. *Chem. Rev*. **2002**, *102*, 4139-4175.

24 Pease, A. R.; Jeppesen, J. O.; Stoddart, J . F.; Luo, Y.; Collier, C. P.; Heath, J . R. *Acc. Chem. Res.* **2001**, *34*, 433-444; Flood, A. H.; Ramirez, R. J. A.; Deng, W. Q.; Muller, R. P.; Goddard, W. A.; Stoddart, J. F. *Aust. J. Chem.* **2004**, *57*, 301-322; Mendes, P. M.; Flood, A. H.; Stoddart, J. F. *Appl. Phys. A* **2005**, *80*, 1197-1209; Orlandini, G.; Groppi, J.; Secchi, A.; Arduini, A.; Kilburn, J. D. *Electrochim. Acta* **2016**, accepted.

1.3.1 Oriented MIMs

The ability of supramolecular structures to perform programmed tasks is strictly connected with their physico-chemical properties and the spatial arrangement of the fragments that constitute their skeleton. One aspect of growing interest, that could expand the applications of these systems in the field of working devices, is the construction of interlocked structures in which the stimuli-promoted movement can be carried out in an unidirectional manner. In principles, the directionality of motion can be governed either by a series of successive and orthogonal chemical transformations, or by the inherent features of the parts of the motors, such as the asymmetry of the components and their mutual spatial arrangement. In particular, the development of motifs in which the reciprocal orientation of the components can be controlled is a fundamental achievement for the realization of catenane-based unidirectional rotary motors and rotaxane-based linear motors.

The macrocycles employed for the construction of MIMs can be grouped in two general categories: those exhibiting a substantially flat shape (as for example crown ethers) and those having a three-dimensional structure, like cucurbiturils, cyclodextrines, resorcinarenes or calixarenes. Since the planar macrocycles and the most symmetric 3D receptors (such as cucurbiturils) are endowed with two palindrome faces, a guest can thread these wheels from both sides yielding the same product (**Figure 1.10a** and **c**).

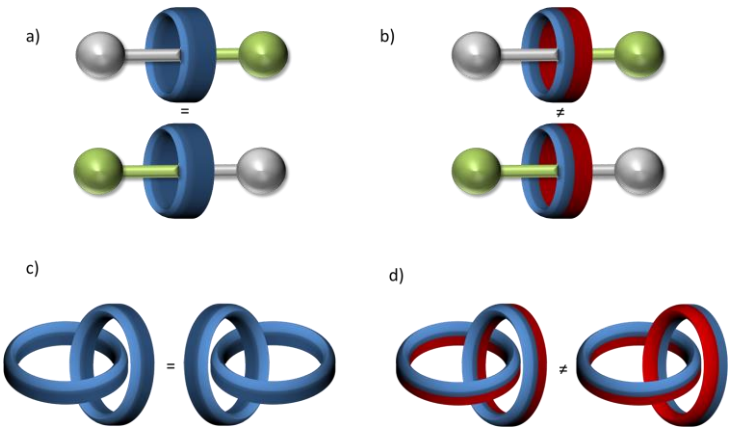

Figure 1.10 *a) Representation of rotaxanes (a) and catenanes (c) composed of palindrome wheels. If facially unsymmetrical macrocycles are employed, the threading of a non-symmetric axle gives rise to orientational rotaxane (b) and catenane (d) isomers.*

On the contrary, when three-dimensional non-symmetric hosts in which the two rims differ either in size or in chemical properties are employed, the threading of a non-symmetric axle gives rise to the formation of a mixture of orientational pseudorotaxane isomers. If bulky stoppers are attached at the termini of the threaded axle, two constitutionally isomeric rotaxanes are obtained (**Figure 1.10b**). Similarly, it is possible to obtain oriented catenanes by exploiting facially unsymmetrical macrocycles (**Figure 1.10d**).

These rotaxane and catenane isomers cannot be interconverted without breaking any mechanical bond, and examples of their selective synthesis have been reported[25], especially exploiting cyclodextrines as wheels. Harada and coworkers[26] were able to synthesize a single orientational pseudorotaxane isomer by tuning the steric hindrance of the two different terminal substituents of the asymmetric axle threaded into a cyclodextrin (see **Figure 1.11a**).

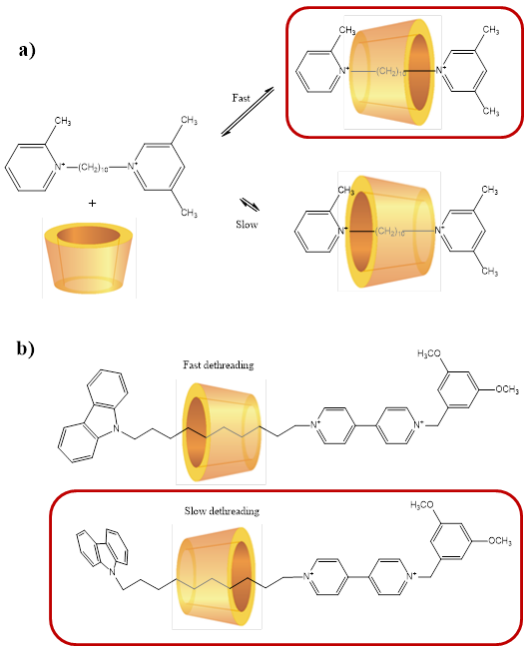

Figure 1.11 *a) The steric hindrance of the groups on the pyridinium-based axle ends was found to control the orientation of the formed pseudorotaxane isomers; b) The conformations of the oriented rotaxanes are responsible for the different threading and dethreading rates.*

[25] Craig, M. R.; Claridge, T. D. V.; Hutchings, M. G.; Anderson, H. L. *Chem. Commun.* **1999**, *16*, 1537-1538; Wang, Q. C.; Ma, X.; Qu, D. H.; Tian, H. *Chem. Eur. J.* **2006**, *12*, 1088-1096.

[26] Oshikiri, T.; Takashima, Y.; Yamaguchi, H.; Harada, A. *J. Am. Chem. Soc.* **2005**, *127 (35)*, 12186-12187.

Also, it is possible to take advantage of the kinetic stabilities of the different orientational isomers formed. This strategy was tackled by Park and coworkers,[27] who showed that a non-symmetric viologen-based axle could slip indifferently into a cyclodextrin from both rims, but the dethreading rate of one orientational isomer was higher. This led to the exclusive formation of the thermodynamically stable isomer after long time equilibration (see **Figure 1.11b**).

Nevertheless, it is possible to differentiate the functionalization of the two rims of the receptor, in order to pivot the interaction with a guest in a controlled geometry through multipoint interactions.[28] As an example, Methyl Orange (MO) has been used as probe to explore the influence of different substituents on the cyclodextrin skeleton on the guest insertion mode.[29] The MO is oriented in a single arrangement inside the *β*-CD cavity (with the dimethylamino group localized towards the secondary side), but this orientation is completely reversed when MO interacts with the anionic sodium *heptakis*[6-deoxy-6-(3-thiopropionate)]-*β*-CD (see **Figure 1.12**):

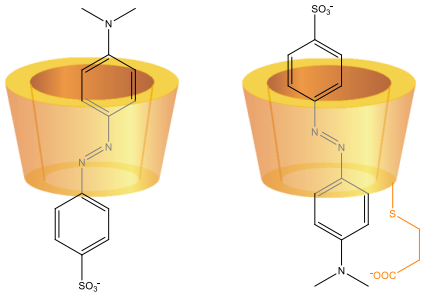

Figure 1.12 *Orientational pseudorotaxane isomers generated upon complexation of MO by cyclodextrins. In the first complex, the guest orients itself inside the cavity with its dipole moment anti-parallel to that of β-CD. The arrangement of the second compound can be easily explained if the repulsive electrostatic forces between the* $-SO_3^-$ *group (MO) and the* $-COO^-$ *(CD) are considered.*

[27] Park, J. W.; Song, H. J. *Org Lett.* **2004**, *6*, 4869-4872.

[28] Safont-Sempere, M. M.; Fernandez, G.; Würthner, F. *Chem. Rev.* **2011**, *111*, 5784-5814.

[29] Mourtzis, N.; Eliadou, K.; Yannakopoulou, K. *Supramol. Chem.* **2004**, *16 (8)*, 587-593.

1.4 Calix[6]arene-based molecular machines prototypes and working devices

Calix[n]arenes are a series of synthetic macrocycles that belong to the class of metacyclophanes, extensively employed in host-guest chemistry as versatile platforms for the synthesis of selective and efficient receptors for charged and neutral species.[30] These compounds are readily accessible in high yield from the base-catalyzed condensation of p-*tert*-butylphenol and formaldehyde,[31] and the size of the obtained macrocycle can be tuned by opportune modification of the reaction conditions. Within the calix[n]arene series, the calix[4]arene has been the most extensively studied, thanks to the possibility to gain easier control on its conformational equilibria and on its regio- and stereoselective functionalization.

Despite the higher conformational mobility of larger calix[5], calix[6] and calix[8]arenes, several synthetic procedures for the partial functionalization of their phenolic rims were established, in order to fix their partial-cone conformation and obtain suitable hosts[30].

Only in the last decade calix[6]arene has been exploited as host for the construction of mechanically interlocked molecules: in fact, it was discovered that an electron-poor guest having an axial symmetry and suitable chemical features can thread the calix[6]arene annulus to yield supramolecular complexes belonging to the classes of pseudorotaxanes, rotaxanes and catenanes.

The first example of a calix[6]arene-based pseudorotaxane was published by our research group in 2000, exploiting the tris(*N*-phenylureido)calix[6]arene derivative **1** as wheel. Calixarene **1** is a three-dimensional non-symmetric heteroditopic host that adopts, on the NMR timescale (see **Figure 1.13a**), a *pseudo-cone*-conformation, decorated with three *N*-phenylureido moieties in alternate position on the upper rim and with three alkyl substituents at the lower rim. It was shown that this receptor is able to take up *N,N'*-dioctylviologen diiodide (**DOV×2I**) in low polarity solvents,[32] giving rise to the pseudorotaxane-type complex **P[1⊃DOV]**, whose structure was investigated in solution through NMR techniques (**Figure 1.13b**).

[30] Gutsche, C. D. *Calixarene, An Introduction, Monographs in Supramolecular Chemistry*, Ed.: J. F. Stoddart, Royal Society of Chemistry, Cambridge, U. K., 2008; *Calixarenes in Action* (Eds. L. Mandolini, R. Ungaro), Imperial College Press, 2000.

[31] Gutsche, C.D.; Dhawan, B.; No, K. H.; Muthukrishnan, R. *J. Am. Chem. Soc.* **1981**, *103 (13)*, 3782-3792.

[32] Arduini, A.; Ferdani, R.; Pochini, A.;Secchi, A.; Ugozzoli, F. *Angew. Chem. Int. Ed.* **2000**, *39 (19)*, 3453-3456.

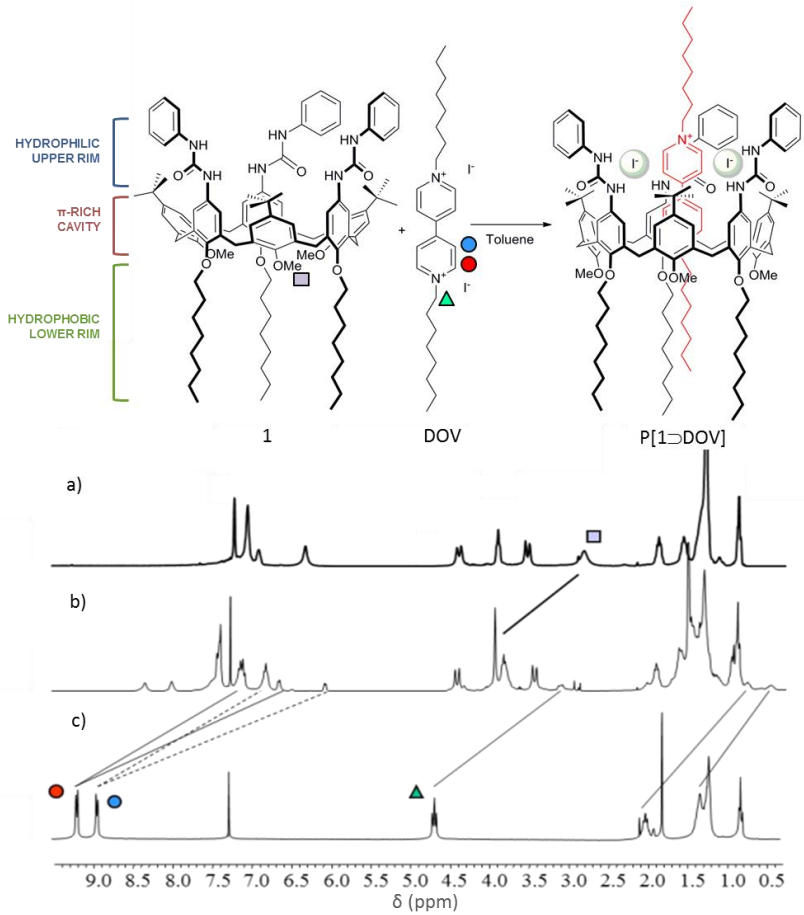

Figure 1.13 *^{1}H NMR spectra of: a) wheel **1** in C_6D_6; b) pseudorotaxane **P[1⊃DOV]** in C_6D_6; c) axle **DOV×2I** in CD_3CN. Adapted from ref. 32, copyright © Wiley-VCH.*

Significantly, upon the formation of the pseudorotaxane complex, the wheel component **1** retains its *pseudo-cone* conformation, as witnessed by the typical AX system of the two doublets at δ = 4.5 and 3.5 ppm (^2J = 15.6 Hz), related to the bridging methylene groups of the macrocycle. Nevertheless, the host undergoes a partial rearrangement as a consequence of the axle threading: the methoxy groups (that are no longer oriented towards the interior of the cavity as in the free receptor) resonate as a sharp singlet at 3.9 ppm, and the NH protons of the ureido groups, involved in hydrogen bonds with iodide anions, show a remarkable downfield shift in comparison with the spectrum of free **1**. The inclusion into the calixarene cavity also affects the chemical shift of several protons of the axial component, especially the methyne protons of the bipyridinium core and the methylene protons that are directly

linked to the positively charged nitrogens, which experience an upfield shift as a consequence of the shielding effect of the electron-rich cavity.

X-ray structure (**Figure 1.14**) obtained from a single crystal confirmed that, in the solid state, the pseudorotaxane complex is stabilized by a synergy of supramolecular interactions that involve all the domains of the calixarene[33]:

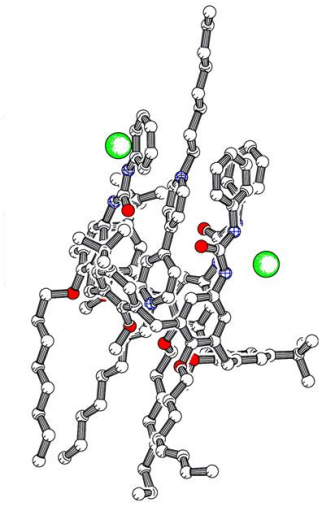

Figure 1.14 *X-ray structure of pseudorotaxane* ***P[1⊃DOV]****.*

In particular, the dicationic portion of the viologen threaded into the calixarene cavity is stabilized by a combination of CH-π and cation-π interactions. Also, a charge-transfer takes place between the electron-poor guest and the π-rich aromatic cavity of the host: this gives rise to a diagnostic red coloration of the pseudorotaxane complex, that is evidenced by the appearance of an absorption band centered at 470 nm in the UV-Vis spectra of these pseudorotaxane species. Moreover, the two anions of the guest can efficiently interact with the phenylureido moieties at the upper rim of the receptor *via* the formation of six highly energetic hydrogen bonds. All together, these combined interactions give rise to a remarkably high apparent association constant (K_a > 10^6 M^{-1}) in low polarity solvents.[34]

It was evidenced that tris(*N*-phenylureido)calix[6]arene-based pseudorotaxanes can be disassembled, for example, by moving from low polar to highly polar solvents: in this case the lack of hydrogen bonds destabilizes the interaction between the components and induces the axle's dethreading. Since the

[33] Ugozzoli, F.; Massera, C.; Arduini, A.; Pochini, A.; Secchi, A. *CrystEngComm.* **2004**, *6*, 227-232.

[34] Credi, A.; Dumas, S.; Silvi, S.; Venturi, M.; Arduini, A.; Pochini, A.; Secchi, A. *J. Org. Chem.* **2004**, *69*, 5881-5887.

bipyridinium core positioned into the axial component is a redox active unit, the rearrangement of these systems can also be triggered electrochemically. Cyclic Voltammetry measurements carried out in dichloromethane on a series of pseudorotaxanes solutions showed that a fast (sub-microsecond timescale) disassembly takes place upon the monoelectronic reduction of the axle's viologen core[34]:

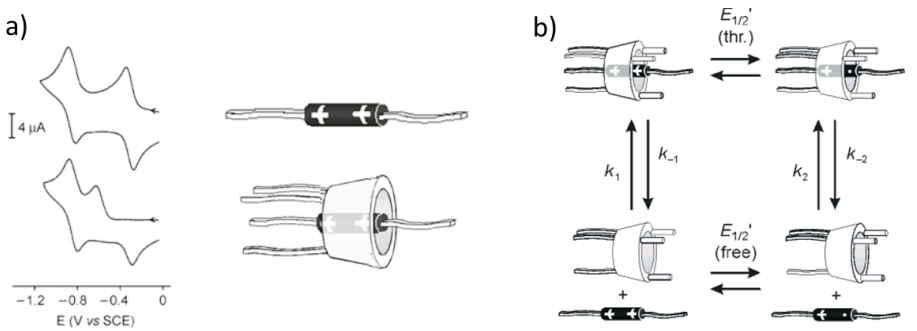

Figure 1.15 *a) Cyclic Voltammetry curves (CH_2Cl_2, 0.05 M tetrabutylammonium hexafluorophosphate, 298 K, scan rate = 0.2 V/s) for the first and second reduction of the 4,4'-bipyridinium unit in free* ***DOV*** *(top) and pseudorotaxane* ***P[1⊃DOV]*** *(bottom); b) Schematic mechanism for the one-electron reduction of* ***P[1⊃DOV]****. Partially adapted from ref. 34, copyright © American Chemical Society.*

As depicted in **Figure 1.15a**, on the pseudorotaxane system the first monoelectronic reduction takes place at a more negative potential value with respect to the free axle in solution. This is due to the stabilization of the viologen in its doubly charged form provided by the aromatic cavity of the calixarene. On the other hand, the potential for the second reduction is comparable for the free and complexed axle, thus meaning that the formed radical-cation dethreads from the wheel and undergoes the second reduction as a free species in solution.

To verify whether the chemical and structural information stored in the two distinct rims of the calixarene wheel play a role in the axle complexation process, we analyzed the outcome of the complexation between **1** and the stoppered viologen-based axle **2**. Indeed, it was evidenced that only the orientational pseudorotaxane isomer $\mathbf{P[1\supset 2]_{up}}$, in which the diphenylacetic stopper is directed towards the upper rim of **1**, was formed, indicating that the axle threading takes places exclusively from

the upper rim of the wheel[35] (see **Figure 1.16**). This behavior was explained considering that: i) in low polarity solvents, the three methoxy groups of the calix[6]arene occupy the cavity and therefore hamper the access of the axle from the lower rim; ii) in low polarity solvents, the axle is present as a tight ion pair. Since the calixarene cavity can host only the cationic portion of the guest, the separation of the bipyridinium core from its counteranions is mandatory. This is accomplished by the ureido groups at the upper rim of the receptor, that efficiently interact with the anions of the axle and pivot the threading process through the upper rim of the wheel.

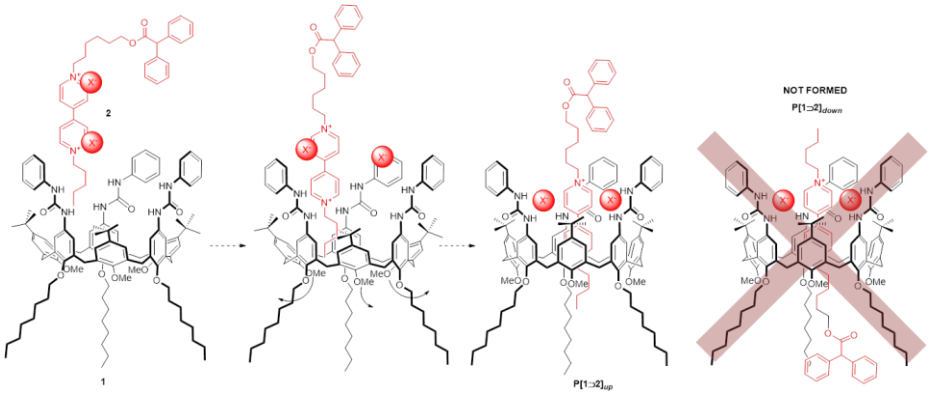

Figure 1.16 *Threading mechanism of a viologen-based stoppered axle in a tris(N-phenylureido)calix[6]arene wheel.*

More recently, it was also demonstrated that simple n-alkyl chains appended to the viologen core can act as kinetic control elements to govern the orientation of the threading of asymmetric axles, to selectively and spontaneously yield oriented pseudorotaxanes.[36] In particular, we have shown that, in low polarity solvents and at room temperature, non-symmetric axles in which the two linear alkyl chains differ in length for at least 7 carbon atoms, preferentially thread the phenylureido wheel **3** from its upper rim with their shorter alkyl chain. As an example, the threading of **C5C18** gives almost exclusively the orientational isomer indicated as **P**[**3**⊃**C5C18**]$_{short}$, and this only partially isomerizes to the corresponding *long* isomer (3:7 = *long* : *short*) after refluxing its toluene solution for 10 days.

35 Arduini, A.; Calzavacca, F.; Pochini, A.; Secchi, A. *Chem. Eur. J.* **2003**, *9 (3)*, 793-799.

36 Arduini, A.; Bussolati, R.; Credi, A.; Secchi, A.; Silvi, S.; Semeraro, M.; Venturi, M. *J. Am. Chem. Soc.* **2013**, *135 (26)*, 9924-9930.

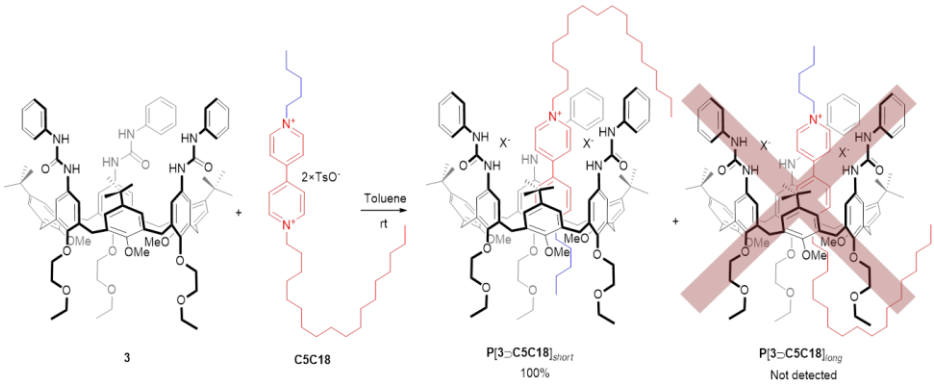

Figure 1.17 *Kinetic self-sorting leads to the selective formation of one out of two possible pseudorotaxane orientational isomers.*

The possibility to gain full control on the threading of viologen salts into calix[6]arene wheels such as **1** and **3** allowed the synthesis of several oriented calix[6]arene-based interlocked structures.[37] For instance, taking advantage of the findings about reversibility and directional threading, the solvent- and light-controlled unidirectional transit of a non-symmetric axle through phenylureido calix[6]arene **3** was achieved[38] by playing around the structural properties of the functional groups anchored at the axle's viologen core.

The viologen-based axle **4** depicted in **Figure 1.18**, containing a photoisomerizable stilbene moiety at one end, was equilibrated with wheel **3** in low polarity media to yield the oriented pseudorotaxane **P[3⊃4]**. Stoppering reaction of this pseudorotaxane, performed at room temperature with diphenylacetylchloride, yielded the corresponding *semi*-rotaxane **R[3⊃4]**. The axle dethreading, induced by the addition of highly polar DMSO, can only occur through the slippage of the stilbene moiety from the lower rim of the wheel, that is in the same direction of the threading process.

[37] Arduini, A.; Ciesa, F.; Fragassi, M.; Pochini, A.; Secchi, A. *Angew. Chem. Int. Ed.* **2005**, *44 (2)*, 278-281; Arduini, A.; Bussolati, R.; Masseroni, D.; Royal, G.; Secchi, A. *Eur. J. Org. Chem.* **2012**, *5*, 1033-1038; Arduini, A.; Bussolati, R.; Credi, A.; Pochini, A.; Secchi, A.; Silvi, S.; Venturi, M. *Tetrahedron* **2008**, *64,* 8279-8286;

[38] Arduini, A.; Bussolati, R.; Credi, A.; Monaco, S.; Secchi, A.; Silvi, S.; Venturi, M. *Chem. Eur. J.* **2012**, *18 (50)*, 16203-16213.

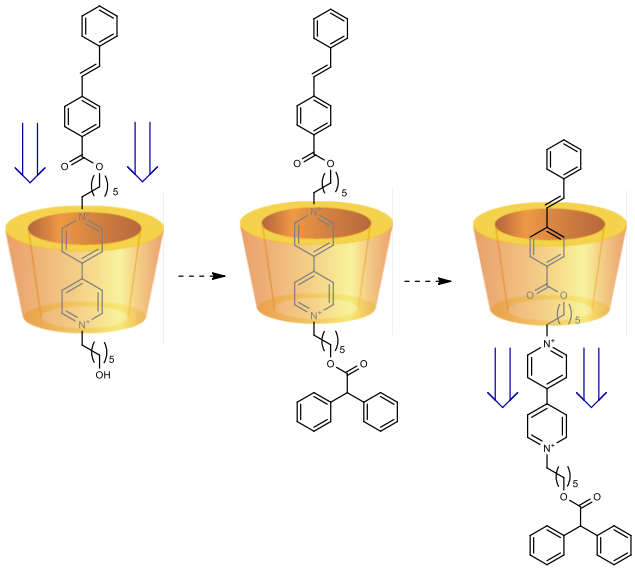

Figure 1.18 *Axle threading through the upper rim of the wheel in low polar solvent, stoppering reaction and axle dethreading induced by polar solvent.*

In this research field, interesting results were reported by the group of Neri and coworkers, who described a general procedure to obtain pseudorotaxanes by employing simple alkoxy calix[6]arene derivatives as wheels and dialkylammonium cations paired to the weekly coordinating tetrakis[3,5-bis(trifluoromethyl)phenyl]borate anion in apolar media.[39] By studying the threading process of the macrocycles toward non-symmetric alkylbenzylammonium guests, the formation of two stereomeric directional pseudorotaxanes was evidenced, in which the *endo*-alkyl and *endo*-benzyl ratios could be varied by changing the length of the axle alkyl chain. It was again evidenced that the structural information present on the axle, together with those on the calixarene wheel (i.e. the bulkiness of the groups at the upper and lower rim), could be exploited to govern the formation of oriented assemblies with a programmable relative orientation of the components.[40]

[39] Talotta, C.; Gaeta, C.; Qi, Z.; Schalley, C. A.; Neri, P. *Angew. Chem. Int. Ed.* **2013**, *52 (29)*, 7437-7441; Gaeta, C.; Talotta, C.; Neri, P. *Chem.Commun.* **2014**, *50*, 9917-9920.

[40] Ciao, R.; Talotta, C.; Gaeta, C.; Margarucci, L.; Casapullo, A.; Neri, P. *Org. Lett.* **2013**, *15 (22)*, 5694-5697; Gaeta, C.; Troisi, F.; Neri, P. *Org. Lett.* **2010**, *12 (9)*, 2092-2095.

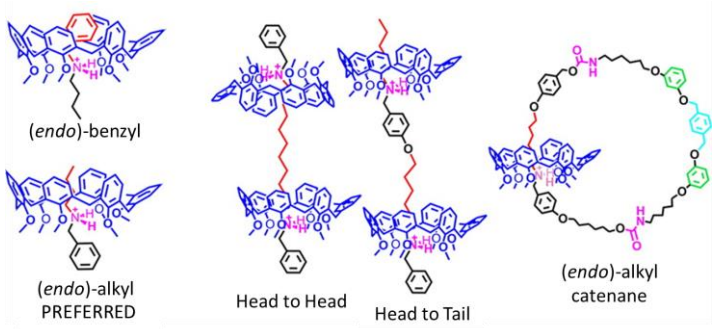

Figure 1.19 *Examples of oriented calix[6]arene-based architectures obtained by exploiting the "endo-alkyl" rule. Modified from ref. 40, copyright © American Chemical Society.*

The potential of these systems to act as molecular level machines was demonstrated by studying the shuttling modes of the corresponding rotaxanes illustrated in **Figure 1.20**.[41] NMR analysis confirmed that, in the positively charged rotaxanes, the n-hexyloxycalix[6]arene encircles the ammonium station; upon deprotonation and generation of the neutral rotaxane, the wheel can shuttle along the two alkyl chains of the dumbbell yielding two translational isomers. Acidic treatment of the neutral rotaxanes restores the original situation.

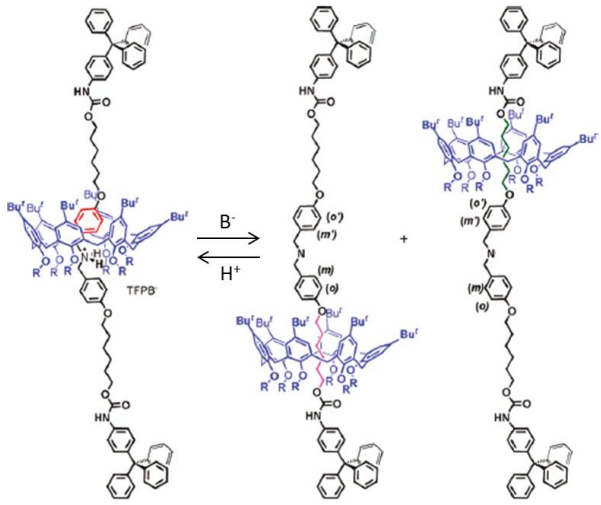

Figure 1.20 *The shuttling behavior of the described rotaxane. Adapted from ref. 41, copyright © American Chemical Society.*

[41] Pierro, T.; Gaeta, C.; Talotta, C.; Casapullo, A.; Neri, P. *Org. Lett.* **2011**, *13 (10)*, 2650-2653.

1.5 Future perspectives

The findings reported in this last part of the chapter evidence the possibility to build calix[6]arene-based interlocked responsive systems, in which the relative orientation of the components can be controlled and whose dynamic properties can be governed through opportune external stimulation. To this state of the art, an appealing development would lie in the transduction of the inherent non-symmetric features of these oriented assemblies into a directionally controlled motion of the components, in order to obtain unidirectional linear and rotary motors. Our recent achievements in this research area are described in this thesis.

CHAPTER 2

WHEEL DIRECTED SUPRAMOLECULARLY-ASSISTED SYNTHESIS OF CALIX[6]ARENE-BASED ORIENTED PSEUDOROTAXANES AND ROTAXANES

2.1 Introduction

As a consequence of Coulombic interactions of a host with its guest, the latter can sustain a modification of its chemical features up to a change of its reactivity. Since the downing of supramolecular chemistry, this has stimulated the ingenuity of scientists to emulate the function of enzymes by manipulating, through synthetic hosts or cages, the energetics and selectivity of reactions through programmed host-guest interactions or confinement.

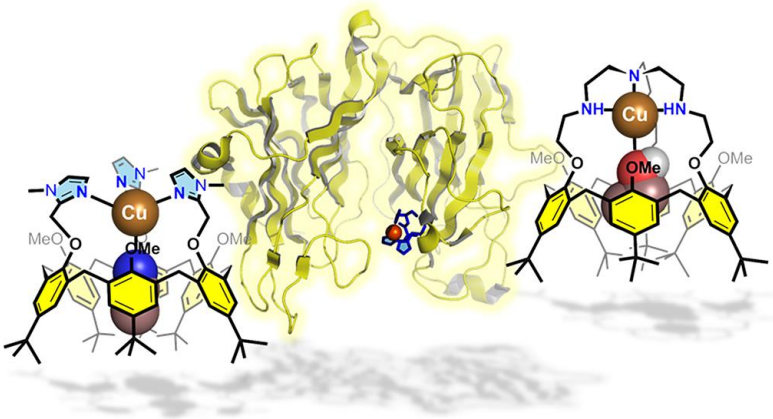

Figure 2.1 *Calix tris(imidazole) funnel complex and calix[6]tren receptor were exploited to mimic the first and second coordination sphere of mono-copper sites of different enzymes. Reproduced from ref. 10, copyright © American Chemical Society.*

As an arbitrary selection of examples, Fujita et al. exploited coordination cages to promote the cavity-directed synthesis of labile silanol oligomers,[1] and for the [2+2]phodimerization of olefins.[2] Using others self-assembled coordination cages, Raymond et al. have successfully catalyzed aza-Cope rearrangements of ammonium substrates.[3] Encapsulation processes in deep resorcinarene-based cavitands have been used by Rebek and co-workers to stabilize a Meisenheimer complex in S_NAr reactions,[4] and for the activation of dienophiles in Dies-Alder reactions.[5] A similar strategy was pursued by the same authors using pseudospherical capsules.[6] Dougherty et al.

[1] Yoshizawa, M.; Kusukawa, T.; Fujita, M.; Sakamoto, S.; Yamaguchi, K. *J. Am. Chem. Soc.* **2001**, *123 (43)*, 10454-10459.

[2] Yoshizawa, M.; Takeyama, Y.; Kusukawa, T.; Fujita, M. *Angew. Chem. Int. Ed.* **2002**, *41 (8)*, 1347-1349.

[3] Fiedler, D.; Bergman, R. G.; Raymond, K. N. *Angew. Chem. Int. Ed.* **2004**, *43 (48)*, 6748-6751.

[4] Butterfield, S. M.; Rebek Jr., J. *Chem. Commun.* **2007**, *16*, 1605-1607.

[5] Hooley, R. J.; Rebek Jr., J. *Org. Biomol. Chem.* **2007**, *5 (22)*, 3631-3636.

[6] Kang, J.; Hilmersson, G.; Santamaría, J.; Rebek, J. *J. Am. Chem. Soc.* **1998**, *120 (15)*, 3650-3656.

exploited a series of cyclophanes derivatives to activate the alkylation of quinolines and delakylation of sulfonium salts.[7] A good example of biomimetic chemistry comes from Breslow et al. who mimicked the catalytic behavior of cytochrome P-450 enzymes by using artificial analogues obtained by linking a porphyrin core with four β-cyclodextrin units.[8] Within this context, calix[4]arenes, because of their π-rich concave aromatic cavity and the possibility to insert and orient in space functional groups and binding sites, have been used as supramolecular catalysts.[9] The larger calix[6]arene platform was used by Reinaud et al. as a tool to mimic the coordination sphere of enzymes active sites[10] (**Figure 2.1**).

In this chapter, we investigated how the engulfment of a positively charged pyridinium-based guest inside the π-rich cavity of tris-(*N*-phenylureido) calix[6]arene host **1** affects its reactivity towards a S_N2 reaction, and we exploited this new supramolecularly assisted approach to achieve the formation of oriented rotaxanes.

2.2 Formation and reactivity of Host-Guest complexes between tris(*N*-phenylureido)calix[6]arene and pyridyl-pyridinium salts: state of the art

Initially, the 1-octadecy-[4,4' bipyridin]-1-ium **2** was selected as suitable guest to study the ability of the calix[6]arene **1** to form inclusion complexes with piridyl-piridinium salts (see **Scheme 2.1**). The occurrence of the complexation between **1** and **2** was first hypothesized by the naked-eye observation that, at room temperature, the non-colored suspension of **2** in weakly polar solvent became immediately homogeneous and orangish when treated with **1**. The NMR spectra of this mixture suggested the presence of several species in solution: the free and complexed wheel, the latter in the form of the two possible orientational pseudorotaxane isomers $\mathbf{P}[\mathbf{1}\supset\mathbf{2}]_{up}$ and $\mathbf{P}[\mathbf{1}\supset\mathbf{2}]_{down}$. The energetic for the formation of $\mathbf{P}[\mathbf{1}\supset\mathbf{2}]$ was investigated through UV/Vis measurements in toluene at T = 333 K, and an apparent binding constant $K = 8.1\times10^4$ M^{-1} was measured.

[7] McCurdy, A.; Jimenez, L.; Stauffer, D. A.; Dougherty, D. A. *J. Am. Chem. Soc.* **1992**, *114 (26)*, 10314-10321.

[8] Breslow, R.; Yang, J.; Yan, J. *Tetrahedron* **2002**, *58 (4)*, 653-659.

[9] Molenveld, P.; Engbersen, J. F. J.; Kooijman, H.; Spek, A. L.; Reinhoudt, D. N. *J. Am. Chem. Soc.* **1998**, *120 (27)*, 6726-6737. Cacciapaglia, R.; Casnati, A.; Mandolini, L.; Reinhoudt, D. N.; Salvio, R.; Sartori, A.; Ungaro, R. *J. Am. Chem. Soc.* **2006**, *128 (37)*, 12322-12330; Salvio, R.; Volpi, S.; Cacciapaglia, R.; Sansone, F.; Mandolini, L.; Casnati, A. *J. Org. Chem.* **2016**, *81 (11)*, 4728-4735.

[10] Le Poul, N.; Douziech, B.; Zeitouny, J.; Thiabaud, G.; Colas, H.; Conan, F.; Cosquer, N.; Jabin, I.; Lagrost, C.; Hapiot, P.; Reinaud, O.; Le Mest, Y. *J. Am. Chem. Soc.* **2009**, *131 (49)*, 17800-17807; Le Poul, N.; Le Mest, Y.; Jabin, I.; Reinaud, O. *Acc. Chem. Res.* **2015**, *48 (7)*, 2097-2106.

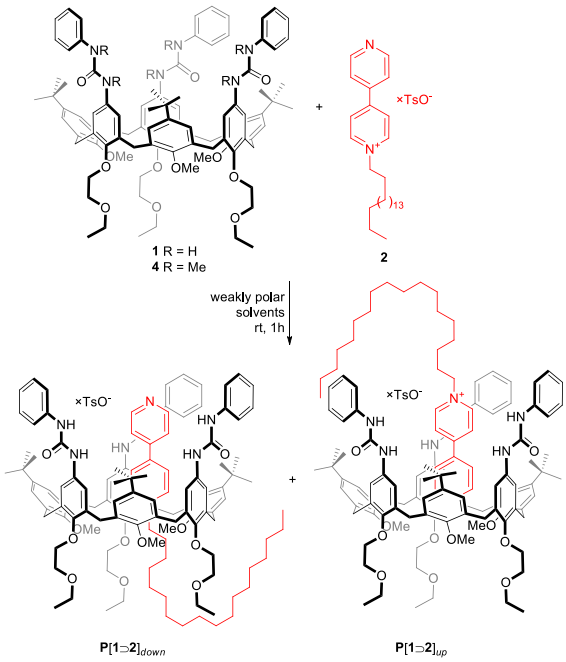

Scheme 2.1 *Orientational pseudorotaxane isomers originating when wheel **1** complexes pyridyl-pyridinium based axle **2**.*

Inspired by the studies of Rebek and co-workers, who demonstrated the reaction rate enhancement toward the Menschutkin reaction of quinuclidine engulfed in a cavitand[11], we hypothesized that in our calix[6]arene-based pseudorotaxane complex **P**[**1**⊃**2**], the engulfment of the positively charged pyridyl-pyridinium guest inside the π-rich cavity could result in an increase of the nucleophilicity of its neutral nitrogen atom towards a S_N2 reaction. To verify such hypothesis, **2** was reacted, in presence of an equimolar amount of **1**, with a series of pentyl derivatives *n*-$C_5H_{11}X$ (**3a-d**; with X = TsO, I, Br and Cl) to yield *N*-pentyl-*N'*-octadecyl viologen salt **C5C18** (see **Scheme 2.2**). The supramolecularly-assisted alkylation of **2** (experiment *A*) was carried out in toluene at *T* = 333 K. The formation of **C5C18** was directly monitored through UV/Vis measurements: indeed, such viologen salt gives rise with **1** to stable oriented pseudorotaxane isomers **P**[**1**⊃**C5C18**]$_{long}$ and **P**[**1**⊃**C5C18**]$_{short}$, which exhibit the typical charge transfer band at λ = 470 nm, regardless the orientation of the axle inside the aromatic cavity.

[11] Purse, B. W.; Gissot, A.; Rebek Jr., J. *J. Am. Chem. Soc.* **2005**, *127 (32)*, 11222-11223.

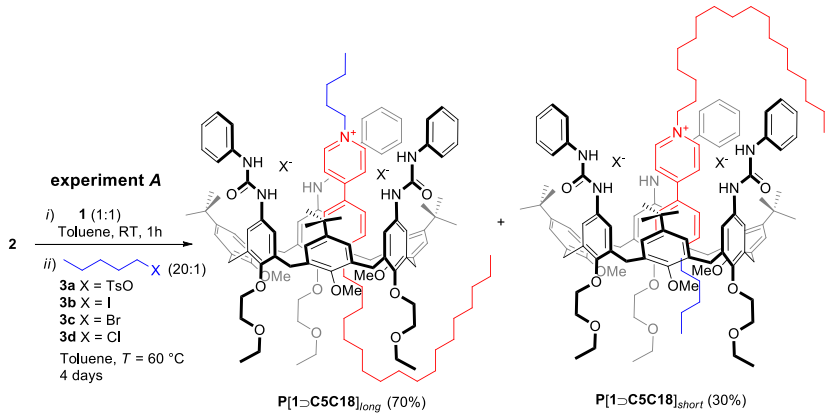

Scheme 2.2 *Supramolecularly-assisted alkylation (experiment A).*

The kinetics of the alkylation reactions were in agreement with a S_N2 reaction mechanism and yielded the kinetic constants gathered in **Table 2.1**. As expected, the tosylate **3a** gave the highest reaction rate, and in general the results obtained for the entire series reflected the ability of the leaving groups (TsO > I > Br > Cl) present in the alkylating agent **3**.

Compound (n-$C_5H_{11}X$)	k (M^{-1} s^{-1})	Relative S_N2 rate
3a (X = TsO)	1.4×10^{-4}	26
3b (X = I)	6.6×10^{-5}	12
3c (X = Br)	1.6×10^{-5}	3
3d (X = Cl)	5.4×10^{-6}	1

Table 2.1 *Kinetic measurements relative to experiment A.*

When a blank experiment (*B,* see **Scheme 2.3**) was carried out employing **3a** as alkylating agent, in the same experimental conditions but in absence of **1**, a kinetic constant of 8.6×10^{-6} M^{-1} s^{-1} was calculated. The comparison of this value with those calculated in experiment *A* evidenced an increment by 16 times of the reaction rate when the alkylation reaction of **2** with **3a** was performed in the presence of **1**.

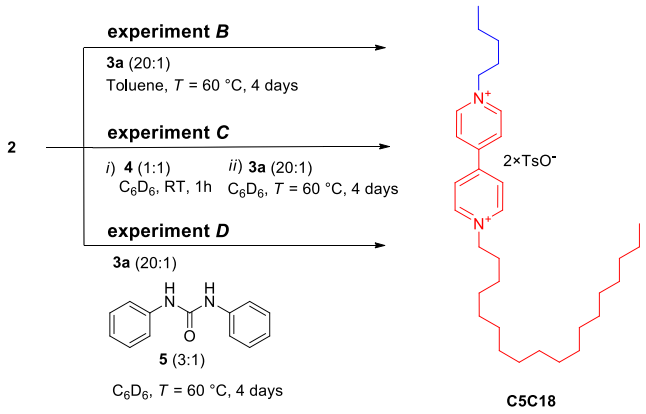

Scheme 2.3 *Blank alkylation experiment B and control alkylation experiments C and D.*

The rate enhancement measured in the supramolecularly-assisted reaction was reasonably ascribed to the following factors: *i*) the engulfment of **2** in the cavity of **1** may strongly enhance the nucleophilicity of its neutral nitrogen thanks to the charge delocalization induced by the electron-rich cavity of the macrocycle (*cavity effect*); and *ii*) the phenylurea groups at the upper rim of **1** might accelerate the alkylation reaction of **2** by binding the tosylate leaving group at the transition state level (*phenylurea effect*).

To investigate the *cavity effect*, the model reaction was accomplished in presence of the calix[6]arene derivative **4** (experiment *C* in **Scheme 2.3**), that, being fully *N*-methylated at its urea groups, is unable to coordinate the tosylate leaving group. After 4 days of stirring at 333K, only a negligible amount of **C5C18** was detected in the reaction mixture. The non-activity of **4** was justified considering that such calix[6]arene derivative is not even able to complex **2**, as verified in a separate ^{1}H NMR experiment.

Experiment *D* (see **Scheme 2.3**) was instead devised to disclose a possible *phenylurea effect*: as the in the model experiment, **2** was reacted with **3a** in presence of 3 equivalents of 1,3-diphenylurea **5**, that would simulate the role of the three *N*-phenylurea units present at the upper rim of **1**. After four days, no traces of **C5C18** salt were found in the reaction mixture.

Overall, experiments *A-D* demonstrated that only the simultaneous presence of the electron-rich cavity and the phenylureido groups at the upper rim of **1** promotes the formation of pseudorotaxane **P**[**1**⊃**2**] and, most important, does accelerate the S_N2 reaction to yield **P**[**1**⊃**C5C18**].

A deep NMR investigation on the orientational outcome of experiment *A* showed that the assistance of **1** also affects the distribution of the resulting possible

orientational pseudorotaxane isomers **P**[**1**⊃**C5C18**]$_{long}$ and **P**[**1**⊃**C5C18**]$_{short}$. As discussed in **Chapter 1**, it is known that non-symmetric axles such as **C5C18** preferentially thread the wheel from its upper rim with their short alkyl chain (in low polarity solvents and at RT), for kinetic reasons. Only a partial isomerization (3:7 = *long* : *short*) is observed after refluxing the pseudorotaxane solution for 10 days. Interestingly, the supramolecularly assisted experiment *A* evidenced the preferential formation of the kinetically non-favored orientational isomer **P**[**1**⊃**C5C18**]$_{long}$ (7:3 = *long* : *short,* **Figure 2.2**).

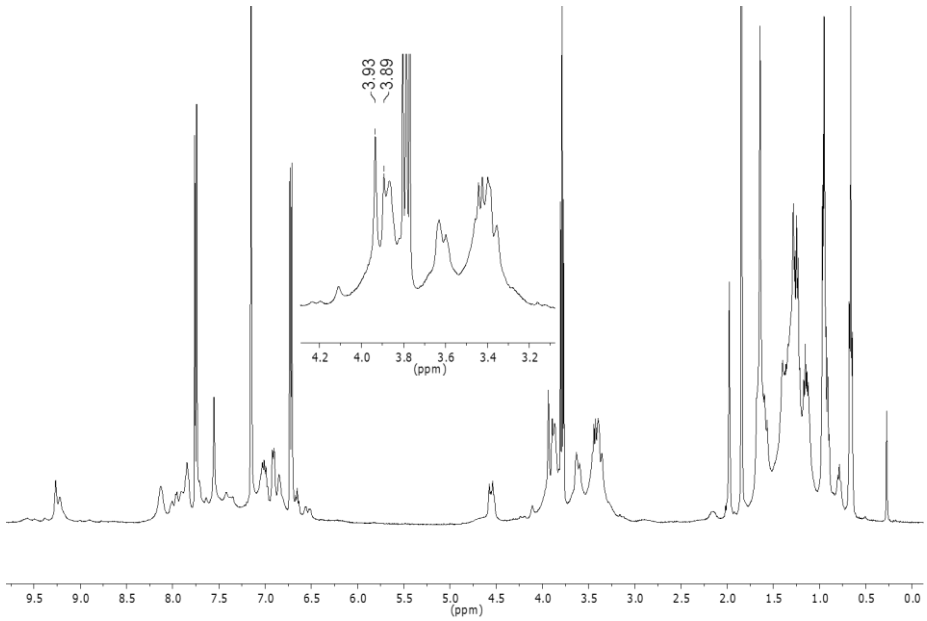

Figure 2.2 *^{1}H NMR spectrum (C_6D_6, 400 MHz) of the outcome of supramolecularly-assisted experiment A. The inset highlights the two singlets amenable to the two orientational pseudorotaxane isomers* ***P[1⊃C5C18]***$_{long}$ *and* ***P[1⊃C5C18]***$_{short}$*, at 3.93 and 3.89 ppm respectively.*

To explain such opposite isomers distribution, we hypothesized that, among the two possible orientational pseudorotaxane isomers **P**[**1**⊃**2**]$_{up}$ and **P**[**1**⊃**2**]$_{down}$ formed upon complexation between **1** and **2**, the latter exhibits a higher reactivity towards the S_N2 alkylation reaction. As a matter of fact, in **P**[**1**⊃**2**]$_{down}$ the deeper engulfment of the positive charge into the electron rich cavity of **1** may result in an increased stabilization, and consequently in an enhanced nucleophilicity with respect to **P**[**1**⊃**2**]$_{up}$. Moreover, in the **P**[**1**⊃**2**]$_{down}$ isomer, the free nitrogen atom of the pyridyl-pyridinium guest **2** is exposed to the bulk and therefore it is more easily attainable,

while in the opposite *up* isomer, the access to the non-alkylated nitrogen is hampered by the presence of the methoxy groups of **1**. In the alkylation reaction of **P**[**1**⊃**2**]$_{down}$, the proximity of the urea groups of **1** could also play a more significant role by binding the leaving group of the alkylating agent **3**, when a highly coordinating anion such as tosylate is employed as leaving group. The presence in the mixture of the "kinetic" isomer **P**[**1**⊃**C5C18**]$_{short}$ can be mainly ascribed to the spontaneous scrambling of the axle **C5C18** inside **1**, that occurs upon heating the toluene solution. To a lesser extent, a possible alkylation of the uncomplexed salt **2** cannot be neglected, after which the resulting axle **C5C18** might thread **1** yielding, in preferential way, the kinetically favored pseudorotaxane isomer **P**[**1**⊃**C5C18**]$_{short}$.

2.3 Supramolecularly assisted synthesis of oriented calix[6]arene-based rotaxanes

To boost the effect of the supramolecular assistance of **1** on the orientational isomers distribution, we attempted to reduce the axle scrambling by placing a bulky substituent on the ending of **2** in order to hamper the rearrangement of the resulting viologen axle into the wheel. Therefore, we carried out a new supramolecularly-assisted alkylation experiment using the stoppered pyridyl-pyridinium salt **6** as the substrate (**Scheme 2.4**):

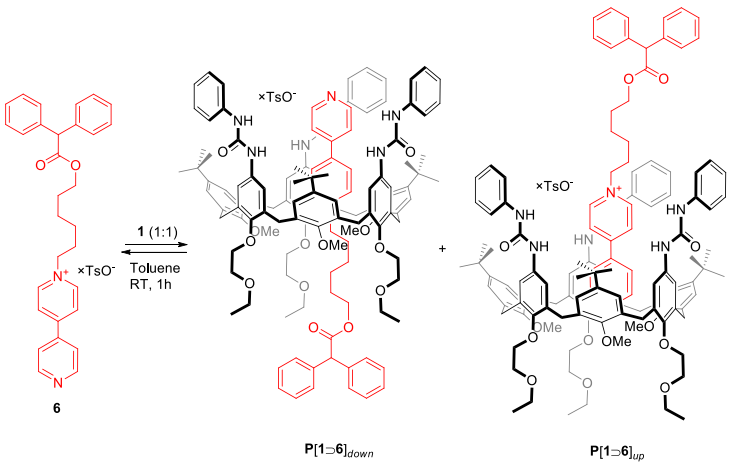

Scheme 2.4 *Orientational pseudorotaxane isomers originating when wheel **1** complexes stoppered pyridyl-pyridinium based axle **6**.*

Also in this case, the self-assembly of a pseudorotaxane complex **P**[**1**⊃**6**] was established by the complete dissolution of **6** and the formation of an orangish

homogeneous solution. As usual, the outcome of this complexation reaction was analyzed by NMR techniques, and the ^{1}H NMR spectrum of this mixture recorded at room temperature showed very broad signals in all low-polar deuterated solvents tested (see **Figure 2.3b** for the spectrum in toluene-d_8). Even raising or lowering the sampling temperature in toluene-d_8 did not appreciably improve the signals resolution (see **Figure 2.3a** and **c**).

2D NMR measurements (COSY and HSQC), carried out at T = 253 K, evidenced the simultaneous presence in the reaction mixtures of different species that could not be univocally identified. Nevertheless, the presence of multiple signals for the methoxy protons at the lower rim of **1**, as well as the presence in the spectrum of at least three resonances at ca. 5 ppm for the methyne proton of the stoppering diphenylacetic group of **6**, could be reasonably ascribed to a mixture of the two possible orientational pseudorotaxane isomers **P**[**1**⊃**6**]$_{down}$ and **P**[**1**⊃**6**]$_{up}$, and to the free salt **6** in equilibrium among them.

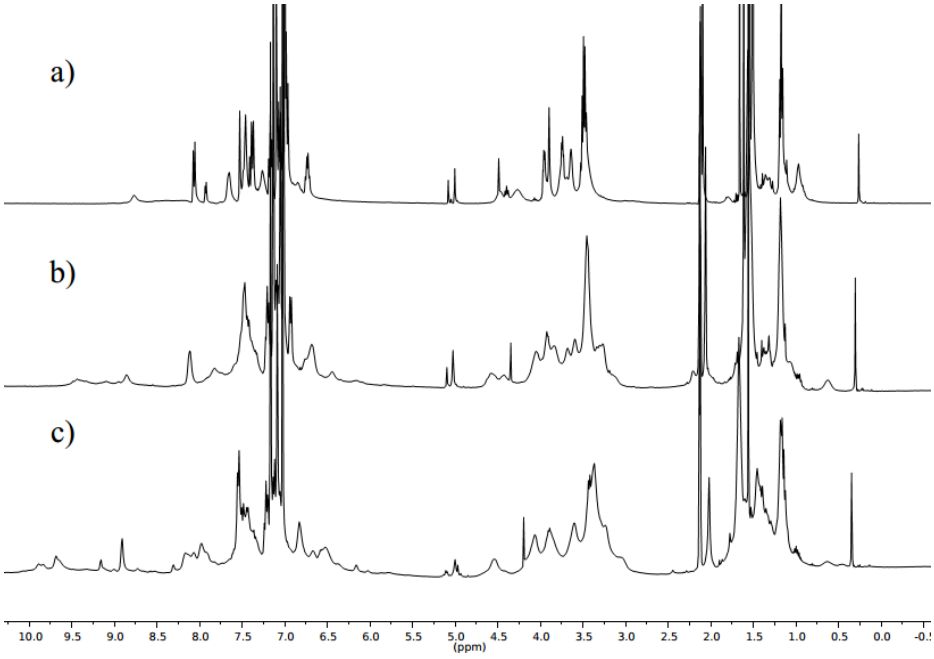

Figure 2.3 *^{1}H NMR spectra (400 MHz, toluene-d8) of **P[1⊃6]** at a) 353 K, b) 295 K and c) 253 K.*

Since the relative amount of these species in solution was difficult to determine, and considering also the results of the supramolecularly-assisted alkylation reaction *A*, we tried to exploit the previously hypothesized higher reactivity of the

down pseudorotaxane isomer to selectively obtain the corresponding oriented rotaxane derivative **R**[**C12C6**]. The reaction mixture was hence reacted with an excess of 12-hydroxydodecyl tosylate **7** in refluxing toluene for 4 days, to achieve the formation of the two possible orientational pseudorotaxane isomers **P**[**1**⊃**8**]$_{up}$ and **P**[**1**⊃**8**]$_{down}$. These latter were neither isolated nor characterized, but directly reacted with diphenylacetyl chloride at room temperature to promote the corresponding rotaxanes formation (see **Scheme 2.5**).

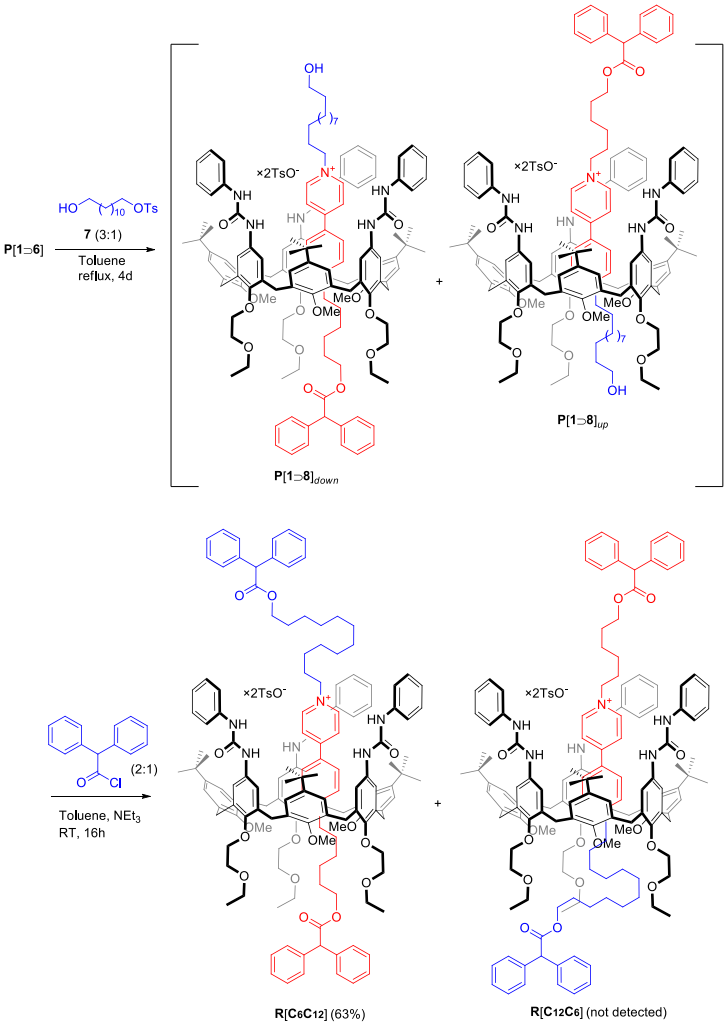

Scheme 2.5 *Supramolecularly-assisted synthesis of oriented rotaxane **R[C12C6]**.*

It is important to underline that, as seen in our previous work, this kind of stoppering reaction, when performed at room temperature, does not cause any isomerization process. Successfully, only the rotaxane isomer **R**[**C12C6**], having the short C6 alkyl chain orientated at the calix[6]arene lower rim, was isolated in good yield after chromatographic separation (63%). No traces of the opposite orientational isomer **R**[**C6C12**] were found in the mixture.

The ^{1}H NMR characterization in benzene-d_6 of the isolated rotaxane **R**[**C12C6**] (see **Figure 2.4a**) was facilitated by the comparison with known symmetric rotaxanes **R**[**C6C6**] and **R**[**C12C12**], having C6 and C12 alkyl spacers between the bis-pyridium core and the stoppers, respectively.[12] The presence of a sharp singlet at δ = 3.88 ppm for the wheel methoxy groups, and only one triplet for each *1'* and *1* methylene groups, at δ = 4.32 and 4.04 ppm respectively, together with the assignment of several diagnostic cross-peaks in the corresponding 2D NMR spectra, unequivocally confirmed the hypothesized geometry of the axial component of **R**[**C12C6**] inside the aromatic cavity of **1**.

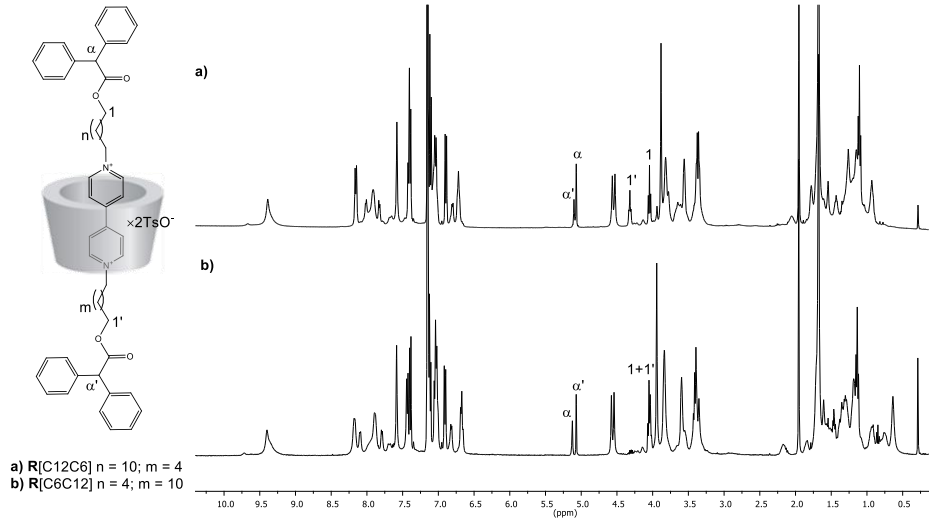

Figure 2.4 *Stack plot of the ^{1}H NMR spectra (C_6D_6, 400 MHz) of rotaxanes: a) **R[C12C6]** and b) **R[C6C12]** (see drawing for proton labelling of the axles).*

This remarkable result indirectly confirms that the reaction between **6** and the alkylating agent **7** must quantitatively take place inside the cavity of **1**. In fact, if we hypothesized a possible alkylation reaction of free **6** outside the calix[6]arene cavity, we would have obtained axle **8** that, as demonstrated in previous works, would have threaded wheel **1** selectively from the upper rim generating, after the stoppering

[12] Arduini, A.; Bussolati, R.; Credi, A.; Pochini, A.; Secchi, A.; Silvi, S.; Venturi, M. *Tetrahedron* **2008**, *64 (36)*, 8279-8286.

reaction, the orientational rotaxane isomer **R**[**C6C12**]. Nonetheless, the outcome of the reaction also illustrates that the supramolecularly-assisted alkylation selectively takes place only on the orientational pseudorotaxane isomer **P**[**1**⊃**6**]$_{down}$ (see **Scheme 2.4**), because if it had occurred on the opposite isomer, **P**[**1**⊃**6**]$_{up}$, after the stoppering reaction we would have obtained again **R**[**C6C12**]. We want also to point out that after the formation of pseudorotaxane **P**[**1**⊃**8**]$_{down}$, no scrambling must take places, because if this was the case, we would have obtained a partial isomerization to **P**[**1**⊃**8**]$_{up}$, that would have led to not detected rotaxane **R**[**C6C12**].

Staring from these results, we envisaged the possibility to synthesize, through this straightforward procedure, rotaxanes bearing the longer alkyl chain oriented toward the calixarene lower rim such as **R**[**C6C12**], that could not be obtained through the kinetically-driven complexation process. According to the protocol followed for **R**[**C12C6**], we carried out a further supramolecularly assisted reaction exploiting salt **9** (see **Scheme 2.6**), that is characterized by a C12 alkyl chain:

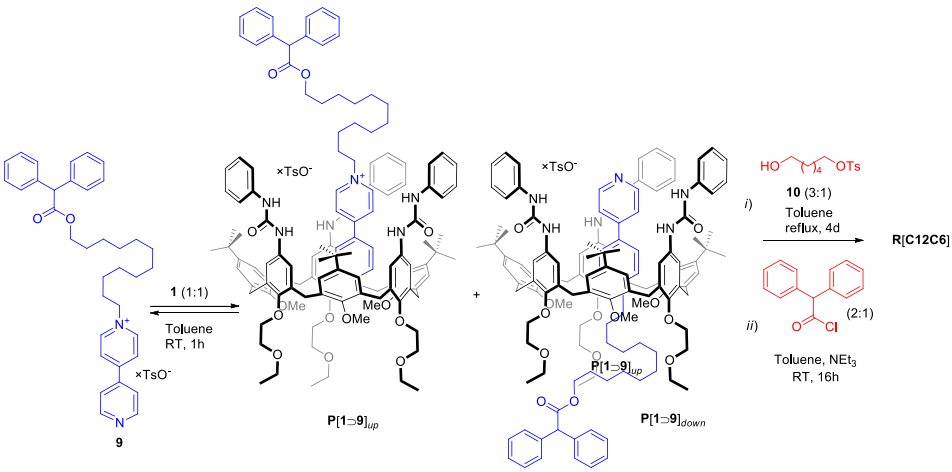

Scheme 2.6 *Supramolecularly-assisted synthesis of oriented rotaxane **R[C6C12]**.*

This salt was first equilibrated with **1** in toluene at room temperature and then refluxed with 6-hydroxyhexyl tosylate **10** for 4 days. After the usual stoppering reaction with diphenylacetylchloride at room temperature, the desired rotaxane **R**[**C12C6**] was isolated in 68% yield after chromatographic separation. NMR analysis in benzene-d_6 (see **Figure 2.4b**) confirmed the exclusive formation of this orientational isomer **R**[**C6C12**]. In particular, the presence of a sharp singlet at δ = 3.94 ppm for the wheel methoxy groups is in agreement with the presence of a C12 alkyl chain in proximity to the lower rim of the calixarene cavity. The chemical shift of the multiplet assigned to the *1* and *1'* methylene groups (4.4 ppm) and the two singlets at 5.12 ppm

and 5.07 ppm relative to the *α* and *α*' methyne protons of the diphenylacetic stoppers confirmed the univocal arrangement of the axle into the macrocycle. Furthermore, several diagnostic cross-peaks in the corresponding 2D NMR spectra were assigned. Also in this case, no traces of the opposite orientational isomer **R**[**C12C6**] were evidenced, thus confirming that this supramolecularly assisted procedure can be easily extended to different pyridyl-pyridinium salts maintaining a predictable and quantitative selectivity on the resulting rotaxane orientation, regardless the length of the alkyl chain appended to the axle.

2.4 Conclusions

In this study, we demonstrated that the tris(*N*-phenylureido) calixarene **1** is able to form stable host-guest complexes with pyridyl-pyridinium salts such as **2**, **6** and **9** in low polarity solvents. Such stabilized substrates can undergo S_N2 alkylation reaction, and the engulfment of the salts into the cavity of **1** results in an enhancement of their nucleofilicity, that leads to an increase up to 16 times of the alkylation reaction rate. This effect was ascribed both to the stabilization of the positively charged pyridine ring, provided by the electron-rich calixarene cavity, and to the presence of the urea moieties at the upper rim of **1**, which are able to bind the anionic leaving group of the alkylating agent. Moreover, we proved that it is possible to achieve a full orientational selectivity in the formed oriented rotaxanes by exploiting the presence of a bulky substituent on the pyridyl-pyridinium salt. In fact, we have shown that upon equilibration between **1** and the stoppered pyridyl-pyridinium salt **6**, both orientational pseudorotaxane isomers **P**[**1**⊃**6**]$_{down}$ and **P**[**1**⊃**6**]$_{up}$ are formed, but only the first one exhibits higher reactivity towards the following alkylation reaction.

The higher reactivity of **P**[**1**⊃**6**]$_{down}$ was justified as follows: a) in this orientational isomer, the positive charge is more deeply engulfed into the electron rich cavity of **1**, and this results in an increased stabilization and an enhanced nucleophilicity; b) the free nitrogen atom of **P**[**1**⊃**6**]$_{down}$ is exposed to the bulk and therefore more easily attainable; c) the proximity of the urea groups of **1** accelerates the reaction by binding the coordinating leaving group of the alkylating agent; and d) in the opposite orientational isomer **P**[**1**⊃**6**]$_{up}$, the access to the non-alkylated nitrogen of **6** is hampered by the presence of the methoxy groups of **1**. This supramolecularly-assisted strategy was proven to be effective also for the synthesis of kinetically unfavored orientational rotaxane isomers bearing the longer alkyl chain directed towards the lower rim of **1**, that could not be obtained through the self-sorting strategy so far employed using pre-formed viologen-based axles. Finally, it is

interesting to remark that this new rotaxanation procedure allowed the formation of oriented rotaxanes as single orientational isomers in higher yields and shorter reaction times compared to traditional sequential procedures, and these interesting results pave the way to the synthesis of more complex and univocally oriented structures.

2.5 Acknowledgments

Thanks to Dr. Guido Orlandini (University of Parma), Dr. Giulio Ragazzon, Prof. Alberto Credi, Prof. Serena Silvi and Prof. Margherita Venturi (University of Bologna).

2.6 Experimental section

Synthesis: All solvents were dried using standard procedures; products $\mathbf{3_{b\text{-}d}}$, **5** and all other reagents were of reagent grade quality obtained from commercial suppliers and were used without further purification. Chemical shifts are expressed in ppm (δ) using the residual solvent signal as internal reference (7.16 ppm for C_6H_6; 7.26 ppm for $CHCl_3$ and 3.31 for CH_3OH). Mass spectra were recorded in ESI mode. Products **1**,[13] **3a**,[14] **4**,[15] **6**,[16] **7**,[17] **10**,[18] **R[C6C6]** and **R[C12C12]**[12] were synthesised according to published procedures.

1-octadecy-[4,4' bipyridin]-1-ium (2): In a 100 ml round-bottomed flask octadecyl 4-methylbenzenesulfonate (1.0 g, 2.4 mmol) and 4,4'-dipyridyl (1.1 g, 7.1 mmol) were dissolved in CH_3CN (50ml) and the solution was refluxed for 24h. Then the solvent was evaporated at reduced pressure and the residue was triturated with EtOAc (3x20 mL) until the product precipitated as a solid compound and was recovered by suction filtration to afford 1.0 g of product **2** as a white solid (64%). ^{1}H NMR (400 MHz, $CDCl_3$ + MeOD): δ = 0.81 (t, ^{3}J(H,H)=7.2 Hz, 3 H, C*H*$_3$), 1.2–1.3 (m, 30 H, aliphatic C*H*$_2$), 1.96 (m, 2 H, N^+-CH_2C*H*$_2$), 2.28 (s, 3 H, Ar-C*H*$_3$), 4.63 (t, ^{3}J(H,H)=7.6 Hz, 2 H, N^+-C*H*$_2$), 7.10 (d, ^{3}J(H,H)=8.0 Hz, 2 H, Ar*H*), 7.65 (d, ^{3}J(H,H)=8.0 Hz, 2 H, Ar*H*), 7.99 (d, ^{3}J(H,H)=6.4 Hz, 2 H, Ar*H*), 8.40 (d, ^{3}J(H,H)=6.4 Hz, 2 H, Ar*H*), 8.82 (d, ^{3}J(H,H)=6.4 Hz, 2 H, Ar*H*), 9.02 (d,

[13] Arduini, A.; Calzavacca, F.; Pochini, A.; Secchi, A. *Chem. - A Eur. J*. **2003**, *9 (3)*, 793-799.

[14] Arduini, A.; Bussolati, R.; Credi, A.; Faimani, G.; Garaudee, S.; Pochini, A.; Secchi, A.; Semeraro, M.; Silvi, S.; Venturi, M. *Chem. - A Eur. J*. **2009**, *15 (13)*, 3230-3242.

[15] Arduini, A.; Credi, A.; Faimani, G.; Massera, C.; Pochini, A.; Secchi, A.; Semeraro, M.; Silvi, S.; Ugozzoli, F. *Chem. - A Eur. J*. **2008**, *14*, 98-106.

[16] Arduini, A.; Ciesa, F.; Fragassi, M.; Pochini, A.; Secchi, A. *Angew. Chemie, Int. Ed*. **2005**, *44 (2)*, 278-281.

[17] Ballot, S.; Noiret, N. *Tetrahedron Lett*. **2003**, *44 (49)*, 8811-8814.

[18] Arduini, A.; Bussolati, R.; Credi, A.; Monaco, S.; Secchi,A.; Silvi, S.; Venturi, M. *Chem. - A Eur. J*. **2012**, *18*, 16203-16213.

^{3}J(H,H)=6.4 Hz, 2 H, Ar*H*). ^{13}C NMR (100 MHz, $CDCl_3$ + MeOD): δ = 14.0, 21.1, 22.6, 26.0, 28.9, 29.3 (2 res), 29.4, 29.5, 29.6 (2 res), 31.5, 31.8, 62.1, 123.2, 125.6, 126.3, 128.8, 140.2, 142.0, 144.1, 145.3, 148.6, 152.6 ppm. ESI-MS(+): m/z (%) = 409 (100) $[M]^+$.

1-(12-(2,2-diphenylacetoxy)dodecyl)-[4,4'-bipyridin]-1-ium 4-methylbenzene sulfonate (9): In a sealed glass reactor, 12-(tosyloxy)dodecyl 2,2-diphenylacetate (0.25 g, 0.45 mmol) and 4,4'-dipyridyl (0.21 g, 1.36 mmol) were dissolved in 20 mL of CH_3CN and heated at 80°C overnight. After cooling at room temperature, the solvent was removed under reduced pressure, and the crude product was purified by precipitation from cold EtOAc (20 mL). The product was collected by Buchner filtration as a white solid (72%). ^{1}H NMR (400 MHz, $CDCl_3$): δ = 1.1–1.3 (m, 16 H, aliphatic CH_2), 1.61 (m, 2 H, O-CH_2CH_2), 1.90 (m, 2 H, N^+-CH_2CH_2), 2.29 (s, 3 H, Ar-CH_3), 4.14 (t, ^{3}J(H,H)=6.8 Hz, 2 H, O-CH_2), 4.73 (t, ^{3}J(H,H)=7.2 Hz, 2 H, N^+-CH_2), 7.11 (d, ^{3}J(H,H)=8.0 Hz, 2 H, Ar*H*), 7.25 (m, 8 H, Ar*H*), 7.60 (m, 2 H, Ar*H*), 7.62 (d, ^{3}J(H,H)=8.0 Hz, 2 H, Ar*H*), 7.76 (d, ^{3}J(H,H)=6.4 Hz, 2 H, Ar*H*), 8.25 (d, ^{3}J(H,H)=6.4 Hz, 2 H, Ar*H*), 8.78 (d, ^{3}J(H,H)=6.4 Hz, 2 H, Ar*H*), 9.24 (d, ^{3}J(H,H)=6.4 Hz, 2 H, Ar*H*). ^{13}C NMR (100 MHz, $CDCl_3$): δ = 21.2, 25.8, 26.1, 28.5, 29.1, 29.5, 31.7, 57.2, 61.6, 65.3, 121.5, 125.9, 127.2, 120.6, 128.8, 138.8, 139.4, 141.0, 143.9, 145.8, 151.2, 153.0, 172.6 ppm. ESI-MS(+): m/z (%) = 535 (100) $[M]^+$.

General procedure for the supramolecularly-assisted rotaxanes synthesis: To a solution of wheel **1** (0.07 mmol) in toluene (20 mL), an equimolar ratio of stoppered salt (0.07 mmol) and an excess of hydroxy-tosylate (0.21 mmol) were added. The orangish resulting solution was refluxed for four days; afterwards, the mixture was cooled to room temperature and diphenylacetyl chloride (0.14 mmol) and triethylamine (0.14 mmol) were added. The solution was stirred at room temperature for 16 hours. The solvent was then evaporated under reduced pressure and the residue was purified by column chromatography (dichloromethane:methanol = 95:5) to afford pure rotaxane.

R[**C12C6**]: product was obtained in 63% yield. ^{1}H NMR (400 MHz, C_6D_6): δ = 9.4 (bs, 6 H), 8.16 (d, ^{3}J = 7.6 Hz, 4 H), 8.1-7.8 (m, 8 H), 7.83 (d, ^{3}J = 6.0 Hz, 2 H), 7.58 (s, 6 H), 7.5-7.3 (m, 10 H), 7.2-7.1 (m, 10 H), 7.1-7.0 (m, 10 H), 6.90 (d, ^{3}J = 8.0 Hz, 4 H), 6.81 (d, ^{3}J = 6.0 Hz, 2 H), 6.8-6.6 (m, 5 H), 5.10 (s, 1 H), 5.07 (s, 1 H), 4.56 (d, ^{2}J = 14.8 Hz, 6 H), 4.33 (t, ^{3}J = 6.2 Hz, 2 H), 4.04 (t, ^{3}J = 6.6 Hz, 2 H), 3.88 (s, 9 H), 3.8 (bs, 6 H), 3.7-3.5 (m, 10 H), 3.5-3.2 (m, 12 H), 2.1 (bs, 2 H), 1.95 (s, 6 H), 1.9-0.6 (m, 83 H). ^{13}C NMR (100 MHz, C_6D_6): δ = 172.0, 171.9, 153.5, 152.9, 148.1, 147.9, 144.4, 143.3, 143.0, 141.3, 139.4, 139.3, 139.0, 137.5, 133.8, 132.2, 129.3, 128.7, 128.6, 128.5, 127.8, 127.6, 127.3, 127.1, 126.5, 125.6, 124.8, 121.1, 118.1, 116.7, 72.4, 69.9, 66.3, 64.9, 61.3, 61.0, 60.7,

57.3, 34.6, 31.5, 29.9, 29.8, 29.7, 29.6, 29.5, 29.3, 28.8, 28.6, 27.8, 26.1, 26.0, 25.8, 22.8, 20.8, 15.2, 14.0. MS (ESI): m/z: 1148.3 $[M\text{-}2TsO]^{2+}$.

R[**C6C12**]: product was obtained in 68% yield. ^{1}H NMR (400 MHz, C_6D_6): δ = 9.4 (bs, 6 H), 8.3-8.0 (bs, 6 H), 8.0-7.7 (m, 10 H), 7.59 (s, 6 H), 7.45 (d, ^{3}J = 7.6 Hz, 4 H), 7.41 (d, ^{3}J = 7.2 Hz, 4 H), 7.2-7.1 (m, 6 H), 7.1-7.0 (m, 10 H), 6.92 (d, ^{3}J = 8.0 Hz, 4 H), 6.83 (d, ^{3}J = 6.0 Hz, 2 H), 6.68 (t, ^{3}J = 6.8 Hz, 6 H), 5.13 (s, 1 H), 5.08 (s, 1 H), 4.58 (d, ^{2}J = 15.2 Hz, 6 H), 4.1-4.0 (m, 4 H), 3.95 (s, 9 H), 3.9-3.7 (m, 8 H), 3.7-3.5 (m, 8 H), 3.5-3.2 (m, 12 H), 2.2 (bs, 2 H), 1.96 (s, 6 H), 1.8 (bs, 2 H), 1.8-1.5 (m, 70 H). ^{13}C NMR (100 MHz, C_6D_6): δ = 172.0, 171.9, 153.5, 152.8, 148.2, 147.9, 144.4, 142.9, 141.2, 139.2, 139.2, 137.5, 133.8, 132.1, 129.3, 128.7, 128.7, 128.6, 128.6, 128.5, 128.3, 127.9, 127.8, 127.7, 127.6, 127.5, 127.2, 127.1, 127.0, 126.5, 125.7, 124.7, 121.2, 118.1, 116.7, 72.4, 70.0, 66.3, 64.7, 60.9, 60.5, 57.4, 57.3, 34.6, 31.5, 30.0, 29.7, 29.2, 28.6, 28.3, 25.8, 25.5, 24.9, 20.8, 15.2. MS (ESI): m/z: 1148.3 $[M\text{-}2TsO]^{2+}$.

CHAPTER 3

STEERING THE PROPERTIES OF PHENYLUREIDO CALIX[6]ARENE THROUGH STRUCTURAL CHANGES

The development of new potential applications of tris(*N*-phenylureido)calix[6]arene-based derivatives and complexes in large interest fields, such as sensing and catalysis, has recently opened the way to new fascinating challenges. To better understand the principles that govern the assembly of the structures that are at the basis of these progresses, we undertook a detailed investigation about how the modification of each domain of the receptor affects the axle complexation process.

3.1 Role of the methoxy groups at the lower rim: study of hydroxy-calix[6]arenes

Concerning the OCH_3 groups at the lower rim, we envisaged that these substituents could induce a minor effect on the selective directional threading. In particular, since in the free receptor -in low polarity solvents and on the NMR timescale- the three methoxy groups are oriented inward the cavity, we hypothesized that they could disfavor, by repulsive intermolecular interactions, the access of the axle through the narrow lower rim.

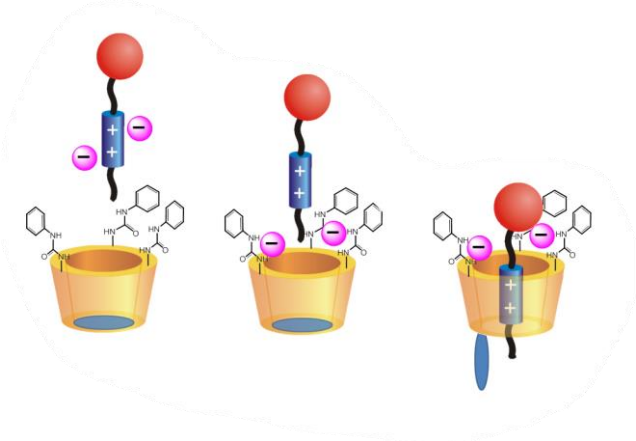

Figure 3.1 *Schematic representation of the axle threading process.*

To determine the extent of this participation, we planned to investigate the behavior of a new hydroxy-calix[6]arene receptor **2**, in which the methoxy groups at the lower rim have been removed (**Scheme 3.1**):

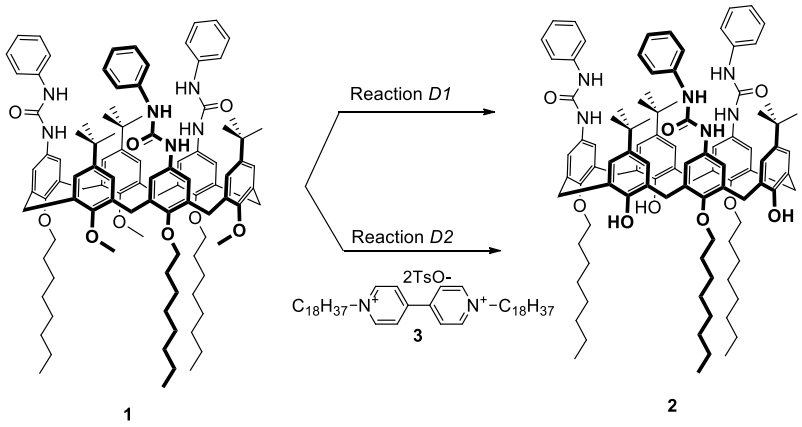

Scheme 3.1 *Reagents and conditions for demethylation reactions D1 and D2: TMSI, $CHCl_3$, 36h, 50°C.*

This strategy requires the demethylation reaction to proceed selectively, without cleavage of the ether bonds linking the longer alkyl chains at the lower rim. Only one procedure for the selective demethylation of a simple calix[6]arene derivative was reported in the literature in the 90's,[1] while a different reaction was recently applied to several multifunctionalized calix[6]arene-based derivatives by Reinaud, Jabin and coworkers.[2] Among the most common dealkylating agents, trimethylsilyl iodide (TMSI) was found to be the most effective and selective one. From their studies, it also emerged that the conformation adopted by the calixarene is crucial for both selectivity and efficiency of the process, and in particular the "*in*" or "*out*" orientation of the methoxy substituents relative to the cavity appears to be a key issue. In collaboration with them, we set up a similar demethylation protocol for receptor **1**. The demethylation reaction (*D1*) was carried out under inert atmosphere by dissolving **1** in anhydrous and degassed $CHCl_3$, adding TMSI (15 equivalents) dropwise and stirring at 50°C. After 8 hours, a second aliquot of TMSI (15 equivalents) was added.

A parallel guest-mediated reaction (*D2*) was carried out in the same experimental conditions, but an equimolar amount of 1,1'-dioctadecyl-4,4'-bipyridinium ditosylate **3** was added in the reaction mixture: the formation of a pseudorotaxane complex between **1** and **3** should prompt the expulsions of the -CH_3 groups from the cavity and therefore facilitate their cleavage.

The progress of the two reactions was initially monitored by high-resolution mass spectrometry in methanol (see **Table 3.1**):

[1] Van Duynhoven, J. P. M.; Janssen, R. G.; Verboom, W.; Franken, S. M.; Casnati, A.; Pochini, A.; Ungaro, R.; de Mendoza, J.; Nieto, P. M.; Prados, P.; Reinhoudt, D. N. *J. Am. Chem. Soc*. **1994**, *116*, 5814-5822.

[2] Danjou, P. E.; De Leener, G.; Cornut, D.; Moerkerke, S.; Mameri, S.; Lascaux, A.; Wouters, J.; Brugnara, A.; Colasson, B.; Reinaud, O.; Jabin, I. *J. Org. Chem.* **2015**, *80*, 5084-5091.

Time (h)	Demethylation *D1*	Guest-mediated Demethylation *D2*
1	**1**; **1**$^{-1Me}$; **1**$^{-2Me}$	**1**; **1**$^{-1Me}$; **1**$^{-2Me}$
2	**1**; **1**$^{-1Me}$; **1**$^{-2Me}$	**1**; **1**$^{-1Me}$; **1**$^{-2Me}$
4	**1**; **1**$^{-1Me}$; **1**$^{-2Me}$; **2**	**1**; **1**$^{-1Me}$; **1**$^{-2Me}$
7	**1**$^{-1Me}$; **1**$^{-2Me}$; **2**	**1**$^{-1Me}$; **1**$^{-2Me}$; **2**
24	**2**	**2**$^{-1octyl}$; **2**$^{-2octyl}$
36	**2**; **2**$^{-1octyl}$	**2**$^{-1octyl}$; **2**$^{-2octyl}$

Table 3.1 *Monitoring of demethylation reactions D1 and D2 with HRMS.*

MS analysis showed that reaction *D1* was successfully completed in 24 hours with good selectivity. Longer reaction times and higher amounts of TMSI led to undesired cleavage of the octyl chains. Contrary to what expected, the selectivity was higher in absence of the viologen guest.

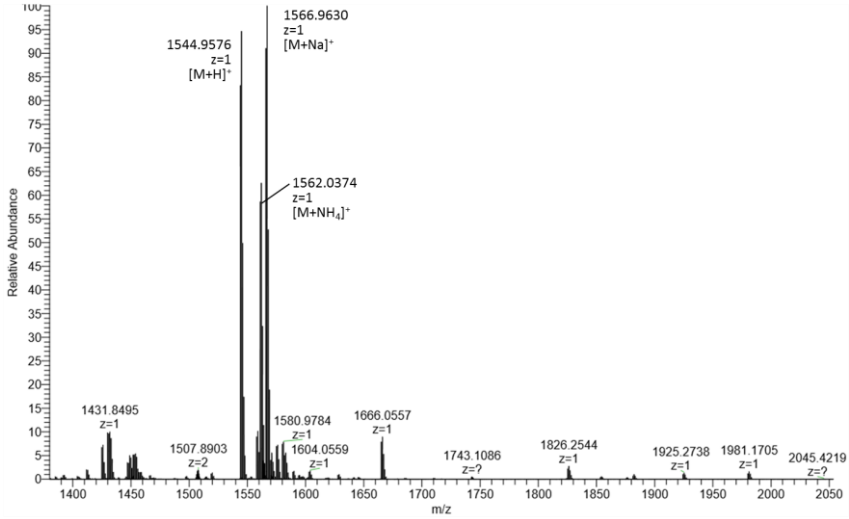

Figure 3.2 *High resolution mass spectrum (MeOH) of demethylation reaction D1 after 24 hours.*

Purification by column chromatography afforded tris-hydroxy-calixarene **2** in up to 80% yield in successive optimized reactions. The ^{1}H NMR spectrum of **2** was compared to the one of known wheel **1** (see **Figure 3.3**). First, it is worth to notice the absence of the broad singlet at ≅ 2.9 ppm relative to the OCH_3 groups. Moreover, the methylene bridging axial and equatorial protons resonate as an unique broad signal around 4 ppm, indicating the higher conformational mobility of this derivative with respect to the methylated precursor. The signals at 3.70, 1.67 and 1.39 ppm are

ascribed to the methylene protons of the octyl chains, and the integration of these peaks confirms the presence of the three alkyl substituents.

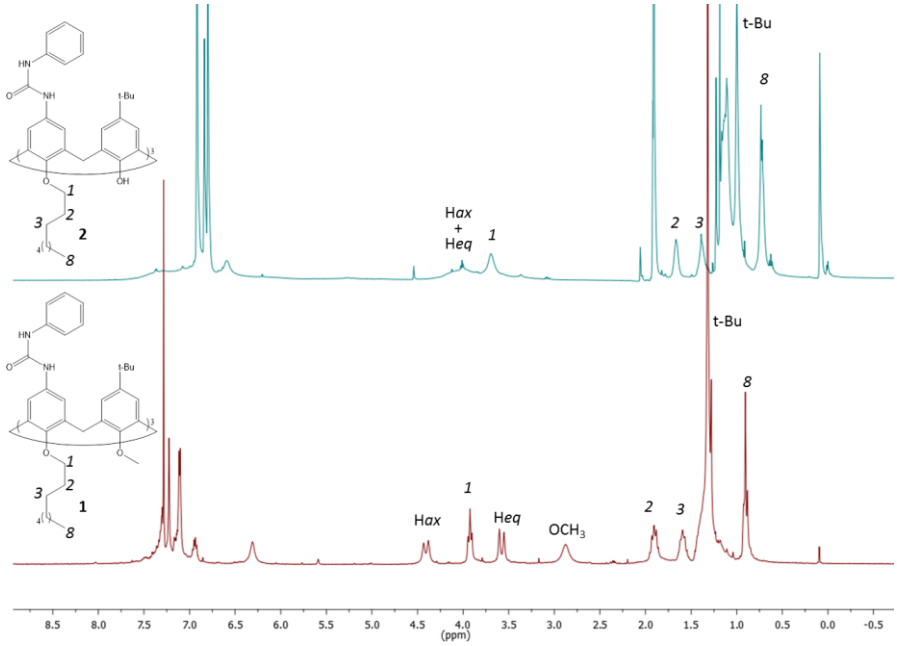

Figure 3.3 *^{1}H NMR spectra of: top) demethylated wheel **2** (500 MHz, toluene-d8); bottom) methylated wheel **1** (300 MHz, $CDCl_3$).*

The ability of **2** to act as host for viologen-based axles was first tested towards dioctylviologen ditosylate (**DOV**). Upon equilibration of equimolar amounts of **2** and **DOV** in low polarity solvent at room temperature, the dissolution of the salt and the appearance of the typical red color were observed, indicating the formation of a pseudorotaxane complex. The energetic for the formation of **P[2⊃DOV]** was investigated through UV/Vis measurements in dichloromethane. A titration experiment was accomplished at room temperature by adding increasing amounts of a 7×10^{-4} M solution of **2** to a 1×10^{-4} M solution of **DOV**.

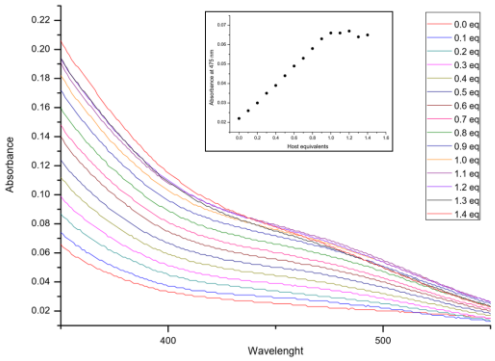

Figure 3.4 *Absorption spectra (CH_2Cl_2, rt, λ = 350-550 nm region) collected in the titration. Inset: absorbance values at λ = 475nm.*

During the titration, a band centered at λ = 475 nm was formed, and the fitting of the absorbance data gave an apparent binding constant log*K* = 6.5 ± 0.3, comparable to the same pseudorotaxane complex bearing methylated wheel **1** (log*K* = 6.8)[3].

The structure of the obtained pseudorotaxane was also investigated through NMR spectroscopy (**Figure 3.5**).

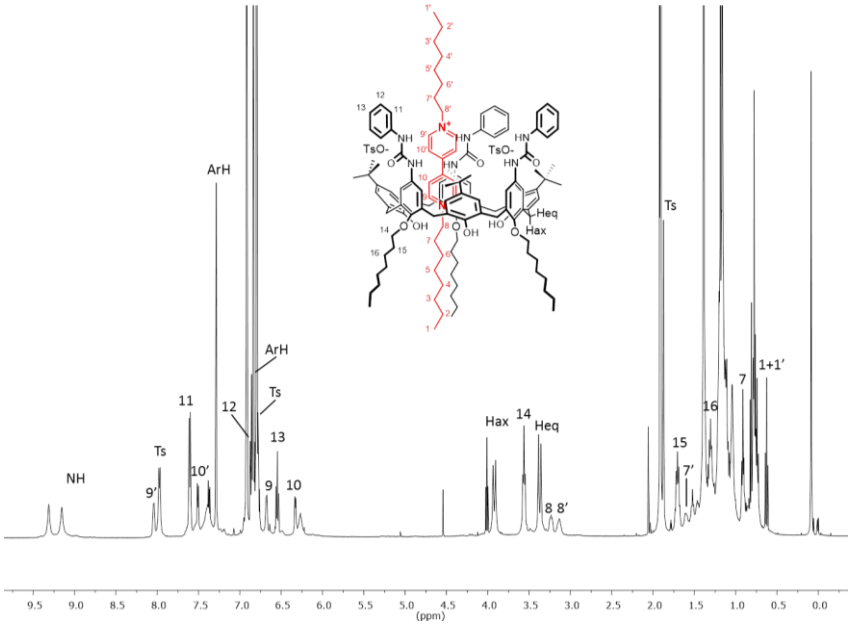

Figure 3.5 *^{1}H NMR spectrum (toluene-d8, 500 MHz) of **P[2⊃DOV]**.*

[3] Credi, A.; Dumas, S.; Silvi, S.; Venturi, M.; Arduini, A.; Pochini, A.; Secchi, A. *J. Org. Chem.* **2004**, *69*, 5881-5887.

The ^{1}H NMR spectrum of **P[2⊃DOV]** in toluene-d8 shows the typical features of the spectra of similar known pseudorotaxanes, such as the upfield shift of the axle (**DOV**) signals due to the inclusion of the latter into the shielding aromatic cavity, as well as their splitting in two series, depending on the proximity of the corresponding protons to the upper or lower rim of the calixarene. A peculiar feature present in the spectrum is the shift at higher fields of the doublet relative to the axial bridging protons (*Hax*) with respect to the same signal found in the spectrum of the methylated wheel **1** (3.9 vs 4.4 ppm). This upfield shift might suggest that **2** retains a *pseudo*-cone conformation on the NMR timescale but with a slightly different geometrical arrangement with respect to **1**.

Once demonstrated the possibility to form inclusion complexes, we investigated the directionality of the axle threading process. To this aim, **2** and the stoppered viologen salt **4** were equilibrated at room temperature in toluene-d8 (**Scheme 3.2**) and the relative arrangement of the components in the resulting pseudorotaxane complex was inferred through NMR measurements (**Figure 3.6**):

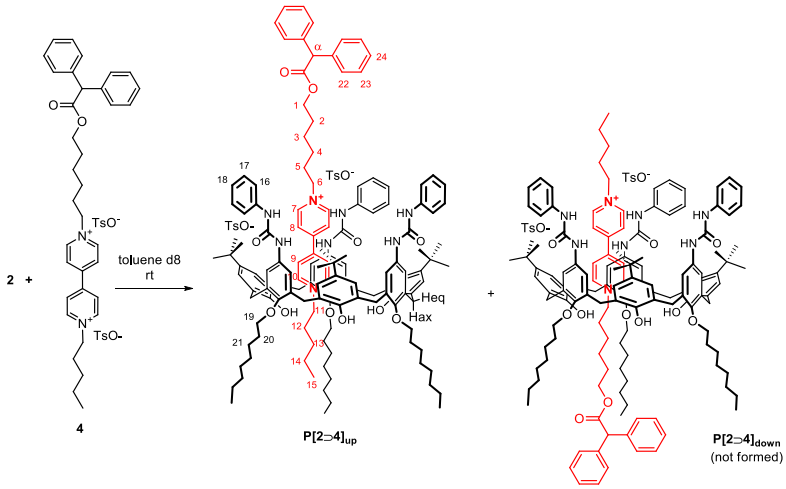

Scheme 3.2 *Formation of pseudorotaxane* ***P[2⊃4]$_{up}$***.

The symmetry of the spectrum suggests the presence of only one out of two possible orientational pseudorotaxane isomers. Also, the presence of a single signal relative to protons *11* and *6*, and the sharp singlet ascribed to methyne proton α, are in agreement with this hypothesis. The chemical shift of the methylene protons *1* in proximity to the diphenylacetic stopper (δ = 3.9 ppm) is in agreement with the presence of a stoppered C6 alkyl chain directed upward, and thus indicates the selective formation of the *up* isomer.

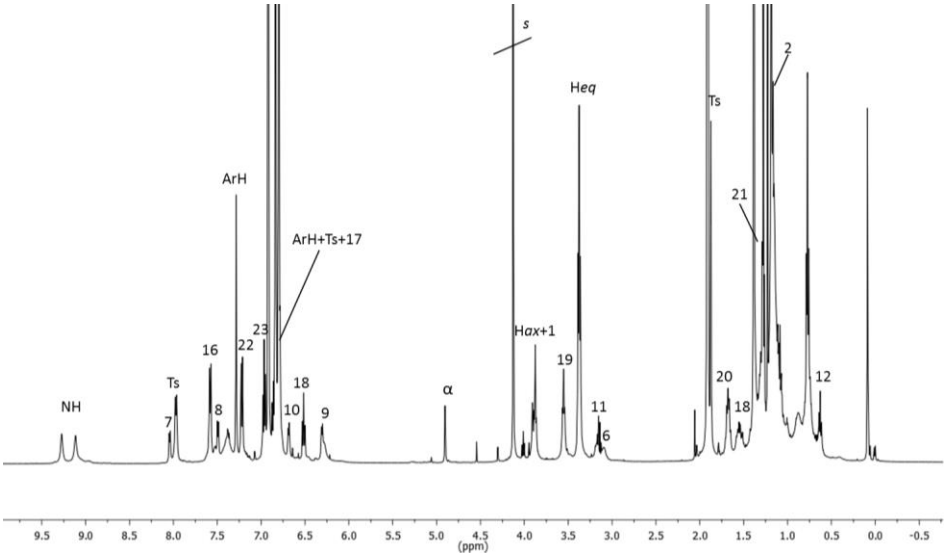

Figure 3.6 *^{1}H NMR spectrum (toluene-d8, 500 MHz) of* ***P[2⊃4]$_{up}$*** *(see* ***Scheme 3.2*** *for labelling).*

This confirms that, in low polarity solvent and at room temperature, the threading of the axle **4** takes place exclusive through the upper rim of **2**, as for the corresponding methylated receptor **1**.

Successively, **2** was equilibrated in toluene-d8 with viologen axle **C5C18** bearing two side chains of different length (**Scheme 3.3**):

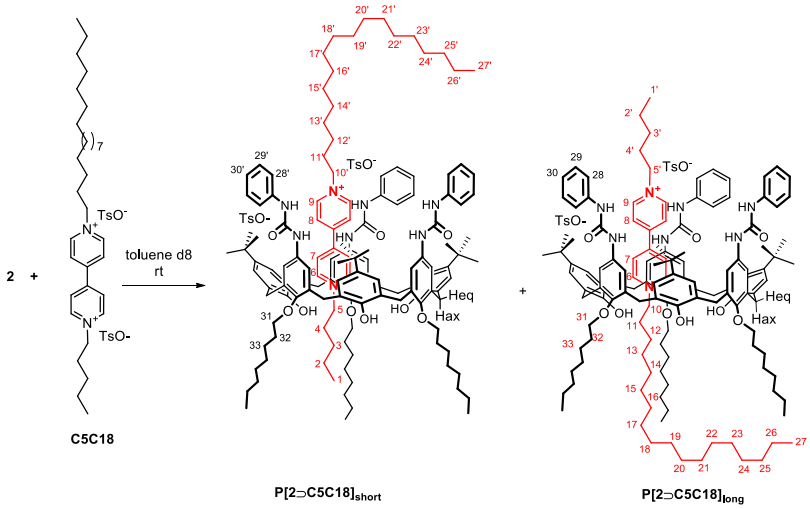

Scheme 3.3 *Formation of pseudorotaxanes* ***P[2⊃C5C18]$_{short}$*** *and* ***P[2⊃C5C18]$_{long}$***.

It is known that this kind of axles preferentially thread methylated wheel **1** with the shorter alkyl substituent for kinetic reasons[4] (detailed explanation is described in **Chapter 1**). 1D and 2D NMR analysis on the newly formed complex demonstrated that this selectivity is not retained when hydroxy-calixarene **2** is employed as host (**Figure 3.7**):

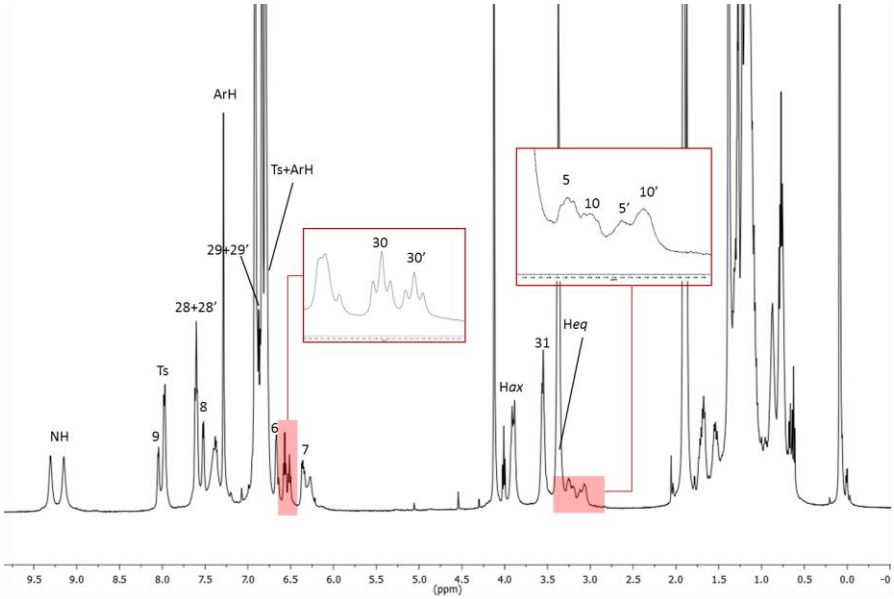

Figure 3.7 *^{1}H NMR spectrum (toluene-d8, 500 MHz) of* ***P[2⊃C5C18]$_{short}$ + P[2⊃C5C18]$_{long}$*** *(see* ***Scheme 3.3*** *for labelling).*

In fact, the presence of four different signals between 3.3 and 3.0 ppm ascribed to protons *5*, *10*, *5'* and *10'*, together with the presence of four different sets of correlations in COSY and TOCSY spectra, indicate the simultaneous presence of the two possible orientational pseudorotaxane isomers. The splitting in two triplets of the signal relative to phenylureidic protons *30* and *30'* is due to the perturbation, in **P[2⊃C5C18]$_{short}$** isomer, induced by the long C18 alkyl chain directed towards the ureidic moieties. Integration of these peaks suggests a ratio between the two isomers *short* : *long* = 60 : 40.

The described demethylation protocol was then extended to other calix[6]arene-based derivatives (**Scheme 3.4**):

[4] Arduini, A.; Bussolati, R.; Credi, A.; Secchi, A.; Silvi, S.; Semeraro, M.; Venturi, M. *J. Am. Chem. Soc.* **2013**, *135 (26)*, 9924-9930.

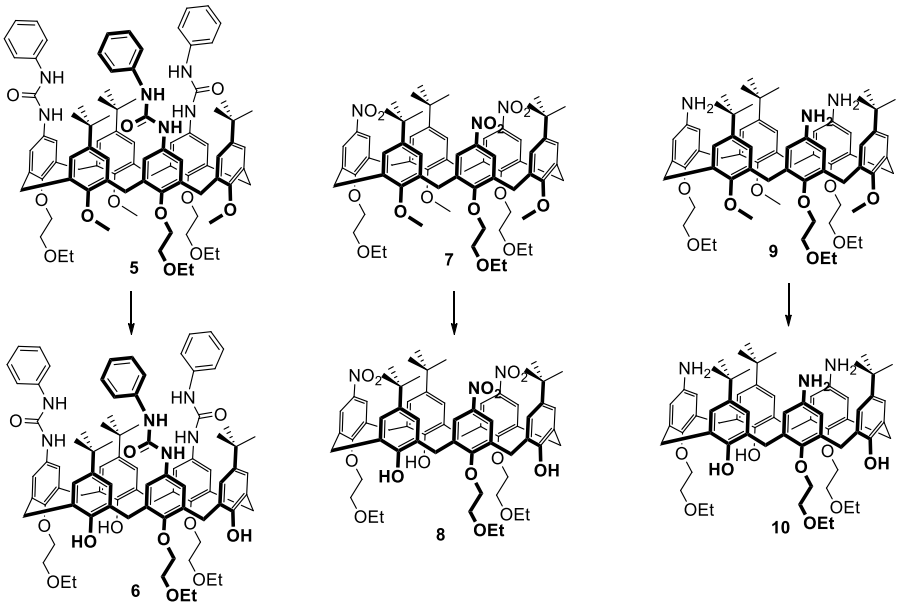

Scheme 3.4 *Synthesis of hydroxy-calix[6]arenes **6, 8** and **10**.*

These new receptors are potentially suitable platforms for further functionalization, since they are equipped with three phenolic moieties that can be exploited as anchoring point for the insertion of new functional groups at the macrocycle lower rim.

Another possible modification of hydroxy-calix[6]arenes is the oxidation of the phenolic rings to yield calix[6]quinones. These peculiar class of receptors, whose skeleton is endowed with redox active units, have attracted considerable attention by virtue of the combination of host-guest, electrochemical and photophysical properties. We therefore performed PbO_2/$HClO_4$ mediated oxidation[5] of tri-hydroxy-calix[6]arene **8**, the only substrate that is compatible with strong acidic and oxidizing conditions. The oxidation was carried out in a 1:1 v/v mixture of dichloromethane and acetone, for each phenol unit were employed 2.5 equivalents of oxidating agent and 15 equivalents of acid, and the concentration of the phenol units was set to 0.06 M. After stirring for one hour at room temperature, the corresponding calix[6]trisquinone **11** was obtained in 60% yield after purification by column chromatography.

[5] Lavendomme, R.; Troian-Gautier, L.; Zahim, S.; Reinaud, O.; Jabin, I. *Eur. J. Org. Chem*. **2016**, 1665-1668.

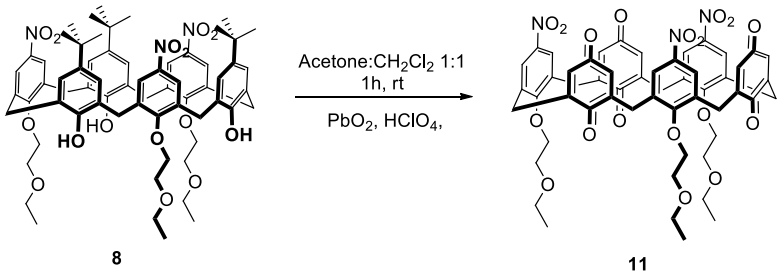

8 11

Scheme 3.5 *Synthesis of calix[6]trisquinone **11**.*

Studies concerning these new obtained receptors are currently undergoing in our laboratories.

3.2 Role of the phenilureido groups at the upper rim: study of bis(*N*-phenylureido)calix[6]arene

From the studies described in **Chapter 1** aimed at disclosing the driving forces for the formation of pseudorotaxane complexes, it emerged that the three ureidic groups of **1** do efficiently interact with the anions of the axle, and participate non only in the separation of the guest tight ion-pair, but also in the stabilization of the final product when coordinating anions are employed. As shown in the crystal structure of a viologen-based pseudorotaxane complex(**Figure 3.8**),[6] the structure is stabilized by the formation of six highly energetical hydrogen bonds.

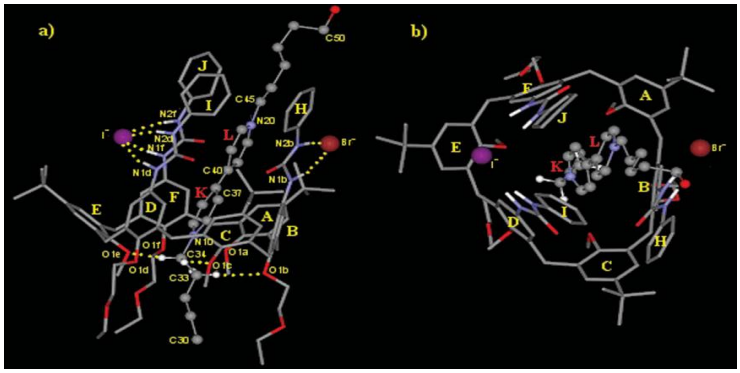

Figure 3.8 *a) X-ray structure of a pseudorotaxane complex formed by tris phenylureido wheel **5** and a viologen-based axle; b) top view. Adapted from ref. 6, copyright © Royal Society of Chemistry.*

[6] Ugozzoli, F.; Massera, C.; Arduini, A.; Pochini, A.; Secchi, A. *CrystEngComm* **2004**, *6 (39)*, 227-232.

In particular, one anion (Br^- in the figure) is coordinated through two hydrogen bonds by two NH of one urea moiety, and the other two ureas simultaneously participate in the stabilization of the second anion (I^- in the figure) by forming four more hydrogen bonds. From these findings, we hypothesized that the presence on the receptor of only two ureas could be sufficient to induce the separation of the ion pair of the guest and therefore guarantee the formation of the complex. To verify such speculation, we designed bis(*N*-phenylureido)calix[6]arene **12**: the synthesis was achieved following a procedure that is similar to the one adopted for the known tris(*N*-phenylureido)calix[6]arene **1**, starting from the 1,2,4,5-tetramethoxy calix[6]arene **13** (**Scheme 3.6**)[7]:

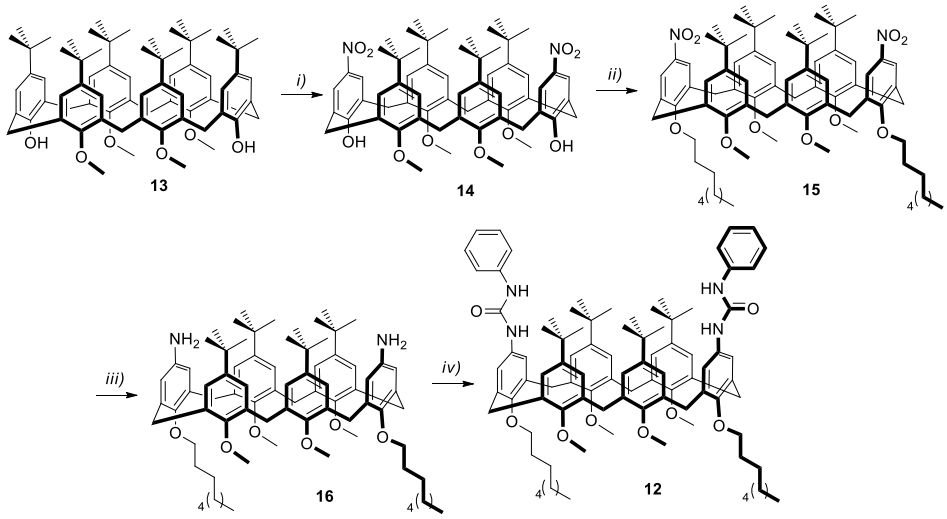

Scheme 3.6 *Reagents and conditions: i) HNO_3/H_2SO_4, CH_2Cl_2 rt, 3 h; ii) 1-Iodooctane, K_2CO_3, CH_3CN, 110°C , 4d; iii) NH_2NH_2, Pd/C, MeOH, reflux, 24 h; iv) Phenyl isocyanate, CH_2Cl_2, rt, 2h.*

The *ipso*-nitration reaction yielded derivative **14**, that was reacted with 1-iodooctane to obtain the alkylated product **15**. Finally, reduction of the nitro groups and reaction

[7] Casnati, A.; Domiano, L.; Pochini, A.; Ungaro, R.; Carramolino, M.; Magrans, J. O.; Nieto, P. M.; Lopez-Prados, J.; Prados, P. *Tetrahedron* **1995**, *51(46)*, 12699-12720. In the methylation reaction, the two major products formed are the 1,3,5-trimethoxy calix[6]arene (precursor of tris(*N*-phenylureido)derivatives) and the tetrasubstituted product **13**. The preferential formation of these regioisomers is justified considering that, upon the insertion of the first methyl substituent, the following alkylations take place in order to guarantee the formation of the highest possible number of intramolecular hydrogen bonds, that concur in the stabilization of the reaction intermediate.

with phenyl isocyanate afforded calix[6]arene **12**, decorated with two phenylureido moieties in the 1,4-diametral position, in 80% yield.

The ^{1}H NMR spectrum of **12** recorded in $CDCl_3$ (see **Figure 3.9a**) exhibits several broad resonances, among which it was possible to evidence the presence of multiple signals assigned to the OCH_3 substituents and the splitting of each bridging methylene signal. No significant changes were observed moving to other low polarity solvents or rising the sampling temperature. These features could be ascribed to the simultaneous presence of different regioisomers, to a high conformational mobility of the product or to aggregation phenomena. The unexpected very low solubility of this derivative in all common solvents tested made us lean towards the latter hypothesis. The addition in the NMR sample of increasing amounts of CD_3OD led to a progressive simplification of the spectrum (see **Figure 3.9b-c**): this allowed, together with several 2D NMR experiments (COSY and HSQC), the identification of all the diagnostic signals, including the three main different signals relative to the bridging methylene protons, two doublets at 4.2 and 3.5 ppm and a broad singlet at 3.8 ppm.

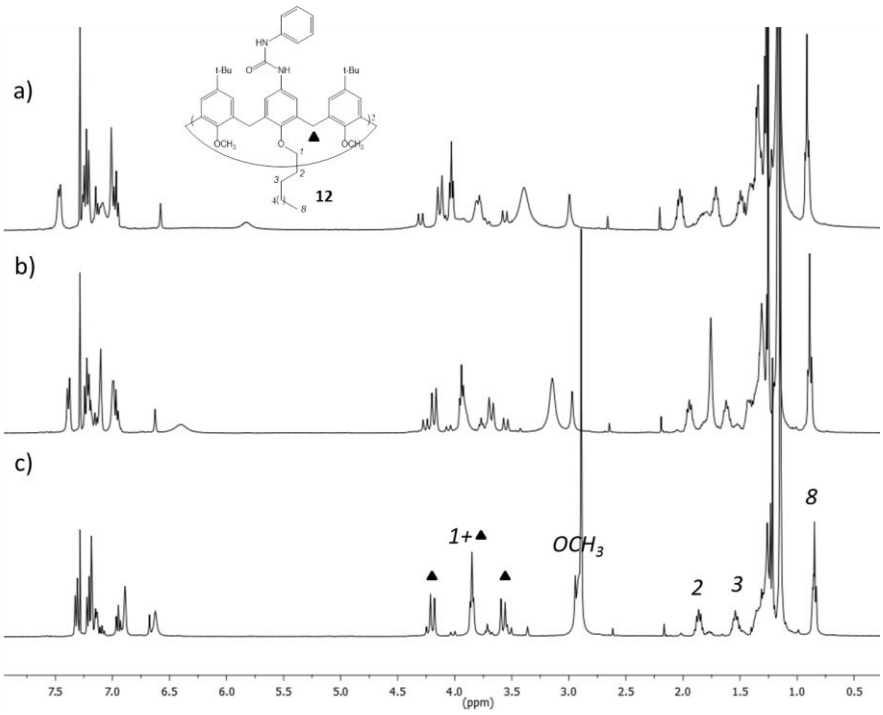

Figure 3.9 *^{1}H NMR spectra of calixarene **12** recorded at 400 MHz in: a) $CDCl_3$; b) $CDCl_3$ + 2% CD_3OD; c) $CDCl_3$ + 7% CD_3OD.*

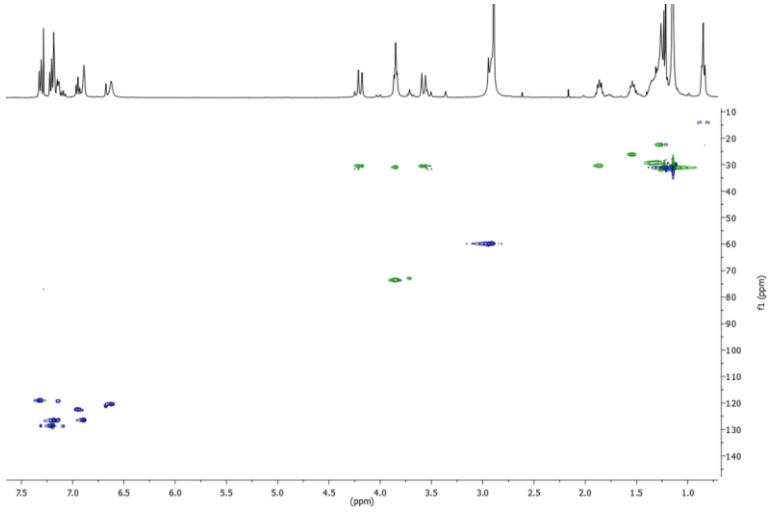

Figure 3.10 *Edited HSQC spectrum of **12** (400 MHz, $CDCl_3$:CD_3OD = 40:2.5).*

Further data for the structural characterization of new receptor **12** came from the solid state structure investigation. The crystal structure of compound **12** was determined *via* synchrotron X-ray diffraction data on single crystals obtained by slow evaporation of a chloroform/methanol solution. In the unit cell, three independent centrosymmetric molecules co-exist, indicated in the discussion as **I**, **II** and **III** (see **Figure 3.11**):

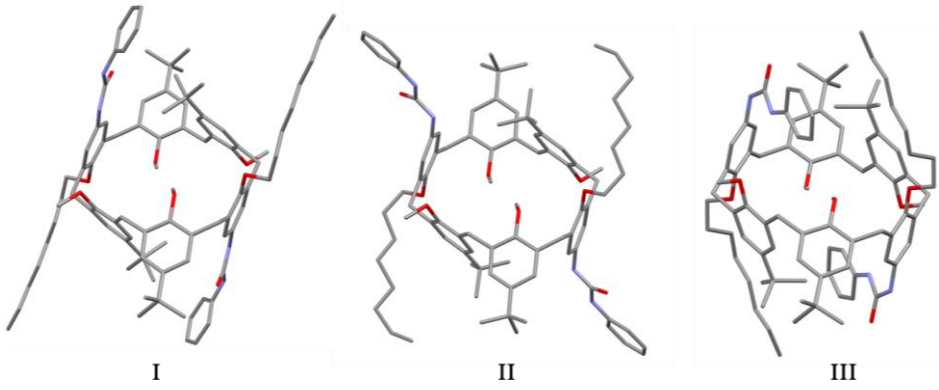

Figure 3.11 *Molecular structures of **I**, **II** and **III**. Hydrogen atoms and solvent molecules have been omitted for clarity.*

In all cases, the receptor adopts an 1,2,3-alternate conformation, in which the two phenylureido moieties face the opposite rims of the calixarene scaffold. In molecule **I**, the substituents lie in the planes defined by the respective aromatic rings of the calixarene, in molecule **II** the urea groups are pointing outwards the cavity, while in molecule **III** the phenylureido pendants are bent towards the openings of the ring. The X-ray analysis confirmed that, in the lattice, the three molecules are regularly connected through hydrogen bonds involving the ureido groups, with the N-H atoms behaving as donors and the oxygen atoms as acceptors (see **Figure 3.12**):

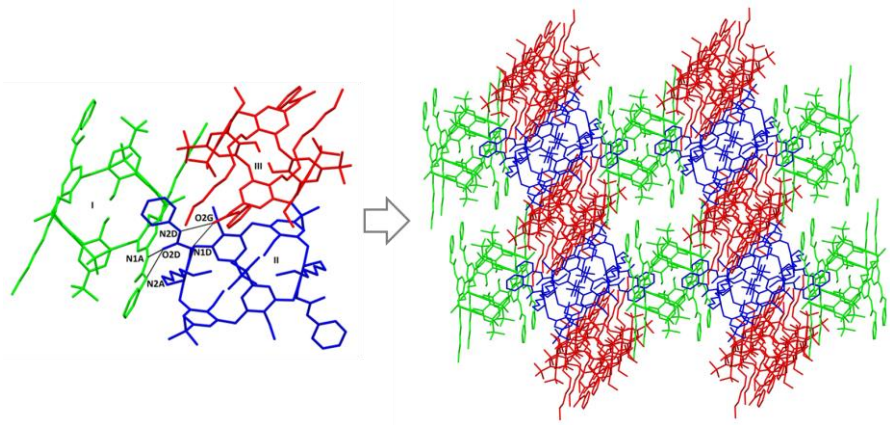

Figure 3.12 *The set of H bonds involving the three independent molecules **I, II** and **III**, with partial labelling scheme. Hydrogen atoms and solvent molecules have been omitted for clarity. H bonds are shown as grey lines.*

The ability of this wheel to act as host for viologen salts was tested in solution by mixing equimolar amounts of **12** and **DOV** in dichloromethane: as observed for similar systems, the dissolution of the salt and the red color of the resulting homogeneous solution indicated the formation of a pseudorotaxane complex. The apparent association constant between host and guest was calculated through a UV/Vis titration experiment, in which aliquots of a 7×10^{-4} M dichloromethane solution of **12** were added to a 1×10^{-4} M solution of **DOV** in the same solvent.

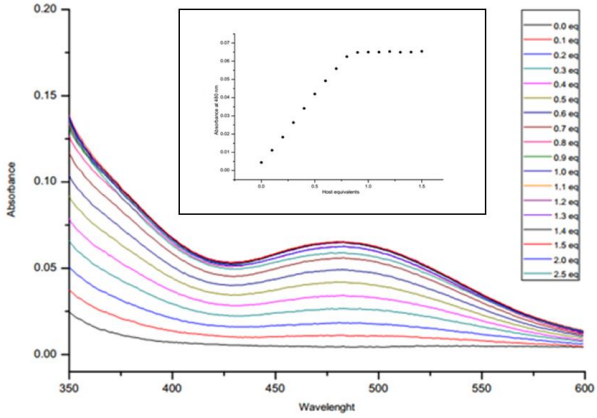

Figure 3.13 *Absorption spectra (CH_2Cl_2, rt, λ = 350-600 nm region) collected in the titration. Inset: absorbance values at λ = 480nm.*

A low energy band centered at λ = 480 nm was formed, and the fitting of the absorption data gave an apparent binding constant log*K* = 5.6 ± 0.1, that is about one order of magnitude lower with respect to the one calculated for tris(*N*-phenylureido) derivative **1**. This is consistent with the ability of the two ureidic groups of **12** to form at most only four hydrogen bonds with the anions of the guest.

The structure of the obtained pseudorotaxane **P[12⊃DOV]** was analyzed by NMR spectroscopy (**Figure 3.14**):

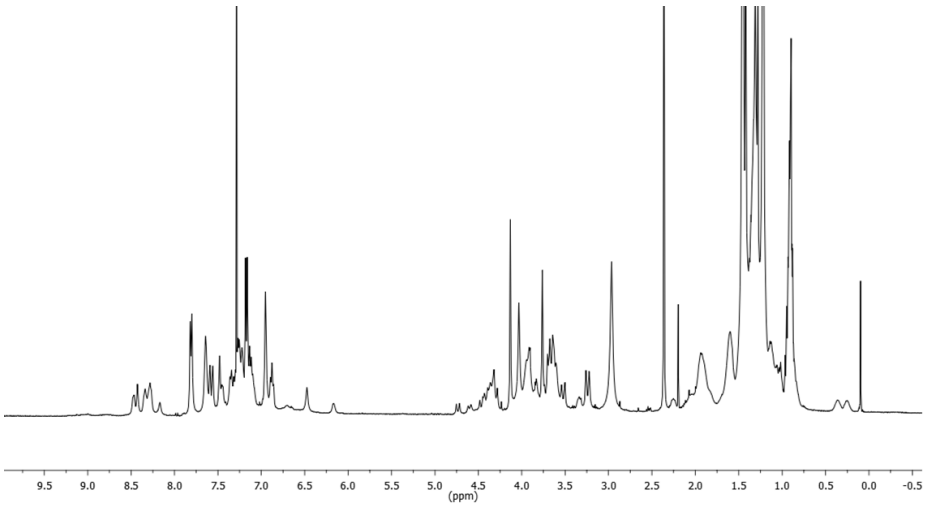

Figure 3.14 *^{1}H NMR spectrum (400 MHz, $CDCl_3$), of **P[12⊃DOV]**.*

The spectrum appears much more complicated if compared to known rotaxanes composed of tris(*N*-phenylureido) wheels. For examples, three different singlets at 4.13, 3.76 and 2.97 ppm related to OCH_3 protons of **12** are displayed, and several doublets relative to the bridging methylene protons are present. The shielding of some resonances attributed to the axle's protons (see for instance the broad signals at 0.36 and 0.24 ppm) indicate the engulfment of the axle into the calixarene cavity. However, further analysis need to be carried out in order to establish the conformation adopted by the calixarene in this pseudorotaxane complex and to find out if aggregation phenomena take place also in the pseudorotaxane system.

3.3 Conclusions

In this chapter, a selective procedure for the cleavage of methoxy groups at the calixarene lower rim was presented. The complexing properties of hydroxy-calix[6]arene **2** towards different viologen-based axles were tested: it emerged that stoppered axles do thread **2** selectively from its upper rim, while the kinetic selectivity induced by the different length of simple alkyl chains appended to the axle is not retained, indicating that the methoxy groups at the lower rim of **1** play a significant role in the self-sorting process. The described demethylation protocol was successfully extended to other calix[6]arene-based intermediates and derivatives **6**, **8** and **10**, in which the presence of free phenolic moieties might enable the insertion of different functional groups at the macrocycles lower rim, or allow the direct oxidation to calix[6]quinones. Moreover, the three OH groups at the macrocycle lower rim might be exploited as a further coordination site on the calix[6]arene skeleton.

Finally, it was also verified that bis(*N*-phenilureido)receptor **12**, decorated with only two ureidic moieties in 1,4-diametral position, ensures the complexation of viologen-based axles in solution. The determination of the crystal structure *via* X-ray diffraction on single crystals showed that receptor **12** adopts, in the solid state, an 1,2,3-alternate conformation and tends to form aggregates held together through a regular network of intermolecular hydrogen bonds. The structure of the obtained pseudorotaxane complex, both in solution and in the solid state, is still under investigation.

3.4 Acknowledgments

Thanks to Dr. Sarah Richards, Dr. Gaël De Leener and Prof. Olivia Reinaud (Université Paris Descartes) for the help in the optimization of the demethylation procedure; thanks to Prof. Franco Ugozzoli and Prof. Chiara Massera (Università di Parma) for the X-ray structure collection and determination.

3.5 Experimental Section

Synthesis: Solvents were dried by following standard procedures, other reagents were of reagent grade quality, obtained from commercial sources and used without further purification. Chemical shifts are expressed in ppm using the residual solvent signal as internal reference. Mass spectra were determined in ESI mode. Compounds **1**[8], **13**[7] and **14**[7] were obtained following reported procedures.

General procedure for demethylation reaction: Methylated wheel (1 eq) was dissolved in anhydrous and degassed $CHCl_3$ (4 mL) under inert atmosphere, and TMSI (15 eq.) was added dropwise through a septum cap. The mixture was stirred at 50°C for 8 hours, after which a second aliquot of TMSI (15 eq.) was added. After 16 hours, the reaction was quenched with water (5 mL). The separated organic phase was dried with $CaCl_2$ and evaporated under reduced pressure.

Hydroxy-calix[6]arene 2: The crude residue was purified by gradient column chromatography (eluent: from dichloromethane to dichloromethane: THF = 98:2), to afford **2** in 80% yield. ^{1}H NMR (500 MHz, toluene-d8): δ = 0.72 (t, ^{3}J(H,H)=6.0 Hz, 9 H, C*H*$_3$), 1.02 (s, 27 H, Ar-Bu^t), 1.1–1.2 (m, 24 H, aliphatic C*H*$_2$), 1.39 (m, 6 H, ArO-CH$_2$CH$_2$C*H*$_2$), 1.67 (m, 6 H, ArO-CH$_2$C*H*$_2$), 3.70 (bs, 6 H, ArO-C*H*$_2$), 4.00 (bs, 12 H, Ar-C*H*$_2$-Ar), 6.59 (bs, 9 H, Ar*H* + N*H*), 6.75 (m, 18 H, Ar*H*), 7.33 (bs, 6 H, Ar*H*). ESI-MS(+): m/z (%) = 1545 (100) [M+H]$^+$, 1562 (100) [M+NH$_4$]$^+$, 1567 (100) [M+Na]$^+$.

Hydroxy-calix[6]arene 6: The crude residue was purified by column chromatography (eluent: hexane: ethyl acetate = 65:35), to afford **6** in 60% yield. ^{1}H NMR (500 MHz, $CDCl_3$): δ = 1.92 (m, 9 H, O-CH$_2$C*H*$_3$), 1.18 (s, 27 H, *Bu*^{t}), 3.58 (bs, 12 H, O-C*H*$_2$CH$_3$ + Ar-CH$_2$), 3.76 (bs, 6 H, ArO-CH2C*H*$_2$), 4.04 (bs, 6 H, ArO-C*H*$_2$), 4.16 (bs, 6 H, Ar-CH$_2$), 6.75-7.75 (m, 27 H, Ar*H*). ESI-MS(+): m/z (%) = 1441 (100) [M+NH$_4$]$^+$; 1448 (100) [M+Na]$^+$.

Hydroxy-calix[6]arene 8: The crude residue was purified by column chromatography (eluent: hexane: THF = 75:25), to afford **8** in 85% yield. ^{1}H NMR (500 MHz, $CDCl_3$): δ = 0.92 (t, ^{3}J(H,H)=7.0 Hz, 9 H, O-CH$_2$C*H*$_3$), 1.16 (s, 27 H, *Bu*^{t}), 3.26 (q, ^{3}J(H,H)=7.0 Hz, 6 H, O-C*H*$_2$CH$_3$), 3.51 (m, 6 H, ArO-CH2C*H*$_2$), 3.91 (bs, 18 H, ArO-C*H*$_2$ + Ar-CH$_2$), 6.73 (bs, 3 H, O*H*), 6.91 (s, 6 H, Ar*H*), 7.78 (s, 6 H, Ar*H).* ESI-MS(+): m/z (%) = 1173 (100) [M+NH$_4$]$^+$.

[8] A. Arduini, F. Ciesa, M. Fragassi, A. Pochini, A. Secchi, Angew. Chem. Int. Ed. **2005**, *44*, 278–281.

Hydroxy-calix[6]arene 10: The crude residue was purified by column chromatography (eluent: hexane: ethyl acetate = 5:5), to afford **10** in 65% yield. ^{1}H NMR (500 MHz, $CDCl_3$): δ = 0.95 (m, 9 H, O-CH_2CH_3), 1.18 (s, 27 H, *Bu*^{t}), 3.48 (bs, 6 H, Ar-CH_2), 3.54 (bs, 6 H, O-CH_2CH_3), 3.63 (bs, 6 H, ArO-CH2CH_2), 3.81 (bs, 6 H, Ar-CH_2), 3.93 (bs, 6 H, ArO-CH_2), 6.01 (s, 6 H, Ar*H*), 6.75-7.75 (m, 21 H, Ar*H*). ESI-MS(+): m/z (%) = 1067 (100) $[M+H]^+$.

Calix[6]trisquinone 11: Hydroxy-calix[6]arene **8** (0.008 g, 0.007 mmol) was dissolved in 0.1 mL of a 1:1 v/v mixture of acetone and dichloromethane. Separately, PbO_2 (0.013 g, 0.052 mmol) and $HClO_4$ (0.019 mL, 0.314 mmol) were dissolved in 0.1 mL of the same mixture. The calix[6]arene solution was slowly added to the oxidant solution, and the resulting mixture was stirred at room temperature for one hour. The mixture was diluted adding dichloromethane (10 mL) and the black solid was filtered off. The organic phase was washed with water, dried over Na_2SO_4, filtered and evaporated under reduced pressure. The crude product was purified by preparative TLC (eluent: hexane:THF = 5:5), and **11** was obtained in 50% yield. ^{1}H NMR (500 MHz, $CDCl_3$): δ = 1.12 (t, ^{3}J(H,H)=7.0 Hz, 9 H, O-CH_2CH_3), 3.49 (q, ^{3}J(H,H)=7.0 Hz, 6 H, O-CH_2CH_3), 3.74 (m, 6 H, ArO-CH2CH_2), 3.90 (bs, 12 H, Ar-CH_2), 4.06 (m, 6 H, ArO-CH_2), 6.23 (bs, 6 H, quinone-*H*), 7.82 (s, 6 H, Ar*H*). ESI-MS(+): m/z (%) = 1047 (100) $[M+NH_4]^+$.

Calix[6]arene 15: A solution of calixarene **14** (0.77 g, 0.77 mmol), K_2CO_3 (0.37 g, 2.68 mmol) and 1-Iodooctane (0.54 mL, 2.68 mmol) was placed in a sealed glass reactor in anhydrous acetonitrile (50 mL). The reaction mixture was heated at 110°C for 4 days. The solvent was then evaporated under reduced pressure, and the residue was taken up in dichloromethane (50 mL) and washed with aqueous 10% HCl (30 mL). The separated organic phase was dried over Na_2SO_4, filtered and evaporated under reduced pressure. Pure product **15** was isolated by precipitation from ethyl acetate in 33% yield. ^{1}H NMR (400 MHz, $CDCl_3$): δ = 0.90 (t, ^{3}J(H,H)=8.0 Hz, 6 H, CH_2CH_3), 1.22 (s, 36 H, *Bu*^{t}), 1.3-1.5 (m, 16 H, aliphatic CH_2), 1.60 (bs, 4 H, O-$CH_2CH_2CH_2$), 1.94 (bs, 4 H, O-CH_2CH_2), 2.97 (s, 12 H, ArO-CH_3), 3.63 (d, ^{2}J(H,H)=12.0 Hz, 4 H, Ar-CH_2), 3.92 (m, 8 H, ArO-CH_2 + Ar-CH_2), 4.35 (d, ^{2}J(H,H)=12.0 Hz, 4 H, Ar-CH_2), 6.96 (s, 4 H, Ar*H*), 7.22 (s, 4 H, Ar*H*), 7.64 (s, 4 H, Ar*H*). ESI-MS(+): m/z (%) = 1232 (100) $[M+H]^+$.

Calix[6]arene 16: In a two-neck flask, under inert atmosphere, product **15** (0.70 g, 0.57 mmol) was dissolved in methanol (150 mL) and dichloromethane (2 mL). Hydrazine monohydrate (2.84 mL, 57.00 mmol) and a tip of spatula of 10% Pd/C were added, and the mixture was refluxed overnight. The hot mixture was then filtered to remove the catalyst and the solvent was removed under reduced pressure. The residue was dissolved in dichloromethane (50 mL) and washed with water to remove the excess of

hydrazine. The separated organic phase was dried over $CaCl_2$, filtered and evaporated under reduced pressure. Product **16** was obtained in quantitative yield and was used without further purification. ESI-MS(+): m/z (%) = 1172 (100) $[M+H]^+$.

Bis(*N*-phenylureido)calix[6]arene 12: In a two-neck flask under inert atmosphere, **16** (0.30 g, 0.26 mmol) was dissolved in anhydrous dichloromethane (50 mL) and phenyl isocyanate (0.09 mL, 0.77 mmol) was added. The solution was stirred at room temperature for one day, after which the solvent was removed under reduced pressure. Product **12** was purified by column chromatography (eluent hexane:ethyl acetate 75:25) in 80% yield. ^{1}H NMR (400 MHz, $CDCl_3$ + MeOD): δ = 0.85 (t, ^{3}J(H,H)=8.5 Hz, 6 H, CH_2CH_3), 1.15 (s, 36 H, *Bu*^{t}), 1.2-1.4 (m, 16 H, aliphatic CH_2), 1.54 (m, 4 H, O-$CH_2CH_2CH_2$), 1.86 (m, 4 H, O-CH_2CH_2), 2.94 (s, 12 H, ArO-CH_3), 3.57 (d, ^{2}J(H,H)=12.0 Hz, 4 H, Ar-CH_2), 3.85 (m, 8 H, ArO-CH_2 + Ar-CH_2), 4.19 (d, ^{2}J(H,H)=12.0 Hz, 4 H, Ar-CH_2), 6.62 (s, 4 H, Ar*H*), 6.71 (s, 4 H, Ar*H*), 6.89 (m, 2 H, Ar*H*), 7.18 (s, 4 H, Ar*H*), 7.20 (m, 4 H, Ar*H*), 7.31 (m, 4 H, Ar*H*). ^{13}C NMR (750 MHz, $CDCl_3$ + MeOD): δ = 14.0, 22.6, 26.3, 29.3, 29.6, 30.5, 31.2, 31.8, 34.1, 59.7, 60.2, 73.7, 119.0, 121.1, 122.5, 122.9, 126.3, 126.7, 126.9, 128.7, 132.1, 132.8, 134.1, 135.4, 136.5, 138.9, 143.5, 146.4, 146.6, 150.4, 152.6, 154.1 ppm. ESI-MS(+): m/z (%) = 1410 (100) $[M+H]^+$.

X-ray data collection and crystal structure determination: The crystal structure of compound **12** was determined by X-ray diffraction methods. Intensity data and cell parameters were recorded at 100(2) K at the ELETTRA Synchrotron Light Source (CNR Trieste, Strada Statale 14, Area Science Park, 34149, Basovizza, Trieste, Italy). The raw frame data were processed using the program package CrysAlisPro 1.171.38.41[9]. The structure was solved by Direct Methods using the SIR97 program[10] and refined on F_o^2 by full-matrix least-squares procedures, using the SHELXL-2014/7 program[11] in the WinGX suite v.2014.1[12]. All non-hydrogen atoms were refined with anisotropic atomic displacements, with the exception of some disordered solvent molecules. The hydrogen atoms were included in the refinement at idealized geometry (C-H 0.95 Å) and refined "riding" on the corresponding parent atoms. The weighting scheme used in the last cycle of refinement was $w = 1/ [\sigma^2 F_o^2 + (0.2410P)^2]$, where $P = (F_o^2 + 2F_c^2)/3$. Crystal data and experimental details for data collection and structure refinement are reported in **Table S3.1**:

[9] CrysAlisPro 1.171.38.41 (Rigaku Oxford Diffraction, 2015).

[10] Altomare, A.; Burla, M. C.; Camalli, M.; Cascarano, G. L.; Giacovazzo, C.; Guagliardi, A.; Moliterni, A. G. G.; Polidori, G.; Spagna, R. *J. Appl. Cryst.* **1999**, *32*, 115-119.

[11] Sheldrick, G. M. *Acta Crystallogr*. **2008**, *A64*, 112-122.

[12] Farrugia, L. J. *J. Appl. Crystallogr*. **2012**, *45*, 849-854; van der Sluis, P.; Spek, A. L. *Acta Cryst., Sect A*. **1990**, *46*, 194-201.

Table S3.1 Crystal data and structure refinement information for **12**.

Compound	$\mathbf{C_{92}H_{120}N_4O_8 \cdot 2/3CHCl_3 \cdot 4/3CH_3OH \cdot 10/3H_2O}$
empirical formula	$C_{94}H_{132.67}Cl_2N_4O_{12.67}$
M	1592.27
crys syst	Triclinic
space group	*P-1*
a/Å	16.071(3)
b/Å	20.134(4)
c/Å	24.107(5)
α/°	98.896(9)
ß/°	98.935(9)
γ/°	110.990(9)
V/Å^3	7005(2)
Z	3
T/K	100(2)
ρ/g cm^{-3}	1.132
μ/mm^{-1}	0.123
F(000)	2580
total reflections	203135

unique reflections (R_{int})	41205 (0.0699)
observed reflections *[F_o>4σ(F_o)]*	29837
GOF on F^{2a}	1.492
R indices *[F_o>4σ(F_o)]*^{b} R_1, wR_2	0.1290, 0.3987
largest diff. peak and hole (eÅ^{-3})	2.540, -2.383

[a)]Goodness-of-fit $S=[\Sigma w(F_o^2-F_c^2)^2/(n-p)]1/2$, where n is the number of reflections and p the number of parameters. [b)]$R_1 = \Sigma \| F_o | - | F_c \| / \Sigma | F_o |$, $wR_2 = [\Sigma[w(F_o^2-F_c^2)^2]/\Sigma[w(F_o^2)^2]]^{1/2}$.

CHAPTER 4

TOWARDS CALIX[6]ARENE-BASED DIRECTIONAL MOLECULAR SHUTTLES

4.1 Introduction

In the field of molecular level machines, the possibility to synthesize and operate with supramolecular systems capable of performing specific movements - i.e. to act as molecular motors - under the action of a defined external energy input, constitutes a fascinating challenge.[1] One of the simplest classes of molecular motors is represented by linear assemblies designed to achieve translational slipping of a macrocyclic component along a threaded axle, defined as molecular shuttles.

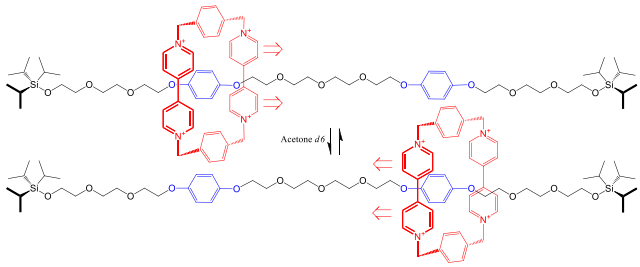

Figure 4.1 *Structure of the first characterized molecular shuttle: the cyclophane ring (red) moves back and forth between the two hydroquinol moieties (blue). The dethreading is prevented by the terminal triisopropylsilyl stoppers.*

This large-amplitude translational motion was first characterized by J. F. Stoddart in solution in 1991 (**Figure 4.1**).[2] Since that report, many mechanically interlocked molecules have been designed, synthesized and shown to mimic the complex functions of macroscopic switches with a wide range of applications, including molecular electronic devices, sensors, nanomechanical systems, and instruments capable of delivering both chemical and biological cargos in a controlled manner. The shuttling motion can be triggered by a plethora of different stimuli, such as thermal treatment,[3] ion coordination,[4] electrochemical[5] or photochemical[6] activation, changes

[1] Silvi, S.; Venturi, M.; Credi, A. *J. Mater. Chem.* **2009**, *19*, 2279-2294; Browne, W. R.; Feringa, B. L. *Nat. Nanotech.* **2006**, *1*, 25-35; Leigh, D. A.; Wong, J. K. Y.; Dehez, F.; Zerbetto, F. *Nature* **2003**, *424*, 174-179; Ragazzon, G.; Baroncini, M.; Silvi, S.; Venturi, M.; Credi, A. *Nat. Nanotech.* **2015**, *10*, 70-75; Feringa, B. L. *Molecular Switches* (Wiley-VCH, Weinheim, Germany, 2001).

[2] Anelli, P. L.; Spencer, N.; Stoddart, J. F. *J. Am. Chem. Soc.* **1991**, *113*, 5131-5133.

[3] Ogoshi, T.; Yamafuji, D.; Aoki, T.; Yamagishi, T. *Chem. Commun.* **2012**, *48*, 6842-6844.

[4] Kelly, T. R. *Acc. Chem. Res.* **2001**, *34 (6)*, 514-522; Caballero, A.; Swan, L.; Zapata, F.; Beer, P. D. *Angew. Chem. Int. Ed.* **2014**, *53*, 11854-11858.

[5] Altieri, A.;Gatti, F. G.; Kay, E. R.; Leigh, D. A.; Martel, D.; Paolucci, F.; Slawin, A. M. Z.; Wong, J. K. Y. *J. Am. Chem. Soc.* **2003**, *125 (28)*, 8644-8654.

[6] Balzani, V.; Credi, A.; Venturi, M. *Chem. Soc. Rev.* **2009**, *38 (6)*, 1542-1550; Brouwer, A. M.; *Science* **2001**, *291*, 2124-2128.

of solvent or pH,[7] and the new spatial arrangement of the components upon the movement can result in a considerable change in the chemical properties of the assembly, including the tuning of luminescence properties, the modification of the reactivity of specific residues or the activation of catalytic behavior.[8]

Molecular switches mainly operate in solution, but in this medium, the molecules are randomly dispersed and their motion is incoherent. Therefore, in order to achieve a higher level of molecular organization, chemists and material scientists are currently investigating about shuttles grafted on active surfaces[9] or incorporated into solid or rigid structures such as the bridging units of MOFs.[10]

One of the major difficulties in the realization of efficient and applicable operating molecular shuttles, however, lies in attaining full control on their directionality. Many examples are present in the literature in which the components of the machine are forced to move in a defined direction one with respect to the other by a series of successive and orthogonal chemical transformations. A more complicated strategy consists in exploiting the structural and chemical information stored in the supramolecular assemblies to induce, with a single external energy input, a spontaneous unidirectional motion of the parts. This involves the availment of inherently non-symmetrical components, arranged in univocally oriented architectures. Indeed, asymmetry is a fundamental factor in the majority of systems reported to date, not only for obtaining unidirectionality of motion, but also for demonstrating it.

4.2 Constitutionally isomeric calix[6]arene-based oriented rotaxanes

Among the class of supramolecular assemblies that can work as prototypes of molecular level machines, rotaxanes are very versatile systems able to perform many programmed tasks, including mechanical-like movement of the macrocyclic component along the threaded dumbbell,[11] and therefore to behave as molecular shuttles.

[7] Ashton, P. R.; Ballardini, R.; Balzani, V;. Baxter, I.; Credi, A.; Fyfe, M. C. T.; Gandolfi, M. T.; Gómez-López, M.; Martinez-Díaz, M. V.; Piersanti, A.; Spencer, N.; Stoddart, J. F.; Venturi, M.; White, A. J. P.; Williams, D. J. *J. Am. Chem. Soc.* **1998**, *120 (46)*, 11932-11942.

[8] Blanco, V.; Leigh, D. A.; Marcos, V.; Morales-Serna, J. A.; Nussbaumer, A. L. *J. Am. Chem. Soc.* **2014**, *136*, 4905-4908; Beswick, J.; Blanco, V.; De Bo, G.; Leigh, D. A.; Lewandowska, U.; Lewandowski, B.; Mishiro, K. *Chem. Sci.* **2015**, *6*, 140-143.

[9] Heinrich, T.; Traulsen, C. H. H.; Holzweber, M.; Richter, S.; Kunz, V.; Kastner, S. K.; Krabbenborg, S. O.; Huskens, J.; Unger, W. E. S.; Schalley, C. A. *J. Am. Chem. Soc.* **2015**, *137*, 4382-4390.

[10] Zhu, K.; O'Keefe, C. A.; Vukotic, V. N.; Schurko, R. W.; Loeb, S. J. *Nat. Chem.* **2015**, *7*, 514-519.

[11] Xue, M.; Yang, Y.; Chi, X.; Yan, X.; Huang, F. *Chem. Rev.* **2015**, *115*, 7398-7501.

Our previous investigation about [2]rotaxanes bearing tris(*N*-phenylureido)-calix[6]arene wheel **1** and 4,4'-bipyridinium-based symmetric axles of different length[12] (**Figure 4.2**), showed that these assemblies exhibit a response to electrochemical stimulation that is influenced by the length of the axle alkyl chains.

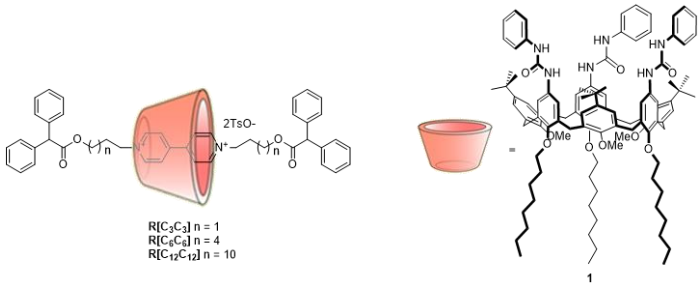

Figure 4.2 *Structure of receptor **1** and previously studied symmetric rotaxanes.*

In these rotaxanes, voltammetry experiments showed that the reduction potentials of the viologen core, and the consequent formation of the corresponding radical-cation, are influenced by the different proximity of the stoppers to the calixarene cavity.

From these results, we planned to investigate whether this class of rotaxanes could act as molecular shuttles and, in particular, if the length of the alkyl chains appended to the viologen core could be exploited as a control element to accomplish a preferential directional motion triggered by electrochemical stimulation. To this purpose, two new series of oriented non-symmetric rotaxanes **R[C_3C_{12}]**, **R[$C_{12}C_3$],** **R[C_6C_{16}]** and **R[$C_{16}C_6$]** (**Figure 4.3**) were devised:

[12] Arduini, A.; Bussolati, R.; Credi, A.; Pochini, A.; Secchi, A.; Silvi, S.; Venturi, M. *Tetrahedron* **2008**, *64*, 8279-8286.

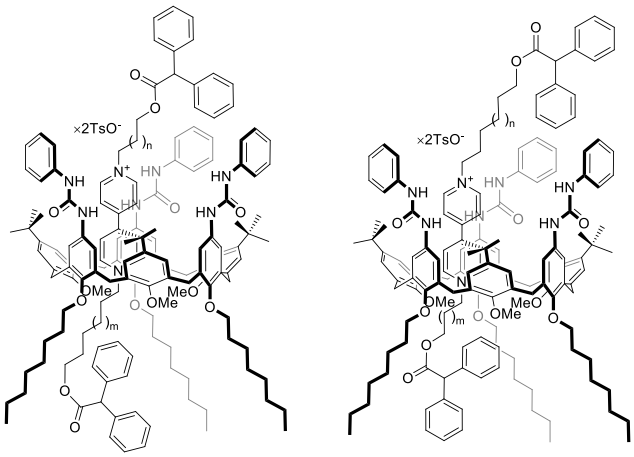

Figure 4.3 *Structure of the asymmetric rotaxanes*.

In these systems, both the axle and the wheel components are non-symmetric: as reported in the introductive chapter, the calixarene **1** presents two rims which differ both for size and chemical properties, and the dumbbells are decorated with two alkyl chains with an appropriate difference in length, in particular one propyl and one dodecyl chain and with one hexyl and one hexadecyl chain. Moreover, in each molecule, the components are arranged in an univocal and controlled relative orientation, giving rise to constitutionally isomeric oriented rotaxanes. Since the functionalized calixarene is non-palindrome, the movement of the wheel towards one side of the axle is chemically not equivalent to the one towards the opposite side, possibly leading to a preferential direction of motion and thus generating specific translational isomers.

4.2.1 Synthesis and structural characterization

In order to achieve the formation of each orientational isomer, we designed axles **2a-c**, functionalized with an alkyl substituent bearing a terminal bulky group that cannot slip through the calix[6]arene rims, and with another alkyl chain ending with an OH moiety. This latter head group neither hampers nor alters the threading process, and it is useful for the attachment of the second stopper upon insertion of dumbbells **2a-c** into the wheel cavity. These axles were synthesized according to **Scheme 4.1**. Tosylate **4**, obtained from the corresponding diol **3**, was first reacted with diphenylacetyl chloride to insert the first stopper. The resulting product **5** was heated to reflux overnight with 4,4'-bipyridine in acetonitrile to give salt **6**. Subsequent alkylation with

the OH-terminated tosylate **4** afforded the monostoppered axles **2a-c** (see experimental for all characterization and synthetic details).

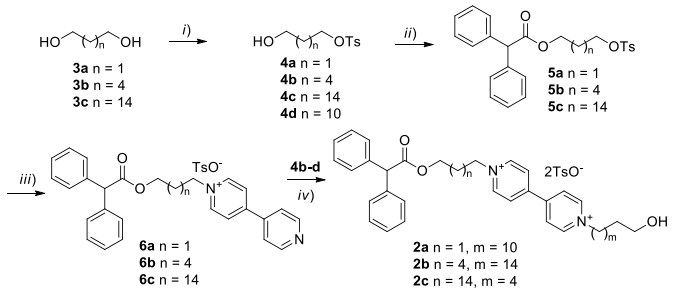

Scheme 4.1: *Reagents and conditions: i) TsCl, NEt_3, DMAP, CH_2Cl_2 rt, 3 h; ii) $Ph_2CHCOCl$, THF rt, 12 h; iii) 4,4'-bipyridine, CH_3CN reflux, 12 h; iv) CH_3CN, reflux, 7 d.*

Selective preparation of oriented assemblies from wheel **1** and axles **2a-c** was possible because of the inherent complexing properties of **1**, explained in detail in the introductive chapter. In fact, previously performed studies demonstrated the selective threading of OH-terminated bipyridinium-based axles from the upper rim of wheel **1**. Indeed, formation of hydrogen bonds between the ureido groups and the anions of the guest favour the insertion of the stoppered axle from the upper rim, whereas the methoxy groups, oriented inward the cavity in the NMR timescale, hamper the access of the dumbbell from the lower rim. For instance, in axle **2a**, the diphenylacetic group prevents the threading of the shortest chain C3, and the univocal insertion of chain C12 from the upper rim of the wheel leads to the exclusive formation of pseudorotaxane **P[1⊃2a]** presenting the orientation depicted in **Scheme 4.2**. This peculiar property was exploited to obtain the desired oriented rotaxanes by a sequential threading-and-stoppering strategy. The same protocol was followed for all the rotaxanes. Wheel **1** was dissolved in toluene and equilibrated for two hours at room temperature with one equivalent of stoppered axle **2a-c**. Upon formation of the oriented pseudorotaxane complexes **P[1⊃2a]**, **P[1⊃2b]**, and **P[1⊃2c]**, indicated by the complete dissolution of the otherwise insoluble axle and by the appearance of a typical dark-red color of the resulting homogeneous solution, a slight excess of triethylamine and diphenylacetyl chloride was added. The mixture was then stirred at room temperature overnight[13]. After chromatographic separation, rotaxanes **R[C_3C_{12}]**, **R[C_6C_{16}]**, and **R[$C_{16}C_6$]** were isolated in 57, 43, and 40 % yield, respectively. The rotaxane **R[$C_{12}C_3$]** was obtained in very poor yield and was contaminated by several

[13] Both equilibration and stoppering reaction were performed at room temperature to avoid any possible scrambling of the axles into **1**, and the consequent formation of mixtures of orientational isomers.

by-products that prevented its full characterization and was therefore excluded from this study.

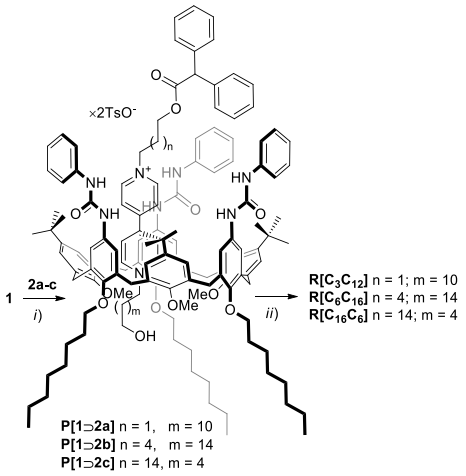

Scheme 4.2 *Reagents and conditions: i)Toluene, rt, 3 h; ii) $Ph_2CHCOCl$, NEt_3, rt, 12 h.*

The properties of these non-symmetric rotaxanes were compared with those of the corresponding symmetrical counterparts. **R[C_3C_3]**, **R[C_6C_6]** and **R[$C_{12}C_{12}$]** are known compounds,[12] whereas **R[$C_{16}C_{16}$]** was synthesized by equilibrating wheel **1** and symmetrical axle **7** in toluene at room temperature and adding two equivalents of triethylamine and diphenylacetyl chloride (**Scheme 4.3**).

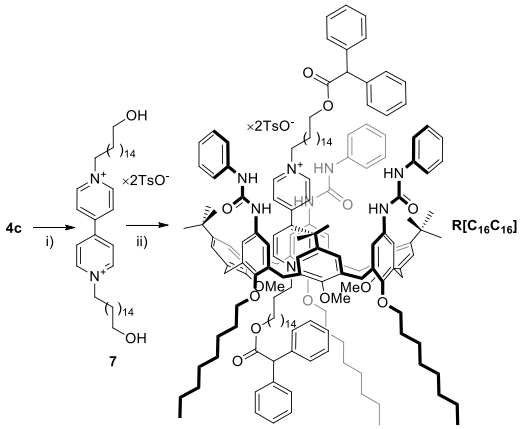

Scheme 4.3 *Reagents and conditions: i) 4,4'-bipyridine, CH_3CN reflux,7 d; ii) a) **1**, toluene, rt, 3 h. b) $Ph_2CHCOCl$, NEt_3, rt, 12 h.*

Each synthesized rotaxane was analyzed by NMR techniques to gain information on the structure and the relative orientation of the components (see expanded regions in **Figure 4.4** and Experimental for full characterization). Significantly, in all the rotaxanes the wheel component **1** exhibits a conformational rearrangement typical of a rotaxane-type assembly. This is evidenced, for instance, by the ^{1}H NMR signal of the NH ureidic protons, involved in hydrogen bonds with anions of the guests, that are remarkably downfield shifted in comparison with the spectrum of free **1**, and by the downfield shift endured by the peak attributed to the methoxy groups that, in the threaded form, are oriented outward the cavity. In the spectra of **R[C_3C_{12}]**, **R[C_6C_{16}]** and **R[$C_{16}C_6$]**, the methoxy groups of the wheel resonate as a sharp singlet at δ = 3.85, 3.86 and 3.80 ppm, respectively. The singlet shape of this signals is diagnostic for the presence of single orientational isomers. Indeed, the chemical shift of methoxy groups is remarkably affected by the proximity of the lower stopper of the axle, and consequently by the length of the lower alkyl chain of the dumbbell. In the presence of a mixture of orientational isomers, this signal would be split. The orientation of the axle into **1** also affects the chemical shift of several protons of the dumbbell component, especially the methyne protons α and α' and the O-CH_2 protons 1 and 1'.

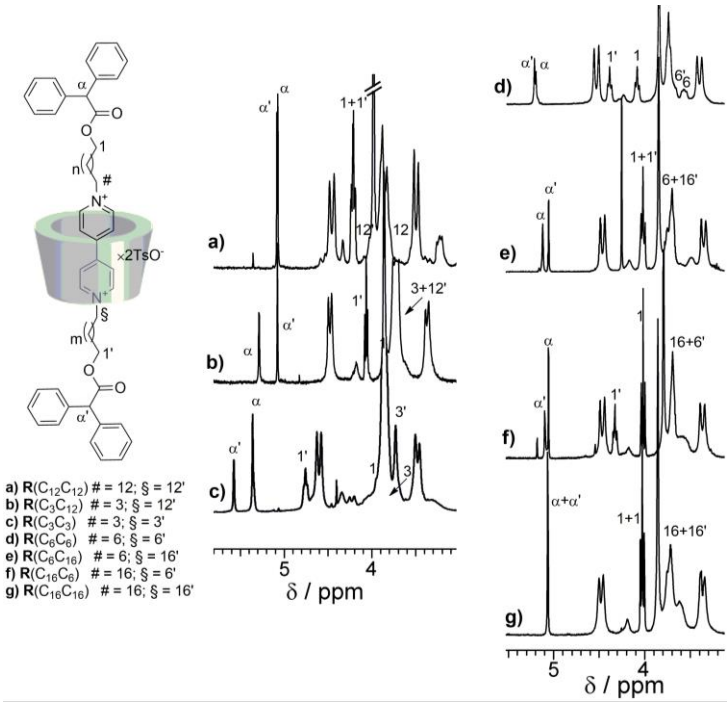

Figure 4.4 *^{1}H NMR spectra (300 MHz, C_6D_6, 3-6 ppm region) of symmetric and asymmetric rotaxanes. See drawing for labelling.*

Comparison of these signals with those found in the ^{1}H NMR spectra of the symmetrical rotaxanes **R[C_3C_3]**, **R[C_6C_6]**, **R[$C_{12}C_{12}$]** and **R[$C_{16}C_{16}$]** provided evidence for the relative orientation of the components. As an example, in **R[C_3C_{12}]**, α and α' protons resonate at δ = 5.30 and 5.07 ppm, respectively, in agreement with the presence of an upward C3 chain and a downward C12 chain. The absence of signals at δ = 5.56 ppm excluded the presence of the opposite orientational isomer with a C3 lower chain. As further evidence, the signal of O-CH_2 protons (1) related to the upper chain of **R[C_3C_{12}]** was detected at 3.7 ppm, confirming the presence of a C3 upper chain. As shown in the symmetrical rotaxane **R[$C_{12}C_{12}$]**, the same signal would be shifted to 4.2 ppm in the opposite orientational isomer with a C12 upper chain. In the same way, the signal of 1' protons located at δ = 4.06 ppm was consistent with a C12 lower chain. In case of a C3 lower chain, this signal would be shifted to δ = 4.74 ppm. Furthermore, the signals of # and § protons, as well as 2D NMR correlations (see Experimental), confirmed the relative orientation of the components. Similarly, the univocal orientation of **R[C_6C_{16}]** and **R[$C_{16}C_6$]** was established. Chemical shifts of the most significant and diagnostic signals are gathered in **Table 4.1**.

Rotaxane	O-CH_3	α	α'	1	1'	#	§
R(C_3C_{12})	3.85	5.30	5.07	3.6-3.8	4.06	3.60	3.60
R(C_3C_3)	3.7-3.9	5.34	5.56	3.7-4.0	4.74	3.50	3.6-3.7
R($C_{12}C_{12}$)	3.90	5.09	5.09	4.1-4.2	4.1-4.2	3.75	3.90
R(C_6C_{16})	3.86	5.13	5.07	4.03	4.03	3.70	3.7-3.8
R($C_{16}C_6$)	3.80	5.06	5.10	4.02	4.33	3.70	3.70
R(C_6C_6)	3.84	5.16	5.17	4.08	4.38	3.60	3.70
R($C_{16}C_{16}$)	3.86	5.07	5.07	4.03	4.03	3.7-3.8	3.7-3.8

Table 4.1 *Chemical shifts (δ, ppm) of some of the most significant signals of synthesized symmetric and non-symmetric rotaxanes; ^{1}H NMR spectra are recorded in C_6D_6 at room temperature with a 300 MHz spectrometer.*

The obtained rotaxanes were also analyzed via UV-Vis absorption measurements (**Figure 4.5**).

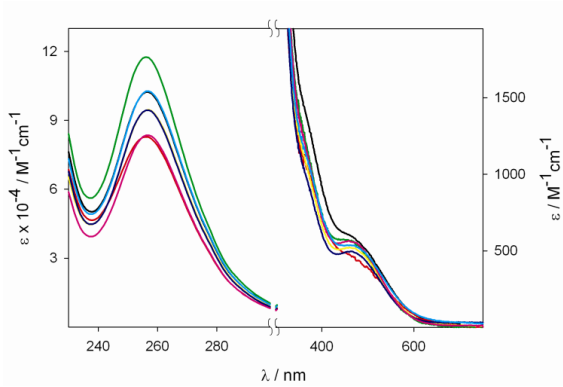

Figure 4.5 *Absorption spectra of the rotaxanes in acetonitrile:* ***R[C12C12]*** *(green);* ***R[C3C3]*** *(black) and* ***R[C3C12]*** *(cyan);* ***R[C6C6]*** *(red) and* ***R[C6C16]*** *(pink);* ***R[C16C16]*** *(yellow, below the blue line) and* ***R[C16C6]*** *(blue).*

In agreement with previous investigations, all the rotaxanes exhibited two main absorption bands: one, more intense and located in the UV region, ascribed to the absorption of the phenylureido moieties and the bipyridinium core, and a second weaker one around 460 nm, arisen from the charge transfer interaction. Both the energy and the absorption coefficient of this latter band are independent of the length of the axles, suggesting that the donor-acceptor electronic coupling, i.e. the extent of encapsulation of the bipyridinium core in the calixarene cavity, is similar for all the rotaxanes. On the other hand, the coefficient of the band in the UV region is not constant. In particular, rotaxanes bearing chains of the same lenght at the upper rim show comparable bands, thus meaning that the proximity of the stopper to the phenylureido moieties has an influence on their absorption.

4.2.2 Electrochemical investigation

Beside the detailed design of the molecular components and the complete assessment of their relative spatial arrangement, other key requirements are the possibility to induce and to detect the relative movement of the parts, and eventually to monitor the direction of motion. We planned to trigger the shuttling via electrochemical stimulation. It is in fact well known that the reduction of the bipyridinium core of the axle weakens the interaction between the components, causing the disassembly of pseudorotaxane-type systems. In rotaxanes, the dethreading is prevented by the bulky stoppers and, indeed, we envisaged that the reduction of the bipyridinium core could induce an oscillation of the wheel along the dumbbell.

Electrochemical investigations were performed by cyclic voltammetry (CV) and differential pulse voltammetry (DPV) on all the rotaxanes and on 1,1'-dioctyl-4,4'-bipyridinium (**DOV**), which was used as a model compound for the bipyridinium unit of the axles. All the potential values are reported versus the standard calomel electrode (SCE). Acetonitrile was chosen as solvent, mainly for reproducibility reasons, but also because some interactions, such as solvophobic effects and hydrogen bonds, are weakened by the polarity of this solvent. We envisaged that this effect could be exploited to maximize the destabilization due to the electrochemical reduction, and cause an easier displacement of the components.

The model compound **DOV** shows two reversible monoelectronic reduction processes at –0.42 and –0.86 V. In presence of an equimolar amount of calix[6]arene **1**, the pseudorotaxane **P[1⊃DOV]** is formed with an association constant around 5×10^4 M^{-1}, meaning that at the concentration of these electrochemical experiments, 25 % of axle is present in its free form. The first reduction process shows two cathodic peaks, related to the free and complexed axle, and only one anodic peak, at the same potential of the free axle. This behaviour suggests that the radical cation is not associated with the calix[6]arene. Indeed, the second reduction process takes place at –0.86 V, that is the same potential of the radical cation derived from free **DOV**, confirming that the pseudorotaxane dissociates after the first reduction. All the rotaxanes show two reversible or quasireversible monoelectronic reduction processes at more negative potential values with respect to the free bipyridinium derivative (all the reduction potentials are gathered in **Table 4.2**). The reversibility of the electrochemical waves suggests that either no conformational rearrangements take place, or the rearrangements are fast on the timescale of the electrochemical experiment. The shift toward negative potential values of the second reduction potential confirms that the reduced forms of the bipyridinium still interact with the calix[6]arene, when the reduction is performed on interlocked complexes.

	E_1 (V)	E_2 (V)
DOV	-0.42	-0.86
R(C_3C_3)	-0.64*	-1.15*
R(C_6C_6)	-0.62	-1.14
R($C_{12}C_{12}$)	-0.62	-1.18
R($C_{16}C_{16}$)	-0.62	-1.24*
R(C_3C_{12})	-0.60	-1.16
R(C_6C_{16})	-0.62	-1.22*
R($C_{16}C_6$)	-0.61	-1.11

Table 4.2 *Electrochemical potentials vs SCE obtained by CV in acetonitrile. *=data obtained by DPV.*

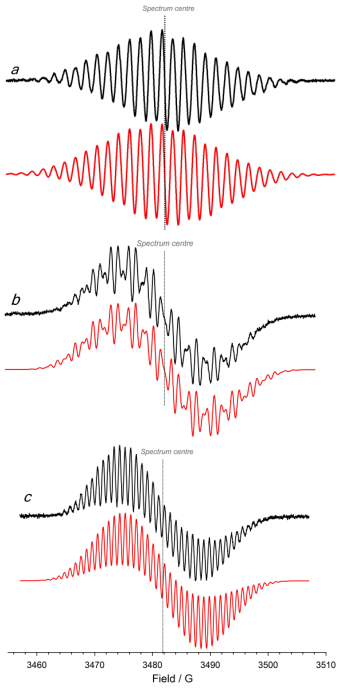

Figure 4.6 *EPR spectra (black) of the radical cation deriving from* ***DOV*** *(a),* ***R[$C_{16}C_{16}$]*** *(b) and* ***R[C_3C_{12}]*** *(c). In red are reported the corresponding theoretical simulations.*

To gain more information on the consequences of electrochemical reduction, we performed EPR experiments on the radical cation of model compound **DOV** and on the synthesized rotaxanes. The radicals were generated inside the EPR cavity by *in situ* electrochemical reduction in deoxygenated acetonitrile at room temperature. The EPR spectrum of free **DOV** (see red line in **Figure 4.6a**) can be simulated on the basis of the coupling of the unpaired electron with two equivalent N atoms, with a hyperfine coupling constant of 4.11 G, and 12 H atoms. The latter can be divided into four protons on the methylene groups of the two chains (α_{CH2} 4.07 G) and two equivalent sets, each of four protons [α (Ar)H_α and α(Ar)H_β] on the aromatic nucleus. The smaller hyperfine coupling constant for these H atoms can be assigned to the aromatic α-protons (1.10 G) whereas the larger coupling can be assigned to the aromatic β protons (1.59 G). The g factor was found to be 2.0031. In the spectra of all the symmetric rotaxanes, a significant change in the shape of the EPR spectrum was clearly observed. As an example, the EPR spectrum obtained after electrochemical reduction of the symmetric rotaxane **R[$C_{16}C_{16}$]** is reported (**Figure 4.6b**). It is evident that the spectra centres no longer correspond to an horizontal line: this feature can be reproduced only by considering a non-symmetric distribution of the spin density in the two heterocyclic rings of the radical cation, confirming that in these rotaxanes the

mono-reduced axle is still confined into the aromatic cavity of **1**. In each case, the g-factor was found to be close to 2.0031.

Also regarding non-symmetric rotaxanes (see as an example **R[C_6C_{16}]** in **Figure 4.6c**), the spectra could be reproduced only by assuming different spin density distribution in the two heterocyclic rings. Moreover, the spectroscopic parameters obtained from the corresponding theoretical simulation were very similar to those measured in the radical cation deriving from the geometrical isomer **R[C_6C_{16}]**.

The fitting parameters obtained by simulation of spectral patterns of all rotaxanes and model **DOV** are summarized in **Table 4.3**:

	a_N	a_N	a_{CH_2}	a_{CH_2}	$a_{(Ar)2H\beta}$	$a_{(Ar)2H\beta}$	$a_{(Ar)2H\alpha}$	$a_{(Ar)2H\alpha}$
DOV	4.11	4.11	4.07	4.07	1.59	1.59	1.10	1.10
R(C_3C_3)	4.34	3.85	4.02	2.76	1.83	1.83	1.19	1.19
R(C_6C_6)	4.34	4.04	4.02	2.72	1.77	1.74	1.10	1.10
R($C_{12}C_{12}$)	4.41	3.92	4.05	2.73	1.83	1.77	1.10	1.06
R($C_{16}C_{16}$)	4.36	4.02	4.02	2.72	1.80	1.76	1.10	1.10
R(C_3C_{12})	4.37	3.82	3.93	2.70	1.99	1.81	1.03	0.96
R(C_6C_{16})	4.42	3.90	3.96	2.69	1.80	1.80	1.14	1.14
R($C_{16}C_6$)	4.32	4.00	4.04	2.66	1.83	1.75	1.18	1.09

Table 4.3 *EPR hyperfine splitting constants (a, Gauss) of radical cations obtained after electrochemical reduction of the bipyridinium unit at r.t. in CH_3CN.*

These observations proved that the bipyridinium radical cations in all the rotaxanes experience a different environment in comparison with the free axle, regardless of the length of the alkyl chains and their position with respect to the wheel. In other words, our results indicate that, after monoreduction of the bipyridinium unit, the wheel is still located close to the radical cation.

4.2.3 Conclusions

In this first part of the chapter, a sequential threading-and-capping strategy, that exploits the spontaneous directional threading of monostoppered viologen axles into a phenylureido calix[6]arene receptor, was presented. This method allows the formation of non-symmetric rotaxanes as single orientational isomers. Cyclic voltammetry and EPR were proven to be effective techniques to steer the dynamic behaviour of these systems. It was evidenced that the proximity of the stoppers to the upper or lower rim of **1** has a slight effect on absorption coefficient in the UV region and on reduction potentials, but has no influence on their dynamic response. Unfortunately, contrarily to what observed for pseudorotaxane assemblies, from the results obtained so far we can state that the bipyridinium reduction alone is not sufficient to induce any

detectable shuttling of the macrocyclic component when the axle is mechanically interlocked in a rotaxane-type structure, regardless of the length of the dumbbell.

4.3 Double-station rotaxanes

From the results described above, it emerged that, before seeking for directionality of motion, the presence of a further recognition element is mandatory to facilitate the displacement and make the electrochemical stimulus effective to promote the shuttling in our interlocked systems. We thus focused our attention on double station rotaxanes, equipped with two distinct recognition sites (stations) on their dumbbell-shaped component, in which the macrocycle can move from one site to the other in a controlled and reversible manner.

To achieve our goal, it is crucial that the two stations exhibit a different association strength with the receptor. If this is the case, the rotaxane can exist as two different equilibrating co-conformations, the populations of which reflect their relative free energies, determined by the extent of the two different sets of non-covalent bonding interactions.

For instance, in the schematic model depicted in **Figure 4.7**, the molecular ring preferentially resides around the first station *A* (*state 0*), until a stimulus that switches off this recognition site (*A* → *A'*) is applied. As a consequence, the system is brought into a non-equilibrium state, and the components subsequently rearrange according to the new potential energy landscape. This process implies the motion of the molecular ring to the second recognition site (station *B*), so that the new equilibrium is reached (*state 1*). If station *A* is switched on again by an opposite stimulus, the original energetical situation is restored, and another co-conformational equilibration occurs. An alternative and complementary approach would be to modify station *B*, through appropriate stimulation, in order to make it a more favored recognition site compared to *A*.

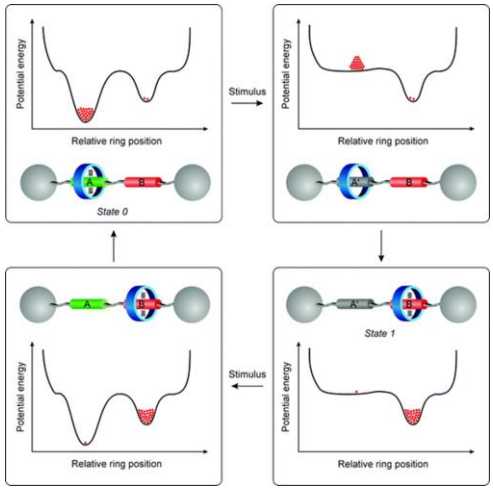

Figure 4.7 *Schematic representation of a double-station rotaxane acting as molecular shuttle and corresponding potential energy landscape for each relative position (modified from ref. 1, copyright © Royal Society of Chemistry).*

4.3.1 Design

The synthesis of novel double station rotaxanes, constituted of triphenylureido calix[6]arene **1** and dialkylviologen-based axles endowed with an ammonium station as second recognition unit on the dumbbell, was devised.

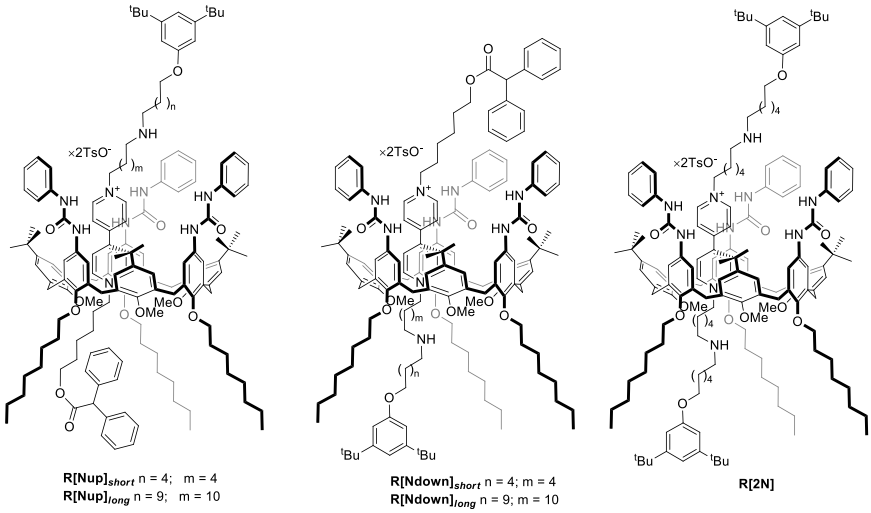

Figure 4.8 *Structure of the double station rotaxanes* ***R[Nup]$_{short}$, R[Nup]$_{long}$, R[Ndown]$_{short}$, R[Ndown]$_{long}$*** *and* ***R[2N]***.

Like in previously examined systems, initially the macrocycle will reasonably reside exclusively around the electron-poor bipyridinium unit, by virtue of the well-known set of supramolecular interactions. Upon reduction, we expect that the weakening of the charge transfer interaction, together with the generation of the second recognition unit through protonation of the secondary amine, may facilitate the slippage of **1** along the dumbbell, until the wheel encircles the ammonium moiety, that is going to be the new most favored station. The association constant between **1** and dialkylammonium guests was never measured; nevertheless, we expect a lower value with respect to viologen dication, but still sufficient[14] to ensure a proper complexation when compared to the radical-cation generated upon reduction.

To gain information about an eventual preferential shuttling direction, pivoted by the inherent asymmetry of **1**, we planned to investigate two different series of orientational rotaxane isomers (*up* and *down*), in which the ammonium station faces the two opposite rims of the macrocycle. To have an insight about the influence of the spacers length, and make sure that the movement is not impeded by neighboring molecular components, each isomer was synthesized with dodecyl (*long*) and hexyl (*short*) alkyl chains. As a control model, also triple-station rotaxane **R[2N]**, bearing an ammonium station in proximity to each rim of **1,** was synthesized.

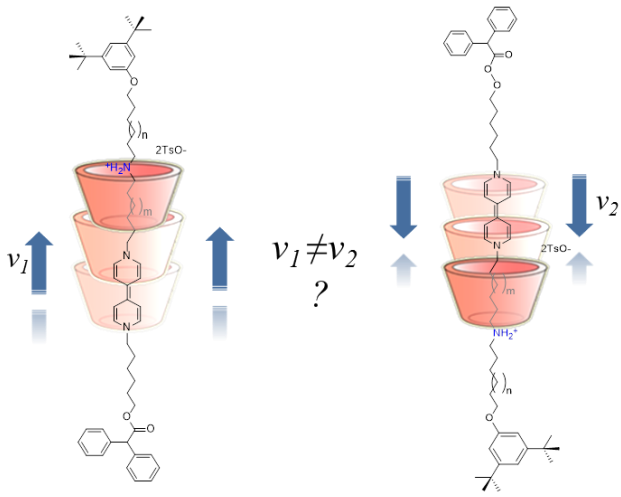

Figure 4.9 *Hypothesized working mode of double station rotaxanes.*

[14] Talotta, C.; De Simone, N. A.; Gaeta, C.; Neri, P. *Org. Lett.* **2015**, *17*, 1006-1009; Casnati, A.; Jacopozzi, P.; Pochini, A.; Ugozzoli, F.; Cacciapaglia, R.; Mandolini, L.; Ungaro, R. *Tetrahedron* **1995**, *51 (2)*, 591-598; Schalley, C. A.; Castellano, R. K.; Brody, M. S.; Rudkevich, D. M.; Siuzdak, G.; Rebek, J. *J. Am. Chem. Soc.* **1999**, *121*, 4568-4579.

4.3.2 Synthesis *via* sequential threading-and-capping strategy

Taking inspiration from the previously followed protocol, we designed the synthesis of axles endowed with a bulky stopper at one end, and a terminal OH group appended at the opposite side. Concerning the *up* isomers, the appropriate axles **8a-b**, in which the secondary amine function is present between the stopper and the viologen unit, were synthesized according to **Scheme 4.4**. Boc-protected aminoalcohol **10** was first treated with *p*-toluenesulphonyl chloride and the resulting product **11** was reacted with 3,5-di-tert-butylphenol to insert the first stopper. The secondary amine was then formed through a nucleophilic substitution between **12** and an excess of 1,6-dibromohexane for **13a** or 1,12-dibromododecane for **13b**. Reaction of bromide **13** with OH-terminated monoalkylviologen **14** afforded axles **8a-b** (see Experimental for detailed synthetical procedures and NMR characterization).

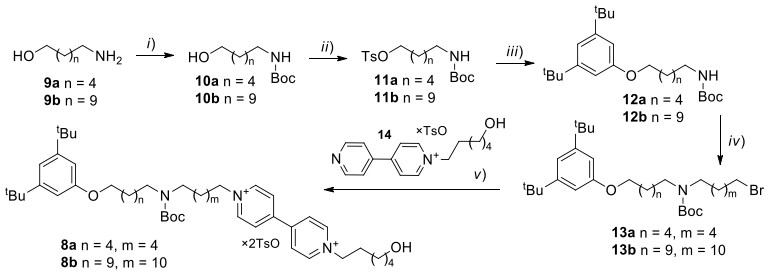

Scheme 4.4: *Reagents and conditions: i) Boc_2O, MeOH/NEt_3, reflux, 2h; ii) TsCl, NEt_3, DMAP, CH_2Cl_2 rt, 8 h; iii) 3,5-di-tert-butylphenol, K_2CO_3, DMF, 80°C, 18 h; iv) a)NaH, DMF, 0°C to rt, 2h; b) 1,6-dibromohexane (**13a**) or 1,12-dibromododecane (**13b**), DMF, rt, 18 h; v) CH_3CN, reflux, 7 d.*

Axles **8a-b** were then equilibrated in toluene at room temperature with an equivalent amount of **1**. The suspension turned homogeneous after three hours and the red color, commonly ascribed to the formation of pseudorotaxane-like structure, was observed. As for non-symmetric rotaxanes, the unidirectional threading of axles from the upper rim of **1**, together with the presence on the salt of a terminal bulky stopper, led to exclusive formation of oriented pseudorotaxanes **P[1⊃8a]** and **P[1⊃8b]** illustrated in **Scheme 4.5**. The following stoppering reaction, performed at room temperature with diphenylacetylchloride and triethylamine, yielded Boc-protected single orientational rotaxane isomers. These products were finally deprotected by addition of trifluoroacetic acid, to obtain double station rotaxanes **R[Nup]$_{short}$** and **R[Nup]$_{long}$** in 55% and 27% yield, respectively.

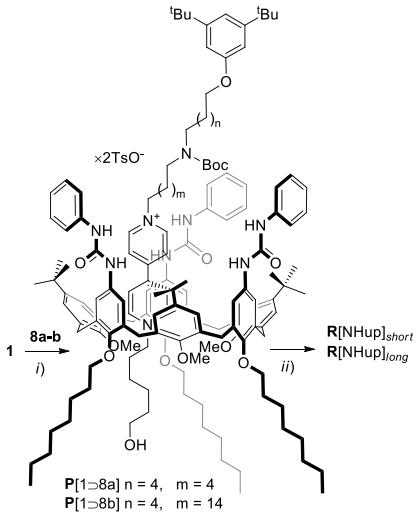

Scheme 4.5 *Reagents and conditions: i)toluene, rt, 3 h; ii) a) $Ph_2CHCOCl$, NEt_3, rt, 12 h; b)TFA, CH_2Cl_2, 3h, rt.*

Regarding the *down* isomers, axles **15a-b**, equipped with the secondary amine function between the viologen unit and the terminal OH group were designed. The synthetical pathway is displayed in **Scheme 4.6** (see Experimental for details). Boc-protected aminoalcohol **10** was first transformed in the silyl ether **16** and then reacted with the appropriate dibromide (1,6-dibromohexane or 1,12-dibromododecane) to obtain the secondary amine **17**. The following step consisted in the deprotection of the -OH group: all common cleavages of the silyl ether attempted with fluoride anion led to fluorination of the terminal bromine of **18**, and therefore quenched its reactivity towards the following nucleophilic substitution. Finally, deprotection with anhydrous $CeCl_3$[15] afforded the chlorinated amine **18**, that presents a terminal hydroxyl moiety and a suitable leaving group (Cl) for the alkylation of bipyridine. The second part of the axle - i.e. the bipyridine **21** functionalized with a stoppered alkyl chain - was obtained by reacting 4,4'-bipyridine with alkylating agent **20**, starting from tosylate **19** and 3,5-di-tert-butylphenol. Residues **18** and **21** were then refluxed in acetonitrile to afford axles **15a-b**.

[15] Ankala, S. V.; Fenteany, G. *Tetrahedron Lett.* **2002**, *43*, 4729-4732.

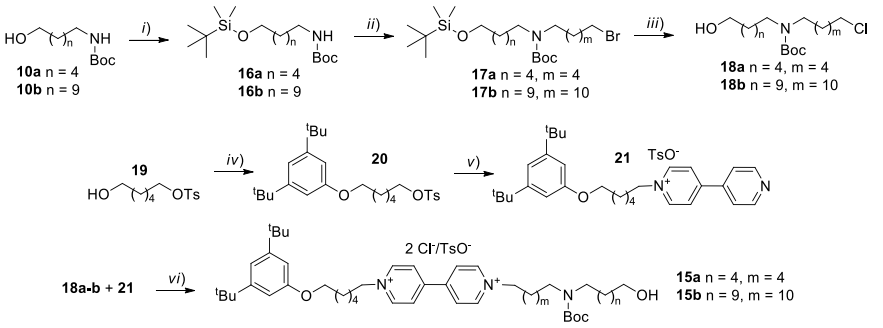

Scheme 4.6: *Reagents and conditions: i) TBDMS-Cl, NEt_3, CH_2Cl_2, 24h; ii) a) NaH, DMF, 0°C to rt, 2h; b) 1,6-dibromohexane (**17a**) or 1,12-dibromododecane (**17b**), DMF, rt, 18 h; iii) $CeCl_3$, CH_3CN/DMF, reflux, 3 d; iv) 3,5-di-tert-butylphenol, K_2CO_3, DMF, 80°C, 18 h; v) 4,4'-bipiridyne, CH_3CN, reflux, 12h; vi) CH_3CN, reflux, 7d.*

Axles **15a-b** were mixed with an equimolar amount of **1** in toluene solution. In this equilibration reaction, no hints of complexation were observed: the reaction mixture never turned red, neither upon heating at reflux for several hours, and salts **15a-b** were still not solubilized. In ESI-MS analysis (performed in MeOH to provide the solubility of the salts) it was possible to identify the m/z peaks related to unreacted reagents, meaning that no side reaction or degradation took place, and **1** was recovered quantitatively after chromatographic separation.

The impossibility to obtain any pseudorotaxane complex was mainly ascribed to the bulkiness of the protected secondary amine and to its tetrahedral geometry, that prevent the threading of the axle bearing the carbamate moiety in proximity to the lower rim of the wheel. For these reasons, we ascertained that this sequential threading-and-capping approach is suitable for the synthesis of the only orientational isomers presenting an upper second station **R[Nup]$_{short}$** and **R[Nup]$_{long}$**.

4.3.3 Synthesis *via* supramolecularly assisted strategy

The threading-and-capping sequential strategy for the formation of rotaxanes has shown remarkable advantages, such as complete orientational selectivity, but its major drawback is the impossibility to obtain assemblies presenting bulky moieties exposed downward or arranged in non-linear conformations, because such dumbbells can not efficiently thread the wheel component. To overcome these limitations, we envisaged to investigate whether the new findings about the supramolecularly assisted synthesis of oriented rotaxanes can be extended to more complicated and

highly functionalized systems, in order to obtain new assemblies that could not be synthesized with traditional procedures.

In **Chapter 2,** it was demonstrated that the alkylation of piridyl-pyridinium salts functionalized with linear alkyl chains, in presence of **1**, takes place preferentially through the cavity of the calix[6]arene, giving rise to the formation of pseudorotaxane structures. If a bulky terminal group is present on the monoalkylviologen, the following assisted alkylation and stoppering reactions lead to the formation of oriented rotaxanes, in which the alkyl chain initially appended to the viologen, regardless its length, is located close to the lower rim of the wheel.

Starting from these results, we planned to verify if the supramolecular assistance and the orientational selectivity are maintained even if different substituents are present both on the salt and on the alkylating agent, and double station rotaxanes **R[Ndown]$_{short}$** and **R[Ndown]$_{long}$** were found to be suitable candidates for this approach. We therefore synthesized the properly designed monoalkylviologen **22**, characterized by the Boc-protected secondary amine function and by the presence of the terminal phenolic stopper. As alkylating agent, we exploited 6-bromohexyl 2,2-diphenylacetate **23**, already equipped with the terminal diphenylacetic stopper. Salt **22**, wheel **1** and bromide **23** were refluxed in toluene in a supramolecularly assisted rotaxanation reaction similar to the ones described in **Chapter 2** (see **Scheme 4.7**), and the reaction was complete after two days.

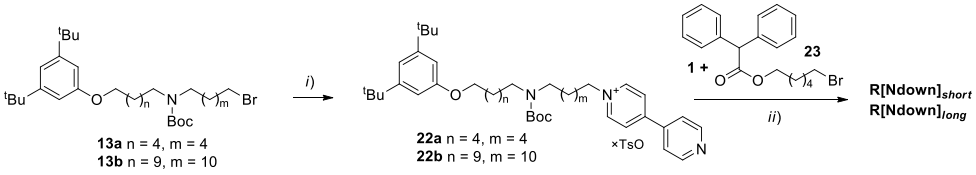

Scheme 4.7: *Reagents and conditions: i) 4,4'-bipiridyne, CH_3CN, reflux, 12h; ii) a)Toluene, reflux, 2d; b)TFA, CH_2Cl_2, rt, 2h.*

Successfully, chromatographic separation of the crude mixture and treatment with trifluoroacetic acid, gave the desired oriented double-station rotaxanes **R[Ndown]$_{short}$** and **R[Ndown]$_{long}$**, isolated in 58% and 69% yield respectively.

The formation of triple station rotaxane **R[2N]** was achieved through an even more simplified supramolecularly assisted reaction. Since the dumbbell is characterized by the presence of two identical chains appended to the viologen core, we envisaged the possibility to obtain in a one-pot reaction:

i) first, salt **22a** from 4,4'-bipyridine and bromide **13a,** and

ii) afterwards, rotaxane **R[2N]**, by simply exploiting the presence of **1** and a stoichiometric excess of **13a**, that is the alkylating agent needed also as the upper part of the axle.

Therefore, wheel **1** was refluxed in toluene in presence of an equimolar amount of 4,4'-bipyridine and a stoichiometric excess (3:1) of **13a**. The reaction was complete after four days, after which chromatographic treatment and acidic deprotection afforded triple station rotaxane **R[2N]** (40%).

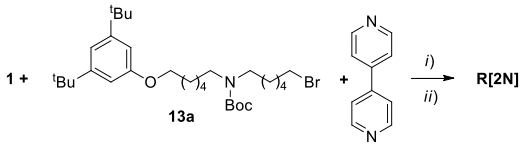

Scheme 4.8: *Reagents and conditions: i) Toluene, reflux, 4d; ii) TFA, CH_2Cl_2, rt, 2h.*

4.3.4 Structural characterization

The obtained rotaxanes were analyzed by NMR techniques to prove the relative arrangement of the components. In all the ^{1}H NMR spectra, the wheel component undergoes some typical modifications that indicate the inclusion of the guest, mainly indicated by the downfield shift of ureidic protons at the upper rim, involved in hydrogen bonding, and methoxy groups at the lower rim that are oriented outward with respect to the cavity. As discussed for asymmetric rotaxanes, the sharp singlet shape of this latter signal implies the presence of single orientational isomers. The methylene bridges resonate as two doublets at ca. 4.4 and 3.3 ppm, indicating that the *cone* conformation is retained.

Comparison between the ^{1}H NMR spectra of the rotaxanes is shown in **Figure 4.10**. In the spectra of the *up* isomers (**R[Nup]**$_{short}$ and **R[Nup]**$_{long}$) the presence of the singlet at 5.10 ppm ascribed to the methyne proton (α) of the diphenylacetic group, and the triplet at 4.33 ppm attributed to the methylene protons (1) adjacent to the same stopper, are in agreement with the presence of a C6 alkyl chain directed toward the lower rim of **1**[16]: this implies that the portion of the axle bearing the amine moiety is positioned in proximity to the upper rim of the wheel. On the contrary, in the spectra of the *down* isomers **R[Ndown]**$_{short}$ and **R[Ndown]**$_{long}$, the signal of the

[16] See comparison with **R[C_6C_6]** in **Table 4.1**.

methyne proton (α') resonates at 5.12 ppm, and the methylene group (1') adjacent to the diphenylacetic stopper gives rise to a triplet at 4.03 ppm. These findings are in agreement with the presence of an upward C6 alkyl chain,[16] thus meaning that the amine moiety is positioned close to the lower rim of **1**.

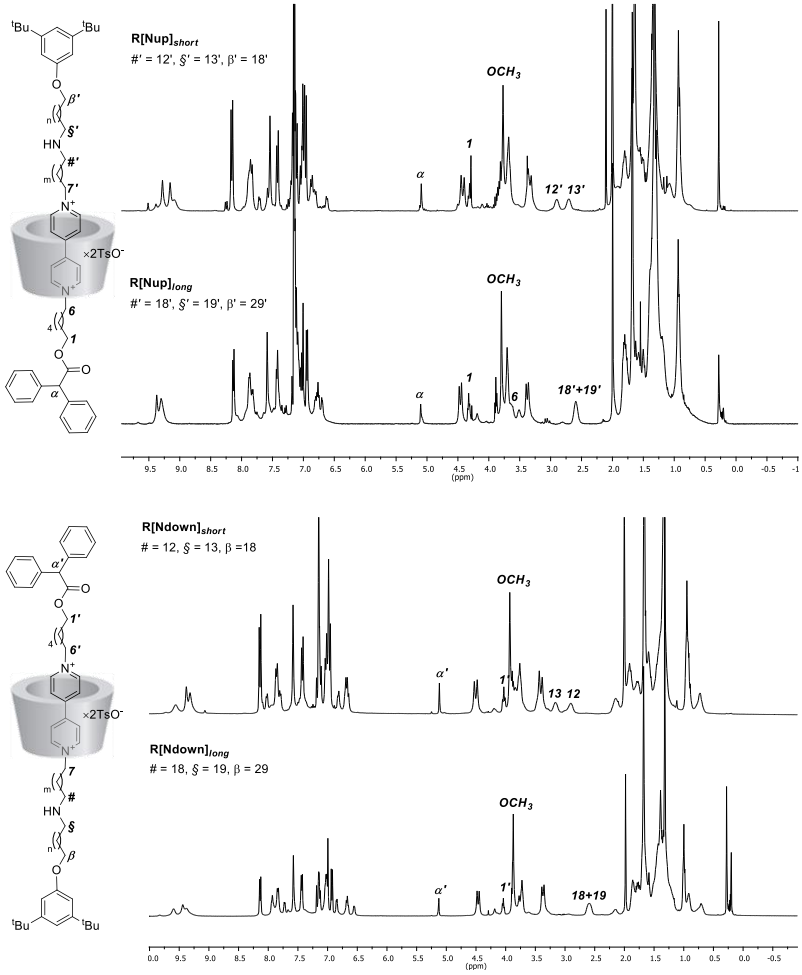

Figure 4.10: *^{1}H NMR spectra (C_6D_6, 400 MHz) of double station rotaxanes.*

In the two rotaxanes characterized by *short* spacers, also the signals of the two methylene groups nearby the amine moiety are affected by the orientation of the axle into **1**. In particular, in rotaxane **R[Nup]$_{short}$** protons (12') and (13') resonate as two broad signals at 2.90 and 2.70 ppm; the same signals are shifted at 2.90 and 3.20 ppm respectively in the opposite orientational isomer **R[Ndown]$_{short}$**. In the *long* isomers, protons (18) and (19) resonate as an unique broad signal centered at 2.60

ppm: these features are probably due to the increased distance of the amine from the cavity. Moreover, for each rotaxane, 2D NMR measurements (COSY, TOCSY, NOESY, HSQC) were carried out to facilitate the complete characterization of the products. In the ^{1}H-^{1}H TOCSY spectra it is possible to evidence a series of correlations that allows to identify the three different alkyl chains present in the dumbbell. As an example, ^{1}H-^{1}H TOCSY spectrum of **R[Ndown]**$_{short}$ is reported (**Figure 4.11**).

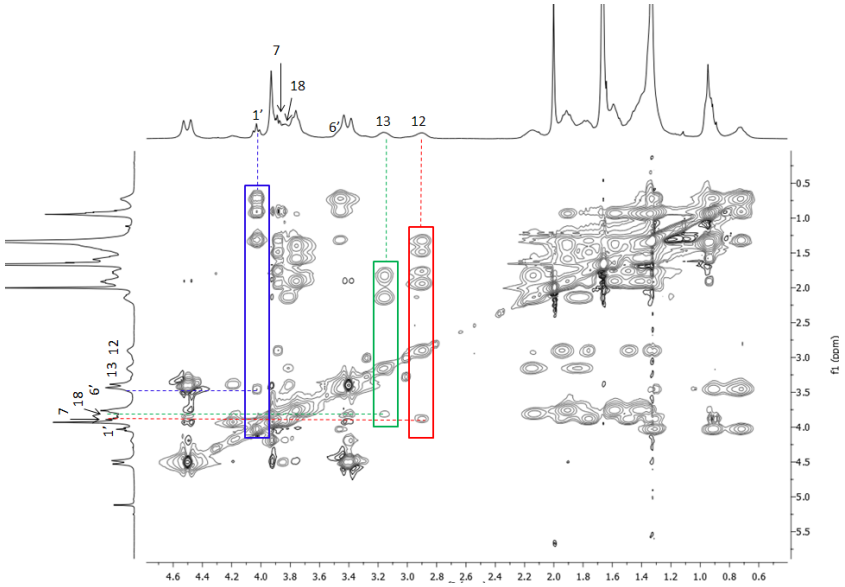

Figure 4.11: *^{1}H-^{1}H TOCSY NMR spectrum (C_6D_6, 400 MHz, mixing time = 80 ms, 0.5-4.7 ppm region) of* ***R[Ndown]***$_{short}$.

The correlations highlighted in red link methylene protons (7) to (12), and are therefore assigned to the spacer between the two stations. The set evidenced in green is ascribed to the alkyl chain that connects the amine station to the lower phenolic stopper (protons 13 to 18). The series of cross peaks that connects methylene protons (1') with methylene protons (6'), encircled in blue, is unequivocally attributed to the upper part of the axle.

The ^{1}H NMR spectrum of triple station rotaxane **R[2N]** (see **Figure 4.12**) exhibits a pattern of signals that reproduces the features of similar double station rotaxanes. It is possible to distinguish the methylene protons linked to the amine moieties in correspondence of the two different rims of **1**. In particular, protons (6) and (7) of the lower branch of the axle resonate at 3.20 and 2.90 ppm, while protons (6') and (7') facing upward give two signals at 2.70 and 2.90 ppm. These chemical shifts

reproduce, as expected, the ones found for the double station *short* isomers. The chemical shifts of most significant signals of each rotaxane are gathered in **Table 4.4**:

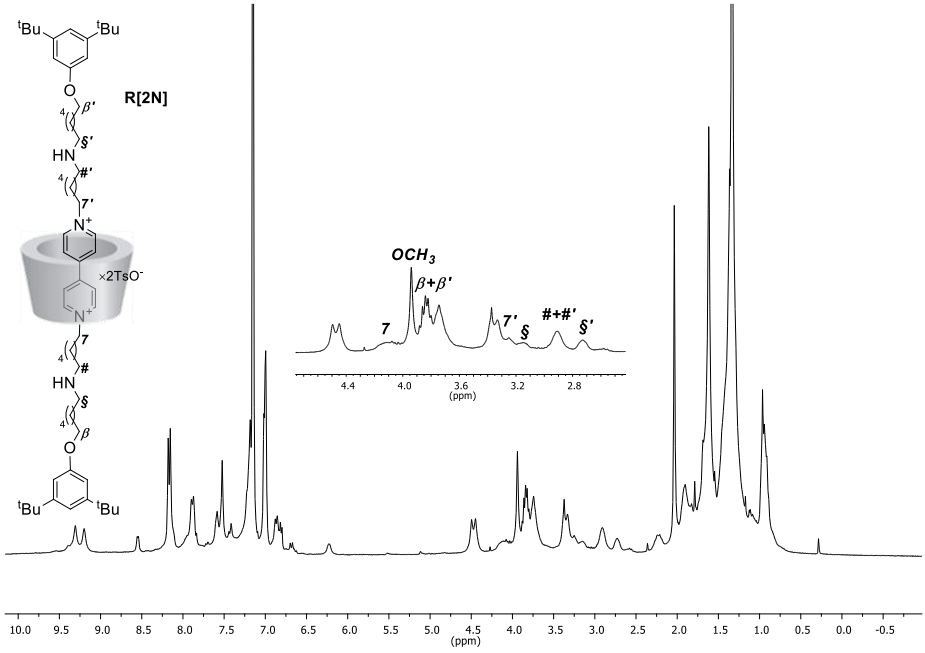

Figure 4.12: *^{1}H NMR spectrum (C_6D_6, 400 MHz) of* ***R[2N]****. Inset: expansion of 2.5-4.5 ppm region.*

	1	1'	#	#'	§	§'
R[C_6C_6]	4.38	4.08	/	/	/	/
R[Nup]$_{short}$	4.31	/	/	2.90	/	2.71
R[Nup]$_{long}$	4.32	/	/	2.59	/	2.59
R[Ndown]$_{short}$	/	4.03	2.90	/	3.16	/
R[Ndown]$_{long}$	/	4.04	2.60	/	2.60	/
R[2N]	/	/	2.91	2.91	3.33	2.73

Table 4.4 *Chemical shifts (δ, ppm) of some of the most significant ^{1}H NMR signals (C_6D_6, 400 MHz) of double station rotaxanes.*

Finally, the formation of the rotaxanes was confirmed by high resolution mass spectrometry (ORBITRAP LQ). For all double station rotaxanes (see **Figure 4.13**) the m/z value and the experimental isotopic distributions perfectly match the corresponding simulated spectra for z=2.

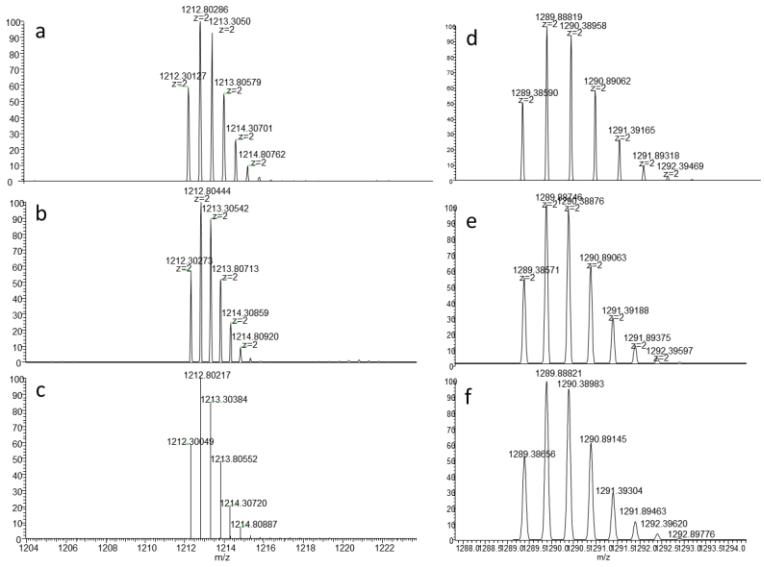

Figure 4.13: *Experimental isotopical distribution of m/z peak found in high resolution mass spectra (ORBITRAP LQ) for a)* ***R[Ndown]$_{short}$*** *b)* ***R[Nup]$_{short}$*** *d)* ***R[Ndown]$_{long}$*** *and e)* ***R[Nup]$_{long}$****. Simulated isotopic patterns for "short" (c) and "long" (f) isomers are reported.*

For triple station rotaxane **R[2N]** (see **Figure 4.14**), two major peaks are present: one at m/z=1258.89734 with z=2, and one at m/z=839.59991 with z=3, attributed to the rotaxane in which one of the amine moieties is protonated.

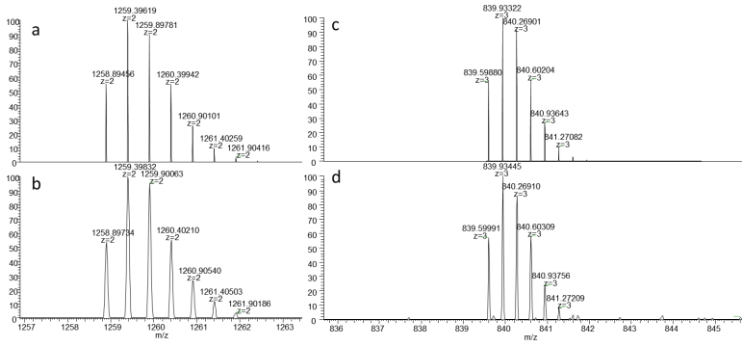

Figure 4.14: *Experimental (b-d) and simulated (a-c) isotopical distribution of peaks found in high resolution mass spectra (ORBITRAP LQ) of* ***R[2N]*** *for m/z =2 and m/z =3.*

4.3.5 Electrochemical study on dynamic behavior

The response of double-station rotaxanes to electrochemical stimulation was steered through Differential Pulse Voltammetry (DPV) measurements in acetonitrile, and the measured potentials were compared to the ones of uncomplexed stoppered dumbbells $\mathbf{A_{short}}$ and $\mathbf{A_{long}}$ (**Figure 4.15**).

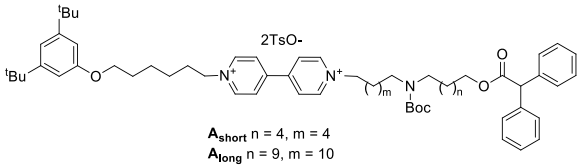

Figure 4.15 S*tructure of the uncomplexed dumbbells* $\boldsymbol{A_{short}}$ *and* $\boldsymbol{A_{long}}$.

To evaluate more in detail the effects of the second recognition unit, for each species the reduction potentials were measured first in presence of the secondary amine in its neutral form, then on the corresponding ammonium rotaxane or axle (generated upon addition of an equimolar amount of triflic acid), and finally after treatment with tributylamine. The obtained values are gathered in **Table 4.5.** For sake of comparison, also the reduction potentials of **DOV** and of symmetric rotaxane **R[C_6C_6]** are reported.

	E_1 (V)	E_2 (V)
DOV	-0.420	-0.860
$\mathbf{R}(N_{up})_{short}$	-0.596	-0.942
$\mathbf{R}(N_{up})_{short}$ + TrH^+	-0.587	-0.904
$\mathbf{R}(N_{up})_{short}$ + TrH^+ + TBA	-0.593	-0.928
$\mathbf{R}(N_{up})_{long}$	-0.606	-0.871
$\mathbf{R}(N_{up})_{long}$ + TrH^+	-0.589	-0.840
$\mathbf{R}(N_{up})_{long}$ + TrH^+ + TBA	-0.606	-0.875
$\mathbf{R}(N_{down})_{short}$	-0.521	-0.932
$\mathbf{R}(N_{down})_{short}$ + TrH^+	-0.509	-0.894
$\mathbf{R}(N_{down})_{short}$ + TrH^+ + TBA	-0.546	-0.932
$\mathbf{R}(N_{down})_{long}$	-0.604	-0.883
$\mathbf{R}(N_{down})_{long}$ + TrH^+	-0.584	-0.872
$\mathbf{R}(N_{down})_{long}$ + TrH^+ + TBA	-0.598	-0.880
$\mathbf{A_{short}}$	-0.410	-0.846
$\mathbf{A_{short}}$ + TrH^+	-0.409	-0.836
$\mathbf{A_{short}}$+ TrH^+ + TBA	-0.402	-0.841

$\mathbf{A}_{long}$	-0.398	-0.849
$\mathbf{A}_{long}$ + TrH^+	-0.399	-0.847
$\mathbf{A}_{long}$+ TrH^+ + TBA	-0.400	-0.848
R(C_6C_6)	-0.620	-1.180

Table 4.5 *Electrochemical potentials vs SCE obtained by DPV in acetonitrile/TEAPF$_6$, [C]=300-400μM.*

In line with previously analyzed systems, all the double-station rotaxanes show two reversible monoelectronic reduction processes. As expected, the first reduction potential of each isomer is shifted towards more negative values with respect to the corresponding free axle in solution, as a consequence of the stabilization of the viologen induced by the calixarene cavity. On the other hand, the second reduction potentials are comparable to the ones of uncomplexed dumbbells: this indicates that, coherently with our initial hypothesis, the electrochemical input induces a rearrangement of the system, that reasonably involves the shuttling of the calixarene towards the more favored second recognition site. As evidenced in the genetic diagram depicted in **Figure 4.16**, it is interesting to notice that both the first and the second reduction potentials of all the rotaxanes are shifted towards less negative values when the reduction is performed on the ammonium rotaxanes. For all the systems, the initial values are re-established when the original situation is restored upon treatment with base.

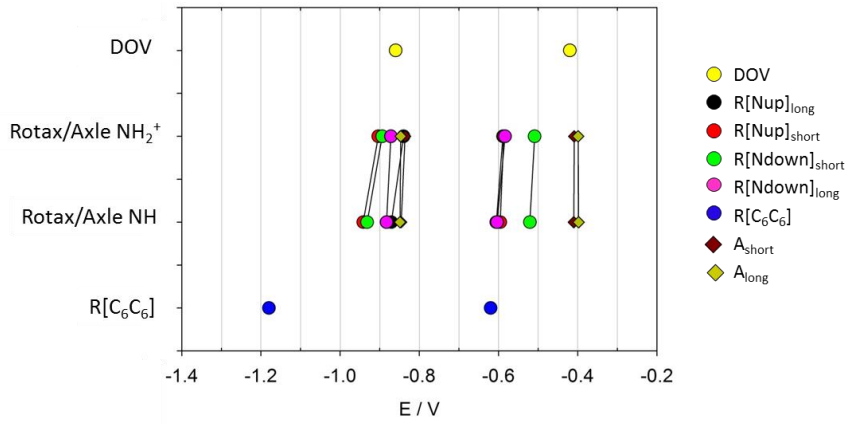

Figure 4.16 *Genetic diagram of the measured reduction potentials.*

As regards the influence of the length of the alkyl spacers, the analysis of the second reduction potentials suggests that the shuttling of the wheel is more favored in the *long* rotaxanes rather than in the *short* isomers.

Concerning the differences between *up* and *down* orientational isomers, these preliminary data do not provide sufficient evidence to determine whether the possible slippage of the wheel takes place preferentially through the upper or the lower rim of the calixarene. The electrochemical study of **R[2N]** will give a significant contribution to clarify these aspects.

The hypothesis of the shuttling motion is also supported by the EPR data recorded in acetonitrile on the electrochemically reduced axles and rotaxanes. The spectra of the mono-reduced double-station rotaxanes reproduce the features shown by the uncomplexed dumbbells (**Figure 4.17**), and the values of the hyperfine coupling constants are in agreement with a symmetric distribution of the two aromatic rings of the bipyridine. These findings, in agreement with voltammetry measurements, confirm that the wheel does not encircle the viologen as soon as the radical-cation is generated.

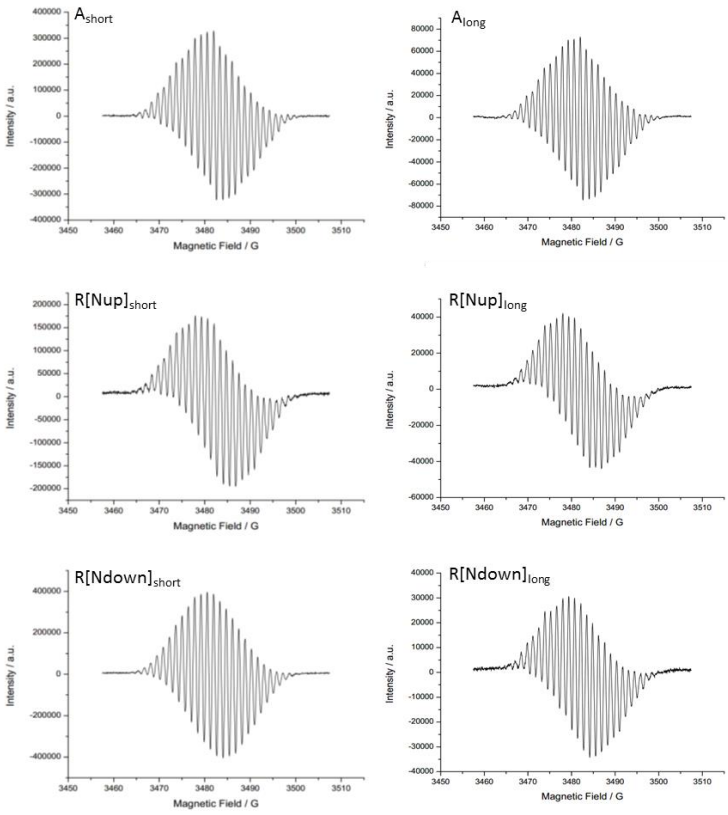

Figure 4.17 *EPR spectra (recorded in acetonitrile) of electrochemically reduced uncomplexed double-station axles and double-station rotaxanes.*

4.3.6 Conclusions

In this second part of the Chapter, the design, the synthesis and the structural characterization of new oriented double-station calix[6]arene-based rotaxanes were presented. The *up* isomers, bearing an ammonium station in proximity to the upper rim of the wheel, were synthesized following a sequential threading-and-capping procedure. The *down* isomers, in which the second recognition unit faces the lower part of the wheel, were obtained exploiting a supramolecularly assisted strategy. The ability of these systems to behave as molecular shuttles driven by electrochemical stimulation was investigated. Differential pulse voltammetry measurements evidenced that, upon the first monoelectronic reduction of the axle's bipyridinium unit, a rearrangement of the systems takes place. This indicates that, coherently with our initial hypothesis, the electrochemical input induces the shuttling of the calixarene towards the more favored second recognition site and the complete reduction of the radical cation to its neutral form takes place outside the calixarene cavity. It is interesting to notice that the protonation of the ammonium station does influence both the first and the second reduction potentials. Nevertheless, preliminary EPR measurements confirmed that the wheel moves away from the viologen core as soon as the radical cation is formed. Further analysis will be carried out to confirm such speculations and to elucidate the eventual differences between the *up* and the *down* isomers. In particular, the study of **R[2N]** will give a significant contribution to clarify these aspects.

4.4 Acknowledgments

Thanks to Dr. Giulio Ragazzon, Prof. Alberto Credi, Prof. Serena Silvi and Prof. Margherita Venturi (University of Bologna) for electrochemical measurements. Thanks to Dr. Paola Franchi and Prof. Marco Lucarini (University of Bologna) for EPR measurements. Thanks to Dr. Andrea Faccini (University of Parma) for high-resolution mass spectrometry measurements.

4.5 Experimental Section

Synthesis: Toluene, THF, acetonitrile and dichloromethane were dried by following standard procedures, other reagents were of reagent grade quality, obtained from commercial sources and used without further purification. Chemical shifts are expressed in ppm using the residual solvent signal as internal reference. Mass spectra

were determined in ESI mode. Compounds **1**,[17] **4–6a**,[18] **4–6b**,[19] **4d**,[20] **R[C_3C_3]**,[12] **R[C_6C_6]**,[12] **R[$C_{12}C_{12}$]**,[12] **14**,[18] **10-11a**,[18] **16a**,[21] **20-21**[22] and **23**[23] were synthesized according to reported procedures.

Electrochemical Experiments: Cyclic voltammetric (CV) experiments were carried out at room temperature in argon-purged acetonitrile (Romil-high dry or Merck-Uvasol) with an Autolab 30 multipurpose instrument interfaced to a PC. The working electrode was a glassy carbon electrode (Amel; 0.07 cm^2); its surface was routinely polished with a 0.3 µm alumina–water slurry on a felt surface. The counter electrode was a Pt wire, separated from the solution by a frit; a Ag wire was employed as a quasi-reference electrode, and ferrocene (Fc) was present as an internal standard [E1/2(Fc+/ Fc) = +0.395 vs. SCE]. Ferrocene was added from a concentrated acetonitrile solution (typically 0.1 M). The concentration of the compounds examined was in the range 2 × 10^{-4} to 4 × 10^{-4} M; tetraetylammonium hexafluorophosphate 0.04 M was added as supporting electrolyte. Cyclic voltammograms were obtained at sweep rates varying typically from 0.02 to 1 V s^{-1}. The IR compensation implemented within the Autolab 30 was used, and every effort was made throughout the experiments to minimize the resistance of the solution. In any instance, the full electrochemical reversibility of the voltammetric wave of ferrocene was taken as an indicator of the absence of uncompensated resistance effects. DPV were performed with a scan rate of 20 mV $^{s-1}$, a pulse height of 75 mV, and a duration of 40 ms. For reversible processes, the same halfwave potential values were obtained from the DPV peaks and from an average of the cathodic and anodic cyclic voltammetric peaks. The potential values for not fully reversible processes were estimated from the DPV peaks. The experimental error on the potential values for reversible and not fully reversible processes was estimated to be ±10 and ±20 mV, respectively. Spectroelectrochemical experiments were performed using the same experimental conditions (solvent, sample concentration, supporting electrolyte and reference) as for cyclic and pulsed voltammetry experiments. Prolonged and vigorous argon purging of the solution was performed to minimize the oxygen content in the investigated solution. Experiments were

[17] Gonzalez, J. J.; Ferdani, R.; Albertini, E.; Blasco, J. M.; Arduini, A.; Pochini, A.; Prados, P.; de Mendoza, J. *Chem. Eur. J.* **2000**, *6*, 73-80.

[18] Arduini, A.; Bussolati, R.; Credi, A.; Faimani, G.; Garaudée, S.; Pochini, A.; Secchi, A.; Semeraro, M.; Silvi, S.; Venturi, M- *Chem. Eur. J.* **2009**, *15*, 3230-3242.

[19] Arduini, A.; Ciesa, F.; Fragassi, M.; Pochini, A.; Secchi, A. *Angew. Chem. Int. Ed.* **2005**, *44*, 278-281.

[20] Ballot, S.; Noiret, N. *Tetrahedron Lett.* **2003**, *44 (49)*, 8811-8814.

[21] Yoritate, M.; Meguro, T.; Matsuo, N.; Shirokane, K.; Sato, T.; Chida, N. *Chem. Eur. J.* **2014**, *20*, 8210-8216.

[22] Boccia, A.; Lanzilotto, V.; Zanoni, R.; Pescatori, L.; Arduini, A.; Secchi, A. *Phys. Chem. Chem. Phys*. **2011**, *13 (10)*, 4452-4462.

[23] Arduini, A.; Calzavacca, F.; Pochini, A.; Secchi, A. *Chem. Eur. J.* **2003**, *9 (3)*, 793-799.

performed in a custom built optically transparent thin-layer electrochemical (OTTLE) cell, having Pt minigrids (ca. 0.3 cm^2) as the working and counter electrodes, and a Ag wire as a pseudo-reference electrode, all melt-sealed into a polyethylene spacer. The thickness of the layer, determined by spectrophotometry, was ca. 180 µm. The electrolysis was controlled by means of the above described Autolab 30 instrument, and the absorption spectra were recorded with an Agilent Technologies 8543 diode array spectrophotometer. The electrolysis times were determined on the basis of the spectral changes observed; that is, the electrolysis was stopped when no further spectral variations occurred. UV/Vis Spectroscopy: Absorption spectra were recorded with Varian Cary 50Bio, Agilent Technologies Cary 300 and Perkin–Elmer Lambda45 spectrophotometers, on air-equilibrated acetonitrile solutions at room temperature (ca.20 °C), with concentrations ranging from 1×10^{-5} to 5×10^{-4} M. Solutions were examined in 1 cm spectrofluorimetric quartz cells. The experimental error on the wavelength values was estimated to be ±1 nm.

EPR Measurements: EPR spectra were recorded at room temperature using an ELEXYS E500 spectrometer equipped with a NMR gaussmeter for the calibration of the magnetic field and a frequency counter for the determination of g-factors that were corrected against that of the perylene radical cation in concentrated sulfuric acid (g = 2.002583). The electrochemical cell was homemade and consisted of an EPR flat cell (Wilmad WG-810) equipped with a 25 × 5 × 0.2 mm platinum gauze (cathode), and a platinum wire (anode). The current was supplied and controlled by an AMEL 2051 general-purpose potentiostat. In a typical experiment, the cell was filled with an acetonitrile solution of the appropriate substrate (ca. 1 mM) containing tetrabutylammonium perchlorate (ca. 0.1 M) as supporting electrolyte. After thoroughly purging the solution with N_2, spectra were recorded at different potential settings in the range 0 to –1.0 V. An iterative least-squares fitting procedure based on the systematic application of the Monte Carlo method was performed to obtain the experimental spectral parameters of the radical species.

16-hydroxyhexadecyl 4-methylbenzenesulfonate (4c): A solution of tosyl chloride (0.23 g, 1.2 mmol) in anhydrous dichloromethane (30 mL) was slowly added to a solution of 1,16-hexadecanediol (0.44 g, 1.7 mmol) in 50 mL of a 1:1 mixture of anhydrous dichloromethane and THF. Triethylamine (0.26 g, 2.55 mmol) and a catalytic amount of DMAP were added. After stirring at room temperature for 5 hours, the reaction was quenched with water (50 mL) and the organic phase was separated, dried over anhydrous $CaCl_2$ and filtered. The solvent was removed under reduced pressure and the residue was purified by column chromatography (n-hexane/ethyl acetate 7:3) to afford **4c** as a white solid (0.26 g, 52%) and 0.2 g of unreacted diol. ^1H

NMR (400 MHz, $CDCl_3$): δ = 1.2–1.4 (m, 24 H, aliphatic CH_2), 1.4-1.7 (m, 4 H, HO-CH_2CH_2), 2.47 (s, 3H, Ar-CH_3), 3.66 (t, ^3J(H,H)=8 Hz, 2 H, HO-CH_2), 4.04 (t, ^3J(H,H)=8 Hz, 2 H, Ar-O-CH_2), 7.37 (d, ^3J(H,H)=8 Hz, 2 H, Ar*H*), 7.81 (d, ^3J(H,H)=8 Hz, 2 H, Ar*H*). ^{13}C NMR (100 MHz, $CDCl_3$): δ = 21.5, 25.2, 25.8, 28.7, 28.8, 29.3, 29.4, 29.5, 29.6 (2 res.), 32.7, 62.6, 70.7, 127.8, 129.8, 133.1, 144.6 ppm. ESI-MS(+): m/z (%) = 435 (90) $[M+Na]^+$, 451 (100) $[M+K]^+$. Mp: 43-46 °C.

16-(tosyloxy)hexadecyl 2,2-diphenylacetate (5c): To a solution of 16-hydroxyhexadecyl 4-methylbenzenesulfonate **4c** (0.57 g, 1.4 mmol) in anhydrous THF (100 mL), diphenylacetyl chloride (0.43 g, 1.85 mmol) was added. After stirring at room temperature for one day, the reaction was quenched with water (50 mL) and extracted with ethyl acetate (2x100 mL). The separated organic phase was dried over Na_2SO_4, evaporated under reduced pressure and the residue was purified by column chromatography (n-hexane/ethyl acetate 8:2), to afford **5c** as a white solid (0.75 g, 88%). ^{1}H NMR (400 MHz, $CDCl_3$): δ = 1.2–1.3 (m, 24 H, aliphatic CH_2), 1.6–1.7 (m, 4 H, Ts-CH_2CH_2 + (C=O)OCH_2CH_2), 2.47 (s, 3 H, Ar-CH_3), 4.04 (t,^3J(H,H) = 6.6 Hz, 2 H, Ts-CH_2), 4.17 (t,^3J(H,H) = 6.6 Hz, 2 H, (C=O)OCH_2), 5.04 (s, 1 H, $(Ph)_2$C*H*), 7.2 - 7.4 (m, 12 H, Ar*H*), 7.82 (d,^3J(H,H)=8 Hz, 2 H, Ar*H*). ^{13}C NMR (100 MHz, $CDCl_3$) δ = 21.6, 25.3, 25.8, 28.5, 28.8, 28.9, 29.2, 29.4, 29.5 (3 res.), 29.6 (2 res.), 29.7, 57.2, 65.3, 70.7, 127.2, 127.9, 128.5, 128.6, 129.8 (2 res.), 138.8, 144.6, 172.5 ppm. ESI-MS(+): m/z (%) = 629 (100) $[M+Na]^+$, 645 (90) $[M+K]^+$. Mp: 58-60 °C.

1-(16-(2,2-diphenylacetoxy)hexadecyl)-[4,4'-bipyridin]-1-ium tosylate (6c): 5c (0.75 g, 1.23 mmol) and 4,4'-bipyridine (0.58 g, 3.7 mmol) were dissolved in anhydrous acetonitrile (50 mL) and heated at reflux overnight. The solvent was then removed under reduced pressure to afford a crude solid residue that was triturated with ethyl acetate (4x25 mL) to give **6c** as a sticky white solid (0.47 g, 50 %). ^{1}H NMR (400 MHz, MeOD): δ = 1.2–1.4 (m, 22 H, aliphatic CH_2), 1.4–1.5 (m, 2 H, (C=O)OCH_2CH_2CH_2) , 1.61 (m, 2 H, N^+-CH_2CH_2), 2.08 (m, 2 H, (C=O)OCH_2CH_2), 2.38 (s, 3 H, Ar-CH_3), 4.17 (t,^3J(H,H) = 6.4 Hz, 2 H, (C=O)OCH_2), 4.68 (t,^3J(H,H) = 7.6 Hz, 2 H, N^+-CH_2), 5.09 (s, 1 H, $(Ph)_2$C*H*), 7.2 - 7.4 (m, 12 H, Ar*H*), 7.72 (d,^3J(H,H)=8 Hz, 2 H, Ar*H*), 7.99 (d,^3J(H,H)=8 Hz, 2 H, Ar*H*), 8.52 (d,^3J(H,H)=6.8 Hz, 2 H, Ar*H*), 8.84 (d,^3J(H,H)=8 Hz, 2 H, Ar*H*), 9.12 (d,^3J(H,H)=8 Hz, 2 H, Ar*H*). ^{13}C NMR (151 MHz, MeOD) δ = 25.4, 25.7, 28.2, 28.7, 29.1, 29.3, 31.0, 56.7, 61.3, 64.8, 122.0, 122.1, 125.4, 125.7, 126.8, 128.2, 128.3, 138.9, 142.2, 145.0, 145.1, 150.3, 150.4, 153.7, 172.9 ppm. ESI-MS(+): m/z (%) = 590 (100) $[M-H]^+$.

General procedure for the synthesis of non-symmetric axles 2a-c: Salt **6a-c** (0.34 eq.) and 16-hydroxydodecyl tosylate **4b-d** (1 eq.) were dissolved in anhydrous acetonitrile

(20 mL) and heated at 100 °C for 7 days. After cooling at 0°C, precipitation of the product was observed.

1-(3-(2,2-diphenylacetoxy)propyl)-1'-(12-hydroxydodecyl)-[4,4'-bipyridine]-1,1'-diium (2a): Pure axle **2a** was collected by Buchner filtration as a sticky white solid (47%). ^{1}H NMR (300 MHz, MeOD): δ = 1.3–1.5 (m, 18 H, aliphatic CH_2), 2.09 (m, 2 H, aliphatic CH_2), 2.37 (s, 3 H, Ar-CH_3), 2.48 (m, 2 H, aliphatic CH_2), 3.55 (t,^{3}J(H,H) = 9 Hz, 2 H, HOCH_2), 4.33 (t,^{3}J(H,H) = 6 Hz, 2 H, (C=O)OCH_2), 4.75 (m, 4 H, N^+-CH_2), 5.09 (s, 1 H, $(Ph)_2$CH), 7.2 - 7.3 (m, 14 H, ArH), 7.69 (d,^{3}J(H,H)=9 Hz, 4 H, ArH), 8.54 (d,^{3}J(H,H)=6 Hz, 2 H, ArH), 8.63 (d,^{3}J(H,H)=6 Hz, 2 H, ArH), 9.9 (d,^{3}J(H,H)=6 Hz, 2 H, ArH), 9.26 (d,^{3}J(H,H)=6 Hz, 2 H, ArH). ^{13}C NMR (75 MHz, MeOD) δ = 20.0, 25.5, 25.8, 28.7, 29.1, 29.2 (2 res.), 29.3, 29.6, 31.2, 32.2, 56.4, 59.3, 61.5, 61.6, 62.0, 125.5, 126.8, 127.1, 128.3 (2 res.), 128.5, 138.7, 140.4, 145.8, 149.6, 149.9, 172.3 ppm. ESI-MS(+): m/z (%) = 593 (100) 594 (60) $[M-H]^+$.

1-(6-(2,2-diphenylacetoxy)hexyl)-1'-(16-hydroxyhexadecyl)-[4,4'-bipyridine]-1,1'-diium ditosylate (2b): The solid was collected by Buchner filtration and purified by further precipitation in acetonitrile at room temperature, to give axle **2b** as a pale-yellow solid (38 %). ^{1}H NMR (300 MHz, MeOD): δ = 1.2–1.5 (m, 28 H, aliphatic CH_2), 1.5–1.6 (m, 2 H, $HOCH_2CH_2$), 1.6 - 1.7 (m, 2 H, $(C=O)OCH_2CH_2$), 2.0 – 2.1 (m, 2 H, N^+-CH_2CH_2), 2.38 (s, 3 H, Ar-CH_3), 3.55 (t,^{3}J(H,H) = 6.6 Hz, 2 H, HOCH_2), 4.17 (t,^{3}J(H,H) = 6.6 Hz, 2 H, (C=O)OCH_2), 4.6 – 4.8 (m, 4 H, N^+-CH_2), 5.09 (s, 1 H, $(Ph)_2$CH), 7.2 - 7.4 (m, 14 H, ArH), 7.69 (d,^{3}J(H,H)=8.1 Hz, 4 H, ArH), 8.65 (d,^{3}J(H,H)=6.6 Hz, 4 H, ArH), 9.24 (m, 4 H, ArH). ^{13}C NMR (100 MHz, MeOD) δ = 20.0, 24.8, 25.2, 25.6, 25.9, 27.9, 28.8, 29.1, 29.2, 29.3, 29.4 (2 res.), 30.9, 31.2, 32.3, 56.9, 61.6, 61.7, 61.9, 64.5, 125.6, 126.9, 128.2, 128.3, 128.5, 138.9, 140.3, 142.3, 145.6, 149.8, 149.9, 172.9 ppm. ESI-MS(+): m/z (%) = 864 (100) 865 (60) $[M+Ts]^+$. Mp: 122-124 °C.

1-(16-(2,2-diphenylacetoxy)hexadecyl)-1'-(6-hydroxyhexyl)-[4,4'-bipyridine]-1,1'-diium ditosylate (2c): The solid was collected by Buchner filtration and purified by further precipitation in acetonitrile at room temperature, to give axle **2c** as a sticky white solid (42%). ^{1}H NMR (400 MHz, MeOD): δ = 1.2–1.5 (m, 30 H, aliphatic CH_2), 1.5–1.7 (m, 4 H, $HOCH_2CH_2$ + $(C=O)OCH_2CH_2$), 2.0 – 2.1 (m, 4 H, N^+-CH_2CH_2), 2.37 (s, 3 H, Ar-CH_3), 3.33 (m, 2 H, HOCH_2), 4.16 (t,^{3}J(H,H) = 6.6 Hz, 2 H, (C=O)OCH_2), 4.6 – 4.7 (m, 4 H, N^+-CH_2), 5.09 (s, 1 H, $(Ph)_2$CH), 7.2 - 7.4 (m, 14 H, ArH), 7.70 (d,^{3}J(H,H)=8.1 Hz, 4 H, ArH), 8.63 (d,^{3}J(H,H)=6.6 Hz, 4 H, ArH), 9.22 (m, 4 H, ArH). ^{13}C NMR (100 MHz, MeOD) δ = 20.0, 25.0, 25.4, 25.5, 25.6, 25.8, 28.2, 28.8, 29.1, 29.2, 29.3 (3 res.), 29.4, 31.2, 31.8, 48.1, 57.0, 61.2, 64.9, 100.0, 125.6, 127.9 (2 res.), 128.2, 128.3, 128.5, 138.9, 140.3, 145.6, 172.9 ppm. ESI-MS(+):m/z: = 692 (100) 693 (50) $[M-H]^+$.

General procedure for the synthesis of non-symmetric rotaxanes R[C_3C_{12}], R[C_6C_{16}], R[$C_{16}C_6$]: Axle **2a-c** (0.065 eq.) was suspended in a solution of **1** (0.065 eq.) in anhydrous toluene (20 mL). The suspension was stirred at room temperature overnight until the solution turned dark-red colored and the axle was completely dissolved. Then triethylamine (0.13 eq.) and diphenylacetyl chloride (0.13 eq.) were added and the solution was stirred at room temperature for one day. After removing the solvent under reduced pressure, the residue was taken up with dichloromethane and the organic phase was washed with water. The organic phase was separated and evaporated under reduced pressure, and the crude product was purified by column chromatography (dichloromethane/methanol 50:1). The isolated rotaxane was re-dissolved in 20 mL of dichloromethane and washed with 0.1 M silver *p*-toluenesulfonate solution in water (50 mL). The organic phase was separated and the solvent was removed under reduced pressure, to afford pure rotaxane as tosylate salt.

Rotaxane R[C_3C_{12}]: Rotaxane was obtained as a red solid (57%). ^{1}H NMR (400 MHz, C_6D_6): δ =0.93 (m, 12 H), 1.10-1.20 (m, 8 H), 1.25-1.35 (bs, 26 H), 1.35-1.45 (bs, 14 H), 1.50-1.60 (m, 12 H), 1.71 (bs, 20 H), 1.83 (m, 8 H), 1.96 (s, 6 H), 3.36 (d, ^{2}J(H,H)=16 Hz, 6 H), 3.7-3.8 (m, 12 H), 3.86 (s, 9 H), 4.06 (t, ^{3}J(H,H)=6 Hz, 2 H), 4.47 (d, ^{2}J(H,H)=16 Hz, 6 H), 5.07 (s, 1 H), 5.30 (s, 1 H), 6.57 (bs, 4 H), 6.75 (bs, 4 H), 6.92 (d, ^{3}J(H,H)=8 Hz, 4 H), 6.95 (bs, 4 H), 7.00-7.10 (m, 4 H), 7.10-7.20 (m, 14 H), 7.40 (d, ^{3}J(H,H)=8 Hz, 4 H), 7.52 (d, ^{3}J(H,H)=8 Hz, 4 H), 7.59 (s, 6 H), 7.75-8.00 (m, 10 H), 8.19 (bs, 4 H), 9.41 (bs, 6H). ^{13}C NMR (100 MHz, C_6D_6): δ = 14.0, 20.8, 22.8, 25.9, 26.6, 28.6, 29.6, 29.9, 30.8, 31.5, 32.0, 34.6, 56.9, 57.3, 58.5, 60.7, 61.2, 64.7, 73.0, 116.6, 118.0, 121.3, 124.8, 125.7, 126.6, 127.1, 128.5, 128.6, 128.7, 128.8, 129.3, 132.0, 133.7, 137.4, 139.2, 139.5, 141.0, 142.9, 143.3, 144.7, 148.3, 152.8, 153.2, 171.7, 171.9 ppm. ESI-MS(+): m/z (%) = 1187 (100) $[M]^{2+}$.

Rotaxane R[C_6C_{16}]: Rotaxane was obtained as a red solid (40%). ^{1}H NMR (300 MHz, C_6D_6): δ =0.72 (bs, 8 H), 0.96 (br t, 9 H + 4 H), 1.13 (m, 8 H), 1.2-1.4 (m, 40 H), 1.56-1.63 (m, 16 H), 1.71 (bs, 20 H), 1.83 (m, 8 H), 1.95 (s, 6 H), 3.36 (d, ^{2}J(H,H)=14 Hz, 6 H), 3.7-3.8 (m, 10 H), 3.86 (s, 9 H), 4.03 (t, ^{3}J(H,H)=6 Hz, 4 H), 4.47 (d, ^{2}J(H,H)=14 Hz, 6 H), 5.07 (s, 1 H), 5.13 (s, 1 H), 6.65 (m, 2 H), 6.74 (m, 2 H), 6.91 (d, ^{3}J(H,H)=8 Hz, 4 H), 6.95-7.10 (m, 10 H), 7.1-7.2 (m, 16 H) 7.35-7.45 (m, 12 H), 7.58 (bs, 6 H), 7.75-7.90 (m, 4 H), 7.12 (m, 2 H), 8.18 (d, ^{3}J(H,H)=8 Hz, 4 H), 9.39 (bs, 6H). ^{13}C NMR (75 MHz, C_6D_6) δ = 14.0, 20.8, 22.8, 25.8, 26.1, 26.5, 28.6, 28.9, 29.2, 29.5, 29.6, 29.7 (3 res.), 29.9 (3 res.), 30.7, 31.5, 31.9, 34.6, 57.3, 60.8, 64.9, 73.1, 116.6, 118.0, 121.0, 124.9, 125.5, 126.5, 127.0, 128.5 (2 res.), 128.6, 128.7, 132.0, 133.6, 137.3, 139.0, 139.3, 139.4, 141.2, 143.3, 148.3, 152.9, 153.4, 171.9 ppm. ESI-MS(+): m/z (%) = 1237 (100) $[M]^{2+}$.

Rotaxane R[$C_{16}C_6$]: Rotaxane was obtained as a red solid (43%). ^{1}H NMR (300 MHz, C_6D_6): δ =0.85-1.00 (bs, 14 H), 1.10 (bs, 6 H), 1.2-1.4 (m, 48 H), 1.51 (bs, 4 H), 1.58 (m, 8 H), 1.70 (bs, 22 H), 1.82 (m, 8 H), 1.95 (s, 6 H), 3.37 (d, ^{2}J(H,H)=14 Hz, 6 H), 3.45-3.65 (bs, 6 H), 3.70 (m, 4 H), 3.80 (s, 9 H), 4.02 (t, ^{3}J(H,H)=6 Hz, 2 H), 4.33 (t, ^{3}J(H,H)=6 Hz, 2 H), 4.48 (d, ^{2}J(H,H)=14 Hz, 6 H), 5.06 (s, 1 H), 5.10 (s, 1 H), 6.61 (m, 2 H), 6.73 (br t, 2 H), 6.89 (d, ^{3}J(H,H)=8 Hz, 4 H), 6.93 (bs, 2 H), 7.00-7.10 (m, 10 H), 7.10-7.20 (m, 12 H) 7.35-7.50 (m, 12 H), 7.59 (bs, 6 H), 7.80-7.90 (m, 10 H), 8.15 (d, ^{3}J(H,H)=8 Hz, 4 H), 9.39 (bs, 6H). ^{13}C NMR (100 MHz, C_6D_6): δ = 14.1, 20.8, 22.8, 25.0, 25.5, 25.8, 26.6, 28.3, 28.6, 29.2, 29.6, 29.7, 29.8 (2 res.), 30.0, 30.1, 30.2, 30.4 (2 res.), 30.8, 31.1, 31.5, 32.0, 34.6, 57.3, 57.4, 60.4, 60.7, 64.6, 64.8, 73.0, 116.6, 118.0, 121.1, 124.8, 125.5, 126.6, 127.1, 127.2, 127.6, 127.8, 128.5, 128.6, 128.7 (2 res.), 128.8, 129.3, 132.1, 133.6, 139.2 (2 res.), 141.1, 142.9, 144.3, 148.3, 152.8, 153.3, 171.9, 172.0 ppm. ESI-MS(+): m/z (%) = 1237 (100) $[M]^{2+}$.

1,1'-bis(16-hydroxyhexadecyl)-[4,4'-bipyridine]-1,1'-diium ditosylate (7): In a sealed glass reactor, **4c** (0.22 g, 0.54 mmol) and 4,4'-bipyridine (0.02 g, 0.13 mmol) were dissolved in 5 mL of anhydrous acetonitrile and heated at 110°C for 7 days. After cooling at room temperature, precipitation of the product was observed. The solid was collected by Buchner filtration and washed with cold acetonitrile. Axle **7** was obtained as a white solid (60 mg, 48%). ^{1}H NMR (300 MHz, MeOD): δ =1.2–1.6 (m, 56 H, aliphatic CH_2), 2.39 (s, 3 H, Ar-CH_3), 3.55 (t,^{3}J(H,H)=6.6 Hz, 4 H, HO-CH_2), 4.74 (t,^{3}J(H,H)=7.5 Hz, 4 H, N^+-CH_2), 7.24 (d,^{3}J(H,H)=8 Hz, 4 H, Ar*H*), 7.69 (d,^{3}J(H,H)=8 Hz, 4 H, Ar*H*), 8.67 (d,^{3}J(H,H)=6.9 Hz, 4 H, Ar*H*), 9.27 (d,^{3}J(H,H)=6.9 Hz, 2 H, Ar*H*). ^{13}C NMR (100 MHz, MeOD): δ = 20.0, 25.5, 25.8, 28.8, 29.1, 29.2 (2 res.), 29.3 (2 res.), 31.2, 32.2, 61.6, 62.0, 125.5, 126.9, 128.5, 140.3, 142.1, 145.6, 149.9 ppm. ESI-MS(+): m/z (%) = 678 (100) 639 (40) $[M-H]^+$. Mp: 165-170 °C.

Rotaxane R[$C_{16}C_{16}$]: Axle **7** (0.05 g, 0.05 mmol) was suspended in a solution of **1** (0.08 g, 0.05 mmol) in anhydrous toluene (20 mL). The suspension was stirred at 50°C for 3 hours until the solution turned dark-red and the axle was completely dissolved. Then triethylamine (15 µL, 0.1 mmol) and diphenylacetyl chloride (25 mg, 0.1 mmol) were added and the solution was stirred at room temperature for one day. After removing the solvent, the residue was portioned between dichloromethane and water. The organic phase was separated and evaporated under reduced pressure, and crude product was purified by column chromatography (dichloromethane/methanol 50:1). The isolated rotaxane was re-dissolved in 20 mL of dichloromethane and washed with 0.1 M silver *p*-toluenesulfonate solution in water (50 mL). The organic phase was separated and the solvent was removed under reduced pressure, to afford rotaxane as a red solid (70 mg, 46%). ^{1}H NMR (300 MHz, C_6D_6): δ = 0.90 (bs, 4 H), 0.96 (br t, 9 H + 4

H), 1.12 (m, 14 H), 1.2-1.4 (m, 64 H), 1.5-1.6 (m, 16 H), 1.73 (bs, 24 H), 1.84 (m, 8 H), 1.96 (s, 6 H), 3.36 (d, ^{2}J(H,H)=12 Hz, 6 H), 3.61 (m, 6 H), 3.72 (m, 4 H), 3.86 (s, 9 H), 4.03 (t, ^{3}J(H,H)=6 Hz, 4 H), 4.48 (d, ^{2}J(H,H)=12 Hz, 6 H), 5.07 (s, 2 H), 6.69 (m, 6 H), 6.83 (m, 2 H), 6.91 (d, ^{3}J(H,H)=9 Hz, 4 H), 7.01 (m, 2 H), 7.03 (br d, 4 H), 7.05 (br d, 4 H), 7.10 (bs, 4 H), 7.12 (bs, 4 H), 7.39 (d, ^{3}J(H,H)=9 Hz, 4 H), 7.58 (bs, 6 H), 7.83 (m, 6 H), 7.95 (m, 2 H), 8.20 (d, ^{3}J(H,H)=9 Hz, 4 H), 9.42 (bs, 6H). ^{13}C NMR (100 MHz, C_6D_6) δ = 14.0, 20.8, 22.8, 25.8, 26.6, 28.6, 28.9, 29.2, 29.6(3 res.), 29.7 (2 res.), 29.8, 29.9 (4 res.), 30.1, 30.2, 30.8, 31.6, 32.0, 34.6, 57.3, 60.8, 64.8, 64.9, 73.0, 116.6, 117.9, 121.0 (2 res.), 124.8 (2 res.), 126.6, 127.0, 127.1, 127.6, 127.8, 128.5 (2 res.), 128.7 (2 res.), 129.4, 139.3, 141.1, 142.9, 144.3, 148.3, 152.9, 153.3, 171.9 ppm. ESI-MS(+): m/z (%) = 1307 (100) $[M]^{2+}$.

N-Boc-11-aminoundecanol 10b: Di-tert-butyl dicarbonate (3.33 g, 15.30 mmol) and triethylamine (1.65 mL, 16.80 mmol) were added to a solution of 11-aminoundecan-1-ol **9b** (2.86 g, 15.30 mmol) in a 9:1 mixture of THF/MeOH (50 mL) under inert atmosphere. The reaction mixture was stirred overnight at room temperature. The solvent was then removed under reduced pressure and the residue was portioned between ethyl acetate and water. The separated organic phase was dried over Na_2SO_4 and evaporated under reduced pressure, to give **10b** (4.16 g, 95%), a colorless oil. ^{1}H NMR (400 MHz, $CDCl_3$): δ = 1.2–1.4 (m, 14 H, aliphatic CH_2), 1.46 (m, 11 H, O*Bu*^{t} + HN-CH_2CH_2), 1.55-1.62 (m, 2 H, HO-CH_2CH_2), 3.16 (t, ^{3}J(H,H)=7.2 Hz,2 H,HN-CH_2), 3.65 (t, ^{3}J(H,H)=6.8 Hz, 2 H, HO-CH_2). ^{13}C NMR (100 MHz, $CDCl_3$): δ = 25.7, 26.7, 27.2, 28.3, 29.2, 29.3, 29.4, 29.5, 32.6, 40.5, 62.5, 78.7, 156.0 ppm. ESI-MS(+): m/z (%) = 288 (100) $[M+H]^{+}$.

11-((tert-butoxycarbonyl)amino)undecyl 4-methylbenzenesulfonate (11b): A solution of tosyl chloride (21.70 mmol) in anhydrous dichloromethane (50 mL) was slowly added to a solution of **10b** (14.50 mmol) in 50 mL of the same solvent. Triethylamine (28.90 mmol) and a catalytic amount of DMAP were added. After stirring at room temperature for one day, the reaction was quenched with water (50 mL) and the organic phase was separated, dried over anhydrous $CaCl_2$ and filtered. The solvent was removed under reduced pressure and the residue was purified by column chromatography (n-hexane/ethyl acetate 8:2) to afford **11b** as a white solid (75%). ^{1}H NMR (400 MHz, $CDCl_3$): δ = 1.2–1.4 (m, 14 H, aliphatic CH_2), 1.46 (m, 11 H, HN-CH_2CH_2 + O*Bu*^{t}), 1.61-1.66 (m, 2 H, O-CH_2CH_2), 2.47 (s, 3 H, Ar-CH_3), 3.11 (bs, 2 H, HN-CH_2), 4.04 (t, ^{3}J(H,H)=6.8 Hz,2 H, O-CH_2), 4.51 (bs, 1 H, N*H*), 7.36 (d, ^{3}J(H,H)=8 Hz, 2 H, Ar*H*), 7.81 (d, ^{3}J(H,H)=8 Hz, 2 H, Ar*H*). ^{13}C NMR (100 MHz, $CDCl_3$): δ = 21.6, 25.3, 26.8, 28.4, 28.8, 28.9, 29.2, 29.3 (2 res.), 29.4, 30.0, 40.6, 70.7, 78.8, 127.8, 129.8, 133.2, 144.6, 156.0 ppm. ESI-MS(+): m/z (%) = 464 (100) $[M+Na]^{+}$.

Tert-butyl (6-(3,5-di-tert-butylphenoxy)hexyl)carbamate (12a): To a solution of **11a** (4.70 mmol) in anhydrous DMF (50 mL), K_2CO_3 (14.10 mmol) and 3,5-di-tert-butylphenol (4.85 mmol) were added. The reaction mixture was stirred for 18 hours at 80°C. After cooling at room temperature, the reaction was quenched with water (50 mL) and extracted with ethyl acetate (3x100 mL). The separated organic phase was dried over Na_2SO_4 and evaporated under reduced pressure. Product was isolated by column chromatography (n-hexane/acetone 80:20) as a colorless oil (53%). ^{1}H NMR (400 MHz, $CDCl_3$): δ = 1.3–1.6 (m, 33 H, aliphatic C*H*$_2$ + Ar-*Bu*^{t} + O*Bu*^{t}), 1.81 (m, 2 H, O-CH$_2$C*H*$_2$), 3.15 (m, 2 H, HN-C*H*$_2$), 3.98 (t, ^{3}J(H,H)=6.4 Hz, 2 H, O-C*H*$_2$), 4.53 (bs, 1 H, N*H*), 6.77 (s, 2 H, Ar*H*), 7.03 (s, 1 H, Ar*H*). ^{13}C NMR (100 MHz, $CDCl_3$): δ = 25.9, 26.6, 28.5, 29.4, 30.1, 31.5, 35.0, 40.6, 67.5, 77.2, 108.8, 114.8, 152.1, 156.0, 158.6 ppm. ESI-MS(+): m/z (%) = 429 (100) 430 (20) $[M+Na]^+$.

Tert-butyl (11-(3,5-di-tert-butylphenoxy)undecyl)carbamate (12b): To a solution of **11b** (8.00 mmol) in anhydrous DMF (50 mL), K_2CO_3 (24.00 mmol) and 3,5-di-tert-butylphenol (7.60 mmol) were added. The reaction mixture was stirred for 18 hours at 80°C. After cooling at room temperature, the reaction was quenched with water (50 mL) and extracted with ethyl acetate (3x100 mL). The separated organic phase was dried over Na_2SO_4 and evaporated under reduced pressure. Product was isolated by column chromatography (n-hexane/THF 85:15) as a colorless oil (43%). ^{1}H NMR (400 MHz, $CDCl_3$): δ = 1.2–1.4 (m, 30 H, aliphatic C*H*$_2$ + Ar-*Bu*^{t}), 1.4-1.5 (m, 13 H, HN-CH$_2$C*H*$_2$ + aliphatic C*H*$_2$ + O*Bu*^{t}), 1.80 (m, 2 H, O-CH$_2$C*H*$_2$), 3.12 (t, ^{3}J(H,H)=6.4 Hz, 2 H, HN-C*H*$_2$), 3.98 (t, ^{3}J(H,H)=6.4 Hz, 2 H, O-C*H*$_2$), 4.51 (bs, 1 H, N*H*), 6.78 (s, 2 H, Ar*H*), 7.03 (s, 1 H, Ar*H*). ^{13}C NMR (75 MHz, $CDCl_3$): δ = 26.1, 26.8, 28.4, 29.3, 29.5 (3 res.), 29.6, 30.1, 30.3, 31.5, 35.0, 40.6, 72.9, 79.1, 108.8, 114.7, 152.1, 156.0, 158.7 ppm. ESI-MS(+): m/z (%) = 499 (100) $[M+Na]^+$.

Tert-butyl (6-bromohexyl)(6-(3,5-di-tert-butylphenoxy)hexyl)carbamate (13a): 12a (1.01 g, 2.50 mmol) was dissolved in anhydrous DMF (50 mL) and cooled at 0°C. NaH (0.20 g of 60 % dispersion in mineral oil, 5.00 mmol) was slowly added and the reaction mixture was stirred for 3 hours at room temperature under inert atmosphere. The orange solution was then cooled again at 0°C and 1,6-dibromohexane (1.82 g, 7.50 mmol) was added dropwise. After stirring for 18 hours at room temperature, the reaction was carefully quenched with water (40 mL) and extracted with ethyl acetate (3x50 mL). The organic phase was dried over Na_2SO_4 and evaporated under reduced pressure. The residue was purified by column chromatography (n-hexane/THF 95:5) to afford **13a** as a colorless oil (0.75 g, 57%). ^{1}H NMR (400 MHz, $CDCl_3$): δ = 1.2–1.4 (m, 22 H, aliphatic C*H*$_2$ + Ar-*Bu*^{t}), 1.4-1.6 (m, 17 H, aliphatic C*H*$_2$ + O*Bu*^{t}), 1.75 -1.9 (m, 4 H, O-

CH_2CH_2 + Br-CH_2CH_2), 3.17 (m, 4 H, N-CH_2), 3.43 (t, ^{3}J(H,H)=6.8 Hz, 2 H, Br-CH_2), 3.98 (t, ^{3}J(H,H)=6.4 Hz, 2 H, HO-CH_2), 6.77 (s, 2 H, Ar*H*), 7.03 (s, 1 H, Ar*H*). ^{13}C NMR (100 MHz, $CDCl_3$): δ = 26.0, 26.1, 26.7, 28.0, 28.5, 30.0, 31.5, 32.8, 33.8, 35.0, 46.9, 47.0, 67.6, 79.0, 108.8, 114.8, 152.1, 155.6, 158.6 ppm. ESI-MS(+): m/z (%) = 590 (100) 592 (98) $[M+Na]^+$.

tert-butyl (12-bromododecyl)(11-(3,5-di-tert-butylphenoxy)undecyl) carbamate (13b): 12b (1.54 g, 3.23 mmol) was dissolved in anhydrous DMF (50 mL) and cooled at 0°C. NaH (0.26 g of 60 % dispersion in mineral oil, 6.45 mmol) was slowly added and the reaction mixture was stirred for 3 hours at room temperature under inert atmosphere. The orange solution was then cooled again at 0°C and 1,12-dibromododecane (3.18 g, 9.70 mmol) was added dropwise. After stirring for 18 hours at room temperature, the reaction was carefully quenched with water (40 mL) and extracted with ethyl acetate (3x50 mL). The organic phase was dried over Na_2SO_4 and evaporated under reduced pressure. The residue was purified by column chromatography (n-hexane/THF 95:5) to afford **13b** as a colorless oil (1.35 g, 58%).^{1}H NMR (400 MHz, $CDCl_3$): δ = 1.2–1.4 (m, 44 H, aliphatic CH_2 + Ar-*Bu*^{t}), 1.4-1.5 (m, 17 H, aliphatic CH_2 + O*Bu*^{t}), 1.80-1.9 (m, 4 H, O-CH_2CH_2 + Br-CH_2CH_2), 3.16 (m, 4 H, N-CH_2), 3.43 (t, ^{3}J(H,H)=6.8 Hz, 2 H, Br-CH_2), 3.98 (t, ^{3}J(H,H)=6.4 Hz, 2 H, HO-CH_2), 6.78 (s, 2 H, Ar*H*), 7.03 (s, 1 H, Ar*H*).^{13}C NMR (100 MHz, $CDCl_3$): δ = 26.2, 26.9, 28.2, 28.5, 28.8, 29.4 (3 res.), 29.5 (4 res.), 29.6 (5 res.), 29.6, 30.4, 31.5, 32.9, 34.1, 35.0, 47.1, 67.8, 78.9, 108.8, 114.8, 152.1, 155.7, 158.7 ppm. ESI-MS(+): m/z (%) = 745 (100) 747 (98) $[M+Na]^+$.

General procedure for the synthesis of axles 8a-b: In a sealed glass reactor, salt **14** (0.23 mmol) and **13** (0.47 mmol) were dissolved in 5 mL of anhydrous acetonitrile and heated at 100°C for 5 days. After cooling at room temperature, the reaction mixture is further cooled at 0°C and precipitation of the product was observed. The solid was collected by Buchner filtration and washed with cold acetonitrile.

1-(6-((tert-butoxycarbonyl)(6-(3,5-di-tert-butylphenoxy)hexyl)amino)hexyl)-1'-(6-hydroxyhexyl)-[4,4'-bipyridine]-1,1'-diium bromide/tosylate (8a): Axle was obtained as a yellow solid (0.15 g, 46%). ^{1}H NMR (300 MHz, MeOD): δ = 1.3–1.6 (m, 45 H, aliphatic CH_2+ Ar-*Bu*^{t} + O-*Bu*^{t}), 1.7–1.9 (m, 2 H, Ar-O-CH_2CH_2), 2.0–2.2 (m, 4 H, N^+-CH_2CH_2), 2.39 (s, 6 H, Ar-CH_3), 3.25 (t,^{3}J(H,H)=6.9 Hz, 4 H, N-CH_2), 3.61 (t,^{3}J(H,H)=6 Hz, 2 H, HO-CH_2), 4.01 (t,^{3}J(H,H)=6 Hz, 2 H, Ar-OCH_2), 4.80 (t, ^{3}J(H,H)=7.5 Hz, 4 H, N^+-CH_2), 6.78 (s, 2H, Ar*H*), 7.06 (s, 1 H, Ar*H*), 7.26 (d,^{3}J(H,H)=8 Hz, 4 H, Ar*H*), 7.72 (d,^{3}J(H,H)=8 Hz, 4 H, Ar*H*), 8.72 (d,^{3}J(H,H)=6.4 Hz, 4 H, Ar*H*), 9.45 (d,^{3}J(H,H)=6.4 Hz, 4 H, Ar*H*). ^{13}C NMR (75 MHz, MeOD): δ = 18.0, 23.8, 23.9, 24.1, 24.2, 24.4, 24.8, 26.0, 26.8, 27.2,

27.4, 27.7, 29.1, 29.6, 30.4, 32.9, 46.2, 59.8, 60.3, 65.8, 77.8, 107.1, 112.8, 124.1, 125.4, 127.1, 138.8, 140.9, 145.4, 148.3, 150.3, 154.5, 157.3 ppm. ESI-MS(+): m/z (%) = 745 (100) $[M-H]^+$.

1-(12-((tert-butoxycarbonyl)(11-(3,5-di-tert-butylphenoxy)undecyl)amino)dodecyl)-1'-(6-hydroxyhexyl)-[4,4'-bipyridine]-1,1'-diium bromide/tosylate (8b): Axle was obtained as a yellow solid (0.13 g, 50%). ^{1}H NMR (400 MHz, MeOD): δ =1.2–1.4 (m, 44 H, aliphatic C*H*$_2$+ Ar-*Bu*^{t}), 1.4–1.6 (m, 21 H, aliphatic C*H*$_2$+ O-*Bu*^{t}), 1.7–1.9 (m, 4 H, aliphatic C*H*$_2$), 2.0-2.2 (m, 4 H, aliphatic C*H*$_2$), 2.38 (s, 3 H, Ar-C*H*$_3$), 3.18 (t,^{3}J(H,H)=7.2 Hz, 4 H, N-C*H*$_2$), 3.58 (t,^{3}J(H,H)=6.4 Hz, 2 H, HO-C*H*$_2$), 3.97 (t,^{3}J(H,H)=6.4 Hz, 2 H, OC*H*$_2$), 4.76 (m, 4 H, N$^+$-C*H*$_2$), 6.74 (s, 2H, Ar*H*), 7.02 (s, 1 H, Ar*H*), 7.24 (d,^{3}J(H,H)=8 Hz, 2 H, Ar*H*), 7.69 (d,^{3}J(H,H)=8 Hz, 2 H, Ar*H*), 8.69 (d,^{3}J(H,H)=6.4 Hz, 4 H, Ar*H*), 9.29 (d,^{3}J(H,H)=6.4 Hz, 2 H, Ar*H*). ^{13}C NMR (100 MHz, MeOD): δ = 20.0, 25.0, 25.6, 25.9 (2 res.), 26.5, 26.6, 27.5 (2 res.), 27.8 (2 res.), 28.3, 28.5, 28.8, 29.1, 29.2 (2 res.), 29.3, 29.4, 30.6, 31.1, 31.2, 31.8, 32.6, 33.1 (2 res.), 34.4, 46.7, 61.2, 61.8, 67.4, 79.2, 108.6, 114.3, 125.5, 126.9, 128.5, 140.3, 142.3, 145.7, 149.8, 151.7, 156.0, 158.8 ppm. ESI-MS(+): m/z: 899 (100) 900 (95) 901 (40) $[M-H]^+$, 1071 (25) 1072 (20) 1073 (18) $[M+TsO]^+$.

General procedure for the sequential synthesis of *up* rotaxanes: Axle **8** (0.03 mmol) was suspended in a solution of wheel **1** (0.03 mmol) in anhydrous toluene (20 mL). The suspension was stirred at room temperature for 3 hours until the solution turned dark-red and the axle was completely dissolved. Then triethylamine (0.04 mmol) and diphenylacetyl chloride (0.04 mmol) were added and the solution was stirred at room temperature overnight. After removing the solvent, the residue was portioned between dichloromethane and water. The organic phase was separated and evaporated under reduced pressure, and crude product was purified by column chromatography (dichloromethane/methanol 50:1). Boc-protected rotaxane was then dissolved in 10 mL of anhydrous dichloromethane and 2 mL of trifluoroacetic acid were added dropwise. The solution turned yellow. After stirring at room temperature for 2 hours, the solvent was evaporated under reduced pressure, re-dissolved in 20 mL of dichloromethane and washed with 0.1M Silver *p*-toluenesulfonate solution in water (50 mL). The organic phase was separated and the solvent was removed under reduced pressure, to afford deprotected rotaxane.

R[Nup]$_{short}$: the product was isolated as a red solid (0.08 g, 55%). ^{1}H NMR (400 MHz, C_6D_6): δ = 0.76 (t, ^{3}J(H,H)=6.0 Hz, 9 H, CH_2CH_3), 0.93 (bs, 2 H, N$^+$-CH_2CH_2), 1.1-1.4 (m, 43 H, Ar-Bu^t + aliphatic C*H*$_2$), 1.4-1.6 (m, 14 H, aliphatic C*H*$_2$), 1.63 (s, 18 H, OAr-Bu^t), 1.79 (m, 2 H, (C=O)OCH$_2$C*H*$_2$), 1.91 (m, 2 H, NH-CH$_2$C*H*$_2$), 2.01 (s, 6 H, Ar-C*H*$_3$), 2.71 (bs, 2 H,

NH-CH_2), 2.91 (bs, 2 H, NH-CH_2), 3.34 (m, 8 H, *eq*CH_2 + N^+-CH_2), 3.68 (m, 4 H, ArO-CH_2(CH_2)$_6$$CH_3$ + N^+-CH_2), 3.77 (s, 9 H, ArO-CH_3), 3.81 (m, 2 H, ArO-CH_2), 4.31 (t, ^{3}J(H,H)=6.0 Hz, 2 H, (C=O)OCH_2), 4.42 (d, ^{2}J(H,H)=12.0 Hz, 6 H, *ax*CH_2), 5.09 (s, 1 H, (C=O)C*H*), 6.59 (d, ^{3}J(H,H)=5.2 Hz, 2 H, Ar*H*), 6.67 (m, 2 H, Ar*H*), 6.87 (m, 3 H, Ar*H*), 6.99 (m, 14 H, Ar*H*), 7.15 (m, 11 H, Ar*H*), 7.42 (d, ^{3}J(H,H)=7.2 Hz, 4 H, Ar*H*), 7.54 (s, 6 H, ArH), 7.70 (d, ^{3}J(H,H)= 5.2 Hz, 2 H, Ar*H*), 7.83 (d, ^{3}J(H,H)=6.8 Hz, 6 H, Ar*H*), 8.15 (m, 2 H, Ar*H*), 8.23 (d, ^{3}J(H,H)=8.0 Hz, 4 H, Ar*H*), 9.0-9.3 (m, 7 H, N*H*). ^{13}C NMR (100 MHz, C_6D_6): δ = 13.2, 20.0, 21.9, 24.6, 25.0, 25.2, 25.6, 25.7, 26.2, 27.1, 27.2, 28.3, 28.7, 28.8, 28.9, 29.9, 30.7, 31.1, 33.8, 33.9, 47.9, 48.2, 56.4, 59.8, 59.9, 60.3, 61.1, 62.8, 64.0, 66.5, 72.3, 108.3, 113.6, 115.8, 117.3, 120.4, 124.0, 124.8, 125.1, 125.7, 126.4, 126.7, 127.0, 127.3, 127.7 (2 res), 127.8, 128.0, 128.5, 128.6, 131.2, 132.8, 136.5, 138.2, 138.6, 140.3, 142.1, 142.5, 143.5, 145.3, 147.5, 151.1, 152.0, 152.5, 158.6, 171.1 ppm. ESI-MS(+): m/z (%) = 1213 (100) 1213.5 (95) $[M]^{2+}$.

R[Nup]$_{long}$: the product was isolated as a red solid (0.03 mg, 27%). ^{1}H NMR (400 MHz, C_6D_6): δ = 0.94 (t, ^{3}J(H,H)=6.0 Hz, 9 H, CH_2CH_3), 1.1-1.3 (m, 57 H, Ar-Bu^t + aliphatic CH_2), 1.4-1.6 (m, 12 H, aliphatic CH_2), 1.69 (s, 18 H, OAr-Bu^t), 1.80 (m, 4 H, (C=O)OCH$_2$CH_2 + NH-CH_2CH_2), 1.99 (s, 6 H, Ar-CH_3), 2.59 (bs, 4 H, NH-CH_2), 3.38 (d, ^{2}J(H,H)=14.4 Hz, 6 H, *eq*CH_2), 3.49 (bs, 2 H, N^+-CH_2), 3.52 (bs, 2 H, N^+-CH_2), 3.70 (bs, 6 H, ArO-CH_2(CH_2)$_6$$CH_3$), 3.79 (s, 9 H, ArO-C$H_3$), 3.88 (t, ^{3}J(H,H)=7.0 Hz, 2 H, ArO-CH_2), 4.32 (t, ^{3}J(H,H)=6.8 Hz, 2 H, (C=O)OCH_2), 4.46 (d, ^{2}J(H,H)=14.4 Hz, 6 H, *ax*CH_2), 5.11 (s, 1 H, (C=O)C*H*), 6.9 (d, ^{3}J(H,H)=5.2 Hz, 2 H, Ar*H*), 6.77 (t, ^{3}J(H,H)=6.8 Hz, 3 H, Ar*H*), 6.83 (d, ^{3}J(H,H)=5.2 Hz, 2 H, Ar*H*), 6.94 (d, ^{3}J(H,H)=8.0 Hz, 4 H, Ar*H*), 7.01 (m, 4 H, Ar*H*), 7.15 (m, 7 H, Ar*H*), 7.43 (m, 4 H, ArH), 7.59 (s, 6 H, Ar*H*), 7.82 (s, 6 H, Ar*H*), 7.88 (d, ^{3}J(H,H)= 5.2 Hz, 2 H, Ar*H*), 8.14 (d, ^{3}J(H,H)=8.0 Hz, 4 H, Ar*H*), 9.2-9.4 (m, 7 H, N*H*). ^{13}C NMR (100 MHz, C_6D_6) δ = 14.0, 20.8, 22.8, 25.7 (2 res.), 25.8 (2 res.), 26.1 (2 res.), 26.4, 26.5, 26.6 (2 res.), 26.7, 28.8, 29.1, 29.2, 29.5 (2 res.), 29.6, 29.7 (2 res.), 29.8 (2 res.), 30.7, 30.8, 31.3, 31.5, 31.6, 31.9, 32.0 (2 res.), 34.6, 34.7, 38.2, 47.4, 47.5, 57.2, 59.7, 60.8, 64.8, 67.5, 73.1, 109.2, 114.4, 116.6, 118.1, 121.2. 124.8, 125.6, 126.4, 127.2, 128.3, 128.4, 128.5, 128.6, 128.7, 128.8, 129.3, 131.7, 132.0, 133.6, 137.3, 139.0, 139.6, 141.2, 142.9, 143.1, 144.1, 148.2, 148.4, 151.9, 152.9, 153.3, 159.5 ppm. ESI-MS(+): m/z (%) = 1290 (100) $[M]^{2+}$.

Tert-butyl (11-((tert-butyldimethylsilyl)oxy)undecyl)carbamate (16b): Tert-butylchlorodimethylsilane (0.89 g, 5.90 mmol) was slowly added to a solution of **10b** (1.43g, 5.00 mmol) and triethylamine (0.61 g, 6.00 mmol) in anhydrous dichloromethane (100 mL). A catalytic amount of DMAP was added. After stirring at room temperature for 2 hours, the reaction was quenched with water (50 mL) and the organic phase was separated, washed with brine, dried over anhydrous $CaCl_2$ and

filtered. The solvent was removed under reduced pressure to afford **16b** as a white oil (1.84 g, 92%). ^{1}H NMR (400 MHz, $CDCl_3$): δ = 0.05 (s, 6H, Si-C*H*$_3$), 0.90 (s, 9 H, Si-*Bu*^{t}), 1.30-1.45 (m, 14 H, aliphatic C*H*$_2$), 1.4-1.5 (m, 13 H, O-*Bu*^{t} + aliphatic C*H*$_2$), 3.10 (bs, 2 H, NH-C*H*$_2$), 3.60 (t, ^{3}J(H,H)=6.8 Hz, 2 H, Si-O-C*H*$_2$), 4.54 (bs, 1 H, N*H*). ^{13}C NMR (100 MHz, $CDCl_3$): δ = -5.3, 14.1, 18.4, 22.6, 25.7, 25.8, 26.0, 26.8, 28.4, 29.3, 29.4, 29.5 (2 res.), 29.6, 30.1, 31.6, 32.9, 40.7, 63.3, 78.9, 156.0 ppm. ESI-MS(+): m/z (100) = 424 (100) 425 (30) $[M+Na]^{+}$.

Tert-butyl (6-bromohexyl)(6-((tert-butyldimethylsilyl)oxy)hexyl)carbamate (17a): 16a (1.45g, 4.40 mmol) was dissolved in anhydrous DMF (100 mL) and cooled at 0°C. NaH (0.35 g of 60 % dispersion in mineral oil, 8.80 mmol) was slowly added and the reaction mixture was stirred for 3 hours at room temperature under inert atmosphere. The solution was then cooled again at 0°C and 1,6-dibromohexane (4.27 g, 17.40 mmol) was added. After stirring for 24 hours at room temperature, the reaction was carefully quenched with water (100 mL) and extracted with ethyl acetate (3x50 mL). The organic phase was dried over Na_2SO_4 and evaporated under reduced pressure. The residue was purified by column chromatography (n-hexane/THF 9:1) to afford ZV136 as a colorless oil (1.19 g, 55%). ^{1}H NMR (400 MHz, $CDCl_3$): δ = 0.009 (s, 6H, Si-C*H*$_3$), 0.86 (s, 9 H, Si-*Bu*^{t}), 1.27 (m, 4 H, aliphatic C*H*$_2$), 1.42 (s, 9 H, O-*Bu*^{t}), 1.4 - 1.5 (m, 10 H, aliphatic C*H*$_2$), 1.82 (m, 2 H, Br-CH$_2$C*H*$_2$), 3.11 (bs, 4 H, N-C*H*$_2$), 3.36 (t, ^{3}J(H,H)=7 Hz, 2 H, Br-C*H*$_2$), 3.56 (t, ^{3}J(H,H)=8 Hz, 2 H, Si-O-C*H*$_2$). ^{13}C NMR (100 MHz, $CDCl_3$): δ = -5.26, 14.1, 18.4, 22.7, 25.6, 25.9, 26.1, 26.7, 28.0, 29.7,30.3, 32.8, 33.8, 46.8, 47.0, 63.2, 79.0, 155.6 ppm. ESI-MS(+): m/z (%) = 516 (97) 518 (100) 519 (30) $[M+Na]^{+}$.

Tert-butyl (12-bromododecyl)(11-((tert-butyldimethylsilyl)oxy)undecyl)carbamate (17b): 16b (1.16 g, 2.90 mmol) was dissolved in anhydrous DMF (100 mL) and cooled at 0°C. NaH (0.23 g of 60 % dispersion in mineral oil, 5.80 mmol) was slowly added and the reaction mixture was stirred for 3 hours at room temperature under inert atmosphere. The solution was then cooled again at 0°C and 1,12-dibromododecane (3.79 g, 11.60 mmol) was added. After stirring for 48 hours at room temperature, the reaction was carefully quenched with water (100 mL) and extracted with ethyl acetate (3x50 mL). The organic phase was dried over Na_2SO_4 and evaporated under reduced pressure. The residue was purified by column chromatography (fron n-hexane 100% to n-hexane/THF 98:2) to afford **16b** as a colorless oil (2.52 g, 54%). ^{1}H NMR (300 MHz, $CDCl_3$): δ = 0.06 (s, 6H, Si-C*H*$_3$), 0.91 (s, 9 H, Si-*Bu*^{t}), 1.28 (m, 28 H, aliphatic C*H*$_2$), 1.46 (s, 9 H, O-*Bu*^{t}), 1.4 - 1.6 (m, 8 H, aliphatic C*H*$_2$), 1.86 (m, 2 H, Br-CH$_2$C*H*$_2$), 3.15 (t, ^{3}J(H,H)=7 Hz, 4 H, N-C*H*$_2$), 3.42 (t, ^{3}J(H,H)=6.8 Hz, 2 H, Br-C*H*$_2$), 3.61 (t, ^{3}J(H,H)=6.6 Hz, 2 H, Si-O-C*H*$_2$). ^{13}C NMR (100 MHz, $CDCl_3$): δ = -5.3, 25.8, 26.0, 26.9, 28.2, 28.5, 28.8,

29.4, 29.5, 29.6, 32.8, 32.9, 34.0, 47.0, 63.3, 78.8, 155.6 ppm. ESI-MS(+): m/z (%) = 648 (95) 650 (100) 651 (40) $[M+H]^+$.

General procedure for the synthesis of 18: 17 (1.56 mmol) was dissolved in a mixture of anhydrous acetonitrile (80 mL) and DMF (10 mL) and anhydrous cerium chloride (3.12 mmol) was added. The reaction mixture was refluxed for 3 days. The solution was then cooled at room temperature and the solvent removed under reduced pressure. The oily residue was taken up with ethyl acetate (100 mL) and washed with water (3x50 mL). The separated organic phase was dried over Na_2SO_4 and evaporated under reduced pressure.

Tert-butyl (6-chlorohexyl)(6-hydroxyhexyl)carbamate (18a): The crude product was purified by column chromatography (n-hexane/THF 6:4) to afford chlorinated product **18a** as a colorless oil (50%). ^{1}H NMR (400 MHz, $CDCl_3$): δ = 1.31 (m, 4 H, aliphatic CH_2), 1.47 (s, 9 H, O-*Bu*^{t}), 1.4 - 1.6 (m, 8 H, aliphatic CH_2), 1.62 (bs, 2 H, HO-CH_2CH_2), 1.79 (m, 2 H, Cl-CH_2CH_2), 3.17 (bs, 4 H, N-CH_2), 3.55 (t, ^{3}J(H,H)=6.4 Hz, 2 H, HO-CH_2), 3.65 (t, ^{3}J(H,H)=6 Hz, 2 H, Cl-CH_2). ^{13}C NMR (100 MHz, $CDCl_3$): δ = 26.2, 26.7, 28.5, 31.0, 32.6, 32.7, 45.0, 46.8, 62.6, 62.9, 79.1, 155.7 ppm. ESI-MS(+): m/z (%) = 336 (100) 338 (30) 337 (20) $[M+H]^+$, 358 (100) 360 (30) 359 (20) $[M+Na]^+$, 374 (100) 376 (30) 375 (20) $[M+K]^+$.

Tert-butyl (12-chlorododecyl)(11-hydroxyundecyl)carbamate (18b): 17b was purified by column chromatography (n-hexane/ethyl acetate 9:1) to afford chlorinated product as a colorless oil (0.22 g, 60%). ^{1}H NMR (400 MHz, $CDCl_3$): δ = 1.27 (m, 28 H, aliphatic CH_2), 1.45 (s, 9 H, O-*Bu*^{t}), 1.4 - 1.6 (m, 8 H, aliphatic CH_2), 1.76 (m, 2 H, Cl-CH_2CH_2), 3.13 (bs, 4 H, N-CH_2), 3.53 (t, ^{3}J(H,H)=6.8 Hz, 2 H, HO-CH_2), 3.63 (t, ^{3}J(H,H)=6.8 Hz, 2 H, Cl-CH_2). ^{13}C NMR (100 MHz, $CDCl_3$): δ = 25.7, 26.9, 28.5, 28.9, 29.4 (2 res.), 29.5 (3 res.), 29.6, 32.6, 32.8, 45.1, 47.0, 63.0, 78.9, 155.7 ppm. ESI-MS(+): m/z (%) = 490 (100) 491 (30) 492 (30) $[M+H^+]$, 512 (100) 513 (30) 514 (30) $[M+Na^+]$, 528 (100) 529 (30) 530 (20) $[M+K]^+$.

General procedure for the synthesis of axles 15a-b: In a sealed glass reactor, salt **21** (0.15 mmol) and chloride **18** (0.30 mmol) were dissolved in 5 mL of anhydrous acetonitrile and stirred at 100°C for 7 days. After cooling at room temperature, 10 mL of ethyl acetate were added and the mixture was further cooled at 0°C to induce the precipitation of the product. The solid was collected by Buchner filtration and washed with cold ethyl acetate.

1-(6-((tert-butoxycarbonyl)(6-hydroxyhexyl)amino)hexyl)-1'-(6-(3,5-di-tert-butylphenoxy)hexyl)-[4,4'-bipyridine]-1,1'-diium chloride/tosylate (15a): Axle was obtained as a sticky white solid (0.09 g, 65%). ^{1}H NMR (400 MHz, MeOD): δ = 1.3–1.6 (m, 36 H, aliphatic C*H*$_2$+ Ar-*Bu*^{t} + O-*Bu*^{t}), 1.83 (t, ^{3}J(H,H)=6.8 Hz, 2 H, Ar-O-CH$_2$C*H*$_2$), 2.14 (t, ^{3}J(H,H)=7.2 Hz, 4 H, N$^+$-CH$_2$C*H*$_2$), 2.37 (s, 6 H, Ar-C*H*$_3$), 3.20 (m, 4 H, N-C*H*$_2$), 3.57 (m, 2 H, HO-C*H*$_2$), 3.99 (t,^{3}J(H,H)=6.0 Hz, 2 H, Ar-OC*H*$_2$), 4.76 (t, ^{3}J(H,H)=7.2 Hz, 4 H, N$^+$-C*H*$_2$), 6.74 (s, 2H, Ar*H*), 7.03 (s, 1 H, Ar*H*), 7.24 (d,^{3}J(H,H)=8 Hz, 4 H, Ar*H*), 7.70 (d,^{3}J(H,H)=8 Hz, 4 H, Ar*H*), 8.66 (d,^{3}J(H,H)=6.0 Hz, 4 H, Ar*H*), 9.27 (d,^{3}J(H,H)=6.0 Hz, 4 H, Ar*H*). ^{13}C NMR (100 MHz, MeOD): δ = 19.9, 25.3, 25.6, 26.3, 27.4, 28.9, 30.5, 31.1, 32.2, 34.4, 61.2, 61.4, 61.8, 67.0, 79.3, 108.5, 114.4, 125.6, 126.9, 128.5, 140.3, 145.7, 149.9, 151.9, 156.0, 158.7, 160.7 ppm. ESI-MS(+): m/z (%) = 745 (100) 746 (50) 747 (20) [M-H]$^+$.

1-(6-(3,5-di-tert-butylphenoxy)hexyl)-1'-(12-((11-hydroxyundecyl)amino)dodecyl)-[4,4'-bipyridine]-1,1'-diium (15b): Axle was obtained as a sticky yellow solid (0.070 g, 88%). ^{1}H NMR (400 MHz, MeOD): δ = 1.3–1.6 (m, 67 H, aliphatic C*H*$_2$+ Ar-*Bu*^{t} + O-*Bu*^{t}), 1.84 (m, 2 H, aliphatic C*H*$_2$), 2.13 (m, 4 H, N$^+$-CH$_2$C*H*$_2$), 2.39 (s, 3 H, Ar-C*H*$_3$), 3.19 (t,^{3}J(H,H)=7.6 Hz, 4 H, N-C*H*$_2$), 3.55 (t,^{3}J(H,H)=6.8 Hz, 2 H, HO-C*H*$_2$), 4.00 (t,^{3}J(H,H)=6.4 Hz, 2 H, Ar-OC*H*$_2$), 4.80 (m, 4 H, N$^+$-C*H*$_2$), 6.75 (s, 2H, Ar*H*), 7.02 (s, 1 H, Ar*H*), 7.25 (d,^{3}J(H,H)=8 Hz, 2 H, Ar*H*), 7.72 (d,^{3}J(H,H)=8 Hz, 2 H, Ar*H*), 8.71 (d,^{3}J(H,H)=6.4 Hz, 4 H, Ar*H*), 9.33 (m, 4 H, Ar*H*). ^{13}C NMR (100 MHz, MeOD): δ = 25.6, 25.9, 26.5 (2 res.), 27.4, 28.8, 28.9, 29.1, 29.2, 29.3, 30.5, 31.1, 31.2, 32.3, 34.4, 61.6, 61.8, 61.9, 67.1, 79.2, 108.6, 125.6, 127.1, 128.5, 140.3, 142.1, 145.7, 149.8, 151.8, 156.1, 158.8 ppm. ESI-MS(+): m/z (%) = 900 (100) [M-H]$^+$.

General procedure for the synthesis of salt 22: Bromide **13** (0.34 mmol) and 4,4'-bipiridyne (1.01 mmol) were dissolved in anhydrous acetonitrile (50 mL) and heated at reflux overnight. The solvent was then removed under reduced pressure to afford a crude solid residue that was triturated with ethyl acetate and hexane (4x25 mL).

1-(6-((tert-butoxycarbonyl)(6-(3,5-di-tert-butylphenoxy)hexyl)amino)hexyl)-[4,4'-bipyridin]-1-ium bromide (22a): 22a was isolated as a sticky yellow solid (0.13 g, 52%). ^{1}H NMR (300 MHz, MeOD): δ = 1.30 (s, 18 H, Ar-*Bu*^{t}), 1.30–1.6 (m, 21 H, aliphatic C*H*$_2$ + O-*Bu*^{t}), 1.78 (t, ^{3}J(H,H)=7.5 Hz, 2 H, Ar-O-CH$_2$C*H*$_2$), 2.19 (t, ^{3}J(H,H)=6.8 Hz, 2 H, N$^+$-CH$_2$C*H*$_2$), 3.22 (t,^{3}J(H,H)=7.3 Hz, 4 H, N-C*H*$_2$), 3.97 (t,^{3}J(H,H)=7.5 Hz, 2 H, Ar-O-CH$_2$C*H*$_2$), 4.75 (t,^{3}J(H,H)=6.8 Hz, 4 H, N$^+$-C*H*$_2$), 6.73 (s, 2H, Ar*H*), 7.01 (s, 1 H, Ar*H*), 8.04 (d,^{3}J(H,H)=8 Hz, 2 H, Ar*H*), 8.56 (d,^{3}J(H,H)=8 Hz, 2 H, Ar*H*), 8.84 (d,^{3}J(H,H)=8 Hz, 2 H, Ar*H*), 9.19 (d,^{3}J(H,H)=8 Hz, 2 H, Ar*H*). ^{13}C NMR (75 MHz, MeOD): δ = 25.6 (2 res.), 26.3, 27.5, 28.3, 29.1, 30.6, 31.0, 31.1, 34.4, 46.5, 61.9, 67.4, 79.3, 108.6, 114.3, 122.3,

125.8, 142.2, 145.2, 150.4, 151.8, 153.5, 156.0, 158.8 ppm. ESI-MS(+): m/z (%) = 645 (100) 646 (95) 647 (80) $[M]^+$.

1-(12-((tert-butoxycarbonyl)(11-(3,5-di-tert-butylphenoxy)undecyl)amino)dodecyl)-[4,4'-bipyridin]-1-ium bromide (22b): Axle was obtained as a sticky yellow solid (0.49 g, 60%). ^{1}H NMR (400 MHz, $CDCl_3$): δ = 1.2–1.4 (m, 52 H, aliphatic C*H*$_2$ + Ar-*Bu*^{t} + C*H*$_2$ + O*Bu*^{t}), 1.77 (t, ^{3}J(H,H)=8 Hz, 2 H, O-CH$_2$C*H*$_2$), 2.08 (t, ^{3}J(H,H)=7 Hz, 2 H, N^+-CH$_2$C*H*$_2$), 3.18 (t, ^{3}J(H,H)=7.4 Hz, 4 H, N-C*H*$_2$), 3.97 (t, ^{3}J(H,H)=8 Hz, 2 H, ArO-C*H*$_2$), 4.73 (t, ^{3}J(H,H)=7 Hz, 2 H, N^+-C*H*$_2$), 6.73 (s, 2 H, Ar*H*), 7.02 (s, 1 H, Ar*H*), 8.03 (d, ^{3}J(H,H)=8 Hz, 2 H, Ar*H*), 8.55 (d, ^{3}J(H,H)=8 Hz, 2 H, Ar*H*), 8.85 (d, ^{3}J(H,H)=8 Hz, 2 H, Ar*H*), 9.17 (d, ^{3}J(H,H)=8 Hz, 2 H, Ar*H*). ^{13}C NMR (100 MHz, $CDCl_3$): δ = 25.8, 26.5 (2 res.), 27.5, 28.8, 29.1, 29.2 (2 res.), 29.3, 29.4, 30.6, 31.1, 34.4, 61.3, 67.5, 79.4, 108.6, 114.5, 122.4, 126.1, 142.2, 145.5, 150.5, 152.0, 153.7, 156.2, 159.1 ppm. ESI-MS(+): m/z (%) = 799 (100) 800 (80) 801 (40) $[M]^+$.

General procedure for the supramolecularly assisted synthesis of *down* rotaxanes: Wheel **1** (0.04 mmol), salt **22** (0.06 mmol) and bromide **23** (0.08 mmol) were suspended in anhydrous toluene (15 mL), and the mixture was stirred for two days at 110°C. After few hours, the mixture turned red and homogeneous. The solvent was then removed under reduced pressure and the residue was portioned between dichloromethane and water. The separated organic phase was evaporated under reduced pressure, and crude product was purified by column chromatography (dichloromethane/methanol 50:1). Isolated Boc-protected rotaxane was then dissolved in 5 mL of anhydrous dichloromethane and 5 mL of trifluoroacetic acid were added dropwise. The red solution turned yellow. After stirring at room temperature for 2 hours, the solvent was evaporated under reduced pressure to give the crude deprotected rotaxane. The residue was re-dissolved in 20 mL of dichloromethane and washed with 0.1M Silver *p*-toluenesulfonate solution in water (30 mL). The organic phase was separated and the solvent was removed under reduced pressure, to afford deprotected rotaxane.

R[Ndown]$_{short}$: Rotaxane was isolated as a red solid (0.06 g, 58%). ^{1}H NMR (400 MHz, C_6D_6): δ = 0.76 (bs, 2 H, N+-CH$_2$C*H*$_2$), 0.95 (t, ^{3}J(H,H)=6.0 Hz, 9 H, CH$_2$C*H*$_3$), 1.1-1.4 (m, 61 H, Ar-Bu^t + aliphatic C*H*$_2$), 1.59 (m, 2 H, aliphatic C*H*$_2$), 1.63 (s, 18 H, OAr-Bu^t), 1.77 (m, 2 H, (C=O)OCH$_2$C*H*$_2$), 1.91 (m, 8 H, NH-CH$_2$C*H*$_2$ + ArO-CH$_2$C*H*$_2$(CH$_2$)$_5$CH$_3$), 2.00 (s, 6 H, Ar-C*H*$_3$), 2.15 (bs, 4 H, aliphatic C*H*$_2$), 2.90 (bs, 2 H, NH-C*H*$_2$), 3.15 (bs, 2 H, NH-C*H*$_2$), 3.40 (m, 8 H, *eq*C*H*$_2$ + N^+-C*H*$_2$), 3.76 (m, 6 H, ArO-C*H*$_2$(CH$_2$)$_6$CH$_3$), 3.82 (m, 2 H, N^+-C*H*$_2$), 3.88 (m, 2 H, ArO-C*H*$_2$), 3.93 (s, 9 H, ArO-C*H*$_3$), 4.03 (t, ^{3}J(H,H)=7.2 Hz, 2 H, (C=O)O-C*H*$_2$), 4.50 (t, ^{2}J(H,H)=15.0 Hz, 6 H, *ax*C*H*$_2$), 5.12 (s, 1 H, (C=O)C*H*), 6.67 (m, 5 H, Ar*H*), 6.82 (d,

^{3}J(H,H)=5.2 Hz, 2 H, Ar*H*), 6.98 (m, 11 H, Ar*H*), 7.15 (m, 10 H, Ar*H*), 7.43 (m, 8 H, Ar*H*), 7.58 (s, 6 H, ArH), 7.80 (d, ^{3}J(H,H)= 5.2 Hz, 2 H, Ar*H*), 7.86 (m, 6 H, Ar*H*), 8.03 (d, ^{3}J(H,H)=5.2 Hz, 2 H, Ar*H*), 8.14 (d, ^{3}J(H,H)=8.0 Hz, 4 H, Ar*H*), 9.2-9.6 (m, 7 H, N*H*). ^{13}C NMR (100 MHz, C_6D_6): δ = 14.1, 20.8, 22.8, 24.9, 25.5, 25.6, 25.9, 26.4, 26.7, 28.3, 29.3, 29.6, 29.8, 30.7, 31.3, 31.5, 32.0, 34.6, 34.8, 38.2, 46.8, 57.4, 60.5, 61.1, 64.7, 67.1, 73.3, 109.0, 114.8, 116.8, 118.1, 121.3, 124.8, 125.7, 126.4, 127.2, 128.6, 128.7 (2 res.), 128.8129.3, 132.0, 133.6, 137.4, 139.2, 139.7, 141.1, 142.9, 143.2, 144.3, 146.3, 148.3, 148.4, 152.1, 152.8, 153.3, 159.2, 172.0 ppm. ESI-MS(+): m/z (%) = 1213 (100) 1213.5 (95) $[M]^{2+}$.

R[Ndown]$_{long}$: product was isolated as a red solid (0.08 g, 69%).^{1}H NMR (400 MHz, C_6D_6): δ = 0.71 (bs, 2 H, N^{+}-CH_2CH_2), 0.91 (bs, 2 H, N^{+}-CH_2CH_2), 0.99 (t, ^{3}J(H,H)=6.0 Hz, 9 H, CH_2CH_3), 1.1-1.5 (m, 69 H, Ar-Bu^{t} + aliphatic CH_2), 1.5-1.7 (m, 44 H, Ar-Bu^{t} + aliphatic CH_2), 1.78 (m, 4 H, aliphatic CH_2), 1.86 (m, 4 H, aliphatic CH_2), 1.98 (s, 6 H, Ar-CH_3), 2.16 (bs, 2 H, NH-CH_2CH_2), 2.58 (bs, 4 H, NH-CH_2), 3.37 (d, ^{2}J(H,H)=14.8 Hz, 6 H, *eq*CH_2), 3.61 (bs, 2 H, N^{+}-CH_2), 3.73 (m, 6 H, ArO-C$H_2(CH_2)_6CH_3$), 3.77 (bs, 2 H, N^{+}-CH_2), 3.87 (m, 11 H, ArO-CH_2 + ArO-CH_3), 4.04 (t, ^{3}J(H,H)=6.8 Hz, 2 H, (C=O)OCH_2), 4.47 (d, ^{2}J(H,H)=14.8 Hz, 6 H, *ax*CH_2), 5.13 (s, 1 H, (C=O)C*H*), 6.55 (d, ^{3}J(H,H)=5.2 Hz, 2 H, Ar*H*), 6.68 (t, ^{3}J(H,H)=7.2 Hz, 3 H, Ar*H*), 6.85 (d, ^{3}J(H,H)=5.2 Hz, 2 H, Ar*H*), 6.93 (d, ^{3}J(H,H)=8.4 Hz, 4 H, Ar*H*), 7.02 (m, 8 H, Ar*H*), 7.12 (s, 1 H, Ar*H*), 7.15 (m, 6 H, ArH), 7.19 (s, 2 H, Ar*H*), 7.44 (d, ^{3}J(H,H)= 7.2 Hz, 6 H, Ar*H*), 7.58 (s, 6 H, Ar*H*), 7.72 (d, ^{3}J(H,H)=5.2 Hz, 2 H, Ar*H*), 7.84 (m, 6 H, Ar*H*), 7.93 (m, 4 H, Ar*H*), 8.14 (d, ^{3}J(H,H)=8.4 Hz, 4 H, Ar*H*), 9.3-9.6 (m, 7 H, N*H*). ^{13}C NMR (100 MHz, C_6D_6) δ = 14.1, 20.8, 22.8, 24.9, 25.5, 25.8, 26.4, 26.7 (2 res.), 26.9, 28.0, 28.3, 28.6, 29.1, 29.2, 29.5, 29.6, 29.7 (3 res.), 29.8 (2 res.), 29.9, 30.0, 30.4, 30.6, 30.8, 31.2, 31.3, 31.5, 31.7, 32.0, 34.6, 34.8, 47.2 (2 res.), 57.4, 60.5, 60.8, 61.1, 64.6, 67.4, 73.0,109.1, 114.6, 116.7, 118.0, 121.3, 124.7, 125.6, 125.4, 127.2, 127.6, 128.6, 128.7 (2 res.), 128.9, 129.3, 132.0, 133.7, 137.3, 139.2, 139.6, 141.0, 142.9, 143.1, 144.1, 147.9, 148.3, 152.0, 152.8, 153.2, 159.4, 172.0 ppm. ESI-MS(+): m/z (%) = 1290 (100) $[M]^{2+}$.

R[2N]: Wheel **1** (0.04 mmol), 4,4'-bipyridine (0.04 mmol) and bromide **13a** (0.12 mmol) were dissolved in anhydrous toluene (15 mL), and the mixture was refluxed For four days. The solvent was then removed under reduced pressure and the residue was portioned between dichloromethane and water. The separated organic phase was evaporated under reduced pressure, and crude product was purified by column chromatography (dichloromethane/methanol 50:1). Isolated Boc-protected rotaxane was then dissolved in 5 mL of anhydrous dichloromethane and 5 mL of trifluoroacetic acid were added. After stirring at room temperature for 2 hours, the solvent was evaporated under reduced pressure and the residue was re-dissolved in 20 mL of

dichloromethane and washed with 0.1M Silver *p*-toluenesulfonate solution in water (30 mL). The separated organic phase was evaporated under reduced pressure, to afford deprotected rotaxane (40%). ^{1}H NMR (400 MHz, C_6D_6): δ = 0.96 (t, ^{3}J(H,H)=6.0 Hz, 9 H, CH_2CH_3), 1.10 (m, 2 H, N^+-CH_2CH_2), 1.1-1.4 (m, 69 H, Ar-Bu^t + aliphatic CH_2), 1.4-1.6 (m, 32 H, OAr-Bu^t + aliphatic CH_2), 1.92 (m, 6 H, ArO-$CH_2CH_2(CH_2)_5CH_3$), 2.04 (s, 6 H, Ar-CH_3), 2.23 (m, 4 H, NH-CH_2CH_2 + N^+-CH_2CH_2), 2.72 (bs, 2 H, NH-CH_2), 2.90 (bs, 4 H, NH-CH_2), 3.14 (bs, 2 H, NH-CH_2), 3.24 (bs, 2 H, N^+-CH_2), 3.35 (d, ^{2}J(H,H)=15.0 Hz, 6 H, *eq*CH_2), 3.74 (bs, 6 H, ArO-$CH_2(CH_2)_6CH_3$), 3.84 (m, 4 H, ArO-CH_2), 3.94 (s, 9 H, ArO-CH_3), 4.14 (bs, 2 H, N^+-CH_2), 4.47 (d, ^{2}J(H,H)=15.0 Hz, 6 H, *ax*CH_2), 6.22 (bs, 2 H, Ar*H*), 6.68 (t, ^{3}J(H,H)=6.8 Hz 3 H, Ar*H*), 6.81 (d, ^{3}J(H,H)=5.2 Hz, 2 H, Ar*H*), 7.00 (d, ^{3}J(H,H)=8.0 Hz, 4 H, Ar*H*), 7.16 (m, 16 H, Ar*H*), 7.42 (s, 6 H, Ar*H*), 7.88 (m, 4 H, ArH), 8.13 (d, ^{3}J(H,H)=8.0 Hz, 4 H, Ar*H*), 8.54 (d, ^{3}J(H,H)=5.2 Hz, 2 H, Ar*H*), 9.0-9.3 (m, 8 H, N*H*). ^{13}C NMR (100 MHz, C_6D_6) δ = 14.0, 14.1, 20.1, 20.8, 22.8, 25.9, 26.4, 29.6, 29.8, 30.1, 30.6, 31.3, 31.4, 32.0, 34.5, 34.8, 47.6, 61.4, 66.3, 67.3, 109.1, 114.6, 116.8, 118.3, 126.0, 126.4, 133.9, 139.9, 140.9, 143.2, 147.9, 148.7, 152.0, 152.7, 153.3, 159.0, 159.4 ppm. ESI-MS(+): m/z (%) = 1259 (100) $[M]^{2+}$.

General procedure for the synthesis of uncomplexed stoppered axles A_{short} and A_{long}: Salt **6b** (1.00 eq.) and the appropriate alkylating agent (**13a** for A_{short} or **13b** for A_{long}, 2.00 eq.) were dissolved in anhydrous acetonitrile (20 mL) and heated at 100 °C for 7 days. The solvent was then removed under reduced pressure, the residue was suspended in ethyl acetate (10 mL) an cooled at 0°C. Precipitation of the Boc-protected products was observed. The axles were separated by Buchner filtration, dissolved in dichloromethane (50 mL) and treated with a molar excess of Trifluoroacetic acid, stirring at room temperature for 2 hours. The solvent was evaporated under reduced pressure to afford stoppered axles A_{short} and A_{long}.

A_{short}: the product was isolated in 60% yield. ^{1}H NMR (400 MHz, MeOD): δ = 1.31 (s, 18 H, Bu^t), 1.4–1.6 (m, 14 H, aliphatic CH_2), 1.6 (m, 2 H, aliphatic CH_2), 1.74 (m, 4 H, aliphatic CH_2), 2.00 (m, 2 H, N^+-CH_2CH_2), 2.12 (m, 2 H, N^+-CH_2CH_2), 2.33 (s, 3 H, Ar-CH_3), 3.00 (m, 4 H, NH-CH_2), 3.97 (t,^{3}J(H,H)=6.0 Hz, 2 H, ArO-CH_2), 4.16 (t,^{3}J(H,H)=6.0 Hz, 2 H, (C=O)O-CH_2), 4.67 (t,^{3}J(H,H)=7.6 Hz, 2 H, N^+-CH_2), 4.77 (t,^{3}J(H,H)=7.6 Hz, 2 H, N^+-CH_2), 5.08 (s, 1H, (C=O)C*H*), 6.75 (s, 2H, Ar*H*), 7.03 (s, 1 H, Ar*H*), 7.2-7.3 (m, 12 H, Ar*H*), 7.69 (d,^{3}J(H,H)=8.0 Hz, 2 H, Ar*H*), 8.64 (d,^{3}J(H,H)=6.0 Hz, 4 H, Ar*H*), 9.22 (d,^{3}J(H,H)=6.0 Hz, 2 H, Ar*H*), 9.28 (d,^{3}J(H,H)=6.0 Hz, 2 H, Ar*H*). ^{13}C NMR (100 MHz, MeOD): δ = 20.0, 24.8, 25.1, 25.2, 25.4 (2 res.), 25.8, 25.9, 27.9, 28.9, 30.5, 30.7, 30.9, 34.4, 56.9, 61.6, 61.7, 64.5, 67.2, 108.6, 114.4, 125.5, 126.9, 128.2, 128.3, 128.6, 138.9, 140.4, 142.3, 145.6, 145.7, 149.8, 149.9, 151.9, 158.8, 172.9 ppm. ESI-MS(+): m/z: 839 (100) $[M-H]^+$.

A_{long}: the product was isolated in 55% yield. ^{1}H NMR (400 MHz, MeOD): δ = 1.31 (s, 18 H, Bu^{t}), 1.4–1.5 (m, 36 H, aliphatic C*H*$_2$), 1.67 (m, 4 H, aliphatic C*H*$_2$), 1.77 (m, 2 H, aliphatic C*H*$_2$), 2.01 (m, 2 H, N^{+}-CH$_2$C*H*$_2$), 2.08 (m, 2 H, N^{+}-CH$_2$C*H*$_2$), 2.36 (s, 3 H, Ar-C*H*$_3$), 2.97 (t, ^{3}J(H,H)=8.0 Hz, 4 H, NH-C*H*$_2$), 3.97 (t,^{3}J(H,H)=6.4 Hz, 2 H, ArO-C*H*$_2$), 4.17 (t,^{3}J(H,H)=6.4 Hz, 2 H, (C=O)O-C*H*$_2$), 4.68 (t,^{3}J(H,H)=7.2 Hz, 2 H, N^{+}-C*H*$_2$), 4.74 (t,^{3}J(H,H)=7.2 Hz, 2 H, N^{+}-C*H*$_2$), 5.08 (s, 1H, (C=O)C*H*), 6.74 (s, 2H, Ar*H*), 7.02 (s, 1 H, Ar*H*), 7.2-7.4 (m, 12 H, Ar*H*), 7.69 (d,^{3}J(H,H)=8.0 Hz, 2 H, Ar*H*), 8.65 (d,^{3}J(H,H)=6.0 Hz, 4 H, Ar*H*), 9.22 (d,^{3}J(H,H)=6.0 Hz, 2 H, Ar*H*), 9.26 (d,^{3}J(H,H)=6.0 Hz, 2 H, Ar*H*). ^{13}C NMR (100 MHz, MeOD): δ = 20.0, 24.8, 25.1, 25.8, 25.9, 26.2, 27.8, 28.8 (3 res.), 29.0, 29.1, 29.2 (2 res.), 30.5, 30.9, 31.2, 34.4, 56.9, 61.7, 61.9, 64.5, 67.5, 108.6, 114.3, 125.5, 126.9, 128.2, 128.3, 128.5, 138.9, 140.4, 145.7, 149.9 (2 res.), 151.8, 158.8, 172.9 ppm. ESI-MS(+): m/z: 993 (100) [M-H]$^{+}$.

CHAPTER 5

CALIX[6]ARENE-BASED ORIENTED CATENANES

AS PROTOTYPES FOR ROTARY MOTORS

5.1 Introduction and state of the art

The chemistry of catenanes, - i.e. mechanically interlocked molecules consisting of two or more entwined macrocycles[1] - has lately experienced a remarkable development, in particular thanks to improved synthetical protocols[2] that disclosed the realization of molecular architectures of increasing complexity. The first synthetical attempts relied on statistical approach,[3] and yielded negligible amounts of the target catenanes. More recently, the progresses in template-directed syntheses provided new elegant and more performing strategies. Various classes of macrocycles have been employed as the basic macroring, and a wide set of non-covalent interactions, such as formation of host-guest adducts[4] and metal coordination,[5] have been exploited to gather the components into preorganized assemblies that can undergo catenation in a predictable and tunable way.

An interesting behavior of properly designed catenanes is the ability of the rings to rotate with respect to one another, that is to behave as rotary motors.[6] To accomplish this task, it is necessary to incorporate into the macrocycles specific functional units that, when properly stimulated, can pivot a controlled conformational rearrangement. Among these systems, catenanes which exhibit an unidirectional circumrotation of the rings (i.e. univocal clockwise on anticlockwise rotation) attract most of attention. The sense of rotation can be governed by the order in which a series of orthogonal chemical transformations is performed. An outstanding example is given by the systems realized by Leigh and coworkers,[7] in which the small rings of [2]- and [3]catenanes move in discrete steps between different binding sites located on a larger interlocked ring. The movements are driven by light, heat or chemical stimuli that change the relative affinity of the components (**Figure 5.1**).

[1] Gil-Ramírez, G.; Leigh, D. A.; Stephens, A. J. *Angew. Chem. Int. Ed.* **2015**, *54*, 6110-6150.
[2] Gibbs-Hall, I. C.; Vermeulen, N. A.; Dale, E. J.; Henkelis, J. J.; Blackburn, A. K.; Barnes, J. K.; Stoddart. J. F. *J. Am. Chem. Soc.* **2015**, *137*, 15640-15643.
[3] Wasserman, E. *J. Am. Chem. Soc.* **1960**, *82*, 4433-4434.
[4] Ashton, P. R.; Goodnow, T. T.; Kaifer, A. E.; Reddington, M. V.; Slawin, A. M. Z.; Spencer, N.; Stoddart, J. F.; Vicent, C.; Williams, D. J. *Angew. Chem. Int. Ed. Engl.* **1989**, *28*, 1396-1399; Anelli, P. L.; Ashton, P. R.; Ballardini, R.; Balzani, V.; Delgado, M.; Gandolfi, M. T.; Goodnow, T. T.; Kaifer, A. E.; Philp, D.; Pietraszkiewicz, M.; Prodi, L.; Reddington, M. V.; Slawin, A. M. Z.; Spencer, N.; Stoddart, J. F.; Vicent, C.; Williams, D. J. *J. Am. Chem. Soc.* **1992**, *114*, 193-218.
[5] Dietrichbuchecker, C. O.; Sauvage, J. P.; Kern, J. M. *J. Am. Chem. Soc.* **1984**, *106*, 3043-3045; Wang, K.; Yee, C. C.; Au-Yeung, H. Y. *Chem. Sci.* **2016**, *7*, 2787-2792.
[6] Spruell, J. M.; Paxton, W. F.; Olsen, J. C.; Benítez, D.; Tkatchouk, E.; Stern, C. L.; Trabolsi, A.; Friedman, D. C.; Goddard, W. A.; Stoddart, J. F. *J. Am. Chem. Soc.* **2009**, *131*, 11571-11580; Meng, Z.; Han, Y.; Wang, L. N.; Xiang, J. F.; He, S. G.; Chen, C. F. *J. Am. Chem. Soc.* **2015**, *137*, 9739-9745.
[7] Leigh, D. A.; Wong, J. K. Y.; Dehez, F.; Zerbetto, F. *Nature* **2003**, *424*, 174-179; Hernandez, J. V.; Kay, E. R.; Leigh, D. A. *Science* **2004**, *306*, 1532-1537.

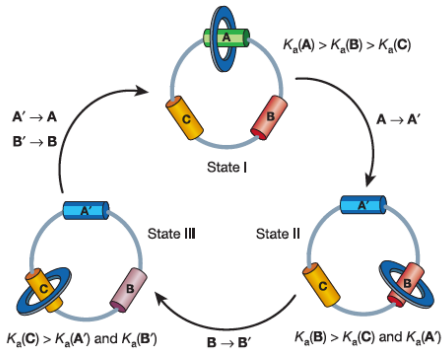

Figure 5.1 *Example of stimuli-induced sequential movement of a macrocycle between different binding sites in Leigh's [2]catenane (reproduced from ref. 7, copyright © Nature Publishing Group)*

The idea to insert a calix[6]arene as one of the macrocyclic components of a catenane was first pursued by Neri[8] and coworkers in 2013: the catenation step consisted in the reaction of the two terminal OH groups of a preformed calix[6]arene-based pseudorotaxane complex with an α-ω di-isocyanate (**Figure 5.2**).

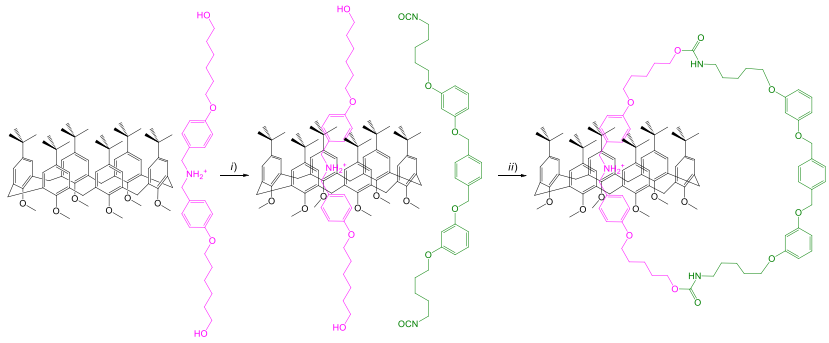

Figure 5.2 *Structure of Neri's through-the-annulus catenated calix[6]arene. Conditions: i) $CHCl_3$; ii) Dibutyltin dilaurate, $CHCl_3$.*

Taking inspiration from this work, and in view of our current interest in the development of new calix[6]arene-based switchable devices, we carried out the synthesis of a tris(*N*-phenylureido)calix[6]arene-based electroactive [2]catenane[9] by

[8] Gaeta, C.; Talotta, C.; Mirra, S.; Margarucci, L.; Casapullo, A.; Neri, P. *Org. Lett.* **2013**, *15* (1), 116-119.
[9] Orlandini, G.; Zanichelli, V.; Secchi, A.; Arduini, A.; Ragazzon, G.; Credi, A.; Venturi, M.; Silvi, S. *Supramol. Chem.* **2016**, *28*, 427-435.

applying the intramolecular ring-closing metathesis reaction (RCM) as the catenation step on a pre-formed pseudorotaxane (**Figure 5.3**):

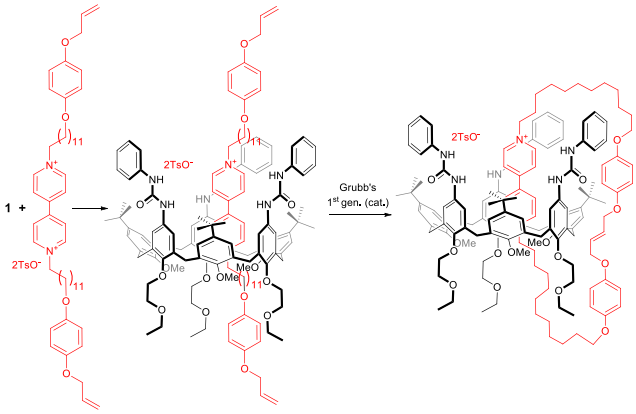

Figure 5.3 *Triphenylureido calix[6]arene-based [2]catenane.*

We exploited the presence of a dicationic viologen unit for the molecular recognition that is at the basis of the formation of the stable pseudorotaxane complex with the calixarene wheel. Each alkyl chain appended to the bipyridinium core bears a terminal alkene function, necessary for the RCM: the length of these alkenyl chains is optimized in order to favor the intramolecular closure and minimize intermolecular oligomerization side reactions. It was demonstrated that an overall length of the cyclic threaded axle of around 40 carbon atoms is the best compromise.

Electrochemical measurements showed that this catenane exhibits two reversible monoelectronic reduction processes, assigned to the first and second reduction of the viologen unit, at –0.60 and –1.13 V (vs. standard calomel electrode, SCE). Both reduction potentials are shifted to more negative values with respect to a free viologen-based axle (e.g. for dioctylviologen derivative $E_{1/2}^{I} = -0.42$ V and $E_{1/2}^{II} = -0.87$ V), in analogy with related single station rotaxane systems discussed in **Chapter 4**. The shift of the two reduction processes indicates that no dethreading of the viologen unit takes place after the reduction, and suggests that a residual interaction exists between the neutral viologen core and the calixarene, thus meaning that no circumrotation movement can be evidenced.

5.2 Synthesis and electrochemical study of double station [2]catenanes

With the final perspective to synthesize stimuli responsive rotary motors, we tackled the synthesis of two new calix[2]catenanes **C[Nup]** and **C[Ndown]**, constituted by receptor **1** and a macrocyclic interlocked ring functionalized with an amine moiety:

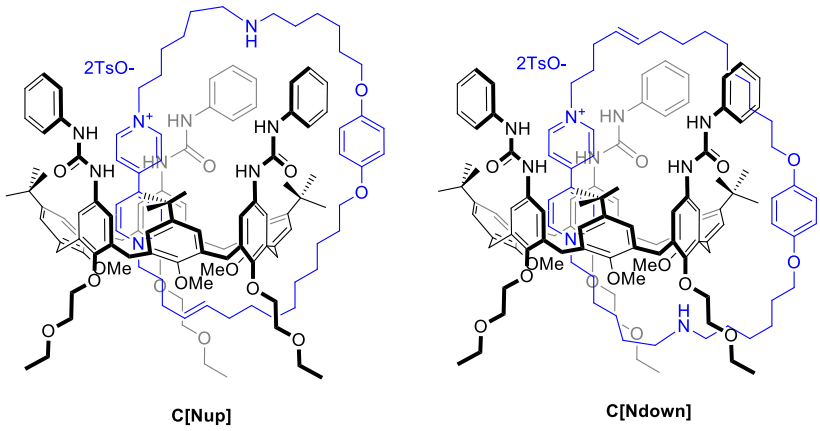

Figure 5.4 *Structures of the target catenanes.*

As for double station rotaxanes described in **Chapter 4**, we expect that the presence of an additional recognition unit for the calixarene cavity (i.e. the protonated ammonium station) should prompt the movement of the wheel along the cyclic dumbbell upon reduction of the bipyridinium core.

The presence of two non-palindrome interlocked macrocycles generates two constitutionally isomeric oriented catenanes, in which the mutual clockwise or anticlockwise circumrotations of the components are not equivalent. To infer if one direction is favored, it is necessary the study of both possible orientational isomers, in which the amine station is situated in proximity to the upper or the lower rim of **1**.

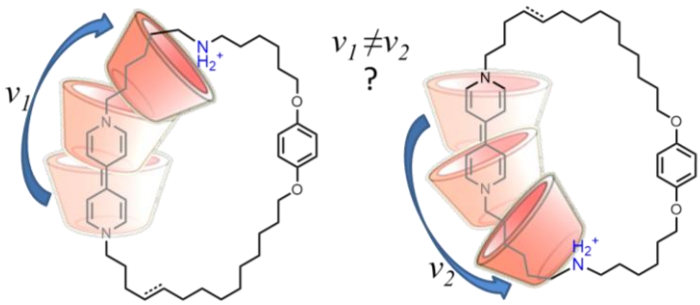

Figure 5.5 *Schematic representation of the circumrotatory motion of double-station catenanes.*

5.2.1 Sequential synthesis of C[Nup]

Taking advantage of the catenation protocol previously described, we planned to synthesize the desired oriented catenane **C[Nup]** starting from a pre-formed pseudorotaxane composed by wheel **1** and viologen axle **7**, obtained as reported in **Scheme 5.1** (see Experimental for details):

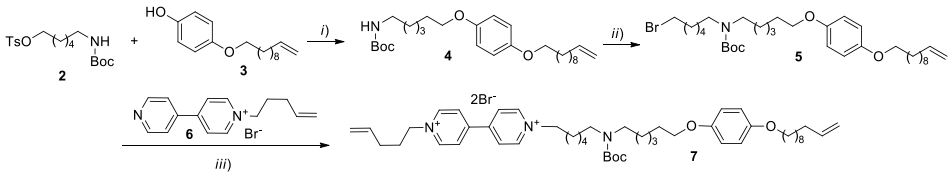

Scheme 5.1 *Reagents and conditions: i) K_2CO_3, DMF, 18h, 80°C; ii) a) NaH, DMF, rt, 2h; b) 1,6-dibromohexane, DMF, rt, 12h; iii) CH_3CN, 110°C, 7d.*

Boc-protected tosylate **2** was first reacted with *p*-hydroxyphenyl undec-10-en-1-yl ether **3** to obtain alkene **4**, and further functionalized with a bromine-terminated hexyl chain. The resulting product **5** was finally reacted with salt **6** to give axle **7**, characterized by one pentenyl substituent and by a longer chain that bears the protected amine moiety (see **Figure 5.6a** for ^{1}H NMR and **Scheme 5.2** for labelling). Each terminus of the axle presents an ω–alkene function that can undergo RCM reaction, and the overall length of the threaded dumbbell is designed to allow the intramolecular closure. Axle **7** was then equilibrated with an equimolar amount of **1** in toluene at room temperature. As validated for similar non-symmetric viologen axles[10], **7** selectively threads **1** from its upper rim with the shortest C5 alkenyl chain, since the longest and highly functionalized side chain acts as kinetic stopper. This gives rise to the oriented pseudorotaxane complex **P[1⊃7up]**, whose structure and relative arrangement were confirmed by NMR analysis:

[10] Arduini, A.; Bussolati, R.; Credi, A.; Secchi, A.; Silvi, S.; Semeraro, M.; Venturi, M. *J. Am. Chem. Soc*. **2013**, *135 (26)*, 9924-9930.

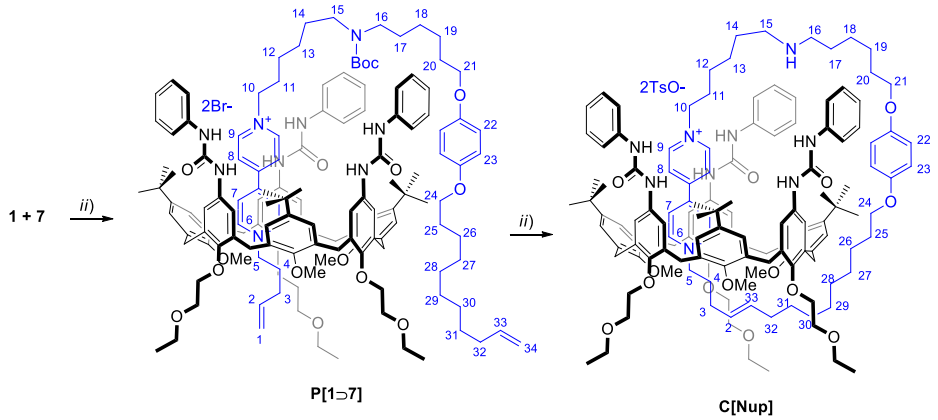

Scheme 5.2 *Reagents and conditions: i)toluene, 12h, rt; ii) a) 2nd gen. Grubbs cat., toluene, rt, 2d; b)TFA, CH_2Cl_2, rt, 3h.*

The ^{1}H NMR spectrum (see **Figure 5.6b** and **Scheme 5.2** for labelling) evidences how the portion of the axle threaded into the electron-rich cavity of **1** is affected by its shielding effect. As expected, this influence is higher for the resonances belonging to the pyridine ring that is more deeply engulfed into the cavity (protons *6* and *7*), rather than for protons *8* and *9*. Also the signals of the methylene groups in proximity to the pipyridinium core (*4*, *5*, *10* and *11*) experience a high field shift due to the complexation. In the central region of the spectrum, two different sets of signals ascribable to terminal alkenes are present. The one that undergoes a remarkable shift ($\Delta\delta \cong 0.5$ ppm) with respect to the free axle is assigned to protons *1* and *2*, located closer to the calixarene; on the other hand, the chemical shifts of protons *33* and *34*, more distant from the cavity, are comparable to the signals of uncomplexed **7**. Furthermore, the presence of a sharp singlet assigned to OCH_3 protons of **1** confirms the formation of a single pseudorotaxane orientational isomer.

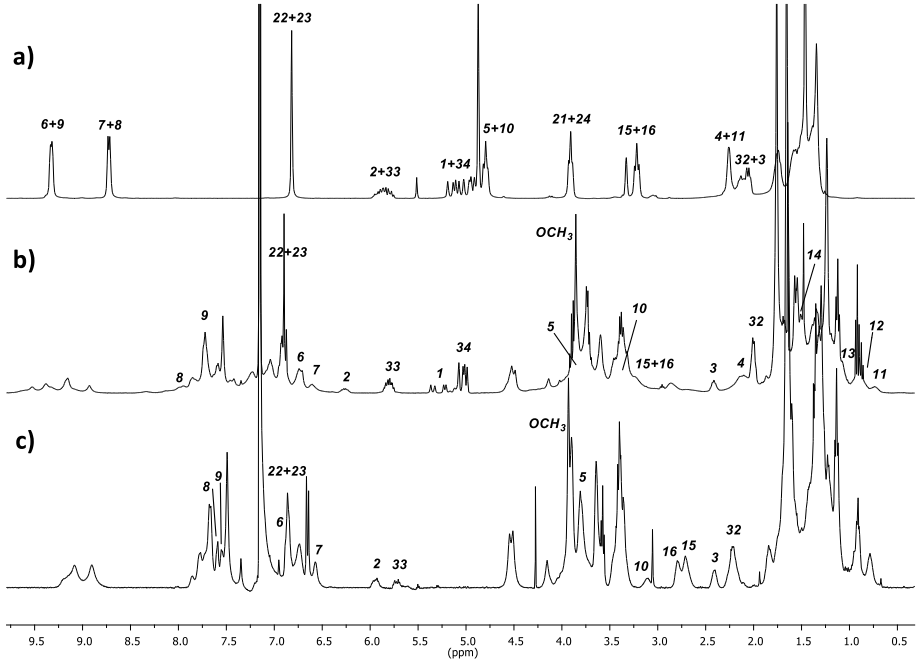

Figure 5.6 *^{1}H NMR spectra recorded at 400 MHz of a) axle **7** in CD_3OD; b)* **P[1⊃7up]** in C_6D_6 and c) **C[Nup]** in C_6D_6.

Besides the dimensions of the macrocycles, other key factors that affect intramolecular cyclization are the concentration of the preformed pseudorotaxane and the molar ratio between pseudorotaxane and metathesis catalyst during the catenation reaction. In agreement with literature data,[11] **P[1⊃7up]** was dissolved in anhydrous and degassed CH_2Cl_2 at 1 mM concentration, and a 15% of 2nd gen. Grubbs catalyst was added. Catenane **C[Nup]** was isolated in 17% yield after chromatographic separation, treated with trifluoroacetic acid to deprotect the amine moiety and subjected to NMR investigation (see **Figure 5.6c** and **Scheme 5.2** for labelling).

The pattern of signals in the ^{1}H NMR spectrum resembles, for several aspects, to that observed for the corresponding pseudorotaxane **P[1⊃7up]**, thus suggesting that the catenation of the axle ring happened through the calixarene annulus. The most relevant evidence of the occurred intramolecular metathesis is the disappearance of the signals of methylene protons *1* and *34*, and the presence of two methyne signals ascribed to the newly formed double bond (protons *2* and *33*). Moreover, in the TOCSY spectrum (see **Figure 5.7**) it is possible to evidence a series of

[11] Kidd, T. J.; Leigh, D. A.; Wilson, A. J. *J. Am. Chem. Soc.* **1999**, *121 (7)*, 1599-1600; Weck, M.; Mohr, B.; Sauvage, J. P.; Grubbs, R. H. *Org. Chem.* **1999**, *64 (15)*, 5463-5471; Guidry, E. N.; Cantrill, S. J.; Stoddart, J. F.; Grubbs, R. H.; *Org. Lett.* **2005**, *7 (11)*, 2129-2132.

correlations that links protons *2* to *32* (blue). These series is also related with protons *33* (red), thus confirming that the intramolecular closure took place. Again, the presence of a sharp singlet ascribed to the OCH_3 protons at the lower rim of **1** is in agreement with the presence of a single orientational catenane isomer.

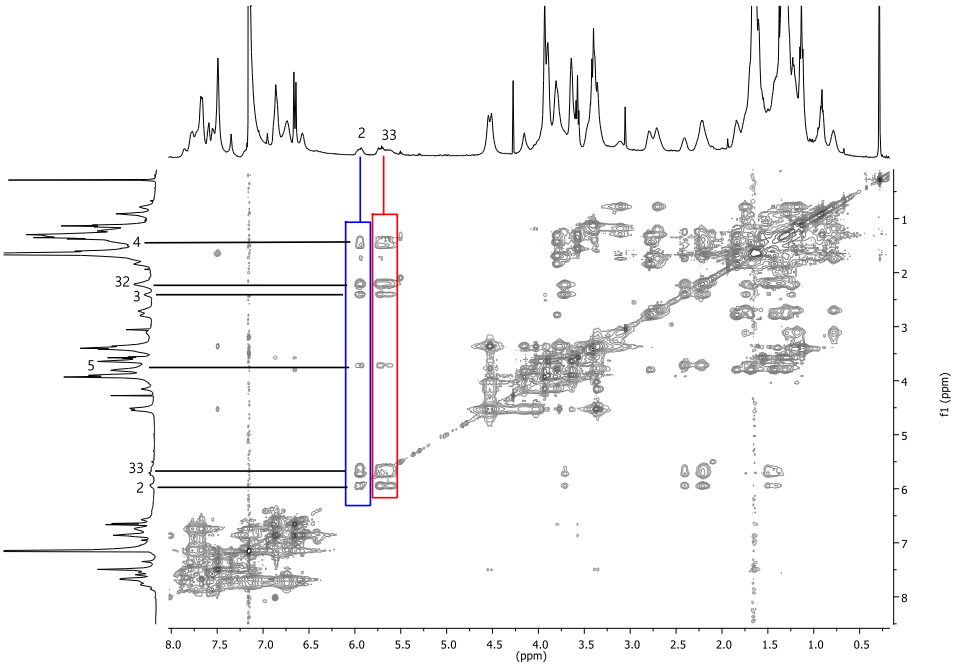

Figure 5.7 *^{1}H-^{1}H TOCSY NMR spectrum (400 MHz, C_6D_6, mixing time = 40 ms) of **C[Nup]**.*

Finally, high resolution mass spectrum (ORBITRAP LQ) confirmed the formation of **C[Nup].** The monoisotopic m/z peak at 1103.67551 is attributed to the doubly charged molecule, while peak at m/z = 2378.36114 to its adduct with one tosylate.

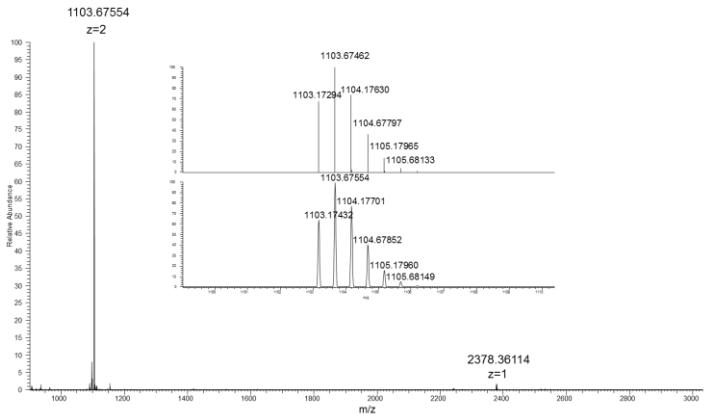

Figure 5.8 *High resolution mass spectrum of catenane **C[Nup]**. Inset: comparison between experimental (bottom) and simulated (top) isotopic distribution for m/z peak at 1103.67551 with z=2.*

5.2.2 Electrochemical investigation on C[Nup]

Electrochemical behavior of **C[Nup]** was investigated through cyclic voltammetry technique. This compound shows two reversible monoelectronic reduction processes at -0.597 and -0.877 V versus the standard calomel electrode SCE (see **Figure 5.9** and **Figure 5.10b**), which are assigned to the first and second reduction of the viologen unit, respectively. The reversibility of the processes confirms that no disassembly of the system takes place upon electrochemical stimulation.

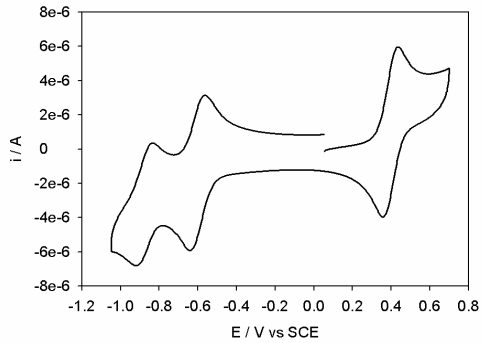

Figure 5.9 *Cyclic voltammogram of an argon-purged acetonitrile solution of catenane C[Nup] (support electrolyte = TEAPF6). The wave in the region of positive potentials is that of ferrocene used as a standard.*

As reported in the genetic diagram depicted in **Figure 5.10**, the first reduction potential of **C[Nup]** is shifted to more negative values with respect to a free viologen-based axle (**DOV** was used as model, see **Figure 5.10e**). This shift is due to the stabilization provided to the bipyridinium by the π–rich cavity of **1**, in analogy with similar single-station rotaxanes (see for comparison **R[C6C6]** in **Figure 5.10a**). On the other hand, the second reduction potential is comparable to the one of free **DOV**, thus meaning that, contrary to what observed for single station catenane, the wheel does not longer interact with the viologen core in its neutral form. These findings make us suppose that a translational movement of the calixarene **1** around the threaded annulus takes place as a consequence of the electrochemical stimulation.

The protonation of the ammonium station induces some changes in the two reduction potentials (see **Figure 5.10c**), and the initial values are re-established when the original situation is restored upon treatment with tributylamine (see **Figure 5.10d**).

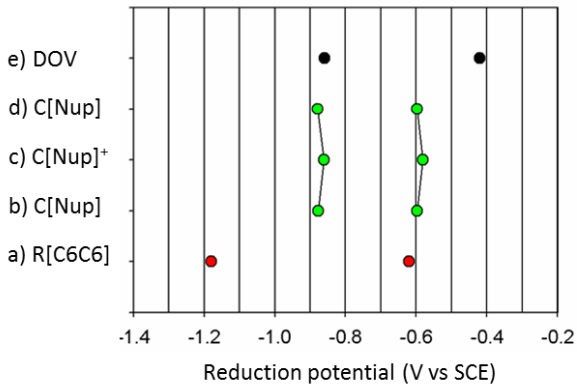

Figure 5.10 *Genetic diagram for the first and second reduction processes in CH_3CN of a) the model compound for single station rotaxanes **R[C6C6]**; b) **C[Nup]**; c) **C[Nup]** upon protonation with one equivalent of triflic acid and d) successive deprotonation with one equivalent of tributylamine; and e) the model compound for free viologen-based salt (**DOV**).*

5.2.3 Attempts of supramolecularly assisted synthesis of C[Ndown]

To establish whether the previously observed movement of **1** along the interlocked ring occurs through a preferential direction, the synthesis of the opposite orientational catenane isomer **C[Ndown]** was tackled. This isomer can't be synthesized through the previously exploited technique, since it is not possible to obtain the corresponding oriented pseudorotaxane bearing the longest and highly functionalized axle chain directed toward the lower rim of **1** *via* spontaneous directional threading.

We therefore set up a supramolecularly assisted reaction to achieve the formation of **P[1⊃7down]** by reacting pyridyl-pyridinium salt **8** with 5-bromo-1-pentene in presence of wheel **1** (see **Scheme 5.3**).

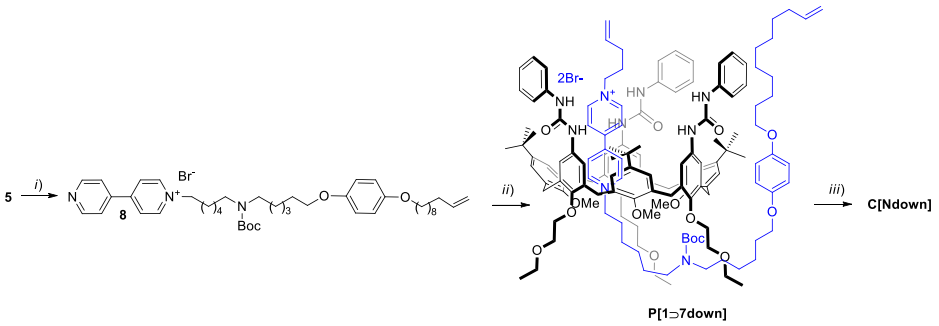

Scheme 5.3 *Reagents and conditions: i) 4,4'-bipyridine, CH_3CN, 80°C, 12h; ii) 5-bromo-1-pentene, toluene, 50°C; iii) 5-bromo-1-pentene, toluene, 50°C, 4d; 2nd gen. Grubbs cat., toluene, rt, 2d.*

As described in **Chapter 2**, we know that monoalkylviologen salts such as **8** form a stable inclusion complexes with **1** in low polar solvents. Among the two possible formed orientational isomers, the one in which the amine functionalized alkyl chain is directed toward the lower rim of **1**, and the free nitrogen of **8** is exposed to the bulk, exhibits higher reactivity towards S_N2 alkylation reactions. We planned to exploit this reactivity to preferentially obtain kinetically unfavored pseudorotaxane **P[1⊃7down]** through its wheel-assisted formation. Wheel **1** and salt **8** were equilibrated in toluene for one hour to achieve the formation of the inclusion complex, and 5-bromo-1-pententene was added. The reaction mixture was slightly heated for four days (the temperature was kept at 50°C to favor alkylation reaction and avoid any possible isomerization process), until the color turned from yellowish to deep red, indicating the formation of a viologen-based pseudorotaxane complex. Grubbs catalyst was then added and the mixture was stirred at room temperature for 48 hours. ESI-MS analysis on the crude reaction mixture evidenced a m/z peak ascribable to the product, but unfortunately, after chromatographic separation, it was not possible to isolate any catenation product in exploitable yield.

5.3 Conclusions

In this Chapter, the synthesis of an oriented electroactive double-station [2]catenane was presented. The strategy involved a ring closing metathesis reaction performed on pre-formed oriented pseudorotaxane. The results provided by voltammetry

measurements resemble the ones found for double-station rotaxanes described in **Chapter 4**, and from these data we can assume that calixarene **1** no longer encircles the viologen core upon its complete reduction. The slight variation of the first reduction potential in comparison with similar rotaxanes suggests that a partial rearrangement might take place already upon the formation of the radical cation, and further EPR investigation will give significant contribution to get further insights on this behavior. The electrochemical measurements will be performed also in dichloromethane in order to maximize the effect of the protonation. The synthesis of the opposite orientational isomer and the study of its dynamic properties are currently undergoing in our laboratory.

5.4 Acknowledgments

Thanks to Dr. Giulio Ragazzon, Prof. Alberto Credi, Prof. Serena Silvi and Prof. Margherita Venturi (University of Bologna) for electrochemical measurements. Thanks to Dr. Andrea Faccini (University of Parma) for high-resolution mass spectrometry measurements.

5.5 Experimental Section

Synthesis: Toluene, THF, acetonitrile and dichloromethane were dried by following standard procedures, other reagents were of reagent grade quality, obtained from commercial sources and used without further purification. Chemical shifts are expressed in ppm using the residual solvent signal as internal reference. Mass spectra were determined in ESI mode. Compounds **1**,[12] **2**[13] and **3**[14] were obtained following reported procedures.

Tert-butyl (6-(4-(undec-10-en-1-yloxy)phenoxy)hexyl)carbamate (4): To a solution of **3** (1.27 g, 4.80 mmol) in anhydrous DMF (100 mL), K_2CO_3 (2.00 g, 14.50 mmol) and **2** (1.98 g, 5.30 mmol) were added. The reaction mixture was stirred for 18 hours at 80°C. After cooling at room temperature, the reaction was quenched with water (100 mL) and extracted with ethyl acetate (3x100 mL). The separated organic phase was dried over Na_2SO_4 and evaporated under reduced pressure. Pure product **4** was isolated by

[12] Casnati, A.; Domiano, L.; Pochini, A.; Ungaro, R.; Carramolino, A.; Oriol Magrans, J.; Nieto, M.; Reinhoudt, D.; Lòpez-Prados, J.; Prados, P.; de Mendoza, J.; Janssen, R. G.; Verboom; W.; Reinhoudt, D. N. *Tetrahedron* ***1995***, *51 (46),* 12699-12720.

[13] Arduini, A.; Bussolati, R.; Credi, A.; Faimani, G.; Garaudee, S.; Pochini, A.; Secchi, A.; Semeraro, M.; Silvi, S.; Venturi, M. Chem. Eur. J. **2009**, *15 (13)*, 3230-3242.

[14] Ornelas, C.; Mery, D.; Cloutet, E.c; Aranzaes, J. R.; Astruc, D. *J. Am. Chem. Soc.* **2008**, *130 (4)*, 1495-1506.

column chromatography (n-hexane/acetone 8:2) as a pale yellow solid (1.29 g, 58%). ^{1}H NMR (400 MHz, $CDCl_3$): δ = 1.3–1.5 (m, 27 H, aliphatic C*H*$_2$ + O*Bu*^{t}), 1.74 (m, 4 H, ArO-CH_2C*H*$_2$), 2.05 (m, 2 H, CH_2=CH-C*H*$_2$), 3.11 (t, ^{3}J(H,H)=6.4 Hz, 2 H, N-C*H*$_2$), 3.88 (t, ^{3}J(H,H)=6.8 Hz, 4 H, ArO-C*H*$_2$), 4.70 (bs, 1 H, N*H*), 4.97 (m, 2 H, C*H*$_2$=CH), 5.81 (m, 1 H, CH_2=C*H*), 6.81 (s, 4 H, Ar*H*). ^{13}C NMR (100 MHz, $CDCl_3$): δ = 14.1, 22.7, 25.8, 26.1, 26.6, 28.4, 28.9, 29.1, 29.3, 29.4 (2 res.), 29.5, 30.1, 31.6, 33.8, 40.5, 68.4, 68.6, 78.9, 114.2, 115.4 (2 res.), 139.1, 153.1, 153.2, 156.0 ppm. ESI-MS(+): m/z (%) = 484 (100) 485 (30) $[M+Na]^+$.

Tert-butyl (6-bromohexyl)(6-(4-(undec-10-en-1-yloxy)phenoxy)hexyl)carbamate (5): **4** (0.50 g, 1.08 mmol) was dissolved in anhydrous DMF (50 mL) and cooled at 0°C. NaH (0.20 g of 60 % dispersion in mineral oil, 2.20 mmol) was slowly added and the reaction mixture was stirred for 1 hour at room temperature under inert atmosphere. The yellow solution was then cooled again at 0°C and 1,6-dibromohexane (0.50 mL, 3.25 mmol) was slowly added. The mixture was stirred for 24 hours at room temperature. The reaction was carefully quenched with water (40 mL) and extracted with ethyl acetate (3x50 mL). The separated organic phase was dried over Na_2SO_4 and evaporated under reduced pressure. The residue was purified by column chromatography (n-hexane/acetone 9:1) to obtain **5** as a colorless oil (0.34 g, 50%). ^{1}H NMR (300 MHz, $CDCl_3$): δ = 1.1–1.7 (m, 33 H, aliphatic C*H*$_2$ + Ar-*Bu*^{t}), 1.88 (m, 4 H, ArO-CH_2C*H*$_2$) 2.03 (m, 2H, Br-CH_2C*H*$_2$), 2.07 (m, 2 H, CH_2=CH-C*H*$_2$), 3.17 (m, 4 H, N^+-C*H*$_2$), 3.41 (t, ^{3}J(H,H)=9 Hz, 2 H, Br-C*H*$_2$), 3.90 (t, ^{3}J(H,H)=6 Hz, 4 H, ArO-C*H*$_2$), 4.96 (m, 2 H, C*H*$_2$=CH), 5.83 (m, 1 H, CH_2=C*H*), 6.82 (s, 4 H, Ar*H*). ^{13}C NMR (100 MHz, $CDCl_3$): δ = 25.9, 26.1, 26.7, 27.9, 28.3, 28.4, 28.5, 28.9, 29.1, 29.4 (2 res.), 29.5, 32.7, 33.8, 46.9, 47.0, 68.4, 68.6, 79.1, 114.1, 115.4 (2 res.), 139.2, 153.1, 153.2, 155.6 ppm. ESI-MS(+): m/z (%) = 624 (95) 625 (40) 626 (100) 627 (38) $[M+H]^+$.

1-(pent-4-en-1-yl)-[4,4'-bipyridin]-1-ium bromide (6): 5-Bromo-1-pentene (0.51 mL, 4.30 mmol) and 4,4'-bipyridine (2.00 g, 12.80 mmol) were dissolved in anhydrous acetonitrile (50 mL) and heated overnight at reflux. After removing the solvent under reduced pressure, the crude residue was triturated with ethyl acetate (4x25 mL) to obtain **6** as a white solid (0.88 g, 68%). ^{1}H NMR (400 MHz, MeOD): δ = 2.2-2.3 (m, 4 H, aliphatic C*H*$_2$), 4.72 (t, ^{3}J(H,H)=6.8 Hz, 2 H, N^+-C*H*$_2$), 5.12 (m, 2 H, C*H*$_2$=CH), 5.86 (m, 1 H, CH_2=C*H*), 6.78 (m, 4 H, Ar*H*), 8.02 (d,^{3}J(H,H)=6 Hz, 2 H, Ar*H*), 8.55 (d,^{3}J(H,H)=6 Hz, 2 H, Ar*H*), 8.85 (d,^{3}J(H,H)=6 Hz, 2 H, Ar*H*), 9.15 (d,^{3}J(H,H)=6 Hz, 2 H, Ar*H*). ^{13}C NMR (100 MHz, MeOD): δ = 29.8, 30.0, 60.8, 115.5, 122.2, 125.8, 136.1, 142.2, 145.2, 150.4 ppm. ESI-MS(+): m/z (%) = 225 (100) 226 (20) $[M]^+$.

1-(6-((tert-butoxycarbonyl)(6-(4-(undec-10-en-1-yloxy)phenoxy)hexyl)amino)hexyl)-1'-(pent-4-en-1-yl)-[4,4'-bipyridine]-1,1'-diium (7): In a sealed glass reactor, salt **6** (0.11g, 0.36 mmol) and bromide **5** (0.34 g, 0.55 mmol) were dissolved in 10 mL of anhydrous acetonitrile and stirred at 110°C for 7 days. After cooling at room temperature, the solvent was evaporated under reduced pressure and the residue was dissolved in ethyl acetate (20 mL). The solution was cooled at 0°C and the precipitation of the product was observed. The yellow solid was collected by Buchner filtration. Axle **7** was obtained as a yellow solid (0.19 g, 55%). ^{1}H NMR (300 MHz, MeOD): δ = 1.3–1.6 (m, 33 H, aliphatic C*H*$_2$+ O-*Bu*^{t}), 1.7-1.8 (m, 4 H, N-CH$_2$C*H*$_2$), 2.0-2.1 (m, 4 H, ArO-CH$_2$C*H*$_2$), 2.26 (m, 4 H, N^{+}-CH$_2$C*H*$_2$), 3.22 (t,^{3}J(H,H)=7 Hz, 4 H, N-C*H*$_2$), 3.92 (t,^{3}J(H,H)=6 Hz, 4 H, ArO-C*H*$_2$), 4.79 (t,^{3}J(H,H)=6 Hz, 4 H, N^{+}-C*H*$_2$), 4.9-5.2 (m, 4 H, CH-C*H*$_2$), 5.7-6.0 (m, 2 H, C*H*-CH$_2$), 6.82 (s, 4H, Ar*H*), 8.72 (d,^{3}J(H,H)=6.4 Hz, 4 H, Ar*H*), 9.31 (d,^{3}J(H,H)=6.4 Hz, 4 H, Ar*H*). ^{13}C NMR (100 MHz, MeOD): δ = 25.6, 25.8, 26.3, 27.4, 28.7, 28.8, 29.1 (3 res.), 29.3, 29.8, 30.1, 31.1, 33.5, 48.2, 61.4, 61.8, 68.1, 68.3, 79.3, 113.3, 115.1, 115.6, 127.0, 136.1, 138.8, 145.7, 149.9 (2 res.), 153.2, 153.3, 156.0 ppm. ESI-MS(+): m/z (%) = 769 (100) 770(95) [M-H]$^{+}$, 669 (100) 670(95) [M-H-BOC]$^{+}$.

Catenane C[Nup]: In a two-neck flask under inert atmosphere, salt **7** (0.07 g, 0.08 mmol) was suspended in a solution of wheel **1** (0.21 g, 0.08 mmol) in anhydrous toluene (80 mL, concentration = 0.001M). The suspension was stirred at room temperature for one day, until the solution turned dark-red and the salt was completely dissolved. Argon was then bubbled into the system for 30', and Second Generation Grubbs' Catalyst (5 mg) was added. The reaction mixture was stirred at room temperature under bubbling argon and monitored with TLC. After 3 days, the solvent was removed and the residue was portioned between dichloromethane and water. The separated organic phase was evaporated under reduced pressure, and the crude protected catenane was purified by column chromatography (dichloromethane/methanol 95:5). The isolated product was then dissolved in 10 mL of anhydrous dichloromethane and 5 mL of trifluoroacetic acid were added dropwise. After stirring for 2 hours at room temperature, the solvent was removed. The residue was then re-dissolved in 20 mL of dichloromethane and washed with 0.1M Silver *p*-toluenesulfonate solution in water (30 mL). The organic phase was separated and the solvent was removed under reduced pressure, to afford catenane as a red solid (0.03 g, 17%). ^{1}H NMR (400 MHz, C_6D_6): δ = δ = 0.78 (m, 2H, N^{+}-CH$_2$C*H*$_2$), 1.1 (t, ^{3}J (H,H) = 6.6 Hz, 9H, OCH$_2$C*H*$_3$), 1.3-1.5 (m, 28H, aliphatic C*H*$_2$), 1.65 (s, 33 H, t-Bu + TsO), 1.80 (m, 2H, aliphatic C*H*$_2$), 2.23 (m, 2H, CH=CH-C*H*$_2$), 2.41 (m, 2H, CH=CH-C*H*$_2$), 2.71 (m, 2H, NH-C*H*$_2$), 2.80 (m, 2H, NH-C*H*$_2$), 3.08 (m, 2H, N^{+}-C*H*$_2$), 3.40 (m, 6H, eqC*H*$_2$), 3.61 (m, 8H, OC*H*$_2$CH$_3$ + N^{+}-C*H*$_2$), 3.81 (m, 10H, ArOCH$_2$C*H*$_2$O + ArOC*H*$_2$), 3.89 (m, 6H, ArOC*H*$_2$CH$_2$O), 3.93 (s, 9H, OC*H*$_3$), 4.45 (d, ^{2}J(H,H) = 11,6 Hz, 6H, ax.C*H*$_2$), 5.71 (m, 1H, CH=C*H*), 5.94

(m, 1H, C*H*=CH), 6.58 (m, 2H, Ar*H*), 6.61 (d, ^{3}J (H,H) = 8.0 Hz, 4H, TsO), 6.76 (m, 2H, Ar*H*), 6.82 (m, 6H, ArH), 7.48 (s, 6H, Ar*H*), 7.50 (m, 2H, Ar*H*), 7.52 (m, 2H, Ar*H*), 7.61 (s, 6H, Ar*H*), 8.8-9.2 (m, 7H, N*H*). ^{13}C NMR (100 MHz, C_6D_6): δ = 14.1, 15.2, 22.8, 24.2, 24.7, 25.5, 26.1 (2 res), 26.5, 28.9, 29.0, 29.2, 29.4, 29.6, 29.8 (2 res), 29.9, 31.3, 31.5, 31.6, 32.0, 32.6, 32.9, 34.5, 38.2, 47.1, 47.6, 59.7, 60.6, 61.1, 62.3, 66.3, 68.0 (2 res), 69.9, 72.5, 115.1, 115.5, 116.3, 116.5, 117.8, 119.2, 121.4, 124.6, 125.6, 127.0, 128.3, 129.0, 129.2, 129.6, 131.5, 132.1, 134.1, 136.8, 140.6, 143.2, 143.9, 148.2, 152.7, 153.0, 153.4, 153.9, 161.7, 162.0, 162.4, 162.7 ppm.

1-(6-((tert-butoxycarbonyl)(6-(4-(undec-10-en-1-yloxy)phenoxy)hexyl)amino)hexyl)-[4,4'-bipyridin]-1-ium bromide (8): 5-Bromo-1-pentene 5 (0.07 g, 0.08 mmol) was dissolved in anhydrous acetonitrile (20 mL) and 4,4'-bipyridine (0.07 g, 0.08 mmol) was added. The reaction mixture was heated at 80°C for 24h. The solvent was evaporated under reduced pressure and the residue was purified by precipitation in hexane. Salt 8 was obtained as a sticky yellow solid (0.07 g, 0.08%). ^{1}H NMR (400 MHz, $CDCl_3$): δ = 1.0-1.5 (m, 33H, aliphatic CH_2 + O-*Bu*^{t}), 1.70 (m, 4H, aliphatic CH_2), 1.92 (m, 2H, aliphatic CH_2), 1.95 (m, 2H, aliphatic CH_2), 3.09 (t, ^{3}J (H,H) = 6,6 Hz, 4H, N-CH_2), 3.84 (t, ^{3}J (H,H) = 6,6 Hz, 4H, Ar-O-CH_2), 4.92 (m, 4H, N^{+}-CH_2 + CH=CH_2), 5.76 (m, 1H, CH2=C*H*), 6.76 (s, 4H, O-Ar*H*), 7.71 (d, 2H, ^{3}J(H,H) = 4.8 Hz, Ar*H*), 8.40 (m, 2H, Ar*H*), 8.82 (d, ^{3}J(H,H) = 4.8 Hz, 2H, Ar*H*), 9.51 (m, 2H, Ar*H*). ^{13}C NMR (100 MHz, $CDCl_3$): δ = 25.8, 26.0, 26.62, 28.5, 28.9, 29.0, 29.4, 29.5, 31.6, 33.7, 46.0, 61.6, 68.4, 68.6, 79.0, 114.1, 115.4, 121.5, 126.0, 139.1, 140.8, 145.6, 151.4, 153.1, 153.2, 153.7, 155.6 ppm. ESI-MS(+): m/z (%) = 701 (100) [M]$^{+}$.

CHAPTER 6

TOWARDS THE SYNTHESIS OF ORIENTED BIS-CALIX[6]ARENE-BASED CONTAINERS: WORK IN PROGRESS AND FUTURE PERSPECTIVES

6.1 Introduction

Molecular capsules are molecular scaffolds endowed with a nanosized cavity isolated from the bulk phase, which can host a complementary guest molecule. These assemblies are of particular interest in the development of containers that can provide stability to highly reactive guests. For examples, some labile molecules such as phosphonium cations[1] or cyclobutadiene[2] could be efficiently stabilized through encapsulation. This approach also enabled the protection of elemental white phosphorus (P_4) thanks to its confinement into self-assembled tetrahedral cages in aqueous solution.[3]

Nevertheless, capsular assemblies create a cavity in which the guest molecules frequently exhibit modifications as consequences of the confinement, and therefore might be exploited as nanoscale "flasks" or reactors able to manipulate the physical and chemical properties of the trapped species.[4]

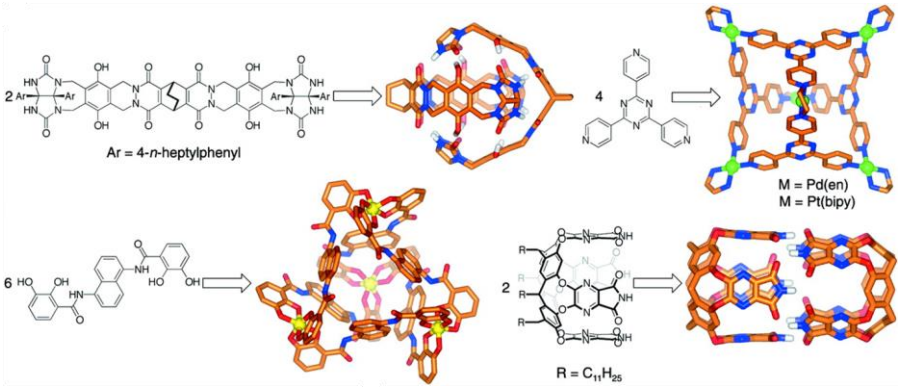

Figure 6.1 *Representative self-assembling molecular capsules (adapted from ref. 4, copyright © 2002, The National Academy of Sciences).*

A peculiar class of molecular flasks is the one in which the hollow cavity is composed by two hemispherical or curved molecules. The group of Rebek and co-workers accomplished the synthesis of several cavitand-based containers held together by a network of reversible interactions or by covalent bridges,[5] and explored their behavior as hosts, supramolecular containers and reactors. As an example, it was

[1] Ziegler, M.; Brumaghim, J. L.; Raymond, K. N. *Angew. Chem. Int. Ed.* **2000**, *39*, 4119-4121.

[2] Cram, D. J.; Tanner, M. E.; Thomas, R. *Angew. Chem.* **1991**, *103*, 1048-1051.

[3] Mal, P.; Breiner, B.; Rissanen, K.; Nitschke, J. R. *Science* **2009,** 324 (5935), 1697-1699.

[4] Hof, F.; Craig, S. L.; Nuckolls, C.; Rebek, J. *Angew. Chem. Int. Ed.* **2002**, *41*, 1488-1508; Qiao, Y.; Zhang, L.; Li, J.; Lin, W.; Wang, Z. *Angew. Chem. Int. Ed.* **2016**, *55*, 12778-12782; Hof, F.; Rebek, J. *Proc. Natl. Acad. Sci. USA* **2002**, *99 (8)*, 4775-4777.

[5] Asadi, A.; Ajami, D.; Rebek, J. *Chem. Commun.* **2014**, *50*, 533-535.

evidenced how the confinement of linear C_{16} to C_{19} alkanes into hydrogen-bonded cavitand complexes entails coiled and compressed conformations.[6] Within this context, several examples of calixarene-[7] or oxacalixarene-based[8] capsules and dimers have been reported to date. By virtue of its higher rigidity and preorganization, the smaller calix[4]arene has been the most exploited building block for the synthesis of self-assembled capsules,[9] in which the components are held together by non-covalent interactions, such as metal coordination[10] and hydrogen bonds networks,[11] or are mechanically interlocked either in a catenane-like fashion[12] or through the insertion of covalent bridges.[13] As far as the larger calix[6]arene is concerned, the problem of controlling its conformational flexibility or blocking it in a *cone* conformation must be overcome. Nevertheless, examples of non-covalent calix[6]arene-based assemblies[14] and covalently-attached dimers have been reported, including the calix[6]tubes proposed by the groups of Prof. Reinaud and Jabin[15] (see **Figure 6.2**):

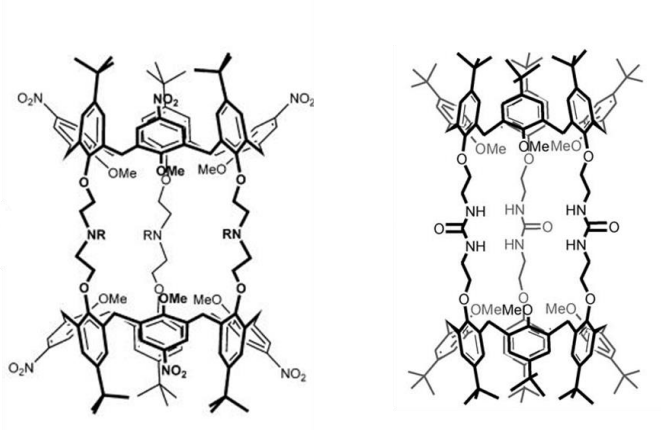

Figure 6.2 *Structures of Jabin's and Reinaud's calix[6]tubes.*

6 Ajami, D.; Rebek, J. *Nat. Chem.* **2009**, *1*, 87-90.

7 Agrawal, y. K.; Bhatt, S. K. *Synth. Commun.* **2007**, *37 (4)*, 551-557; Rebek, J. *Chem. Commun.* **2000**, *8*, 637-643.

8 Zhong, Z.; Ikeda, A.; Shinkai, S. *J. Am. Chem. Soc.*, **1999**, *121 (50)*, 11906-11907.

9 Yamanaka, M.; Kobayashi, K. *Asian J. Org. Chem.* **2013**, *2*, 276-289; Rebek, J. *Chem. Commun.* **2000**, 637-643.

10 Liu, M.; Liao, W.; Hu, C.; Du, S.; Zhang, H. *Angew. Chem. Int. Ed.* **2012**, *51*, 1585-1588.

11 MacGillivray, L. R.; Atwood, J. L. *Nature* **1997**, *389*, 469-472.

12 Chasm M.; Ballester, P. *Chem. Sci.* **2012**, *3*, 186-191.

13 Puchnin, K.; Zaikin, P.; Cheshkov, D.; Vatsouro, I.; Kovalev, V. *Chem. Eur. J.* **2012**, *18*, 10954-10968.

14 Rincòn, A. M.; Prados, P.; de Mendoza, J. *Eur. J. Org. Chem.* **2002**, *4*, 640-644.

15 Le Gac, S.; Zeng, X.; Reinaud, O.; Jabin, I. *J. Org. Chem*, **2005***, 70 (4)*, 1204-1210; Moerkerke, S.; Ménand, M.; Jabin, I. *Chem. Eur. J.* **2010**, *16*, 11712-11719.

Our research group tackled the synthesis of double calix[6]arenes *via* self-assembly, in low polarity solvents, of two tricarboxy[16] or *N*-triureido[17] derivatives, held together by hydrogen bond networks. These latter dimers showed good recognition properties toward *N*-substituted pyridinium guests, and were also able to encapsulate solvent molecules such as dichloromethane and benzene. Furthermore, we studied the formation and the complexation properties of covalently-linked double calix[6]arenes with imino and 1,4-phenylendiimino bridges,[18] and the ability of an oriented head-to-tail derivative to form a pseudorotaxane complex by threading a viologen salt was demonstrated[19] (**Figure 6.3**). From these findings, it emerged that the dimerization of calix[6]arene scaffolds could be an appealing method to enhance, or at least modify, their binding properties in solution, and to create new hosts endowed with bigger and more tunable cavities. However, it was evidenced that, in the head-to-tail dimer, only the calix[6]arene annulus decorated with ureido moieties on its upper rim actively takes part in the axle's complexation mechanism.

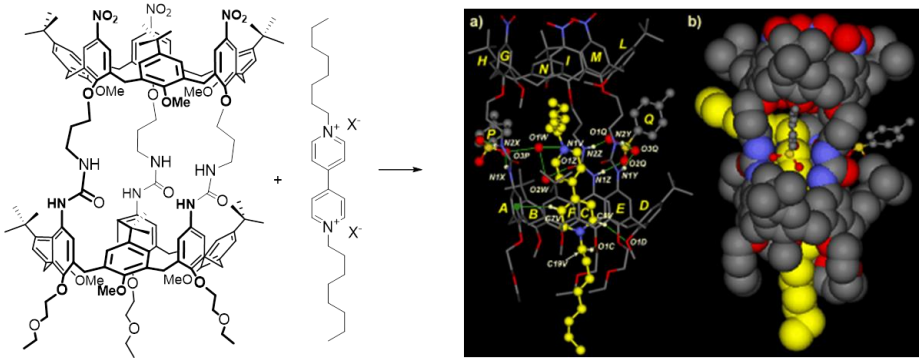

Figure 6.3 *Head-to-tail calix[6]arene dimer and X-ray structure of the complex with DOV.*

To get further insights into these aspects, we designed the synthesis of new oriented head-to-head bis-calix[6]arene receptors, in which both the macrocyclic components are decorated with tris(*N*-phenylureido) groups in correspondency of their upper rims. Our interest is primarily focused on the modification of the physico-

16 Arduini, A.; Domiano, L.; Ogliosi, L.; Pochini, A.; Secchi, A.; Ungaro, R. *J. Org. Chem.* **1997**, *62*, 7866-7868.

17 González, J. J.; Ferdani, R.; Albertini, E.; Blasco, J. M.; Arduini, A.; Pochini, A.; Prados, P.; de Mendoza, J. *Chem. Eur. J.* **2000**, *6 (1)*, 73-80.

18 Arduini, A.; Ferdani, R.; Pochini, A.; Secchi, A. *Tetrahedron* **2000**, *56*, 8573-8577.

19 Arduini, A.; Credi, A.; Faimani, G.; Massera, C.; Pochini, A.; Secchi, A.; Semeraro, M.; Silvi, S.; Ugozzoli, F. *Chem. Eur. J.* **2008**, *14*, 98-106.

chemical and electrochemical properties of electron-poor trapped molecules, but it would be also interesting to better investigate about the pathways followed by the guests to access the cavity (i.e. whether the threading takes place from the terminal poles or from the equatorial portals of the receptor). A possible further development in this field might be the realization of a "two hosts-one guest" system, whose binding mode could eventually be governed by external stimulation.

In this chapter, two synthetic strategies for the realization of oriented head-to-head covalently linked bis-calix[6]arene-based receptors are thus presented.

6.2 Hetero-bis-calix[6]arene *via* click reaction

In this first approach, the target capsule **3** is constituted by two different calix[6]arene wheels that are three-point covalently bridged *via* a Cu^{I}-catalyzed alkyne-azide "click" cycloaddition with the formation of three triazole linkers:

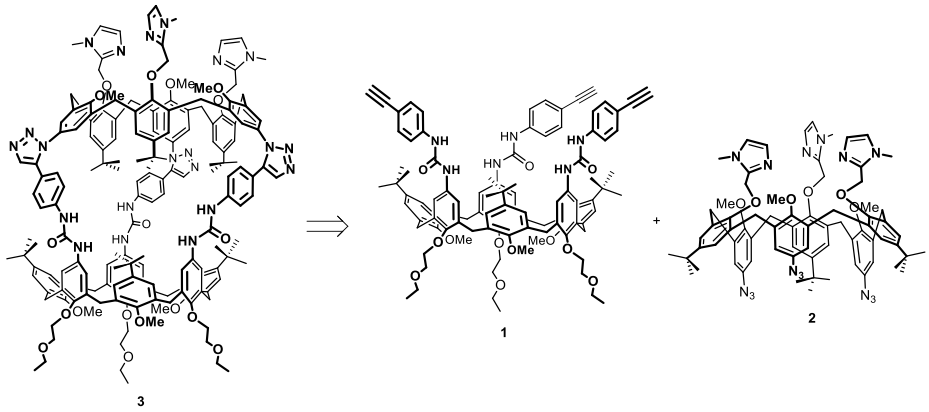

Scheme 6.1 *Target capsule **3** and calixarene monomers **1** and **2**.*

The first component is the trifenilureido calix[6]arene derivative **1**, in which the three aromatic rings of the phenylurea moieties at the upper rim are decorated with alkyne moieties. This was obtained by reacting the tris-amino calixarene **7** with the alkyne-functionalized isocyanate **6**, as reported in **Scheme 6.2**:

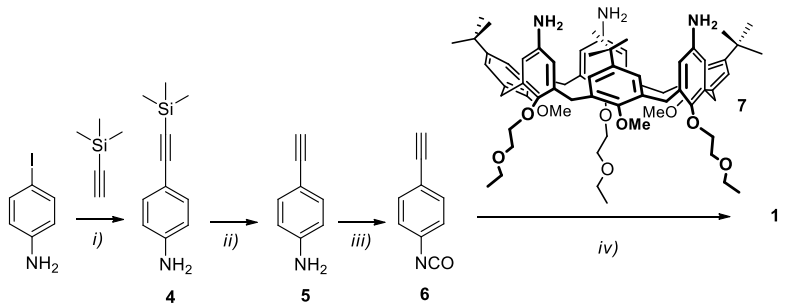

Scheme 6.2 *Reagents and conditions: i) CuI, NEt_3, $Pd(PPh_3)_2Cl_2$, THF, rt, 2 h; ii) K_2CO_3, MeOH/CH_2Cl_2, reflux, 4 h; iii) Triphosgene, NEt_3, CH_2Cl_2, rt, 1 h; iv) CH_2Cl_2, rt, 3 h.*

The second component is the tris-azido calix[6]arene **2**, equipped with *N*-methylimidazole ligands at the lower rim, whose synthesis was reported in previously published procedures[20].

Once tackled the synthesis of the two macrocycles, we explored different reaction conditions for the alkyne-azide coupling. The copper sulphate/sodium ascorbate catalytic system was tested in two different solvent mixtures (THF/water,[21] Entry 1 in **Table 6.1**, and dichloromethane/water,[22] Entry 2 in **Table 6.1**) and stoichiometric ratios. In both cases, only negligible traces of the target dimer were evidenced in the mass spectra of the crude reaction mixtures (see **Figure 6.4**), while the most intense m/z peaks were ascribed to unreacted starting material. We also tried to exploit $[(CH_3CN)_4Cu]PF_6$ as a different source of Cu(I) catalyst that can be used in low polar media in absence of water[23] (Entry 3 in **Table 6.1**), but after reacting for four days no traces of the coupling were evidenced.

Entry	$CuSO_4 \cdot 5H_2O$	Sodium Ascorbate	$[(CH_3CN)_4Cu]PF_6$	Solvent	T (°C)	t (h)
1	4.0 eq.	8.0 eq.	/	THF/Water 1:1	25	15
2	0.6 eq.	1.2 eq.	/	CH_2Cl_2/Water 1:1	60	60
3	/	/	1.0 eq.	CH_2Cl_2	25	90

Table 6.1 *Reaction conditions tested for the coupling reaction.*

[20] Colasson, B.; Save, M.; Milko, P.; Roithová, J.; Schröder, D.; Reinaud, O. *Org. Lett.* **2007**, *9 (24)*, 4987-4990.

[21] Rebilly, J. N.; Bistri, O.; Colasson, B.; Reinaud, O. *Inorg. Chem*. **2012**, *51 (10)*, 5965-5974.

[22] Colasson, B.; Le Poul, N.; Le Mest, Y.; Reinaud, O. *Inorg. Chem.* **2011**, *50 (21)*, 10985-10993.

[23] Fu, X.; Zhang, Q.; Rao, S. J.; Qu, D. H.; Tian, H. *Chem. Sci.* **2016**, *7*, 1696-1701.

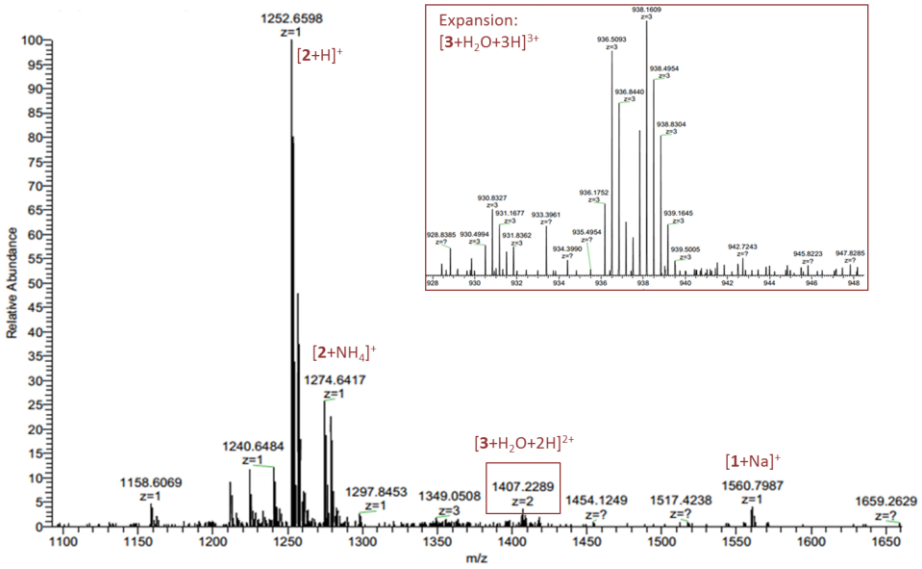

Figure 6.4 *Mass spectrum of the crude reaction mixture of Entry 1.*

To facilitate the intermolecular click reaction, we envisaged the possibility to exploit a ditopic guest to promote the spatial proximity and the correct mutual arrangement of the two calixarene monomers, and favor the formation of dimers versus oligomers (see **Scheme 6.3**). The threading of a guest into the wheels should also induce a rigidification of the calix[6]arene scaffolds, and reduce their conformational mobility.

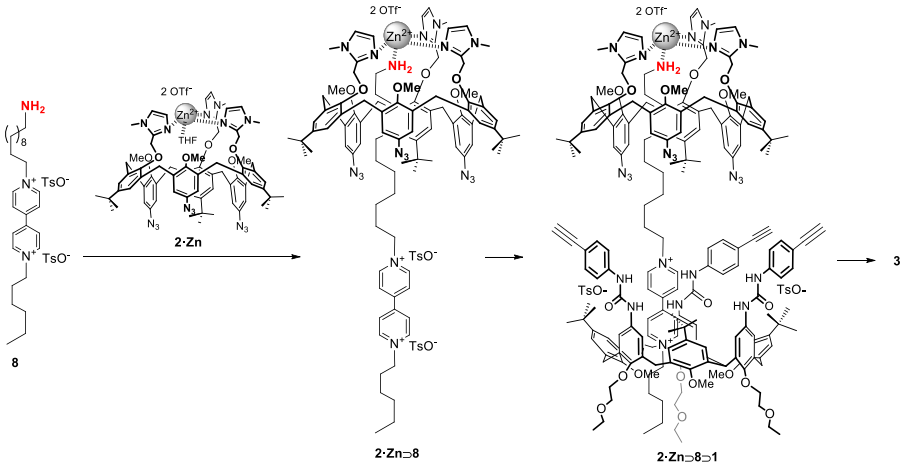

Scheme 6.3 *Templated approach for the synthesis of capsule **3**.*

Trifenilureido calix[6]arenes such as **1** are known for the affinity toward electron-poor species, especially dialkylviologen based salts, while tris-azido calix[6]arene **2** exhibits good complexing properties toward primary amines, *via* the formation of a zinc complex at the lower rim of the wheel[24]. On these bases, we designed as templating agent the viologen salt **8,** decorated with a primary amine moiety at one end.

First, the zinc complex **2·Zn** was synthesized by reacting calixarene **2** with zinc triflate in THF. Subsequently, the 1:1 adduct between the amine-terminated salt and the azido-calixarene was formed by adding a solution of **2·Zn** in 400 µL of CD_3CN to a solution of **8** in 20 µL of MeOD with 2 equivalents of triethylamine (the presence of at least a 5% of methanol was mandatory for the solubility of the salt, while the base was necessary to assure the presence of the terminal primary amine in its neutral form).

The structure of the complex was confirmed by ^{1}H-NMR analysis (see **Figure 6.5a**). In particular, both the methylene protons connecting the imidazole ligands to the calixarene scaffold and the aromatic protons of the calixarene core experience a downfield shift due to the rearrangement of the host. Moreover, the protons of the alkyl chain in proximity of the complexed amine resonate at very high fields because of the shielding effect of the calixarene cavity.

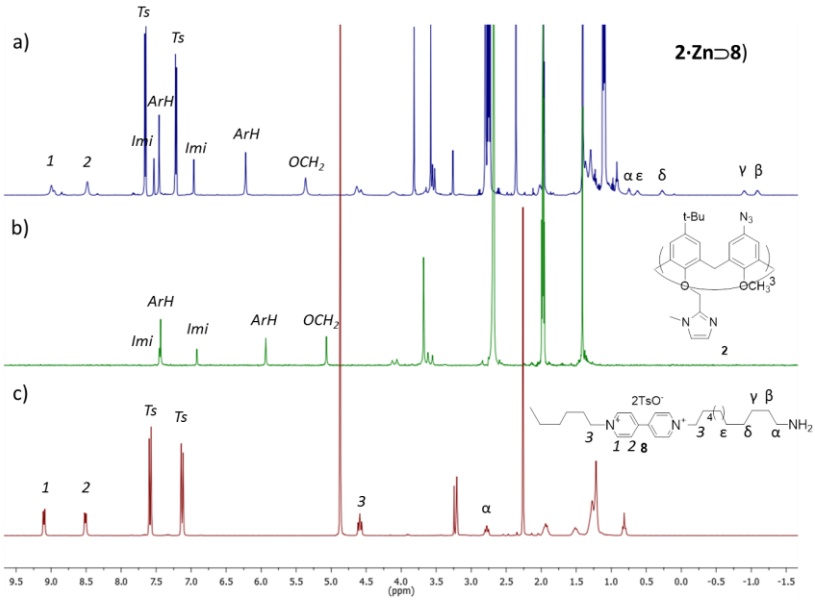

Figure 6.5 *^{1}H NMR spectra of a) **2·Zn⊃8** complex in a 20:1 CD_3CN:MeOD mixture, 500 MHz; b) tris-azido calixarene **2** in CD_3CN, 250 MHz; c) Axle **8** in MeOD, 400 MHz.*

[24] Colasson, B.; Reinaud, O. *J. Am. Chem. Soc.* **2008**, *130*, 15226-15227; Menard, N.; Reinaud, O.; Colasson, B. *Chem. Eur. J.* **2013**, *19*, 642-653.

The following step consisted in the formation of the ternary complex **2·Zn⊃8⊃1**: as known, the bipyridinium pendant should thread wheel **1** from its upper rim, generating the oriented pseudorotaxane depicted in **Scheme 6.3**, in which the two calixarenes are arranged in the desired head-to-head orientation. An important factor that needs to be taken into account is that the interaction between wheel **1** and the viologen salt involves the formation of highly energetic hydrogen bonds, and therefore is inefficient in polar media such as the acetonitrile/methanol mixture. Unfortunately, every attempt to obtain the precursor **2·Zn⊃8** complex in low polarity solvents failed, because of the very low solubility of wheel **2** in these media. We tentatively tried to achieve the formation of the **2·Zn⊃8⊃1** complex by adding to the 1:1 aggregate previously formed in acetonitrile an equimolar amount of wheel **1**. As expected, only a pale orangish coloration was evidenced, thus indicating that the phenylureido calixarene did not efficiently interact with the viologen unit of the templating salt. After heating the mixture at 80°C for three days, both in absence and in presence of the Cu catalyst, no peaks indicating the formation of the desired product were detected in the mass spectra.

The inefficiency of this protocol was mainly ascribed to the different polarity conditions needed for the stabilization of the two inclusion complexes. Nevertheless, regardless the employment of a templating agent, the formation of a triazole ring is a sterically demanding reaction, and the presence of the bulky t-Bu groups at the upper rims of the two calixarenes might prevent the coupling.

6.3 Homo-bis-calix[6]arene *via* transesterification reaction

A different synthetic approach for the synthesis of the homo-bis-calix[6]arene **11** was devised (see Scheme 6.4). In this system, the two tris(*N*-phenylureido) wheels **9** decorated with *tert*-butyl ester moieties on their upper rims encircle the tetra-charged viologen derivative **10**, in which two cationic stations are present:

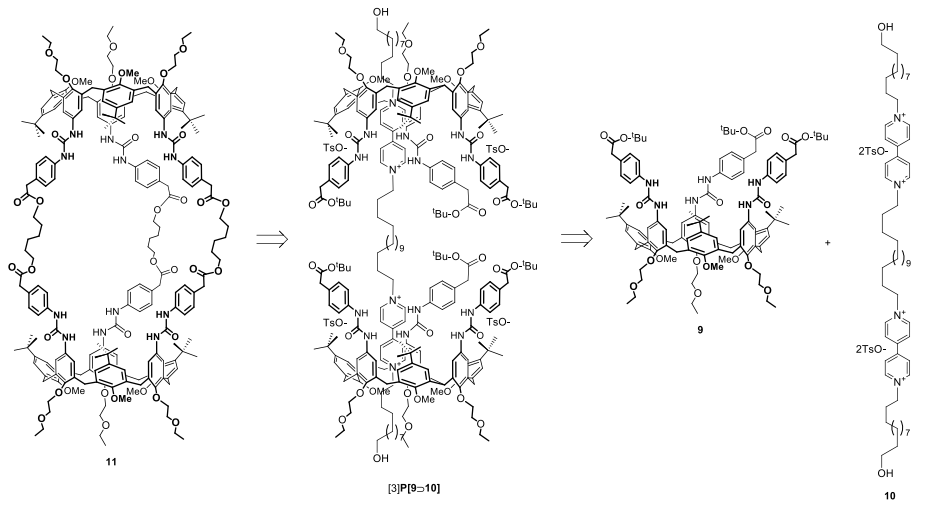

Scheme 6.4 *Templated approach for the synthesis of bis-calix[6]arene **11**.*

We hypothesize that, after the formation of the oriented [3]pseudorotaxane, the *in situ* deprotection of the acidic groups of the wheels and the following reaction with an appropriate linker could lead to the formation of a three-point bridged dimer. For an efficient templating effect, the length of the alkyl chain between the two viologen units of the axle should be adjusted in order to allow the simultaneous complexation of two calixarene derivatives without steric impediments. Starting from previously obtained experimental data[25], for this first attempt a spacer of 16 methylene units was used. Calixarene **9** was obtained by the reaction of tris-amino calixarene **7** with isocyanate **14**, as shown in **Scheme 6.5**:

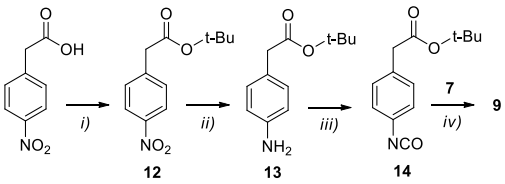

Scheme 6.5 *Reagents and conditions: i) t-BuOH, DCC, DMAP, CH_2Cl_2, rt, 3 h; ii) NH_2NH_2, Pd/C, MeOH, rt, 30'; iii) Triphosgene, NEt_3, CH_2Cl_2, rt, 1 h; iii) CH_2Cl_2, rt, 3 h.*

To achieve the formation of axle **10**, the pyridyl-pyridinium salt **15** was reacted with hexadecane-1,16-diyl bis(4-methylbenzenesulfonate) **16** as reported in **Scheme 6.6**:

[25] In previoulsy reported experiments (Dr. Guido Orlandini, PhD Thesis, 2016) it was evidenced that a short C6 spacer on a bis-viologen salt sterically hampers the simultaneous complexation of two calixarene derivatives. In the same study, a C12 spacer was proven to be sufficient for the complexation of two tris(*N*-phenylureido)calix[6]arene wheels that did not bear any further functionalization on their uper rims.

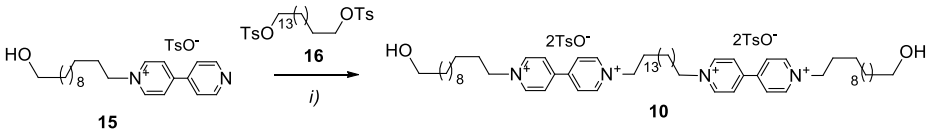

Scheme 6.6 *Reagents and conditions: i) CH_3CN, 110°C, 5 d.*

The obtained axle was then equilibrated with a two-fold amount of wheel **9** in C_6D_6. The mixture was slightly heated at 50 °C to favor the formation of the complex without losing the orientational selectivity of the complexation. After three days, a deep red coloration of the solution was observed, indicating the successful formation of a pseudorotaxane-type complex, whose structure was inferred through NMR techniques (**Figure 6.6b**):

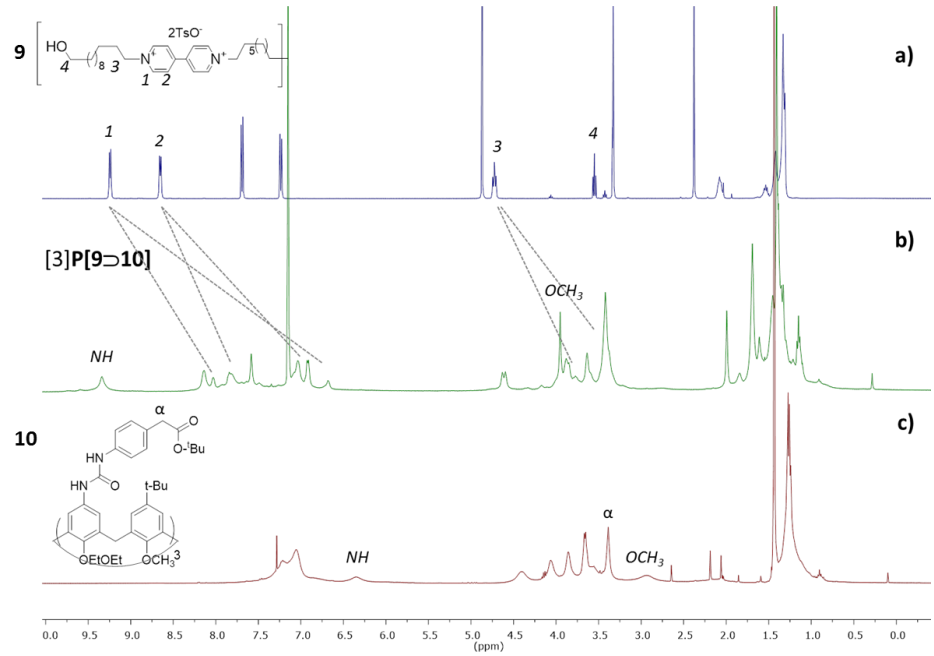

Figure 6.6 *^{1}H NMR spectra (400 MHz) of a) axle **10** in MeOD; b) [3]pseudorotaxane [3]**P**[**9**⊃**10**] in C_6D_6; c) wheel **9** in $CDCl_3$.*

In the ^{1}H NMR spectrum of [3]**P**[**9**⊃**10**], several diagnostic signals indicate the successful threading of the axle into two macrocycles. The inclusion of the axle is witnessed by the upfield shift of the methylene protons close to the positively charged nitrogens, induced by the shielding effect of the electron-rich cavity of **9**. The same can be said for the aromatic protons of the bipyridinic cores. The absence of signals

ascribable to the free axle in the region between 8.5 and 9.5 ppm (see comparison with spectrum of free **10**, **Figure 6.6a**) confirms the quantitative complexation of both the positively charged stations. The expected orientational arrangement of the components in the [3]pseudorotaxane was also proven: the presence of a sharp singlet signal at 3.95 ppm relative to the OCH_3 groups of **9** indicates that both the wheels interact with the salt with the same relative orientation.

Another key parameter involved in this strategy is the adjustment of the length of the covalent linker according to the distance between the two calixarenes, dictated by the span between the two bipyridinium moieties. Considering the C16 spacer on the axle, we chose to employ 1,6-hexanediol as linker.

To the [3]pseudorotaxane solution were hence added the diol and a catalytic amount of *p*-toluenesulphonic acid, and the mixture was heated at 80°C overnight. The full characterization of the obtained product is still undergoing.

6.4 Conclusions and Perspectives

These preliminary studies evidenced the difficulties in obtaining aggregates in which two calix[6]arene-based conformationally mobile units are multipoint linked *via* covalent bonds. From our investigation, it emerged that it is possible to arrange in space the building blocks of the capsule by exploiting a ditopic guest as templating agent. Among the two pathways tested, the latter seems to be the most versatile and promising one. However, further experiments need to be carried out in order to adjust parameters such as the length of the axles spacer and the diol linker, and different reactions for the closure of the dimer (including the formation of amides) will be explored. Nevertheless, an accurate theoretical modelling will be pursued.

6.5 Acknowledgments

Thanks to Dr. Jean-Noel Rebilly and Prof. Olivia Reinaud (Université Paris Descartes) for the advice and the collaboration in the first synthetic strategy, and to Dr. Assia Hessani (Université Paris Descartes) for MS measurements.

6.6 Experimental section

Synthesis: All solvents were dried using standard procedures; all reagents were of reagent grade quality obtained from commercial suppliers and were used without

further purification. Chemical shifts are expressed in ppm (δ) using the residual solvent signal as internal reference (7.16 ppm for C_6H_6; 7.26 ppm for $CHCl_3$ and 3.31 for CH_3OH). Products **2**[20], **7**[26] and **16**[27] were synthesised according to published procedures.

4-((trimethylsilyl)ethynyl)aniline (4): In a 100 ml two-necked flask 4-Iodoaniline (2.0 g, 9.1 mmol) and triethylamine (8.4 g, 83.0 mmol) were dissolved in anhydrous THF (20mL). CuI (0.2 g, 0.8 mmol) and $Pd(PPh_3)_2Cl_2$ (0.3 g, 0.5 mmol) were added and the mixture was stirred for 4 hours at room temperature. The solvent was evaporated at reduced pressure and the residue was dissolved in ethyl acetate (50 mL), washed with water (50 mL) and filtered over celite to remove the exhaust catalyst. The solvent was removed under reduced pressure and the residue was dissolved in hexane (50 mL) and cooled at 0°C, until the product precipitated as a sticky white solid, that was recovered by suction filtration in 80% yield. ^{1}H NMR (400 MHz, $CDCl_3$): δ = 0.25 (s, 9 H, Si-C*H*$_3$), 3.94 (bs, 2 H, N*H*$_2$), 6.60 (d, ^{3}J(H,H)=8.8 Hz, 2 H, Ar*H*), 7.29 (d, ^{3}J(H,H)=8.8 Hz, 2 H, Ar*H*). ^{13}C NMR (100 MHz, $CDCl_3$ + MeOD): δ = 0.2, 91.4, 106.0, 112.5, 114.6, 133.4, 146.8 ppm.

4-ethynylaniline (5): Product **4** (1.1 g, 5.6 mmol) was dissolved in 20 mL of methanol and 10 mL of dichloromethane. K_2CO_3 (3.9 g, 28.0 mmol) was added and the mixture was stirred under reflux for four hours, after which the solvent was removed under reduced pressure. The residue was portioned between dichloromethane and water, and the separated organic phase was dried over $CaCl_2$, filtered and evaporated to yield **5** as a pale yellow solid (95%). ^{1}H NMR (400 MHz, $CDCl_3$): δ = 2.98 (s, 1 H, C≡C*H*), 3.81 (bs, 2 H, N*H*$_2$), 6.60 (d, ^{3}J(H,H)=8.8 Hz, 2 H, Ar*H*), 7.29 (d, ^{3}J(H,H)=8.8 Hz, 2 H, Ar*H*). ^{13}C NMR (100 MHz, $CDCl_3$): δ = 74.9, 84.4, 111.4, 114.6, 133.5, 147.0 ppm.

1-ethynyl-4-isocyanatobenzene (6): Product **5** (0.2 g, 1.5 mmol) was dissolved in anhydrous dichloromethane (50 mL), and triethylamine (0.2 g, 1.8 mmol) was added. Separately, triphosgene (0.1 g, 0.5 mmol) was dissolved in 5 mL of anhydrous dichloromethane. The amine solution was carefully added to the triphosgene solution, and the resulting mixture was stirred at room temperature for one hour. The solvent was removed under reduced pressure and the product was extracted from the sticky residue with hexane. Product **6** was recovered in 80 % yield and directly used without further purification.

[26] Gonzalez, J. J.; Ferdani, R.; Albertini, E.; Blasco, J. M.; Arduini, A.; Pochini, A.; Prados, P.; De Mendoza, J. *Chem. - A Eur. J.* **2000**, *6 (1)*, 73–80.

[27] Muranaka, K.; Sano, A.; Ichikawa, S.; Matsuda, A. *Bioorg. Med. Chem.* **2008** , *16 (11)*, 5862-5870.

Calixarene 1: In a two necked flask, tris-amino calixarene **7** (0.1 g, 0.1 mmol) was dissolved in anhydrous dichloromethane under inert atmosphere. Isocyanate **6** (0.1 g, 0.4 mmol) was added, and the mixture was stirred at room temperature for 3 hours. The reaction mixture was washed with water and evaporated under reduced pressure. The product was purified by column chromatography (eluent dichloromethane:ethyl acetate = 9:1). Wheel **1** was obtained in 60% yield. ^{1}H NMR (400 MHz, $CDCl_3$): δ = 1.1-1.3 (m, 36 H, CH_2CH_3 + t-Bu), 2.9 (bs, 9 H, OCH_3), 3.02 (s, 3 H, C≡C*H*), 3.5 (bs, 6 H, eq-CH_2), 3.67 (m, 6 H, OCH_2CH_3), 3.86 (bs, 6 H, $ArOCH_2CH_2$), 4.08 (bs, 6 H, $ArOCH_2$), 4.37 (bs, 6 H, ax-CH_2), 6.25 (bs, 6 H, N*H*), 7.0-7.4 (m, 24 H, Ar*H*). ESI-MS(+): m/z (%) = 1539 (80) $[M+H]^+$, 1561 (100) $[M+Na]^+$, 1577 (60) $[M+H]^+$.

Calixarene 2·Zn: Calixarene **2** (0.10 g, 0.07 mmol) was dissolved in THF (3 mL) and an equimolar amount of $Zn(OTf)_2$ (0.29 g, 0.07 mmol) was added. The obtained mixture was stirred at room temperature for 3 hours until all the zinc salt was dissolved, and the solvent was then evaporated under reduced pressure. The residue was taken up in the minimum amount of THF (1 mL), diethyl ether was added (10 mL) and the resulting heterogeneous mixture was centrifuged in order to separate solid **2·Zn**, that was further washed with diethyl ether. **2·Zn** was obtained as a white solid (95%).

Axle 8: A solution of 1-hexyl-[4,4'-bipyridin]-1-ium tosylate (0.3 g, 1.5 mmol) and 11-((*tert*-butoxycarbonyl)amino)undecyl tosylate (1.3 g, 2.9 mmol) in anhydrous acetonitrile was heated at 110°C for five days in a Shlenk reactor. The reaction mixture was then cooled at 0°C and precipitated BOC-protected axle was isolated by Buchner filtration. The axle was then dissolved in a dichloromethane /methanol 1:1 mixture and treated with 2 mL of Trifluoroacetic acid at room temperature for 4 hours. After removing the solvent under reduced pressure, deprotected axle **8** was obtained as a sticky yellow solid (55%). ^{1}H NMR (400 MHz, MeOD): δ = 0.79 (t, ^{3}J(H,H)=9.2 Hz, 3 H, CH_2CH_3), 1.1-1.3 (m, 20 H, aliphatic CH_2), 1.50 (m, 2 H, NH_2-CH_2CH_2), 1.92 (m, 4 H, N^+-CH_2CH_2), 2.24 (s, 6 H, $ArCH_3$), 2.76 (t, ^{3}J(H,H)=8.0 Hz, 2 H, NH_2-CH_2), 4.57 (t, ^{3}J(H,H)=8.0 Hz, 4 H, N^+-CH_2), 7.11 (d, ^{3}J(H,H)=8.1 Hz, 4 H, Ar*H*), 7.56 (d, ^{3}J(H,H)=8.1 Hz, 4 H, Ar*H*), 8.49 (d, ^{3}J(H,H)=6.6 Hz, 4 H, Ar*H*), 9.08 (d, ^{3}J(H,H)=6.6 Hz, 4 H, Ar*H*). ESI-MS(+): m/z (%) = 410 (100), 411 (60) $[M]^{2+}$.

***tert*-Butyl 2-(4-nitrophenyl)acetate (12):** 2-(4-nitrophenyl)acetic acid (2.5 g, 13.8 mmol) was dissolved in 25 mL of anhydrous dichloromethane, and *tert*-butanol (3.1 g, 41.8 mmol) and DMAP (1.4 g, 11.0 mmol) were added. The mixture was cooled at 0°C and DCC 4.1 g, (4.1 g, 19.8 mmol) was slowly added. The solution was stirred at room temperature for three hours, after which the formation of a white precipitate (DCU) was observed. The solid was filtered off through Buchner filtration, and the organic

phase was washed with water (50 mL) and evaporated under reduced pressure. Product **10** was purified by column chromatography (eluent hexane: ethyl acetate = 7:1) as a colorless oil (70%).^{1}H NMR (400 MHz, $CDCl_3$): δ = 1.45 (s, 9 H, t-Bu), 3.65 (s, 2 H, C*H*$_2$), 7.46 (d, ^{3}J(H,H)=8.0 Hz, 2 H, Ar*H*), 8.19 (d, ^{3}J(H,H)=8.0 Hz, 2 H, Ar*H*). ^{13}C NMR (100 MHz, $CDCl_3$): δ = 27.9, 42.3, 81.7, 123.6, 130.2, 142.1, 147.1, 169.4 ppm. ESI-MS(+): m/z (%) = 238 (100) $[M+H]^+$.

***tert*-Butyl 2-(4-aminophenyl)acetate (13):** To a solution of **10** (1.8 g, 7.6 mmol) in methanol (20 mL) kept under nitrogen flux, hydrazine (2.4 g, 76.0 mmol) and a tip of spatula of Pd/C were added. After stirring at room temperature for 30', the solution was vacuum filtered over celite under inert atmosphere. The solvent was evaporated under reduced pressure and the residue was portioned between dichloromethane and water. The separated organic phase was dried over $CaCl_2$, filtered and evaporated to dryness to quantitatively afford **11** as a colorless oil. ^{1}H NMR (400 MHz, $CDCl_3$): δ = 1.45 (s, 9 H, t-Bu), 3.42 (s, 2 H, C*H*$_2$), 3.53 (bs, 2 H, N*H*$_2$), 6.66 (d, ^{3}J(H,H)=8.0 Hz, 2 H, Ar*H*), 7.07 (d, ^{3}J(H,H)=8.0 Hz, 2 H, Ar*H*). ^{13}C NMR (100 MHz, $CDCl_3$): δ = 28.1, 41.8, 80.5, 115.2, 124.7, 130.0, 145.2, 171.6 ppm. ESI-MS(+): m/z (%) = 208 (100), 209 (25) $[M+H]^+$.

***tert*-Butyl 2-(4-isocyanatophenyl)acetate (14):** Product **11** (0.7 g, 3.6 mmol) was dissolved in anhydrous dichloromethane (10 mL), and triethylamine (0.4 g, 4.3 mmol) was added. Separately, triphosgene (0.3 g, 1.2 mmol) was dissolved in 5 mL of anhydrous dichloromethane. The amine solution was carefully added to the triphosgene solution, and the resulting mixture was stirred at room temperature for one hour. The solvent was removed under reduced pressure and the product was extracted from the sticky residue with hexane. Product **12** was recovered in 82 % yield and directly used without further purification.

Calixarene 9: In a two necked flask, tris-amino calixarene **7** (0.1 g, 0.1 mmol) was dissolved in anhydrous dichloromethane under inert atmosphere. Isocyanate **12** (0.1 g, 0.4 mmol) was added, and the mixture was stirred at room temperature for 3 hours. The reaction mixture was washed with water and evaporated under reduced pressure. The residue was taken up in the minimum amount of ethyl acetate, hexane (10 mL) was added and the mixture was cooled at 0°C to favor the precipitation of the product. After two hours, the formed precipitate was isolated by Buchner filtration and washed with hexane. Wheel **9** was obtained in 78% yield as a white solid. ^{1}H NMR (400 MHz, $CDCl_3$): δ = 1.0-1.3 (m, 36 H, CH_2CH_3 + Ar-tBu), 1.45 (s, 27 H, COO-tBu), 2.9 (bs, 9 H, OC*H*$_3$), 3.39 (s, 6 H, Ar-C*H*$_2$-C=O), 3.55 (bs, 6 H, eq-C*H*$_2$), 3.58 (m, 6 H, OCH_2CH_3), 3.86

(bs, 6 H, ArOCH$_2$C*H$_2$*), 4.06 (bs, 6 H, ArOC*H$_2$*), 4.41 (bs, 6 H, ax-C*H$_2$*), 6.35 (bs, 6 H, N*H*), 6.9-7.4 (m, 24 H, Ar*H*). ESI-MS(+): m/z (%) = 1810 (100) [M+H]$^+$, 1833 (100) [M+Na]$^+$.

1-(12-hydroxydodecyl)-[4,4'-bipyridin]-1-ium 4-methylbenzenesulfonate 15: 12-hydroxydodecyl 4-methylbenzenesulfonate (0.6g, 1.6 mmol) was dissolved in anhydrous acetonitrile (100 mL) and 4,4'-bipyridine (0.4 g, 2.4 mmol) was added. The reaction mixture was refluxed overnight, and the solvent was evaporated under reduced pressure. Product **15** was purified by trituration in ethyl acetate and obtained in 56% yield as a white solid. ^{1}H NMR (400 MHz, MeOD): δ = 1.3-1.4 (m, 16 H, aliphatic C*H$_2$*), 1.54 (m, 2 H, HO-CH$_2$C*H$_2$*), 2.08 (m, 2 H, N$^+$-CH$_2$C*H$_2$*), 2.38 (s, 3 H, ArC*H$_3$*), 3.55 (t, ^{3}J(H,H)=6.4 Hz, 2 H, HO-C*H$_2$*), 4.68 (t, ^{3}J(H,H)=7.6 Hz, 2 H, N$^+$-C*H$_2$*), 7.23 (d, ^{3}J(H,H)=8.0 Hz, 2 H, Ar*H*), 7.71 (d, ^{3}J(H,H)=8.0 Hz, 2 H, Ar*H*), 8.00 (d, ^{3}J(H,H)=6.8 Hz, 2 H, Ar*H*), 8.51 (d, ^{3}J(H,H)=6.8 Hz, 2 H, Ar*H*), 8.84 (d, ^{3}J(H,H)=6.8 Hz, 2 H, Ar*H*), 9.12 (d, ^{3}J(H,H)=6.8 Hz, 2 H, Ar*H*). ESI-MS(+): m/z (%) = 341 (100) [M]$^+$.

Axle 10: A solution of pyridil-pyridinium salt **15** (0.26 g, 0.50 mmol) and hexadecane-1,16-diyl bis(4-methylbenzenesulfonate) **16** (0.14 g, 0.25 mmol) in anhydrous acetonitrile was heated at 110°C for five days in a Schlenk reactor. The reaction mixture was then cooled at room temperature, and precipitated axle **10** was isolated by Buchner filtration in 40% yield as a white powder. ^{1}H NMR (400 MHz, MeOD): δ = 1.3-1.4 (m, 58 H, aliphatic C*H$_2$*), 1.54 (m, 4 H, HO-CH$_2$C*H$_2$*), 2.06 (m, 8 H, N$^+$-CH$_2$C*H$_2$*), 2.39 (s, 12 H, ArC*H$_3$*), 3.55 (t, ^{3}J(H,H)=6.8 Hz, 4 H, HO-C*H$_2$*), 4.73 (t, ^{3}J(H,H)=7.2 Hz, 8 H, N$^+$-C*H$_2$*), 7.24 (d, ^{3}J(H,H)=8.0 Hz, 8 H, Ar*H*), 7.69 (d, ^{3}J(H,H)=8.0 Hz, 8 H, Ar*H*), 8.65 (d, ^{3}J(H,H)=6.8 Hz, 8 H, Ar*H*), 9.24 (d, ^{3}J(H,H)=6.8 Hz, 8 H, Ar*H*). ^{13}C NMR (100 MHz, MeOD): δ = 19.9, 28.7, 28.8, 29.1, 29.2 (2 res.), 29.3 (3 res.), 29.4 (2 res.), 31.2, 32.3, 61.6, 61.9, 125.5, 126.9, 128.5, 140.3, 142.3, 145.6, 149.9 ppm. ESI-MS(+): m/z (%) = 1420 (100) [M-TsO]$^{3+}$.

The Author

Valeria Zanichelli was born in Reggio Emilia in 1989. She obtained the bachelor degree in Industrial Chemistry (110/110) in 2011 under the supervision of Prof. E. Dalcanale at the University of Parma, working on the self-assembly of supramolecular polymers. In the same research group, she obtained the master degree in Industrial Chemistry (110/110 cum laude) in 2013 with a thesis entitled "Synthetical approaches to the monofunctionalization of cavitands with fluorophores". Since 2014 she is carrying out her PhD at the University of Parma under the supervision of Prof. A. Arduini. Her research is focusing on the design, the synthesis, the structural characterization and the evaluation of the working modes of calix[6]arene-based molecular machines prototypes. During the PhD (January 2016 – May 2016), she joined as a visiting student the group of Chimie Bioinorganique Supramoléculaire headed by Prof. O. Reinaud at the Laboratoire de Chimie & Biochimie Pharmacologiques et Toxicologiques, Université Paris Descartes – CNRS UMR 8601, Paris (FR). The results achieved during her PhD are described in this thesis.

List of Publications

Orlandini, G.; Zanichelli, V.; Secchi, A.; Arduini, A.; Ragazzon, G.; Credi, A.; Venturi, M.; Silvi, S. "Synthesis by Ring Closing Metathesis and Properties of an Electroactive Calix[6]arene [2]Catenane", *Supramolecular Chemistry* **2016,** *28*, 427–435.

Zanichelli, V.; Ragazzon, G.; Arduini, A.; Credi, A.; Franchi, P.; Orlandini, G.; Venturi, M.; Lucarini, M.; Secchi, A.; Silvi, S. "Synthesis and Characterization of Constitutionally Isomeric Oriented Calix[6]arene-Based Rotaxanes", *Eur. J. Org. Chem.* **2016**, 1033-1042.

Vita, F.; Vorti, M.; Orlandini, G.; Zanichelli, V.; Massera, C.; Ugozzoli, F.; Arduini, A.; Secchi, A. "Synthesis and Recognition Properties of Calix[4]arene Semitubes as Ditopic Hosts for N-alkylpyridinium Ion Pairs", *Cryst. Eng. Comm* **2016**, *18*, 5017-5027.

Orlandini, G.; Ragazzon, G.; Zanichelli, V.; Degli Esposti, L.; Baroncini, M.; Silvi, S.; Venturi, M.; Credi, A.; Secchi, A.; Arduini, A. "Plugging a bipyridinium axle into multichromophoric calix[6]arene wheels bearing naphthyl units at different rims", *Chemistry Open*, in press.

Orlandini, G.; Zanichelli, V.; Secchi, A.; Arduini, A.; Ragazzon, G.; Silvi, S.; Credi, A.; Venturi, M. "Wheel directed supramolecularly-assisted synthesis of calix[6]arene-based oriented pseudorotaxanes and rotaxanes" (in preparation).

Ringraziamenti

Grazie a Arturo e Andrea per avermi dato la possibilità di intraprendere questo percorso, per tutti i consigli, per avermi insegnato tantissime cose (chimiche e non) e per avermi aiutata a valorizzare i miei punti di forza.
Grazie al gruppo del Prof. Alberto Credi dell'Università di Bologna, e in particolare a Giulio, per la collaborazione nella maggior parte dei progetti.
Grazie a Olivia e a tutto il suo gruppo per avermi ospitata e per avermi fatto scoprire una città bellissima come Parigi.
Grazie al Capitano Guido e a Francesco, con cui ho condiviso la maggior parte del tempo in laboratorio, ai borsisti-casinisti Nicolò e Carola (che rimane sempre la mia Meredith) e a tutti i tirocinanti e tesisti che mi hanno dato una mano e a cui spero di aver insegnato qualcosa: Mattia, Francesco, Anureet, Sabrina, Luca, Margherita, Jennifer, Simone, Valeria…siete proprio tanti!
Grazie a tutti i compagni di studi che hanno condiviso fatiche e divertimento per questi lunghi otto anni.
Grazie alla mia famiglia che ancora una volta mi ha incoraggiata e supportata.
Grazie a Alessandro per non avermi mai permesso di mollare e per tutto quello che ci aspetta.
Grazie alle mie amiche favolose che sono sempre un punto fermo e irrinunciabile.